CONTRACTOR REPORT

SAND87–7024
Unlimited Release
UC–270

Investigation of Potential Islanding of Dispersed Photovoltaic Systems

Robert A. Jones, Thomas R. Sims
Southern Electric International
PO Box 2625
Birmingham, AL 35202

Ali Imece
Auburn University
Montgomery, AL 36849

Prepared by Sandia National Laboratories Albuquerque, New Mexico 87185 and Livermore, California 94550 for the United States Department of Energy under Contract DE-AC04-76DP00789

Printed October 1988

Issued by Sandia National Laboratories, operated for the United States Department of Energy by Sandia Corporation.

Printed in the United States of America
Available from
National Technical Information Service
U.S. Department of Commerce
5285 Port Royal Road
Springfield, VA 22161

NTIS price codes
Printed copy: A15
Microfiche copy: A01

Distribution
Category UC-270

SAND87-7024
Unlimited Release
Printed October 1988

INVESTIGATION OF POTENTIAL ISLANDING OF DISPERSED PHOTOVOLTAIC SYSTEMS

Robert A. Jones, Thomas R. Sims
Southern Electric International

Al Imece
Auburn University

Sandia Contract 59-3704

ABSTRACT

Photovoltaic sources feed power back to a utility through static power converters (SPCs) during normal operation. The SPCs are designed to shut down when the utility grid is abnormal; however, it has been shown that they continue to operate or "run-on" under certain abnormal conditions. This research was designed to establish the conditions of load vs. generation under which run-on would occur. Computer simulations were made of a TESLACO self-commutated SPC and of a Gemini line-commutated SPC. The results of the simulations were verified by laboratory and field tests. Run-on was found to occur only when there was a very close match between PV generation (SPC output) and connected load. For the TESLACO, under matched-load conditions, run-on was limited to 4 seconds, due to destabilizing circuits and internal trip mechanisms. For the Gemini, external VAR support, necessary for matched-load conditions, allows the unit to run-on indefinitely. The addition of internal trip mechanisms based on sensing frequency and voltage, available from the Gemini manufacturer, reduced run-on to an extremely low probability event. The research did not reveal any dynamic interaction among multiple TESLACOs, multiple Geminis, or among TESLACOs and Geminis within an island that would cause the island to persist longer than it would for a single SPC.

ACKNOWLEDGEMENTS

The authors wish to acknowledge the tremendous contribution made by Dennis Hand and Marty Page of Georgia Power Company in planning and executing the laboratory and field tests. We also wish to acknowledge the contribution made by Ed Ney and Dennis Keebaugh of Georgia Power in handling the administration of the project. We wish to acknowledge the assistance given by Linda Smith of Southern Company Services in performing the computer simulations. The authors wish to acknowledge the guidance and editorial suggestions by John Stevens of Sandia National Laboratories. We also wish to acknowledge the editorial suggestions by Gobind Atmaram of Florida Solar Energy Center, Don Wallace of Alabama Solar Energy Center, and Hans Meyer of Omnion Power Engineering Corporation. We wish to thank Oleg Wasynczuk and Paul Krause of Paul Krause and Associates for supplying computer models for the TESLACO and Gemini static power converters. We wish to thank the personnel of the Energy Research Test Facility of the Tennessee Valley Authority for their assistance in performing the field tests. Finally, we wish to thank George Vachtsevanos of the Georgia Institute of Technology for his assistance and his development of a simplified model of the APCC static power converter.

TABLE OF CONTENTS

LIST OF FIGURES

EXECUTIVE SUMMARY

The safety of line crew personnel and others is a major concern of electric utilities regarding the widespread use of grid-connected photovoltaic (PV) power sources. PV sources feeding power back to the electric utility grid through static power converters (SPCs), which are designed to shut down when disconnected from the grid, have been shown to continue to operate under certain simulated conditions when disconnected from the utility. Tests for isolated operation or "running on" of self-commutated single inverters conducted at Sandia National Laboratories have resulted in control circuit modifications for some designs, which have improved the shut-down characteristics of those SPCs. Little was known about the effectiveness of those modifications in preventing isolated operation or "islanding" of several SPCs in parallel. It was conjectured that multiple SPCs might interact dynamically under certain conditions to prevent the shut-down logic from working properly. The purpose of this research was to show if islanding of multiple SPCs will occur and to establish boundary conditions under which it will occur. To accomplish this research the project was split into three tasks:

1. Computer simulations
2. Laboratory testing
3. Field testing

The primary emphasis of the research was to use computer simulations to define the boundary conditions under which islanding could occur. The purpose of the laboratory and field tests was to validate the results of the simulations.

Computer simulations of PV arrays, SPCs, and a utility system were made using the Electromagnetic Transients Program (EMTP). Because of a limited availability of detailed data on commercially available SPCs, only two were chosen to be modeled and analyzed with detailed computer simulations - a self-commutated, 4000-watt, SPC manufactured by TESLACO and a line-commutated, 6000-watt, Gemini SPC manufactured by Windworks, Inc. Numerous simulations were made to understand what impact various system parameters had on islanding. Among those examined were the mismatch between watts and vars of load and watts and vars of generation within a possible island, the effect of the type of load, the effect of distribution feeder characteristics and the effect of solar insolation variations and load variations during an islanding condition. The parameter found to have the most significant impact on run-on time for both the TESLACO SPC and the Gemini SPC was the mismatch between load and generation.

Under no conditions did the TESLACO SPC exhibit a sustained islanding condition. It always shut down eventually after the island was disconnected from the utility. For certain combinations of load and generation in the island, it could run on for up to 3.8 seconds but would always shut down. The TESLACO would shut down within approximately two cycles if the mismatch between watts of load and watts of generation was greater than approximately 40% of the rating of the SPC (1600 watts). It would shut down within two cycles if the mismatch between vars of load and vars of generation was greater than 20% of the rating (800 vars). When the mismatches were less than these, the TESLACO would run on from a few cycles to a few seconds.

The Gemini SPC can run on indefinitely for a specific range of load conditions. If the load within the island supplies 60% or more of the pre-island reactive power requirement of the Gemini, and if the watts of load do not exceed 130% of the watts supplied by the Gemini, then the SPC will run on indefinitely (until the load-generation match changes to values outside these boundaries). One other boundary condition was implied by the results of the laboratory and field tests. The Gemini must be in the continuous conduction mode of operation for indefinite islanding to occur. That is, the output of the unit must be greater than approximately 35-40% of the unit's rating. This boundary condition was not due to any protective circuit. Computer simulations implied that this boundary condition may have been specific to the unit tested and may not hold true in general for all Geminis. While it is felt that all of these boundary conditions could exist simultaneously within an island, the probability of this occuring has not been determined.

If the load is outside of these boundaries when the island is formed, the SPC shuts down within five cycles. The boundaries could be reduced considerably by the addition of an overvoltage relay and an over/under frequency relay. These are features which the manufacturer offers, but the unit tested did not include them. Simulations indicated that with these additions the mismatch in watts of load to watts of generation must be less than approximately 25% (actual value depends on setting of over-voltage relay) and the mismatch in vars of load and the reactive requirement of the SPC must be less than approximately 3% (actual value depends on setting of frequency relays) for the SPC to run on indefinitely. The probability of having a var mismatch this small should be relatively low.

The analysis of potential islands with both a TESLACO and a Gemini did not reveal any dynamic interaction between the two that would make one SPC run on longer than it would if it were in an island by itself. In general the watt and var mismatch in the potential island with both a TESLACO and a Gemini determined how long the TESLACO ran on. When the TESLACO shut down (as it always did), the resulting mismatch between load and generation determined if the Gemini shut down or ran on indefinitely. Also no dynamic interaction was found between multiple TESLACOs within an island or between multiple Geminis within an island.

Laboratory and field tests were performed that verified the results of the computer simulations. No indefinite run on of a properly functioning TESLACO was produced. One TESLACO SPC tested had a bad capacitor in the phase-locked loop circuit, which allowed it to run on indefinitely. When the circuit board containing the phase-locked loop was replaced, the TESLACO SPC always shut down when disconnected from the utility. This experience suggests the need for manufacturers of SPCs to test the units for islanding as part of their factory testing. The laboratory and field tests verified that a Gemini SPC could run on indefinitely for the boundary conditions described above. No dynamic interaction between multiple SPCs was seen in the laboratory and field tests.

The results of this project indicate that sustained islanding is not a concern for utilities if only TESLACO SPCs are within a potential island. Sustained islanding is a concern for utilities if Gemini SPCs which do not have overvoltage and over/under frequency relays are within a potential

island. However, the probability of having a sustained island can be greatly reduced by having these relays either in the Gemini or in the interface between the utility and the Gemini SPC. It is recommended that these protective features always be included.

In addition to the extensive analyses performed for the TESLACO SPC and the Gemini SPC, a brief analysis was made of the islanding potential of an SPC made by American Power Conversion Corporation (APCC). Based on a simplified

model of the SPC, it appears that the APCC cannot be put into an indefinite run-on condition. If the net load within an island is resistive or inductive, the APCC will shut down immediately (within a cycle). If the net load has an impedance angle greater than 2° leading, the SPC will also shut down immediately. If the net load has an angle between 0° to 2° leading, the unit will run on for a short time (up to one second in the limited amount of simulations made). Further detailed analysis is necessary to quantify further the run-on potential of the APCC.

I. INTRODUCTION

Electric power utilities have been concerned about the impact of photovoltaic (PV) generation on their systems [1-4]. One of the major issues is "islanding," or the isolated operation of grid-interconnected PV systems following the utility power interruption [5-7]. The problem is illustrated in Figure 1-1, which shows a utility-interconnected residential PV system diagram. Under normal conditions the static power converter (SPC) converts the dc power generated by the PV array to ac power supplying both local and remote loads. If the generation is greater than the load demand, the difference is fed back to the utility; otherwise the utility supplies the difference. But in all cases the following equation holds when the SPC is operating synchronized to the utility:

$$P_{Generation} = P_{Load} + P_{Grid} \cdot \qquad (1\text{-}1)$$

If the utility de-energizes its distribution line for any reason the P_{Grid} becomes zero and the generated power is forced to be equal to P_{Load}. Depending upon the initial mismatch between the generated and load powers and the control algorithm of the SPC, the system operating voltage and frequency will move to a new operating point. The utility wants the SPC to sense these variations and disconnect itself from the line rapidly. This requirement is necessary primarily for the safety of the line crew who must repair the supposedly disconnected line. Furthermore the SPC's reaction time is also important due to the possible reclosure of the utility circuit breaker. Optimally the SPC control and protection logic must sense the

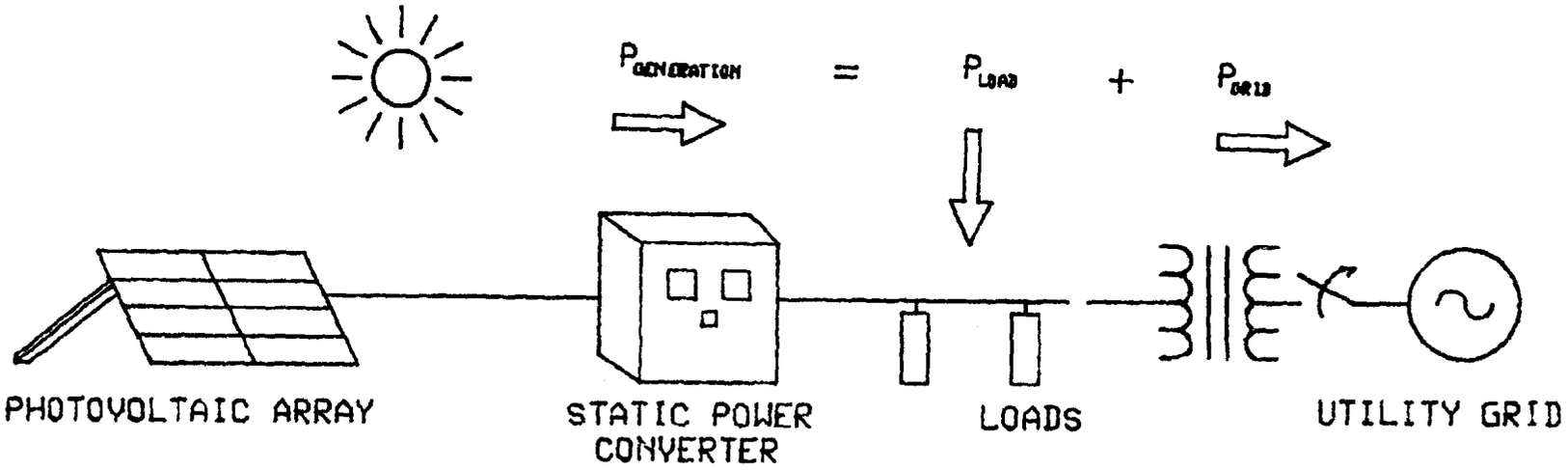

Figure 1-1. Utility Interconnected Residential Photovoltaic System.

utility power interruption and take itself off line before the minumum automatic reclosing time of the utility. If P_{Grid} is initially close to zero, the operating point will not deviate much from its original condition, and it will be difficult for the SPC protection circuit to detect any change.

This report presents the results of an organized theoretical and experimental investigation on this potential problem. The objective of the research was to develop a computer model for residential grid-interconnected PV systems to predict the conditions that lead to islanding.

In previous studies, hybrid computer simulations were performed by Purdue University to demonstrate the dynamic behavior of the isolated PV systems [5,6]. Also several experiments were performed by electric power utilities that demonstrated the islanding potential of commercially available SPCs [7]. In these computer simulations and experimental studies only general behavior of the isolated systems was considered. No special effort was made in quantifying the effects of system parameters.

In this study, the effects of system parameters on islanding were investigated in terms of windows; that is, the system variable was varied over a range of values and its effect on the islanding performance of the SPC was observed. These windows, the boundary conditions under which islanding occurs, were quantified by computer simulations. The computer simulation results were first validated in a laboratory, then in a field environment.

In the computer simulations and experiments, special emphasis was given to the power mismatch between the generation and the load. Both real and reactive power mismatches were varied and their effects on the duration of the island were characterized. This process was repeated for different load types and feeder characteristics so that their effects on the islanding were also understood.

In addition, variations of both load and atmospheric conditions were investigated as to their effect on the island. Also, the ability of two or more SPCs operating in parallel to sustain an island was addressed.

For this project two commercially available SPCs were selected for detailed modeling and analysis. One was a self-commutated unit manufactured by TESLACO and the other was a line-commutated unit manufactured by Windworks, Inc. The TESLACO was developed under contract to the US Department of Energy. The Windworks unit was developed through private funding. The main body of this report plus appendices A, B, and C deal with the islanding potential of these two SPCs. Appendix D contains a simplified model and a brief analysis of the islanding potential for a self-commutated SPC manufactured by American Power Conversion Corporation.

1.1 Definitions

The terminology used in current literature to describe the conditions and modes of PV system isolated operation may cause confusion; such as "running on," "islanding," "multiple-islanding," etc. For this report the following definitions will apply.

"Isolated operation" or more commonly "islanding" refers to the condition of the PV system during the time between the loss of utility and shut-down of the last SPC.

The "run-on time" is defined as the time elapsed between the utility power interruption and the shutdown of the SPC.

If the islanding involves only one SPC, it will be referred to as "single-SPC-islanding." If there is more than one SPC, then islanding formed due to the parallel operation will be called "multiple-SPC-islanding."

During islanding the system parameters, such as voltage and frequency, may converge to a new operating condition and the rates of change may become very small. "Transient islanding" covers the behavior of the isolated PV system during the period between the start of islanding and shut-down of the last SPC, or the time that system parameters converge to a new operating point. If the system parameters converge, "sustained islanding" refers to the condition of the isolated PV system until the utility breaker recloses.

BLANK PAGE

II. ANALYTICAL PREDICTION OF ISLANDING CONDITIONS

2.1 Photovoltaic System Modeling

A block diagram of a utility-interconnected PV system is shown in Figure 2.1-1. As shown in this figure, the PV array is the dc power source, converting sunlight to electricity. The dc energy is fed to the static power converter (SPC), and after conversion into the ac form, it is injected into the utility grid and is supplied to the loads. The role of the SPC goes beyond dc-to-ac conversion. It is also responsible for properly interfacing the PV array to the inverter, and the inverter to the utility, as well as providing overall PV power system control and protection [8-10]. The control unit of the SPC determines the PV system performance and ensures conversion of dc power to high-quality, utility-compatible, ac power in a safe, reliable and efficient manner. Commercially available SPCs for photovoltaic applications are basically of two types; self-commutated and line-commutated. There are considerable differences between the operational characteristics of these two types of SPCs and they are described in the literature in detail [11-21]. These operational differences, however, have only a secondary influence on the islanding characteristics of SPCs. The primary influence is the control and protection circuitry.

In regard to the operational performance of SPCs, islanding is one of the issues that electric power utilities must resolve before they accept large-scale penetration of photovoltaic systems into the utility grid. To characterize the islanding operation of SPCs, a computer model of utility-interconnected photovoltaic systems was developed.

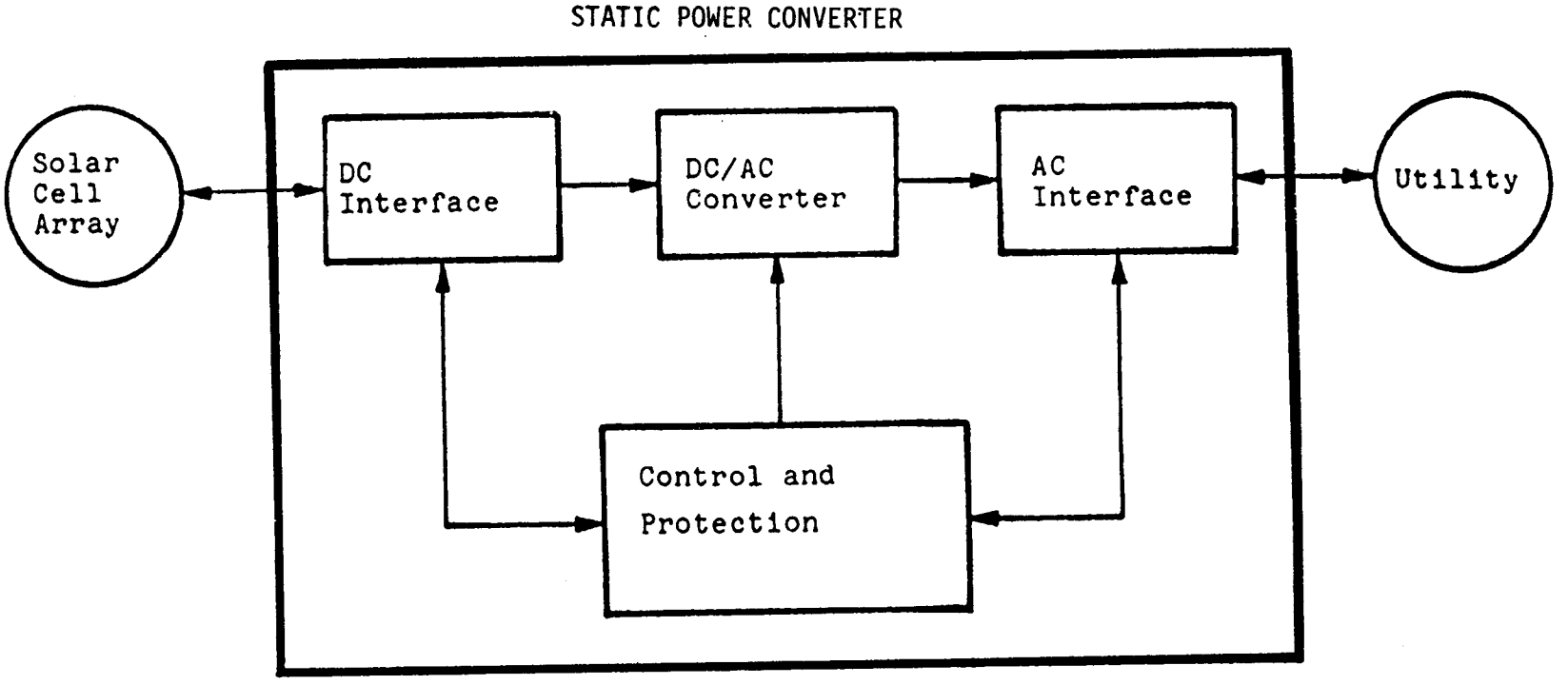

Figure 2.1-1. Block Diagram of a Photovoltaic System.

This computer modeling effort was accomplished using the Electromagnetic Transients Program (EMTP) residing at the Southern Company Services computing facilities. This program was originated by Bonneville Power Administration but has been further developed by many utilities, universities, and others over the years. The program has widespread usage among electric utilities both in this country and internationally. It is a very general program with which electrical equipment can be modeled using basic elements such as resistors, capacitors, diodes, and inductors [22].

As mentioned before, the utility-interconnected photovoltaic system is composed of several components such as the photovoltaic array, the static power converter, the loads and the utility grid. The model for each component was developed individually by considering the philosophy of the EMTP. Then, the models were combined to characterize the total PV system.

The photovoltaic array model was composed of a nonlinear analytical equation describing the output current-voltage characteristics of the array in terms of solar radiation, cell temperature, number of series and parallel solar cells forming the array, and certain cell parameters. The details of the model are presented in Appendix A.

For the SPC modeling, two commercially available SPC designs were identified and their manufacturers were contacted to obtain technical information on the specifics of the designs. The first SPC was a self-commutated unit with its operation based on the high frequency link approach. The second SPC was a line-commutated model that used silicon controlled rectifiers (SCRs) as the power switching devices. The detailed description of the self-commutated

and line-commutated SPC models are presented in Appendices B and C, respectively. The models include the power and control stages of the SPCs as well as their protection logic at the ac interface. The action of the protection devices was simulated to disconnect the SPC from the ac system when the system parameters such as the voltage and/or the frequency were out of tolerance.

The loads on the utility system include both active and passive types. Active type loads refer to equipment such as induction motors for which the equivalent model considers the effect of the inertia and back EMF of the motor. In order to obtain a realistic computer model for an induction motor, tests were performed on the 1-hp motor that was going to be used in the lab test portion of the project. This was a capacitor start motor with its starting winding connected to the midpoint of its stator winding. The tests performed on the motor included a no load test, a locked rotor test without the starting winding connected, and a locked rotor test without the starting capacitor or the main rotor winding connected. Data from these tests were used to derive the equivalent circuit shown in Figure 2.1-2.

Passive loads are those which do not supply voltage or current to the feeder after the utility is disconnected. These loads were represented primarily by resistances and inductances. Passive loads include such items as incandescent lights, electric ranges, and water heaters.

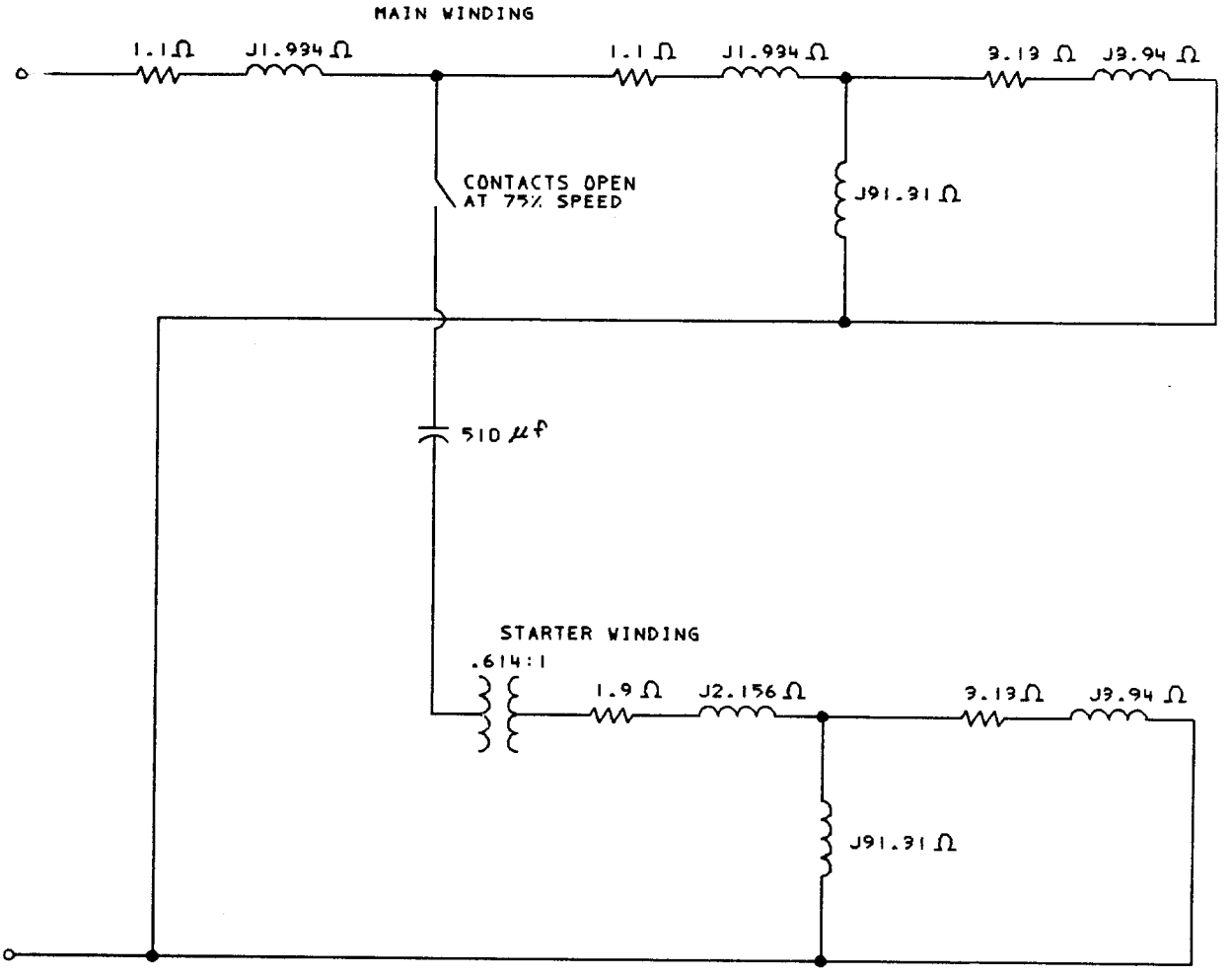

FIGURE 2.1-2 EQUIVALENT CIRCUIT FOR 1HP MOTOR

The elements of the utility grid model included transformers, distribution feeders and power factor correction capacitor banks. In the model, the utility grid was represented by a sinusoidal voltage source in series with an impedance.

After incorporating individual models of the PV system into the EMTP, simulations showing the dynamic behavior of the SPCs under islanding conditions were performed. The results of the simulations are given in terms of the run-on times, which enable a fair comparison of different SPCs in terms of their islanding performance. The details of the simulations are provided in the next two sections.

2.2 Analytical Results for a TESLACO Self-Commutated Static Power Converter

The self-commutated SPC used in this project was a single phase, 4-kW unit manufactured by TESLACO. This device utilizes push-pull buck converter switching at 20 kHz to convert the dc input into a fully rectified sine wave. This sine wave is subsequently unfolded by a four transistor bridge to produce 60-Hz sine-wave power output. The buck converter is controlled by an internally generated reference wave, so that its output is essentially an amplified version of the reference wave. The reference wave is produced by a phase-locked loop, which locks it in phase with the terminal voltage of the SPC. The TESLACO SPC operates at a near unity power factor. The phase-locked loop also contains control circuitry that will detect a loss-of-utility condition. These circuits will allow the TESLACO to shut itself down if its internal reference wave becomes 6° out of phase with its terminal voltage. Without the utility connected, the control circuits are designed to drive the phase difference between the internal reference wave and the terminal voltage to a value larger than 6° and therefore to shut down. The results of this project indicate that these control circuits work very well in that no indefinite run-on conditions were obtained for the TESLACO. It always shuts down within a few seconds after disconnection from the utility.

A block diagram model for a TESLACO static power converter was obtained from Paul Krause and Associates as a result of their work at Purdue University. This model was implemented on the Electromagnetic Transients Program (EMTP).

Details of the computer model and the implementation of the model on EMTP are given in Appendix B. Many computer simulations were made to determine what parameters are important in assessing the run-on time of the TESLACO SPC. Among the parameters investigated were the mismatch between load and generation within an island, type of load, distribution feeder characteristics, the number of SPCs within the island, and load variation and solar insolation variation after separation from the utility.

Effect of Mismatch Between Load and Generation

The most significant parameter for run-on times for the TESLACO is the mismatch between load and generation. The general trend is for shorter run-on times to be associated with larger mismatches between load and generation. Table 2.2-1 illustrates this trend. The effect of a watts mismatch between load and generation is different from the effect of a var mismatch. When the PV system and load are disconnected from the utility, the terminal voltage of the TESLACO changes almost immediately to a new magnitude, which is determined by the amount of mismatch between watts generated and the watts of resistive load within the island. For example, if the resistive load is 10% less than the watts generated, the voltage will increase by a factor of $\sqrt{1.1}$ so that the watts consumed by the resistive load will equal the watts generated. The change in terminal voltage produces a phase error within the phase-locked loop because of the response of the line filter. This phase error increases with time and eventually reaches 6° at which time the unit shuts itself down.

When there is a mismatch between vars generated and vars consumed by the load within an island, the phase of the terminal voltage undergoes a change when the utility is disconnected. The phase change is in a direction to try to balance the var generation with the var load. The control circuitry of the TESLACO acts to increase this phase error with time, and eventually the error reaches 6° and the unit shuts down. The run-on times of the TESLACO were found to be much more sensitive to mismatches in vars than they were to mismatches in watts. For example, with var load matched to vars generated, a resistive load that is 40% greater or less than the watts generated will cause the TESLACO to shut down consistently within one cycle of disconnection from the utility. For the TESLACO operating at rated output of 4000 watts, this amounts to a load-to-generation mismatch of 1600 watts. However, with watt load matched to watts generated, a var mismatch of only 800 vars will consistently cause the TESLACO to shut down within one cycle. Therefore, the run-on time is more sensitive to mismatches in vars than it is to mismatches in watts.

When the load and generation within an island have mismatches in both watts and vars, then some interesting results can occur. For some cases the phase error produced by the watt mismatch can tend to cancel the phase error produced by the var mismatch and produce a long run-on time. For other cases the two phase errors tend to reinforce each other and a short run-on time is obtained. Further explanation of this effect is made after the zero crossing effect is described in the next paragraph.

Another effect that was seen in the computer simulations was a variation in run-on times depending on whether the switch disconnecting the potential

Table 2.2-1 Effect of Type of Load

	Case Description	Net Flow From Island to System		Run-On Times (sec.)	
		Watts	Vars	Negative-to-Positive Interruption	Positive to-Negative Interruption
T-1A	Primarily resistive load; local load.				
	1X. Load watts and vars matched to generation.	.08	.02	1.608	1.616
	2X. Load watts 10% less than generation; vars matched.	400	0	.941	1.076
	3X. Load watts 10% more than generation; vars matched.	-400	0	1.158	.917
	4X. Load watts 20% less than generation; vars matched.	800	0	.808	1.076
	5X. Load watts 20% more than generation; vars matched.	-800	0	1.050	.817
	6X. Load watts 30% less than generation; vars matched.	1200	0	.004	.004
	7X. Load watts 30% more than generation; vars matched.	-1200	0	.005	.004
	1X1. Load watts matched to generation; vars slightly mismatched.	.1	3.9	1.880	1.847
	2X1. Load watts 10% less than generation; vars slightly mismatched.	379	10	.740	1.59
	3X1. Load watts 10% more than generation; vars slightly mismatched.	-413	9	1.41	.683
	4X1. Load watts 20% less than generation; vars slightly mismatched.	778	10	.492	1.83
	5X1. Load watts 20% more than generation; vars slightly mismatched.	-808	9	1.43	.515
	6X1. Load watts 30% less than generation; vars slightly mismatched.	1177	11	.016	1.20
	7X1. Load watts 30% more than generation; vars slightly mismatched.	-1201	12	1.948	.021
	8X1. Load watts 40% less than generation; vars slightly mismatched.	1575	16	-	.004 -
	9X1. Load watts 40% more than generation; vars slightly mismatched.	-1594	14	.004	

Table 2.2-1 Effect of Type of Load (continued)

	Case Description	Net Flow From Island to System		Run-On Times (sec.)	
		Watts	Vars	Negative-to-Positive Interruption	Positive to-Negative Interruption
T-IC	Resistive and inductive load; local load; capacitance added.				
	1. Load watts and vars matched to generation.	.07	.07	1.496	1.471
	2. Load watts 10% less than generation; vars matched	400	0	.907	1.001
	3. Load watts 10% more than generation; vars matched	-400	0	1.016	.842
	6. Load vars 400 more than generation; watts matched.	0	-400	.025	.141
	6A. Load vars 400 less than generation; watts matched.	0	400	.076	.026
	8. Load watts 20% less than generation; vars matched.	800	0	.600	.793
	9. Load watts 20% more than generation; vars matched.	-800	0	.733	.634
	2S. Load watts 10% less than generation; vars slightly mismatched.	376	10	.742	1.71
	3S. Load watts 10% more than generation; vars slightly mismatched.	-416	9.5	1.425	.785
	4S. Watts slightly mismatched; Load capacitance reduced by 10%.	-19	-42	.913	.972
	5S. Watts slightly mismatched; Load capacitance increased by 10%	-20	62	.812	.753
	6S. Load vars 400 more than generation; watts slightly mismatched.	-14	-392	.133	.307
	7S. Load vars 800 more than generation; watts slightly mismatched.	-8	-790	.008	.008

Table 2.2-1 Effect of Type of Load (continued)

	Case Description	Net Flow From Island to System		Run-On Times (sec.)	
		Watts	Vars	Negative-to-Positive Interruption	Positive to-Negative Interruption
T-ID	Resistive and capacitive load; 1 Hp motor modeled; Local load only.				
	1. Load watts and vars matched to generation.	0	0	1.750	1.758
	2. Load watts 10% less than generation; vars matched.	400	0	1.008	1.584
	3. Load watts 10% more than generation; vars matched.	-400	0	1.184	1.092
	4. Load vars 400 less than generation; watts matched.	0	400	.026	.025
	5. Load vars 400 more than generation; watts matched.	0	-400	.041	.092
	6. Load watts 20% less than generation; vars matched.	800	0	.757	1.782
	7. Load watts 20% more than generation; vars matched.	-800	0	1.009	.918
	2S. Load watts 10% less than generation; vars slightly mismatched.	376	15	.907	1.30
	3S. Load watts 10% more than generation; vars slightly mismatched.	-	-	.635	.792
	4S. Load vars 400 less than generation; watts slightly mismatched.	-20	-382	.173	.190
	5S. Load vars 400 more than generation; watts slightly mismatched.	-26	419	.185	.158

island from the utility opened on a positive-to-negative zero crossing of the current wave or on a negative-to-positive zero crossing. This phenomenon can be understood when there is a net watt mismatch within the island by referring to Figures 2.2-1 through 2.2-4. The signals that are compared in the phase-locked-loop are the internal reference wave shifted by -90° and a filtered version of the terminal voltage. The filter produces a steady-state phase shift of -90°. These two signals are compared once every cycle at a negative-to-positive zero crossing to determine the phase error and to make a phase correction in the internal reference wave. When the switch opens to create the island and there is a net watt mismatch, the voltage in the island changes in a direction to balance the watt load and generation. This voltage change is a change in input to the line filter. The line filter produces a dc offset in its output which is the terminal voltage comparison signal. As shown in Figure 2.2-1, for a case with a net flow from the island to the system of -400 watts (load is 400 watts greater than generation), the offset is in the positive direction when the current is interrupted on a negative-to-positive zero crossing. This results in a small apparent phase error at the negative-to-positive zero crossing of the signals, which occurs 270° later (Figure 2.2-2). Since the negative-to-positive crossing is the one being checked in order to adjust the internal reference wave, a small phase error is seen, and the control circuitry eventually drives the phase error to 6° and shuts down relatively slowly. The situation is the opposite when the current is interrupted on a positive-to-negative zero crossing as shown in Figures 2.2-3 and 2.2-4. The dc offset is in the opposite direction, and the apparent phase error at the zero crossing of the signals that is being checked (only 90° later) is larger. Therefore, it takes less time for this case to reach 6° phase error and to shut down.

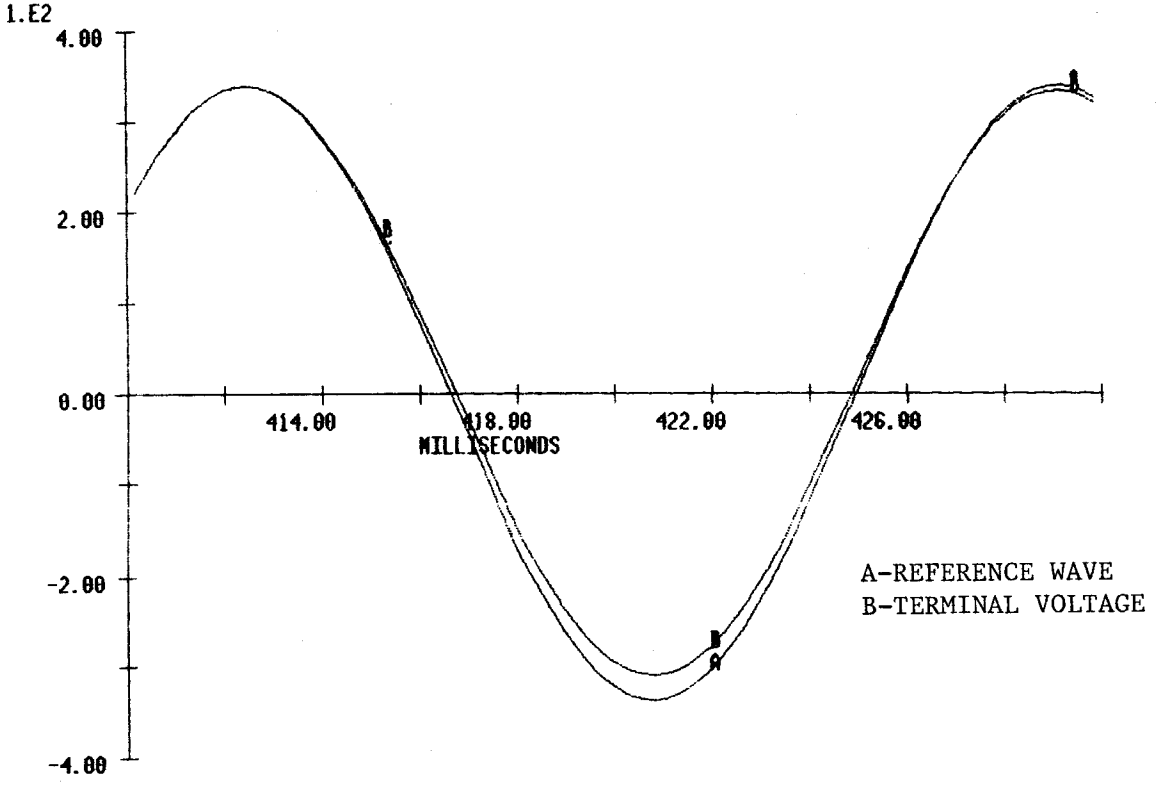

Figure 2.2-1 Phase comparator signals for a negative-to-positive zero crossing interruption.

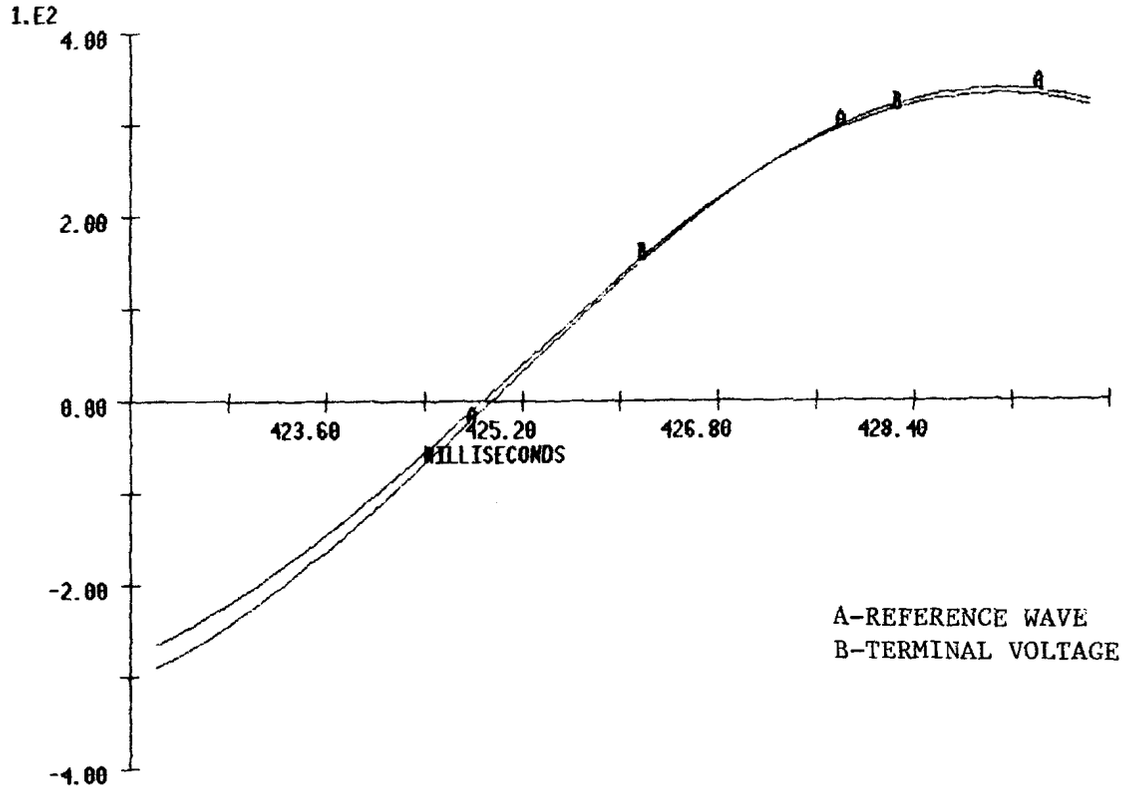

Figure 2.2-2 Phase comparator signals at the zero crossing which is being checked for apparent phase error(negative-to-positive interruption).

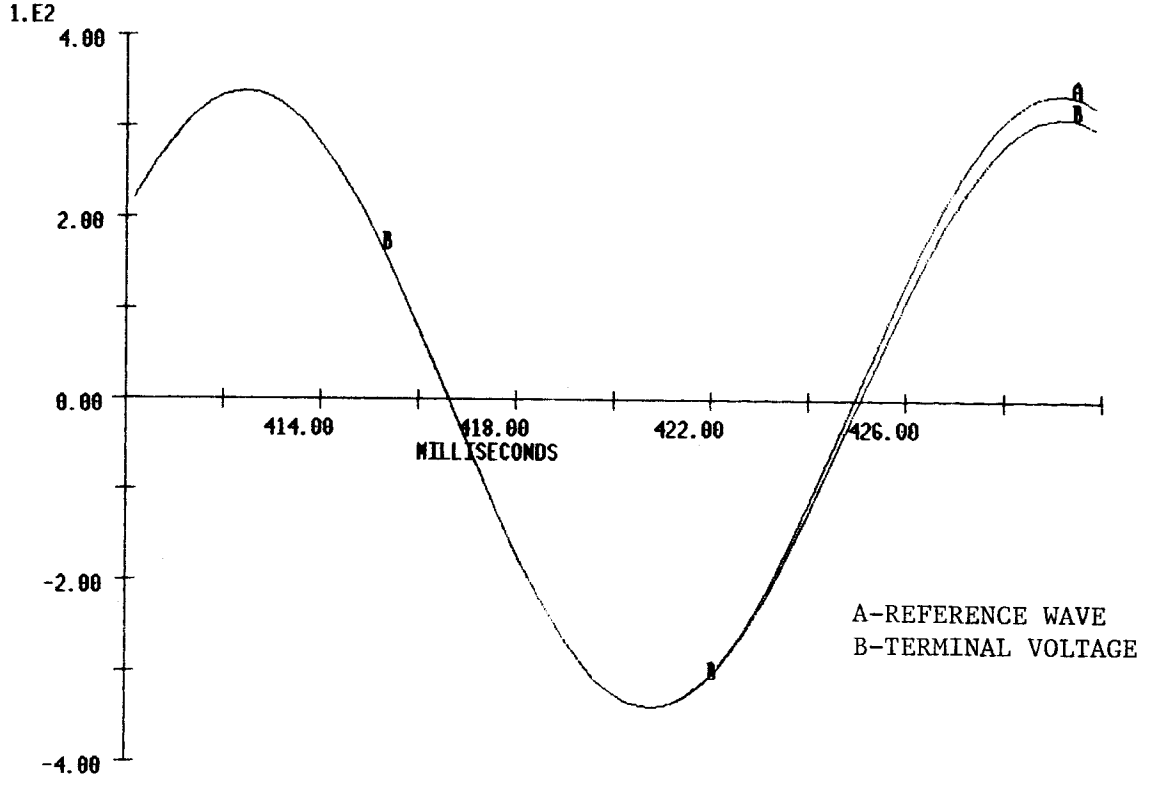

Figure 2.2-3 Phase comparator signals for a positive-to-negative zero crossing interruption.

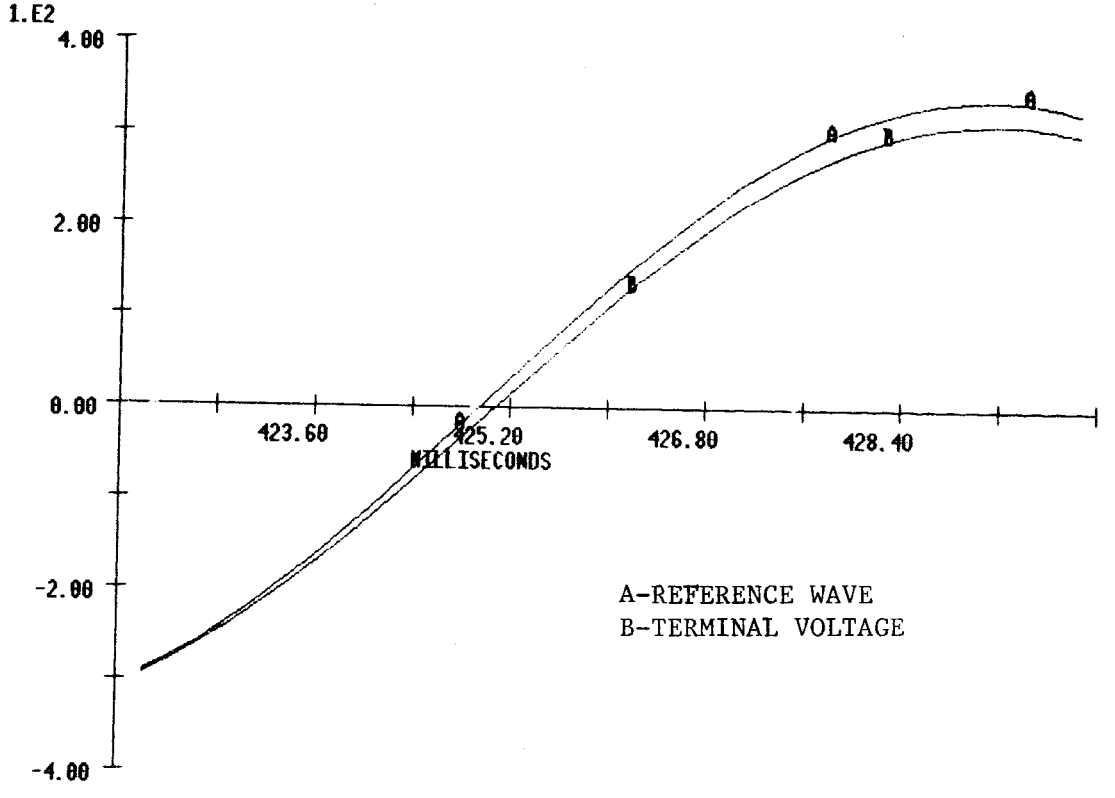

Figure 2.2-4 Phase comparator signals at the zero crossing which is being checked for apparent phase error (positive-to-negative interruption).

When the net flow from the island to the system is +400 watts, the situation is just the opposite from that described above. The current from the island to the system has the opposite polarity from the current in the case described above. The results of a negative-to-positive zero crossing interruption are therefore equivalent to the results of the positive-to-negative zero crossing interruption described above. Similarly, the results of a positive-to-negative zero crossing interruption are equivalent to the negative-to-positive results from the previous case. This explains the correlation seen in the table of results between negative-to-positive run-on times for a case with a certain percentage smaller load than generation and positive-to-negative run-on times for a case with the same percentage greater load than generation.

Now that an explanation of the zero crossing effect has been given, a description can be given of what happens when the net mismatch of load and generation within an island consists of both watts and vars. As stated earlier, for some cases the effects of the watt mismatch and the var mismatch tend to cancel each other and thereby produce a longer run-on time. For other cases the two effects tend to reinforce each other and a shorter run-on time is produced. This is illustrated in Figure 2.2-5, which shows the run-on times for a series of cases in which the net watts out to the system were held constant at -400 watts. The net var mismatch was varied from -40 to 40 vars. For negative-to-positive zero crossing interruptions, the effect of a positive var mismatch of approximately 8 vars produced the longest run-on time. As shown previously in Figure 2.2-2, the phase error produced by a negative-to-positive zero crossing interruption in a case with a -400 watts mismatch is in a negative direction (reference wave lags the terminal

FIGURE 2.2-5 RUN-ON TIMES VERSUS VAR MISMATCH AS WATT MISMATCH IS HELD CONSTANT AT -400.

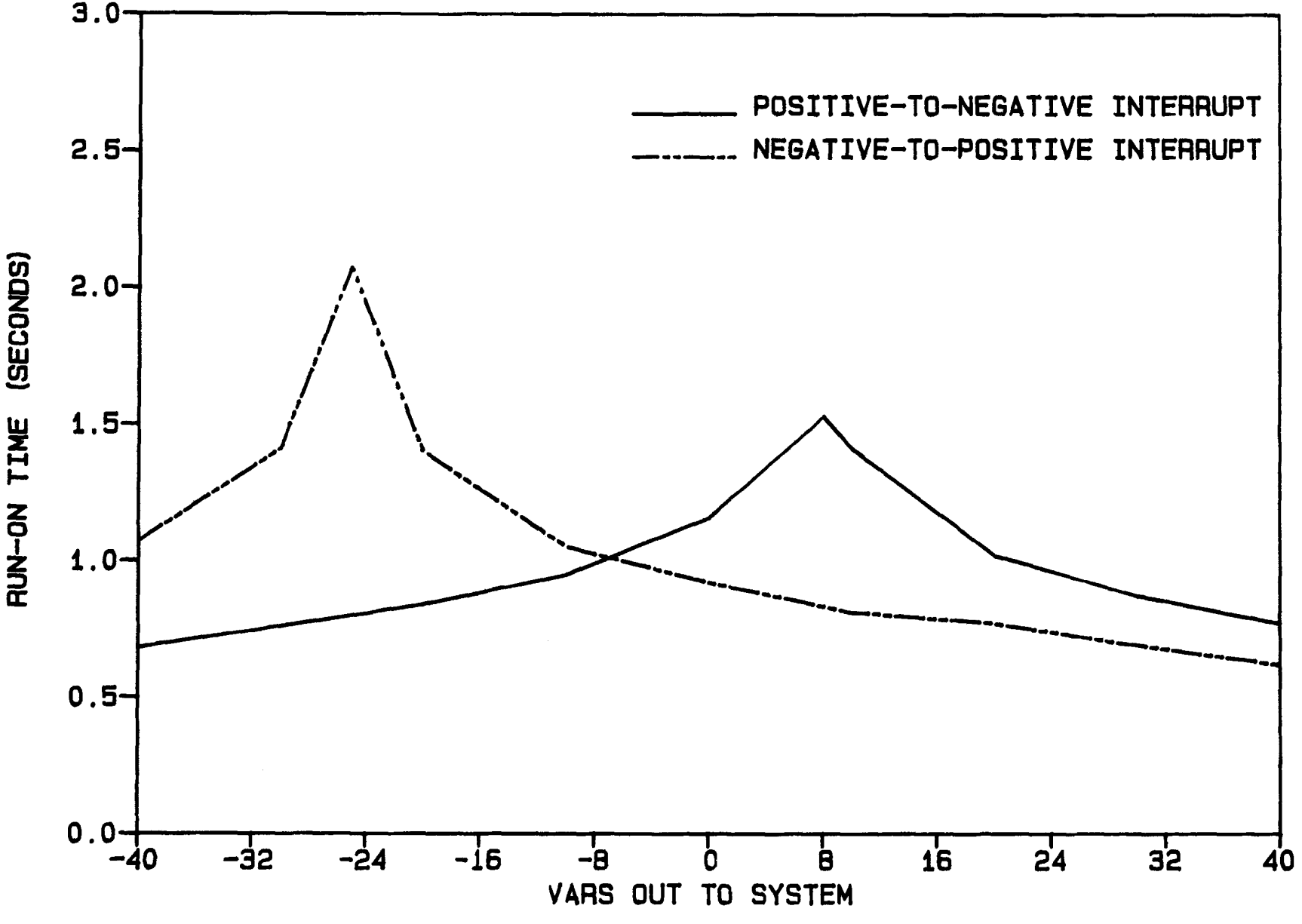

voltage). When an island is created that has a net var mismatch, the terminal voltage of the TESLACO changes phase in a direction to eliminate the mismatch. The output impedance of the TESLACO is essentially a 12-ohm resistor. To produce vars the phase angle of the terminal voltage must shift its phase angle ahead of the internal reference voltage. Conversely, to reduce var output the terminal voltage must shift its phase angle back relative to the reference wave. Therefore, when the var mismatch is 8 vars positive, the terminal voltage must shift back relative to the reference wave. This is in the opposite direction to the shift caused by the -400 watts mismatch, and the two effects cancel to produce a relatively long run-on time.

For a positive-to-negative zero crossing interruption, the longest run-on time occurred for a var mismatch of -25 vars. This can be understood by realizing that for a -400 watt mismatch case, a positive-to-negative zero crossing interruption produced an initial phase error opposite to that produced by a negative-to-positive interruption and larger in magnitude. To cancel this phase error, the var mismatch must be negative and larger in magnitude. Thus, the longest run-on was obtained for a var mismatch of -25.

When the watts mismatch is +400 instead of -400 watts, the curves would be very similar to Figure 2.2-5 if the labels negative-to-positive and positive-to-negative are swapped. All the previous discussion would also be applicable with the two zero crossing interruptions swapped.

Effect of Distribution Feeder Characteristics

A series of computer simulations was run to determine the significance of the characteristics of a distribution feeder that might be included in a potential island. These simulations included a TESLACO static power converter, 7200-240/120 volt transformers, distribution feeders, and loads as shown in Figure 2.2-6. For these simulations the loads were primarily resistive. Three different distribution feeder configurations were simulated. These are shown in Figure 2.2-7. These configurations were some that were found on the 12-kV distribution feeder to which the Alabama Solar Energy Center is connected. The conductor sizes were chosen to give a range of impedances for the feeder. Table 2.2-2 gives the results of these simulations. The feeder characteristics made virtually no difference in the run-on times. This result is reasonable when the impedance of the feeder is compared to the impedances of the transformers and the load. The feeder impedance is insignificant. The only influence that the feeder will have on run-on times is through the amount of capacitance to ground that it has. As far as run-on times are concerned, a feeder can be treated as a lumped capacitor. Its influence will then be how much it contributes to the var mismatch between load and generation within a potential island.

Effect of Type of Load

The effect of the type of load on the run-on times of the TESLACO static power converter was investigated by computer simulation. For passive loads (constant impedance type), this effect was found to be not very significant.

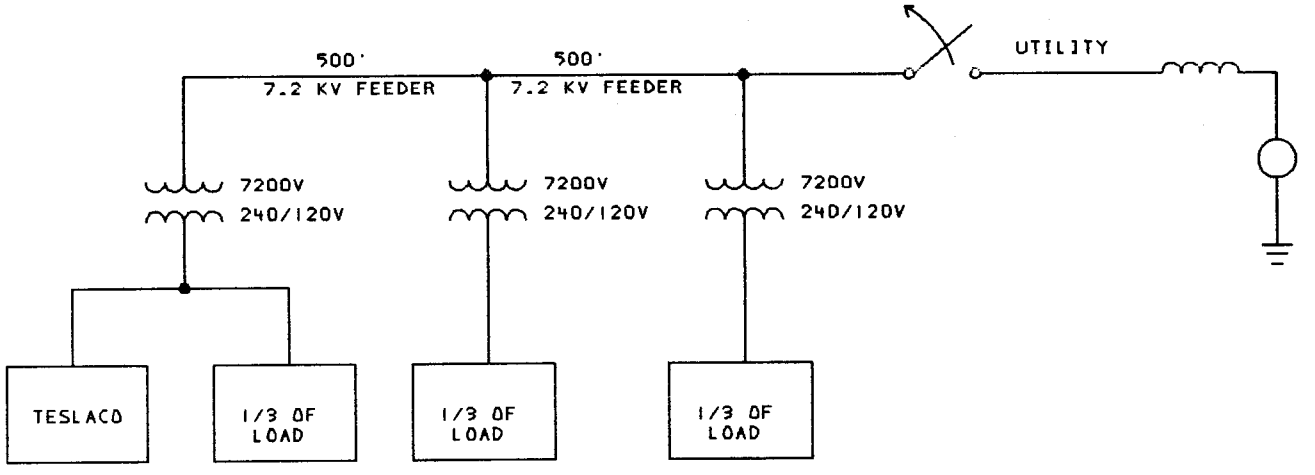

FIGURE 2.2-6 SYSTEM MODELED FOR DETERMINING EFFECT OF FEEDER

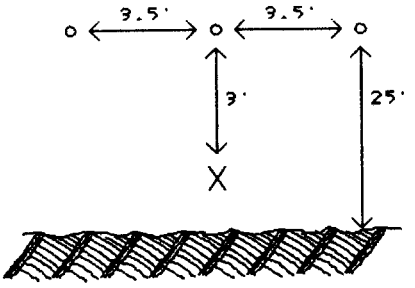

PHASE CONDUCTOR: 4/0 ALUMINUM
NEUTRAL CONDUCTOR: 2/0 ALUMINUM

(A)BASE CASE CONFIGURATION

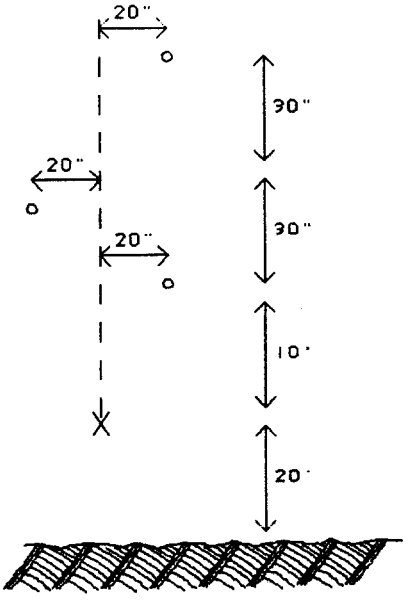

PHASE CONDUCTOR: 336 ACSR
NEUTRAL CONDUCTOR: 4/0 ACSR

(B) CONFIGURATION WITH SMALLER IMPEDANCE

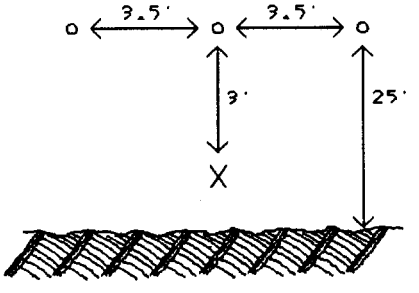

PHASE CONDUCTOR: 1/0 ALUMINUM
NEUTRAL CONDUCTOR: 1/0 ALUMINUM

(C) CONFIGURATION WITH LARGER IMPEDANCE

FIGURE 2.2-7 DISTRIBUTION FEEDER CONFIGURATION

Table 2.2-2 Effect of Distribution Feeder Characteristics

	Case Description	Net Flow From Island to System		Run-On Times (sec.)	
		Watts	Vars	Negative-to-Positive Interruption	Positive to-Negative Interruption
T-1B	Primarily resistive load; one third of load at SPC; One third of load 500' down feeder; One third of load 1000' down feeder.				
	1. Watts load matched to generation.	-23	-96	.65	.69
	2. Watts load 10% less than generation.	376	-96	.41	.67
	3. Watts load 10% more than generation.	-422	-96	.58	1.18
	1A. Same as 1 except with smaller conductor.	-23	-99	.62	.62
	2A. Same as 2 except with smaller conductor.	376	-99	.41	.67
	3A. Same as 3 except with smaller conductor.	-422	-99	.58	1.11
	1B. Same as 1 except with larger conductor.	-23	-98	.62	.64
	2B. Same as 2 except with larger conductor.	376	-98	.41	.67
	3B. Same as 3 except with larger conductor.	-422	-98	.58	1.14

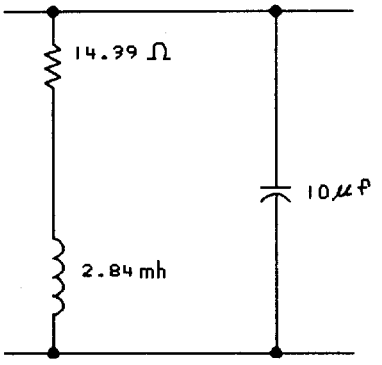

(A) LOAD FOR CASE IAIX

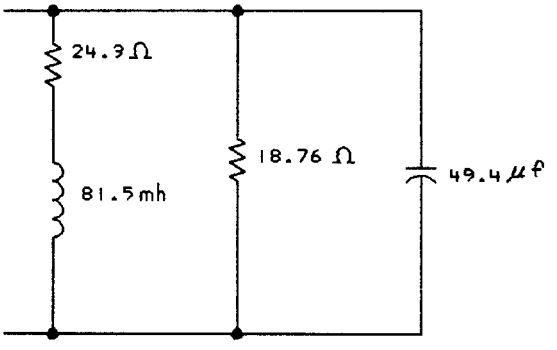

(B) LOAD FOR CASE ICI

FIGURE 2.2-8 COMPARISON OF TWO DIFFERENT TYPES OF LOAD

Several cases were run in which the net watt and var output from the island was the same but the make-up of the load was different. The run-on times for these cases were not very different. This can be seen by comparing cases IA1X and IC1, IA2X and IC2, IA3X and IC3 in Table 2.2-1. For the series of cases designated X, the load was the combination of R, L, and C shown in Figure 2.2-8a. This load was primarily resistive and had only small amounts of inductance and capacitance. The load in the C-series of cases was as shown in Figure 2.2-8b. The RL-series load was representative of the load impedance of a 1-hp motor. The R- and C-shunt elements were adjusted to give the same net watts and vars of load as were used in the X-series of cases. The C-series of cases had a much larger total of capacitance than the X-cases. However, the run-on times obtained for comparable cases were very similar.

When an induction motor is a part of the load, the run-on times for a specific watt and var mismatch can be different from the run-on time when the load is a constant impedance type with the same watt and var mismatch. When the watt and var mismatch is near zero, the two types of loads have virtually the same run-on times. For this type case the voltage does not change when the island is created. If the voltage does not change the motor acts like a constant impedance, and therefore the two cases have similar run-on times. When there is a watt mismatch within the island, the voltage changes when the island is created. This causes the power factor of the motor to change and thus the apparent impedance of the motor to change. Therefore, the two run-on times will be different.

FIGURE 2.2-9 VARIATION OF P AND Q OF 1HP MOTOR AS TERMINAL VOLTAGE IS VARIED

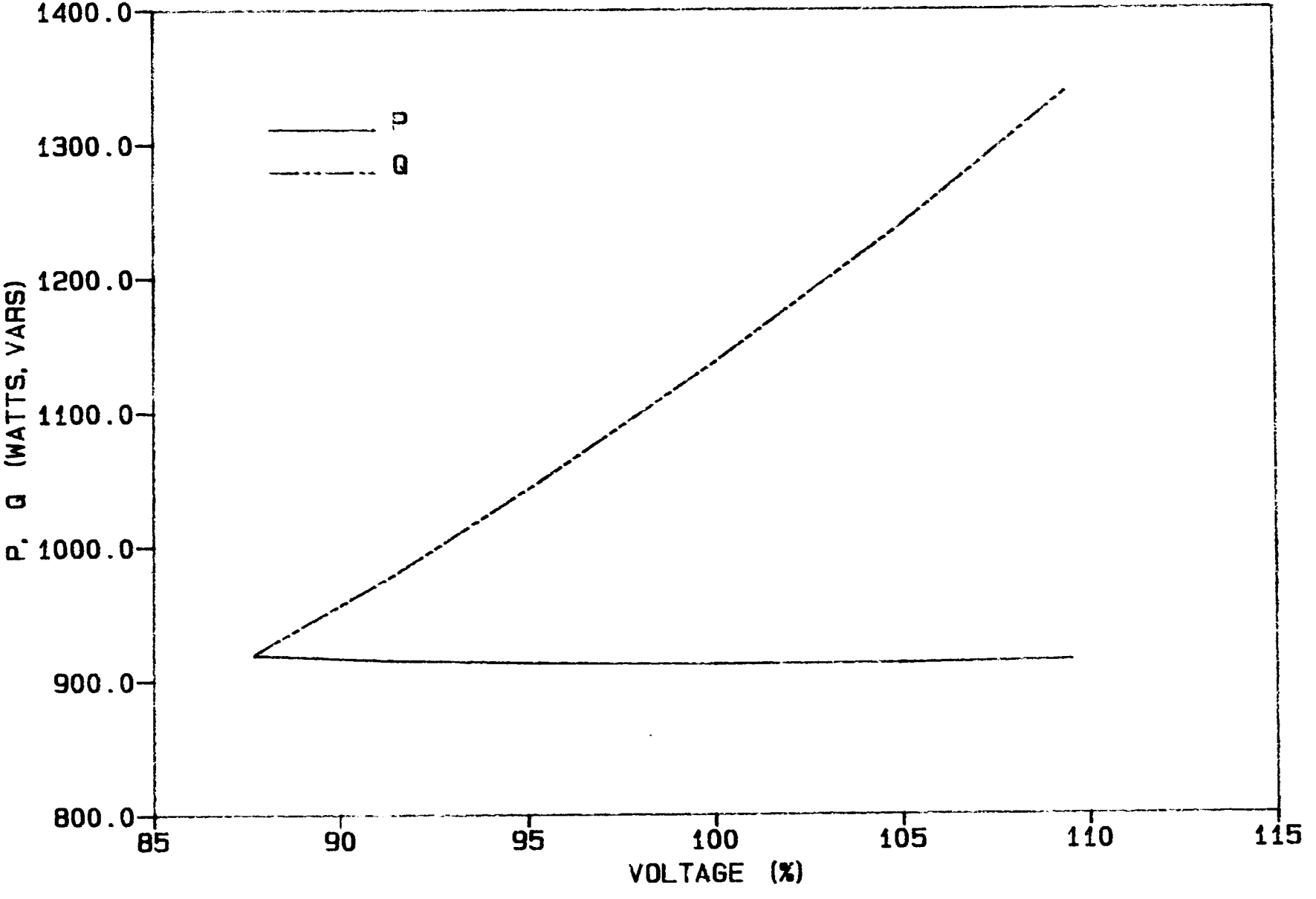

The different run-on time for the case with motor load can still be analyzed in terms of watt and var mismatch. The key to this is knowing how the watts and vars taken by an induction motor change as the voltage is changed. Figure 2.2-9 shows this relationship, which was determined using the EMTP induction motor model. The power taken by the motor remains relatively constant. The vars taken by the motor increase as the voltage increases, but do not increase as much as the square of the voltage. The vars produced by capacitance within the island increase in proportion to the square of the voltage. Thus, if the initial voltage change when the island is created is positive, the initial var mismatch becomes larger. Compare cases IC2 and ID2 and cases IC3 and ID3 in Table 2.2-1. The difference in the cases is that cases ID2 and ID3 have a 1-hp induction motor modeled, and cases IC2 and IC3 have an RL-series impedance that takes the same amount of watts and vars (912 watts and 1151 vars) as the 1-hp motor does at normal voltage. Cases IC2 and ID2 initially have 400 watts less load than generation and have var loads balanced with var generation. When the island is created the voltage rises so that the watts of the load will match the watts of generation. Since the watts taken by the motor in case ID3 change very little with voltage and the watts taken by the constant impedance representing a motor in case IC2 change with the square of the voltage, the voltage in the island rises somewhat higher in case ID2 than it does in IC2. The var load and var generation (due to capacitance) both change as the square of the voltage in case IC2 so that the var mismatch remains approximately zero. However, in case ID2 the vars required by the motor do not increase as much as the vars generated by the capacitance. Therefore, a positive var mismatch is created. Case ID2 is effectively like moving a short distance to the right away from the zero var

line in Figure 2.2-5. The difference between run-on times for positive-to-negative and negative-to-positive zero crossing interruptions tends to increase. This is what you see when comparing case ID2 to IC2; the difference in run-on times for positive-to-negative and negative-to-positive interruptions is greater.

Cases IC3 and ID3 initially have a load 400 watts more than generation and have var load balanced to generation. When the island is created, the voltage must decrease. Reasoning similar to that given above leads to the conclusion that case ID3 winds up with a negative var mismatch and is effectively like moving a short distance to the left away from the zero var line in Figure 2.2-5. This tends to decrease the difference between negative-to-positive and positive-to-negative run-on times.

Another effect of having an induction motor as part of the load was noted. Increasing the amount of inertia of the motor generally tended to increase the run-on time of the TESLACO. The simulations made to study this effect are summarized in Table 2.2-3. The only difference between the four simulations given in the table was in the amount of inertia represented for the motor. It appears that increasing the inertia of the motor allowed the motor to hold its terminal voltage (and that of the TESLACO) more constant in magnitude and phase. This reduced the phase error initially detected in the phase-locked loop of the TESLACO and resulted in a longer run-on time. The trend of increasing run-on time for increasing inertia did not always hold. Going from three times the base case inertia (case ID12X) to six times the base case inertia (case ID12Y) resulted in approximately the same run-on time. It is not known why this occurred.

Table 2.2-3 Effect of Inertia of Motor Load

	Case Description	Net Flow From Island to System Watts	Vars	Run-On Times (sec.)
T-ID	Resistive and capacitive load; 1 Hp motor modeled; local load only.			
	12. Base case with actual inertia of motor.	40.0	-.01	1.616
	12X. Three times inertia of base case.	39.3	.45	1.882
	12Y. Six times inertia of base case.	39.3	.46	1.834
	12Z. One third inertia of base case.	39.5	.47	1.449

Effect of the Number of SPCs in the Island

Several computer simulations were made with two TESLACOs within an island and one was made with four TESLACOs within an island. The results of these simulations are given in Table 2.2-4. With each of the TESLACOs producing maximum output (4000 watts), and with the load twice what it was in the single TESLACO cases, run-on times were obtained in the two TESLACO cases that were very similar to those obtained in the corresponding single TESLACO cases. For example, compare cases IB1, IB2 and IB3 in Table 2.2-2 with IIB1, IIB2 and IIB3 in Table 2.2-4. In the IIB series the two TESLACOs were located 1000 feet apart on the same feeder that was used in the IB series. The loads in the IIB series were approximately double but were adjusted slightly to make the overall watt and var mismatch twice that for the IB series. The run-on times for these cases were virtually the same.

Also shown in Table 2.2-4 is a series of cases for which the two TESLACOs were separated by 3000 feet of distribution feeder. One of the units was producing 4000 watts and the other was producing 2000 watts. All the load for this series was located at the end of the feeder with the TESLACO that was producing 2000 watts. This insured that there would be a great deal of power flowing on the feeder for this series of cases. In case IIF1 and IIF2, with load watts and vars matched to generated watts and vars, the run-on times were approximately 1.6 seconds. This was very similar to the run-on times for a single TESLACO balanced case. The run-on times for the 10% and 20% load mismatched cases were also fairly similar. For all of these cases, when one TESLACO reached a 6° phase error and shut down, the load-generation mismatch for the other became so great that it shut down only a half-cycle later.

Table 2.2-4 Effect of More Than One TESLACO Within the Island

	Case Description	Net Flow From Island to System		Run-On Times (sec.)*	
		Watts	Vars	Negative-to-Positive Interruption	Positive to-Negative Interruption
T-IIB	Two TESLACOs separated by 1000' feeder; one third of load local to each unit; One third of load located halfway between units; Each unit producing 4 KW; Primarily resistive load.				
	1. Watts load matched to generation.	-46	-192	.631	.656
	2. Watts load 10% less than generation.	753	-192	.427	.627
	3. Watts load 10% more than generation.	-844	-192	.585	1.334
T-IIF	Two TESLACOs separated by 3000 feeder; all loads local to the units.				
	1. Load watts and vars matched to generation. Unit 1 producing 4 KW; Unit 2 producing 3 KW.	-5	25	1.529	1.554
	2. Load watts and vars matched to generation. Unit 1 producing 2 KW; Unit 2 producing 4 KW.	-15	21	1.654	1.654
	3 Load watts 10% less than generation. vars slightly mismatched; Unit 1 producing 2 KW; Unit 2 producing 4 KW.	558	24	.825	1.580
	4. Load watts 10% more than generation; vars slightly mismatched. Unit 1 producing 2 KW; Unit 2 producing 4 KW.	-638	19	1.078	.750
	5. Load watts 20% less than generation; vars slightly mismatched. Unit 1 producing 2 KW; Unit 2 producing 4 KW.	1157	25	.592	1.117
	6. Load watts 20% more than generation; vars slightly mismatched. Unit 1 producing 2 KW; Unit 2 producing 4 KW.	-1242	14	1.042	.058
T-IV	Four TESLACOs - local loads.				
	1. Load watts and vars matched to generation.	0	0	1.312	-

*Note: Both SPCs shut down at the same time.

For the case with four TESLACOs within the island, the system was modeled as shown in Figure 2.2-10. The only simulation made for this situation was for load watts and vars matched to generated watts and vars. This case gave a run-on time of 1.3 seconds. It appears that adding more TESLACOs in the island does not tend to stabilize the island and keep it energized longer. A multiple TESLACO island behaves much the same as a single TESLACO island.

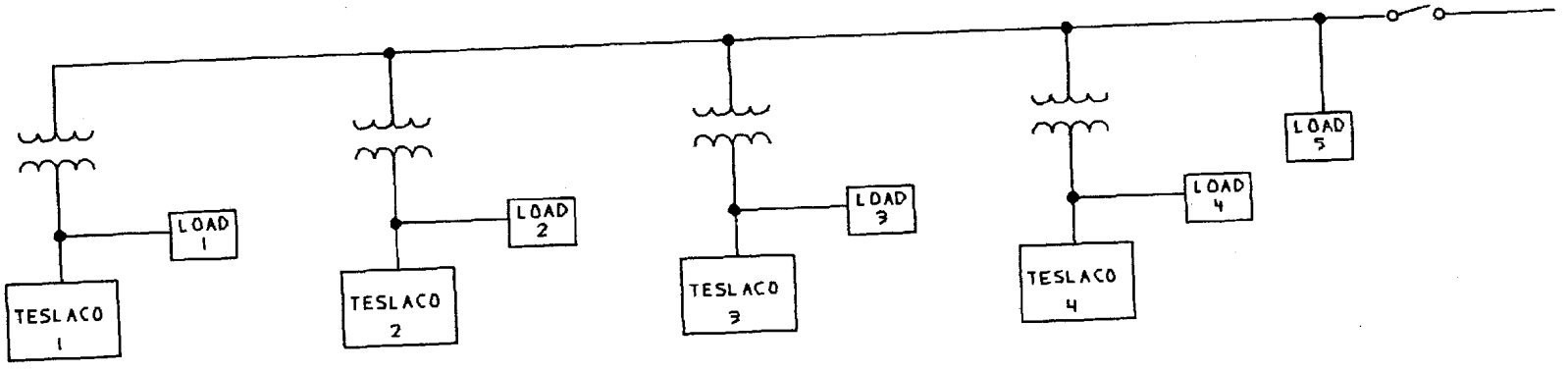

FIGURE 2.2-10 SYSTEM CONFIGURATION FOR FOUR TESLACO CASE

Effect of Load Variation and Solar Insolation Variation

Most of the computer simulations were made with constant loads and constant solar insolation. In a realistic system these two parameters can vary during the duration of an island. The most probable effect of having variable loads and solar insolation is to reduce the run-on time. It is possible, however, for the changes to increase the run-on time. These effects were studied briefly and the results are summarized in Table 2.2-5.

When an island is created, the phase error between a TESLACOs internal reference wave and its terminal voltage eventually increases to 6 degrees, and then the device shuts itself down. There can be a transient period for a few cycles after the island is created in which the phase error takes a jump and then decreases. After this period the phase error steadily increases in magnitude. If a change in load or in solar insolation causes a phase shift that is opposite to this error, then a longer run-on time can be achieved. In case IA2XI a decrease in solar insolation produced a run-on time that was .34 seconds longer than it would have been without the decrease. This case initially had approximately 400 watts more generation than load. The reduction in solar insolation from 100 mW/cm2 to 90 mW/cm2 reduced the output of the TESLACO by about 400 watts, thereby achieving more of a balance between load and generation. This had the effect of reducing the phase error and delaying the inevitable shutdown by a short time.

A step change of watts load can cause a different phase shift depending on the time during a cycle that the change occurs. Cases IA1XL2 to IA1XL2C in Table 2.2-5 illustrate this effect. The only difference among the cases is

Table 2.2-5 Effect of Load and Solar Insolation Changes

	Case Description	Net Flow From Island to System		Run-On Times (sec.)	
		Watts	Vars	Negative-to-Positive Interruption	Positive to-Negative Interruption
T-1A	Primarily resistive load; local load.				
	1X. Load watts and vars matched to generation	.08	.02	1.608	1.616
	1XL1. Same as 1X except add 200 watts load at .500 seconds after island begins.	.08	.02		1.566
	1XL2. Same as 1X except subtract 200 watts load at .499 seconds after island begins.	.08	.02		2.299
	1XL2A. Same as 1X except subtract 200 watts load at .503 seconds after island begins	.08	.02		1.599
	1XL2B Same as 1X except subtract 200 watts load at .507 seconds after island begins.	.08	.02		1.499
	1XL2C Same as 1X except subtract 200 watts load at .511 seconds after island begins.	.08	.02		1.574
	1XL2E Same as 1X except subtract 400 watts load at .499 seconds after island begins.	.08	.02		1.632
	2X Load watts 10% less than generation; vars balanced.	400	0	.941	1.076
	2XI Same as 2X except ramp down insolation from 1000 W/M2 to 900 W/M2 in .3 seconds starting .5 seconds after island begins.	400	0	1.283	.901
	2XLI Same as 2X except add 400 watts load at .3 seconds after island begins.	400	0	1.016	1.042

the time at which the 200-watt reduction in load took place. For Case IA2XL2 the run-on time was increased by .7 seconds over the case with no load change. It is theoretically possible to have a series of load changes or solar insolation changes each of which will momentarily reduce the phase error and delay the eventual shutdown of the TESLACO. In this fashion, much longer run-on times could possibly be achieved. In order for this to happen, the load or insolation changes must be of appropriate magnitude and occur only at certain times during a 60-Hz cycle. It is very unlikely that load changes on a utility system or solar insolation changes would cause an island to persist for more than a second longer than it would have in the first place.

Unfolder Errors

Several of the computer simulations resulted in what has been termed unfolder errors. This is a condition in which the unfolder circuitry does not function properly and the output of the TESLACO is a rectified sine wave. This phenomenon had been seen before in a previous simulation of a TESLACO SPC [6]. For the unfolder circuitry to work properly, zero crossings of the terminal voltage of the TESLACO must be detected. When the SPC is connected to a utility there will always be zero crossings and the unfolder circuitry will work properly. However, when the TESLACO is in an islanding condition the terminal voltage does not always cross zero.

As explained in Appendix B, the internal reference wave of the TESLACO is a fully rectified sine wave. When in an islanding mode, the load within the island determines the phase angle of the terminal voltage with respect to the reference wave. If the terminal voltage leads the reference wave, it will cross zero prior to the reference wave's reaching zero and beginning to increase again. Thus, a zero crossing in the terminal voltage will always occur. However, if the terminal voltage lags behind the reference wave, the reference wave will decrease to zero and begin to increase prior to the terminal voltage's crossing zero. When the reference wave reaches zero and begins to increase, it produces a transient, which propagates through the TESLACO. This transient will sometimes force the terminal voltage away from zero, thereby preventing a zero crossing and the resultant action of the unfolder.

Two adjustments were found that could be made to the load in order to eliminate the unfolder errors. One adjustment is to make the load more inductive. This tends to advance the phase of the terminal voltage with respect to the reference wave and therefore to allow zero crossings to occur. A second adjustment is to increase the capacitance in the load. More capacitance in the load tends to slow the response of the circuit to the transient that is produced when the reference wave stops decreasing and begins to increase. This has the effect of allowing the terminal voltage to cross zero. For the simulations that resulted in unfolder errors, capacitance and inductance were added to the load so that the net vars of the load were unchanged. This always allowed the simulation to run without unfolder errors.

Summary of Computer Simulations

The following observations were made from the results of the computer simulations of the TESLACO self-commutated SPC.

1. The run-on time for the TESLACO will be different depending on whether the island was created by interrupting current on a negative-to-positive zero crossing or on a positive-to-negative zero crossing.

2. The composition of the load within an island is not very important in influencing run-on times. The net amount of watts and vars of load is of primary importance.

3. Distribution feeder conductors and configurations have little influence on run-on times.

4. Run-on time is more sensitive to mismatches in var load and generation within an island than it is to mismatches in watts.

5. Two TESLACOs within an island at the same location will have the same run-on times as one TESLACO at that location with half the load.

6. Run-on times are not increased by having more than one TESLACO within an island. If anything they are decreased somewhat.

7. Unfolder errors can occur for some load conditions. This refers to an operation in which the unfolder circuitry of the TESLACO does not work properly and the output of the SPC is a fully rectified sine wave instead of a normal sine wave.

8. The longest run-on times for the TESLACO can occur for two conditions: 1) when the mismatch between load and generation in the island is approximately zero; and, 2) when there is a watt mismatch of several hundred watts and the var mismatch is in the range of 5 to 25 vars.

9. The TESLACO will shut down immediately (within two cycles) if the watts mismatch is in the range of 40% of the device's rating or if the var mismatch is in the range of 20% of the device's rating.

A series of lab tests was designed to verify many of the observations made above. A number of tests were planned to make sure that the TESLACO would not run on indefinitely regardless of how well the load was matched to generation. The TESLACO lab tests are summarized in Section 3.2.

BLANK PAGE

2.3 Analytical Results for a Gemini Line-Commutated Static Power Converter

The Gemini static power converter modeled in this project was a line-commutated 6-kW single-phase converter. A block diagram model of the Gemini converter was supplied by Paul Krause and Associates. In this project, a detailed model was developed for the EMTP digital computer program based on the Krause model. Details of the computer model along with verification of the EMTP model based on a comparison with results from Krause's analog computer model are given in Appendix C. The EMTP computer model was then used to predict the operation of the converter following disconnection from the utility (islanding).

A typical single Gemini islanding simulation setup is shown in Figure 2.3-1. In most cases the solar insolation was assumed to be constant resulting in a constant power output of the array. The converter has a voltage and current regulator circuit that acts to hold the array dc voltage to a constant value equal to a user-set reference voltage. The regulator circuit maintains the constant array voltage by adjusting the SCR firing times, which vary the converter output current. Details of the regulator circuit and converter operation are given in Appendix C. The final stage of the converter is a 350/240-V step-down transformer. This transformer was modeled as an ideal transformer with its through impedance.

Local loads were then modeled on the terminals of the converter. In most cases the loads were combinations of parallel R-L-C elements. In a few

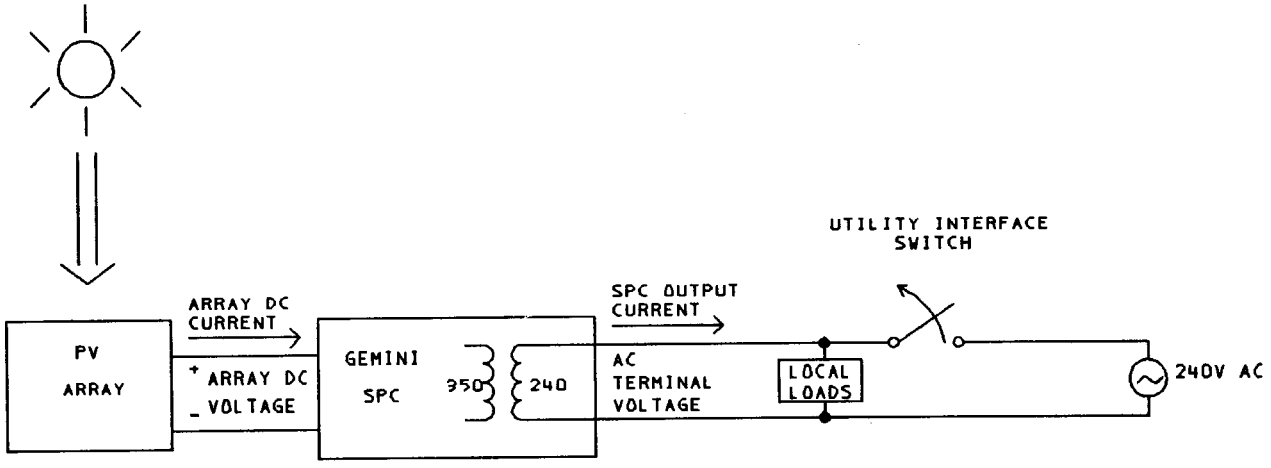

FIGURE 2.3-1 TYPICAL SINGLE **GEMINI** SIMULATION SET UP

simulations rotating loads were modeled in detail to examine their effect on the island conditions. The total load was adjusted to allow the desired power flow through the utility switch prior to islanding for the various islanding conditions. The EMTP simulations were started and allowed to run for 400 ms to reach a steady-state operating condition, and then the utility interface switch was opened.

There are two major differences between the simulation results reported for the TESLACO SPC and the simulation results for the Gemini. In our simulation of the TESLACO SPC it was found that the zero crossing at which current is interrupted to form an island (positive-to-negative or negative-to-positive) had an impact on the run-on time. Many of the Gemini SPC cases were run with the island being formed following interruption at each type of zero crossing, but this did not change the case results. Only one zero crossing is reported for the Gemini; the interruption occurs on the first zero crossing of the converter output current after 400 ms of simulation. The second difference is that the concept of "run-on time" described for the TESLACO has less significance for the Gemini. This is clarified later in this discussion. Many of the cases ran on indefinitely. In order to determine other characteristics that would be significant in classifying the Gemini islanding conditions, the island voltages and currents were monitored.

The Gemini could shut down during an islanding condition for either of two reasons. The first would be a commutation failure.
This is discussed at length with the effects of load types. The second reason would be operation of the Gemini's undervoltage monitor in its control

circuitry. The converter trips off if the ac terminal voltage is less than approximately 80% of its normal peak value of 339.4 V. Given these restrictions, there may be practical load conditions that will cause the Gemini to continue to operate after an island is formed. This type of operation is not desirable from a utility's standpoint. The frequency of the ac terminal voltage in islanding operation is dependent on the local load and PV generation. The frequency variation from 60 Hz when islanding occurs appears to be the most significant factor that could be monitored to determine if the utility supply has been lost. Therefore, the frequency of the islanding system was monitored in our simulations.

Two factors complicate the analysis of the Gemini converter. The first is that the output current contains a significant amount of harmonics. The local loads used in the computer model and the loads to be used in the laboratory experiments are parallel R-L-C elements. These loads draw mainly fundamental (60-Hz) current when connected to the utility. Prior to islanding, the Gemini's harmonic current flows through the utility switch and out to the system. It is very difficult to "zero out" this current, thus power flows out to the system. Therefore, we do not have a zero power mismatch type of case for the Gemini. In our simulations, a Fourier transform of the ac terminal voltage and output current waveforms for the cycle just before opening of the utility interface switch were calculated. The fundamental component of the voltage and current in this cycle was used to calculate the watt and var output. A "balanced load" was calculated to be equal to this fundamental volt-ampere output.

The second factor complicating the analysis was the mode of operation; either continuous current or discontinuous current. The mode of operation depends on the power available from the array and the selection of converter dc reference voltage that fixes the array voltage. A description of the two modes is given in Appendix C. Most Gemini simulations were run in both operating modes.

Effects of Load Types

The initial group of simulations had local loads that were resistive only. During the first commutation period following the opening of the utility switch, the SCR bridge was short-circuited. As described in Appendix C, normal commutation for a line-commutated converter requires that the utility source (or island load in this case) attempt to force current back through two of the four SCRs to cut them off. In the case of a resistive load, the load voltage drops to zero during commutation. All four of the SCRs remained closed and the output of the Gemini dropped to zero. For this reason, R-C loads were used for most of the remaining simulations. During commutation, the capacitance of the load has a stored voltage across it. When the SCR bridge shorted out, this voltage attempted to drive reverse current through two of the SCRs, allowing normal commutation. In all of our simulations in which the local load supplied 60% or more of the reactive power requirements and the watt load was less than 130% of the output of the Gemini prior to islanding, the unit ran on indefinitely.

For this reason, run-on time does not have the significance that it did for the TESLACO unit. In reviewing the early simulation results it was apparent

that the watt and var mismatch at the time an island formed was the important parameter which dictated the characteristics of the resulting island voltages and currents. Several cases were run to demonstrate that the net watt and var mismatches were the important parameters. This was accomplished by running cases with an R-only load and comparing them to an R plus a parallel L-C load. The L-C load was sized so that its reactive contributions canceled each other. In both cases the unit shut down in less than one cycle. Cases with parallel R-C loads were also run and compared to R-C plus another parallel L-C load section. The parallel L-C section was sized so that its reactive power contributions cancelled each other. The results of these two types of cases were the same. Therefore, the makeup of the load was not significant. Only the net watt and var mismatch was important.

The final type of local load that was modeled included rotating machinery. The EMTP universal machine model described in Section 2.1. was used to model a single-phase induction motor in detail.

In early simulations, the Gemini and local loads were connected through a typical distribution transformer and feeder to a substation. A utility breaker opening was modeled in the simulations to initiate the island. After being convinced that the losses of the distribution transformer and the capacitance of the distribution line behaved similar to an equivalent lumped load model, the cases were simplified.

The resistive and capacitive local load was varied in $\pm$ 1%, $\pm$ 3%, $\pm$ 5%, $\pm$ 10%, and $\pm$ 50% steps to study the effect of watt and var mismatches on the island voltages and currents. The effect of real and reactive power

mismatches is discussed separately in the next two sections. The effect of motor load in the island is described following the watt and var mismatch discussion.

The fundamental component of the voltage remains fairly constant before and after the island for a "matched load" case. The composite terminal voltage waveform including all harmonics does not remain the same. The net result is that the composite ac terminal waveform is reduced in magnitude when the island is formed. When an island is formed with the Gemini and a balanced local load (watts and vars), the array voltage, output fundamental component of watts and vars, and ac terminal voltage frequency remain fairly constant. The unit runs on indefinitely in both modes of current operation.

Effects of Real Power Mismatch

If only real power is flowing (a watt mismatch) at the time when the utility interface switch opens to form an island, the fundamental component of the island voltage adjusts to a value equal to the square root of the power out of the converter times the resistive load in the island. The effect of varying the output watt mismatch is shown in Table 2.3-1. The important trends are summarized below:

	GEMINI OUTPUT	TERMINAL VOLTAGE	
		60 Hz	
	pf	MAG	FREQ
Island load > generation	increase	decrease	constant
Island load = generation	constant	constant	constant
Island load < generation	decrease	increase	constant

Table 2.3-1 Simulation Results for Cases Where The Watt Mismatch is Varied

CASE	WATT AND VAR MISMATCH	PRE-ISLAND CONDITIONING AC TERM VOLTAGE	SPC WATTS	SPC VARS	FREQ	AFTER 500 MS OF ISLAND AC TERM VOLTAGE	SPC WATTS	SPC VARS	FREQ	RUN-ON
G-1 SINGLE UNIT GEMINI STATIC POWER CONVERTER										
A. LOCAL LOAD ONLY AT THE POWER CONVERTER TERMINALS										
1. CONTINUOUS CURRENT MODE										
a. RESISTIVE LOAD MATCHED TO GENERATION, NO REACTIVE LOAD	.033-j4979	240.	3901.	-4979.	60.					1 cycle
b. RESISTIVE LOAD MATCHED TO GENERATION, CAPACITIVE LOAD MATCHED TO GEMINI'S VAR REQUIREMENT	.001-j.001	240.	3901.	-4979.	60.	240.04	3886.	-4953.	59.6	Indef.
c. VARY RESISTIVE LOAD VS. GENERATION, CAPACITIVE LOAD MATCHED TO GEMINI'S VAR REQUIREMENT										
1. RESISTIVE LOAD 1% LESS THAN GENERATION	39.-j.001	240.	3901.	-4979.	60.	241.93	3947.	-5905.	60.3	Indef.
2. RESISTIVE LOAD 3% LESS THAN GENERATION	13.-j.001	240.	3901.	-4979.	60.	245.07	3998.	-5251.	60.8	Indef.
3. RESISTIVE LOAD 5% LESS THAN GENERATION	185-j.001	240.	3901.	-4979.	60.	246.08	3931.	-5258.	60.3	Indef.
4. RESISTIVE LOAD 10% LESS THAN GENERATION	389-j.002	240.	3901.	-4979.	60.	251.97	3873.	-5490.	60.7	Indef.
5. RESISTIVE LOAD 50% LESS THAN GENERATION	1951-j.003	240.	3901.	-4979.	60.	327.71	3971.	-9107.	56.5	1 cycle
6. RESISTIVE LOAD 1% MORE THAN GENERATION	-39.9-j.001	240.	3901.	-4979.	60.	238.90	3905.	-4936.	59.7	Indef.
7. RESISTIVE LOAD 3% MORE THAN GENERATION	-119-j.001	240.	3901.	-4979.	60.	237.93	3952.	-4833.	60.3	Indef.
8. RESISTIVE LOAD 5% MORE THAN GENERATION	-205+j.000	240.	3901.	-4979.	60.	234.89	3934	-4770	60.0	Indef.
9. RESISTIVE LOAD 10% MORE THAN GENERATION	-388+j.000	240.	3901.	-4979.	60.	229.30	3934.	-4538.	59.3	Indef.
10. RESISTIVE LOAD 50% MORE THAN GENERATION	-1950-j.005	240.	3901.	-4979.	60.					1/2 cycle
11. RESISTIVE LOAD 20% MORE THAN GENERATION	-781.9+j.000	240.	3901.	-4979.	60.	220.39	3993.	-4173	58.3	Indef
12. RESISTIVE LOAD 30% MORE THAN GENERATION	-1165+j.001	240.	3901.	-4979.	60.					5 cycles
13. RESISTIVE LOAD 40% MORE THAN GENERATION	-1548+j.001	240.	3901.	-4979.	60.					1 cycle

Table 2.3-1 (cont'd.) Simulation Results for Cases Where The Watt Mismatch is Varied

CASE	WATT AND VAR MISMATCH	PRE-ISLAND CONDITIONING AC TERM VOLTAGE	SPC WATTS	SPC VARS	FREQ	AFTER 500 MS OF ISLAND AC TERM VOLTAGE	SPC WATTS	SPC VARS	FREQ	RUN-ON
G-1 SINGLE UNIT GEMINI STATIC POWER CONVERTER										
A. LOCAL LOAD ONLY AT THE POWER CONVERTER TERMINALS										
2. DISCONTINUOUS CURRENT MODE										
a. RESISTIVE LOAD MATCHED TO GENERATION, NO REACTIVE LOAD	.025-j2988.	240.	1975.	-2988.	60.					1 cycle
b. RESISTIVE LOAD MATCHED TO GENERATION, CAPACITIVE LOAD MATCHED TO GEMINI'S VAR REQUIREMENT	.000-j.001	240.	1971.	-2967.	60.	239.70	1927.	-3026.	61.0	Indef.
c. VARY RESISTIVE LOAD VS. GENERATION, CAPACITIVE LOAD MATCHED TO GEMINI'S VAR REQUIREMENT										
1. RESISTIVE LOAD 1% LESS THAN GENERATION	19.41+j.001	240.	1975.	-2988.	60.	242.25	1984.	-3044.	60.7	Indef.
2. RESISTIVE LOAD 3% LESS THAN GENERATION	57.10+j.001	240.	1975.	-2988.	60.	245.87	2008.	-3137	60.4	Indef.
3. RESISTIVE LOAD 5% LESS THAN GENERATION	93.36+j.000	240.	1975.	-2988.	60.	246.59	2000.	-3161.	60.7	Indef.
4. RESISTIVE LOAD 10% LESS THAN GENERATION	178.17+j.000	240.	1975.	-2988.	60.	250.47	1975.	-3287.	60.3	Indef.
5. RESISTIVE LOAD 50% LESS THAN GENERATION	987.5-j.027	240.	1975.	-2988.	60.	311.58	2110.	-5489.	53.7	Indef.
6. RESISTIVE LOAD 1% MORE THAN GENERATION	-19.80+j.001	240.	1975.	-2988.	60.	240.10	1985.	-2991.	60.7	Indef.
7. RESISTIVE LOAD 3% MORE THAN GENERATION	-60.34+j.001	240.	1975.	-2988.	60.	237.87	1988.	-2936.	60.7	Indef.
8. RESISTIVE LOAD 5% MORE THAN GENERATION	-103.11+j.001	240.	1975.	-2988.	60.	235.71	1997.	-2883.	60.7	Indef.
9. RESISTIVE LOAD 10% MORE THAN GENERATION	-196.00+j.000	240.	1975.	-2988.	60.	232.50	2080.	-2835.	61.0	Indef.
10. RESISTIVE LOAD 50% MORE THAN GENERATION	-987.9-j.006	240.	1975.	-2988.	60.					1 cycle

These trends are illustrated in Figures 2.3-2 and 2.3-3 where the local load is 50% greater than and 50% less than generation. The 50% greater case would actually shut down in one cycle. The shut-down logic was disabled so the effect of local mismatch would be pronounced on the plot.

Effect of Reactive Power Mismatch

If only reactive power is flowing (a var mismatch) at the time when the utility interface switch opens to form an island, the steady-state magnitude of the fundamental component of ac terminal voltage of the island remains fairly constant. A transient voltage condition occurs, which may cause the Gemini's undervoltage relay to operate. This occurred for var mismatches of 40% or more. The power factor of the Gemini is a function of the ac terminal voltage; therefore, it remains fairly constant in the island. Since the Gemini's var requirement does not change, the frequency of the island ac terminal voltage will be forced to change. The effect of varying the var producing load is reported in Table 2.3-2. A summary of the important trends is given below:

	GEMINI OUTPUT	TERMINAL VOLTAGE	
	pf	60 Hz MAG	FREQ
Island producing vars prior to separation	constant	constant	decrease
Island vars balanced prior to separation	constant	constant	constant
Island receiving vars prior to separation	constant	constant	increase

FIGURE 2.3-2 CASE G_I.A.1.c.10

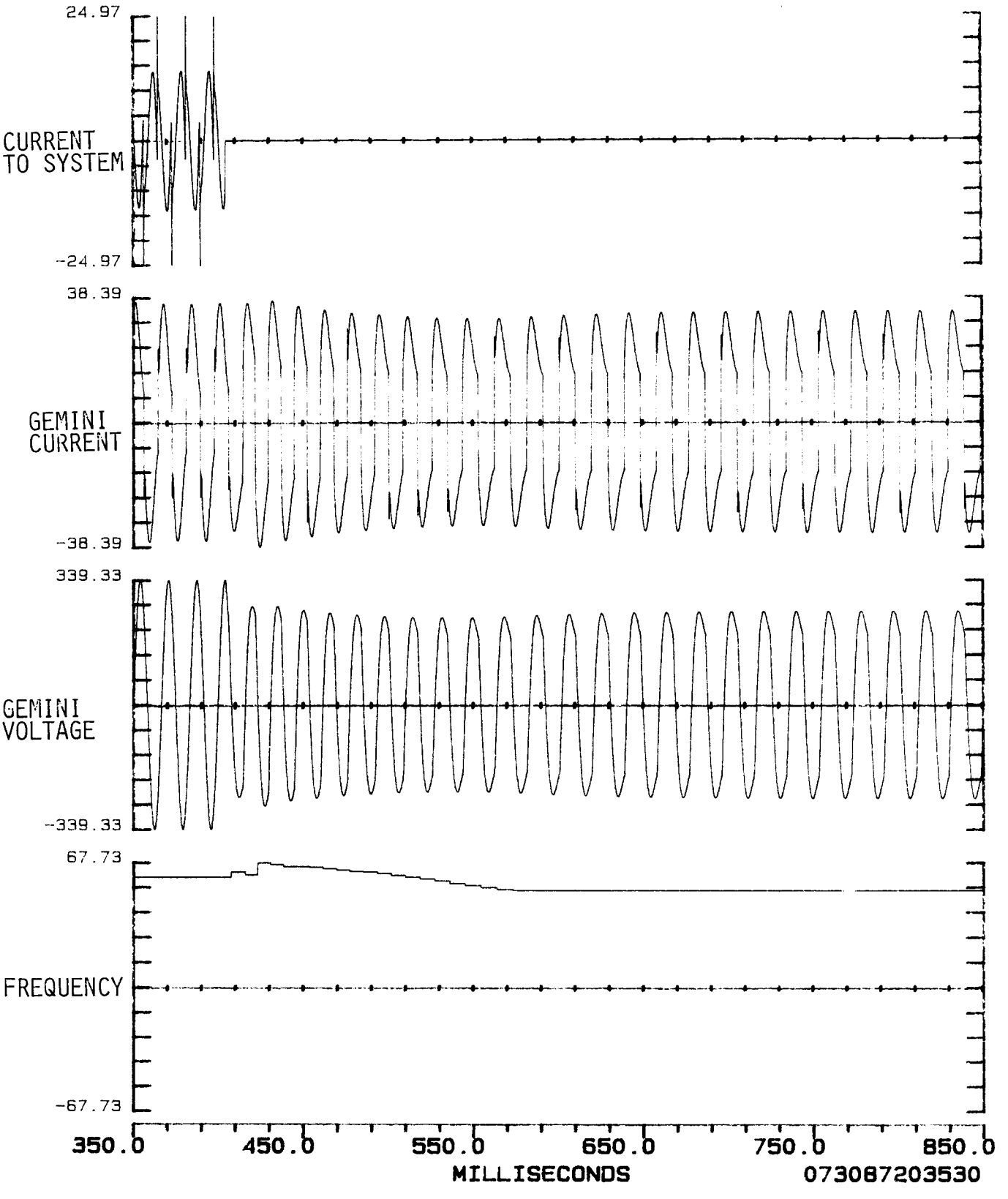

FIGURE 2.3-3 CASE G_I.A.1.c.5

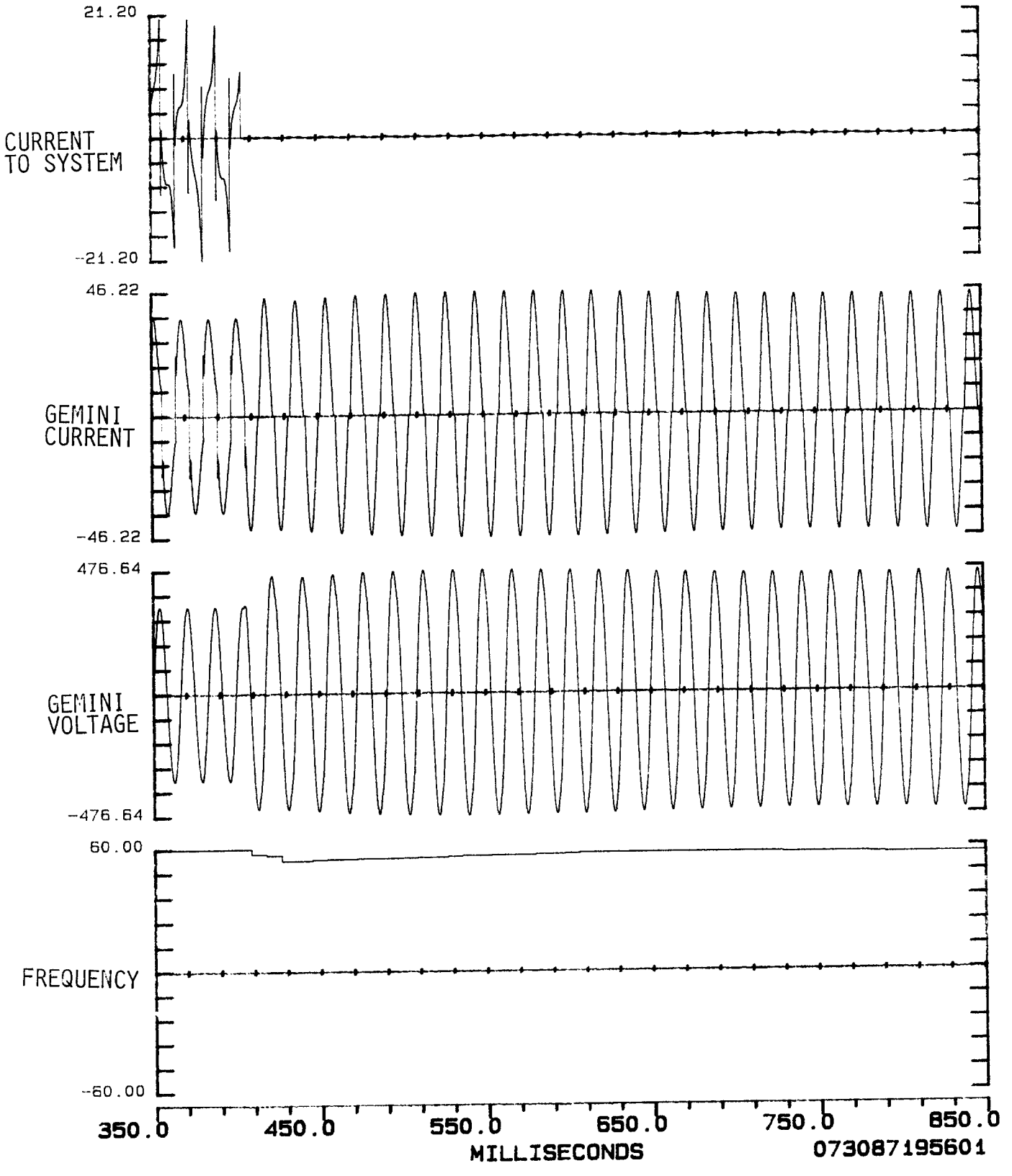

Table 2.3-2 Simulation Results for Cases Where The Var Mismatch is Varied

CASE	WATT AND VAR MISMATCH	PRE-ISLAND CONDITIONING AC TERM VOLTAGE	SPC WATTS	SPC VARS	FREQ	AFTER 500 MS OF ISLAND AC TERM VOLTAGE	SPC WATTS	SPC VARS	FREQ	RUN-ON
G-1 SINGLE UNIT GEMINI STATIC POWER CONVERTER										
A. LOCAL LOAD ONLY AT THE POWER CONVERTER TERMINALS										
1. CONTINUOUS CURRENT MODE										
d. RESISTIVE MATCHED TO GENERATION, VARY CAPACITIVE LOAD VS. GEMINI'S VAR REQUIREMENT										
1.	CAPACITIVE LOAD 1% LESS THAN VAR REQUIREMENT .000-j49.9	240.	3901.	-4979.	60.	240.3	3908.	-4979.	60.3	Indef.
2.	CAPACITIVE LOAD 3% LESS THAN VAR REQUIREMENT .001-j149.8	240.	3901.	-4979.	60.	241.0	3932.	-4869	61.4	Indef.
3.	CAPACITIVE LOAD 5% LESS THAN VAR REQUIREMENT .004-j249.5	240.	3901.	-4979.	60.	244.7	4163.	-4952.	63.1	Indef.
4.	CAPACITIVE LOAD 10% LESS THAN VAR REQUIREMENT .006-j497.07	240.	3901.	-4979.	60.	227.8	3404.	-4837.	65.0	Indef.
5.	CAPACITIVE LOAD 50% LESS THAN VAR REQUIREMENT .016-j2486.	240.	3901.	-4979.	60.					1 cycle
6.	CAPACITIVE LOAD 1% MORE THAN VAR REQUIREMENT -.004+j49.9	240.	3901.	-4979.	60.	239.7	3917.	-4997.	59.3	Indef.
7.	CAPACITIVE LOAD 3% MORE THAN VAR REQUIREMENT -.011+j149.9	240.	3901.	-4979.	60.	241.5	4025.	-5022.	58.7	Indef.
8.	CAPACITIVE LOAD 5% MORE THAN VAR REQUIREMENT -.001+j 247.3	240.	3901.	-4979.	60.	244.41	3990	-5002.	57.7	Indef.
9.	CAPACITIVE LOAD 10% MORE THAN VAR REQUIREMENT -.003+j 497.3	240.	3901.	-4979.	60.	244.89	3811.	-4993.	55.7	Indef.
10.	CAPACITIVE LOAD 50% MORE THAN VAR REQUIREMENT -.020+j 2486.	240.	3901.	-4979.	60.				43.7	Indef.
11.	CAPACITIVE LOAD 20% LESS THAN VAR REQUIREMENT -.088-j 994.	240.	3901.	-4979.	60.	204.0	2593.	-4302.	72	Indef.
12.	CAPACITIVE LOAD 30% LESS THAN VAR REQUIREMENT -014-j 1491	240.	3901.	-4979.	60.	221.0	3376.	-2959.	80.6	Indef.
13.	CAPACITIVE LOAD 40% LESS THAN VAR REQUIREMENT -006-j 1988	240.	3901.	-4979.	60.					1 Cycle

Table 2.3-2 (cont'd.) Simulation Results for Cases Where The Watt Mismatch is Varied

CASE	WATT AND VAR MISMATCH	PRE-ISLAND CONDITIONING AC TERM VOLTAGE	SPC WATTS	SPC VARS	FREQ	AFTER 500 MS OF ISLAND AC TERM VOLTAGE	SPC WATTS	SPC VARS	FREQ	RUN-ON
G-I SINGLE UNIT GEMINI STATIC POWER CONVERTER										
A. LOCAL LOAD ONLY AT THE POWER CONVERTER TERMINALS										
2. DISCONTINUOUS CURRENT MODE										
d. RESISTIVE MATCHED TO GENERATION, VARY CAPACITIVE LOAD VS. GEMINI'S VAR REQUIREMENT										
1. CAPACITIVE LOAD 1% LESS THAN VAR REQUIREMENT	.000-j30.39	240.	1975.	-2988.	60.	236.85	1911.	-3031.	61.4	Indef.
2. CAPACITIVE LOAD 3% LESS THAN VAR REQUIREMENT	.000-j91.20	240.	1975.	-2988.	60.	237.55	1875.	-2933.	62.1	Indef.
3. CAPACITIVE LOAD 5% LESS THAN VAR REQUIREMENT	.001-j152.00	240.	1975.	-2988.	60.	237.07	1843.	-2850	63.5	Indef.
4. CAPACITIVE LOAD 10% LESS THAN VAR REQUIREMENT	-.003-j304.02	240.	1975.	-2988.	60.	234.14	2136.	-2825.	67.1	Indef.
5. CAPACITIVE LOAD 50% LESS THAN VAR REQUIREMENT	.010-j1520.	240.	1975.	-2988.	60.					1 Cycle
6. CAPACITIVE LOAD 1% MORE THAN VAR REQUIREMENT	-.001+j30.40	240.	1975.	-2988.	60.	239.95	1980.	-3056.	60.3	Indef.
7. CAPACITIVE LOAD 3% MORE THAN VAR REQUIREMENT	-.002+j91.21	240.	1975.	-2988.	60.	240.85	1969.	-3078.	59.6	Indef.
8. CAPACITIVE LOAD 5% MORE THAN VAR REQUIREMENT	-.003+j152.01	240.	1975.	-2988.	60.	240.29	1956.	-3137.	59.0	Indef.
9. CAPACITIVE LOAD 10% MORE THAN VAR REQUIREMENT	-.003+j304.01	240.	1975.	-2988.	60.	236.50	1923.	-3192.	57.4	Indef.
10. CAPACITIVE LOAD 50% MORE THAN VAR REQUIREMENT	-.013+j1520.	240.	1975.	-2988.	60.	215.50	998.	-2339.	47.7	Indef.

Effects of Motor Load in Island

A detailed machine model was developed and used in combination with R-L-C loads to provide the boundary conditions described in Table 2.3-3. The motor cases demonstrated the same general relationships observed in the passive load cases. In all islanding cases the frequency undergoes a transient when the island is formed. It oscillates around its new steady-state value for a half-second or more before reaching a constant value. When a motor is in the load, the oscillations seem to be larger in value and take a longer period of time to damp out.

Table 2.3-3 Simulation Results for Cases Where The Local Load Includes a Motor

CASE	WATT AND VAR MISMATCH	PRE-ISLAND CONDITIONING AC TERM VOLTAGE	SPC WATTS	SPC VARS	FREQ	AFTER 500 MS OF ISLAND AC TERM VOLTAGE	SPC WATTS	SPC VARS	FREQ	RUN-ON
G-I SINGLE UNIT GEMINI STATIC POWER CONVERTER										
D. LOCAL LOAD ONLY AT THE POWER CONVERTER TERMINALS INCLUDING MOTOR LOAD										
1. CONTINUOUS CURRENT MODE										
a. RESISTIVE LOAD MATCHED TO GENERATION, NO REACTIVE LOAD	.024-j6115.48	240.	3901.	-4979.	60.					1/2 cycle
b. RESISTIVE LOAD MATCHED TO GENERATION, CAPACITIVE LOAD MATCHED TO GEMINI'S VAR REQUIREMENT	.000-j.003	240.	3901.	-4979.	60.	233.47	4059.	-4885	61.	Indef.
c. VARY RESISTIVE LOAD VS. GENERATION, CAPACITIVE LOAD MATCHED TO GEMINI'S VAR REQUIREMENT										
4. RESISTIVE LOAD 10% LESS THAN GENERATION	388.69+j.001	240.	3901.	-4979.	60.	245.14	3943.	-5146.	60.4	Indef.
9. RESISTIVE LOAD 10% MORE THAN GENERATION	-389.88-j.010	240.	3901.	-4979.	60.	236.98	4214.	-4544.	58.9	Indef.
d. RESISTIVE MATCHED TO GENERATION, VARY CAPACITIVE LOAD VS. GEMINI'S VAR REQUIREMENT										
4. CAPACITIVE LOAD 10% LESS THAN GEMINI'S VAR REQUIREMENT	-.001-j553.98	240.	3901.	-4979.	60.	248.11	4901.	-5415.	72.5	Indef.
9. CAPACITIVE LOAD 10% MORE THAN GEMINI'S VAR REQUIREMENT	.004+j608.00	240.	3901.	-4979.	60.	235.61	3648.	-5196.	55.7	Indef.

Table 2.3-3 (cont'd.) Simulation Results for Cases Where The Local Load Includes a Motor

CASE	WATT AND VAR MISMATCH	PRE-ISLAND CONDITIONING: AC TERM VOLTAGE	SPC WATTS	SPC VARS	FREQ	AFTER 500 MS OF ISLAND: AC TERM VOLTAGE	SPC WATTS	SPC VARS	FREQ	RUN-ON
G-1 SINGLE UNIT GEMINI STATIC POWER CONVERTER										
D. LOCAL LOAD ONLY AT THE POWER CONVERTER TERMINALS INCLUDING MOTOR LOAD										
2. DISCONTINUOUS CURRENT MODE										
a. RESISTIVE LOAD MATCHED TO GENERATION, NO REACTIVE LOAD	.023-j4124	240.	1975.	-2988.	60.					1/2 cycle
b. RESISTIVE LOAD MATCHED TO GENERATION, CAPACITIVE LOAD MATCHED TO GEMINI'S VAR REQUIREMENT	.006+j.001	240.	1975.	-2988.	60.	239.79	2010.	-3001.	60.6	Indef.
c. VARY RESISTIVE LOAD VS. GENERATION, CAPACITIVE LOAD MATCHED TO GEMINI'S VAR REQUIREMENT										
4. RESISTIVE LOAD 10% LESS THAN GENERATION	197.03+j.003	240.	1975.	-2988.	60.	255.65	1994.	-3405.	59.6	Indef.
9. RESISTIVE LOAD 10% MORE THAN GENERATION	-196.89-j.002	240.	1975.	-2988.	60.	219.25	1955.	-2477.	60.3	Indef.
d. RESISTIVE MATCHED TO GENERATION, VARY CAPACITIVE LOAD VS. GEMINI'S VAR REQUIREMENT										
4. CAPACITIVE LOAD 10% LESS THAN GEMINI'S VAR REQUIREMENT	.008-j297.55	240.	1975.	-2988.	60.	201.16	1256.	-1517.	57.7	Indef.
9. CAPACITIVE LOAD 10% MORE THAN GEMINI'S VAR REQUIREMENT	.004+j297.52	240.	1975.	-2988.	60.	240.29	1947.	-3192.	58.3	Indef.

Insolation Variation During Islanding

For the Gemini converter the watt output is directly related to the insolation. If the insolation is reduced a sufficient amount that the ac terminal voltage drops below 80% of its nominal value the unit will shut down in one cycle. A simulation of this case is given in Figure 2.3-4. The Gemini was allowed to island for 200 ms. The insolation was then decreased until the unit shut down.

Load Variation After Islanding

The Gemini converter has control circuitry to sense the reduction of the peak ac terminal voltage to below 80% of its nominal value. The simulation of load variation was made by adding a watt load in 10% steps from 100% to 150% of matched load every 200 ms after a sustained island was formed. The reactive load was assumed constant. The result of this simulation is given in Figure 2.3-5. The unit was shut down by the low voltage control after the third step was switched in. Another simulation was run in which 20% steps of inductive load were switched in after a sustained island had formed. These were designed to cancel the local capacitance's var production. The frequency of the terminal voltage increased, and the capacitive load provided the vars required by the inductive load following each step of inductive load. The unit continued to island, as illustrated in Figure 2.3-6, even after the inductive load had a 60-Hz var requirement equal to the capacitors' 60-Hz var production capability. This is interesting because cases of this type shut down immediately when inductance and capacitance of these values were in the load at the time the island was formed. It appears that a transient condition at the time of interruption caused a commutation failure that shut down the previous cases.

FIGURE 2.3-4 VARY INSOLATION

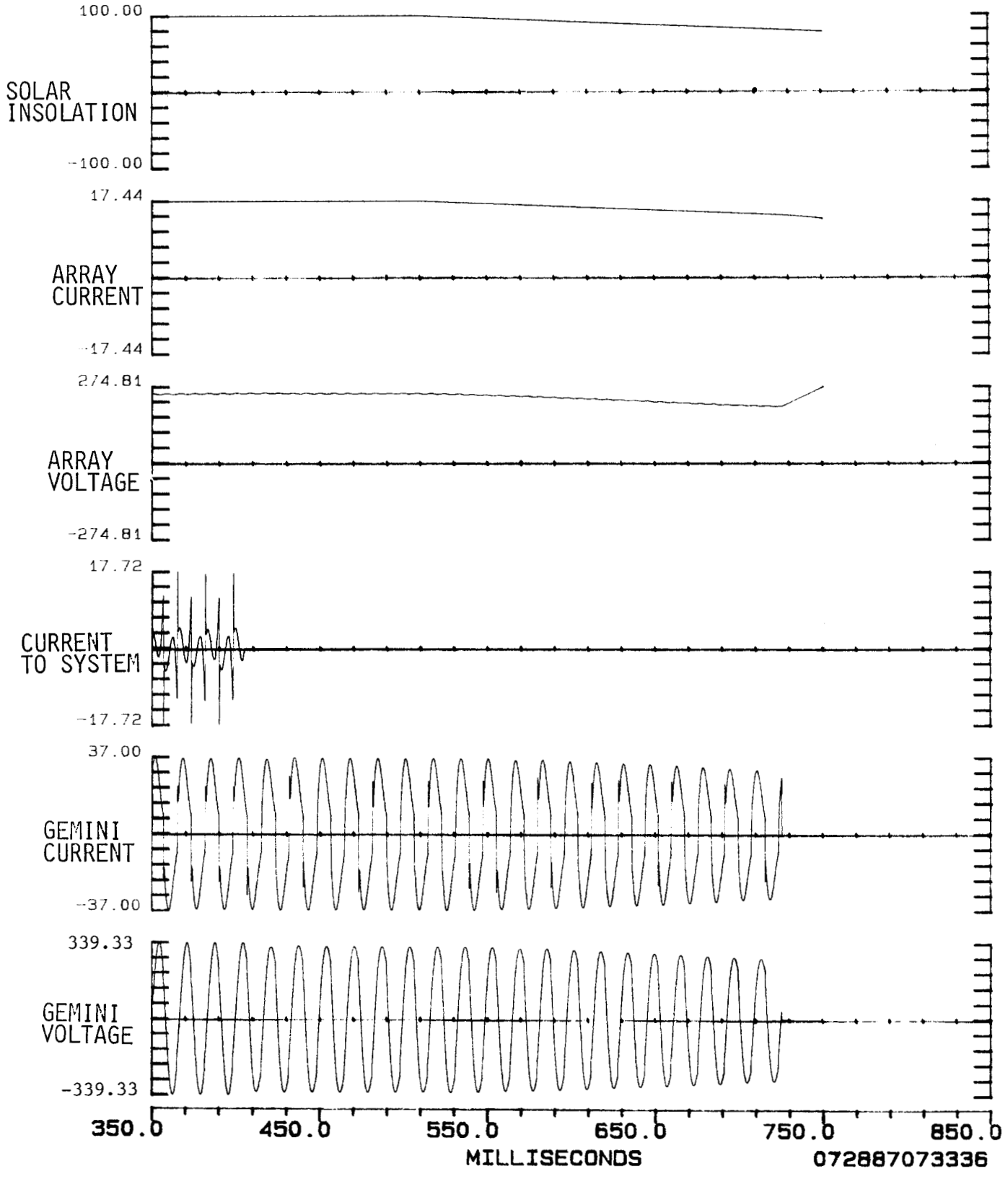

FIGURE 2.3-5 VARY WATT LOADING

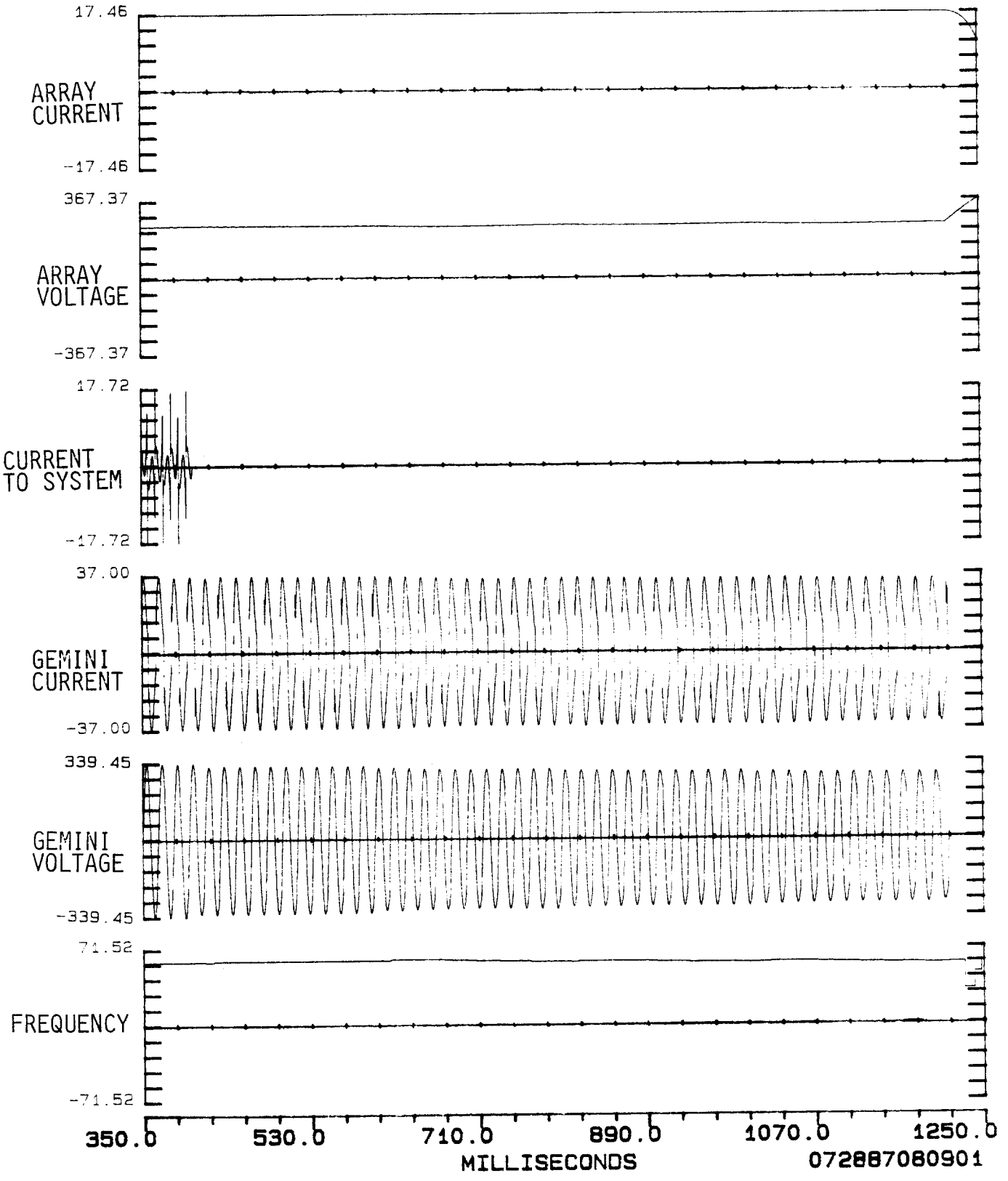

FIGURE 2.3-6 VARY VAR LOADING

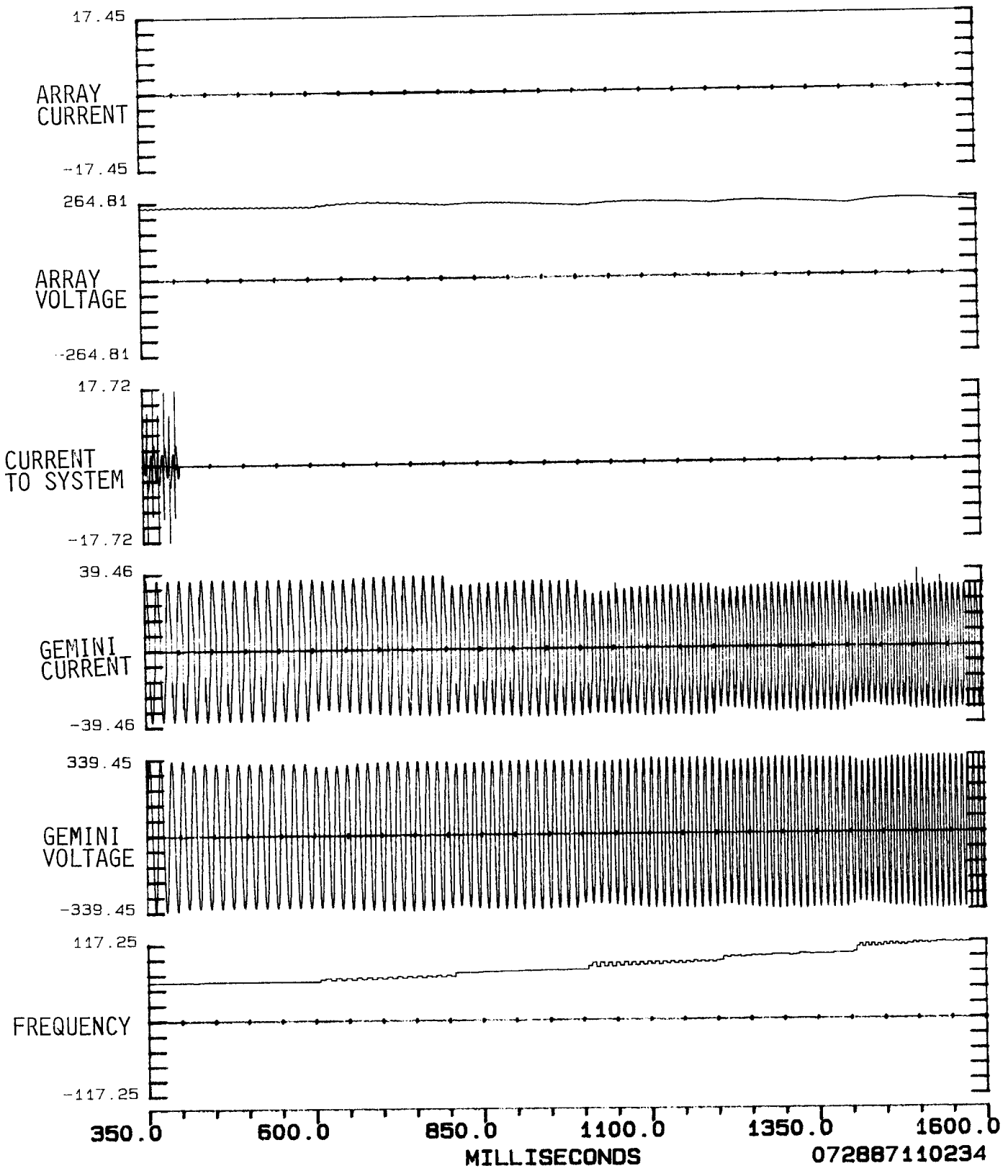

Conclusions from the Simulations and Proposed Laboratory Testing.

The following observations were made from the results of the Gemini computer simulations.

1. The Gemini can form a sustained island if the following load/generation conditions exist and if the unit does not have over/under frequency and overvoltage protective circuits.

   a. The island load must be able to supply 60% or more of the pre-island Gemini var requirement.

   b. The island watt load must not exceed 130% of the watt generation of the Gemini.

2. If the Gemini has over/under frequency (± 1 Hz) and over/under voltage protection (± 10%) either in the device itself or in the interface between the device and the utility, then the conditions for sustained islanding become much more restrictive.

   a. The island load must supply an amount of vars which is within 3% of the pre-island var requirement of the Gemini.

   b. The island watt load must be within 25% of the watt generation of the Gemini.

3. The watt and var mismatch at the island boundary is the most important factor in determining the characteristics of the island. Watt mismatches affect the magnitude of the ac voltage. Var mismatches affect the frequency of the ac voltage.

4. The makeup of the load is not important, only the resulting mismatch as just described. This indicates that feeder characteristics and distributed load do not have a significant role in determining islanding results.

5. Motor load in the island behaves basically the same as passive loads, but the time required to reach steady-state island conditions (voltage magnitude and frequency) is longer.

6. A sufficient reduction in insolation during islanding will cause the Gemini to shut down due to low voltage.

7. The variation of load during islanding has different effects based on the type of load.

    a. Increasing watt loading above 130% of Gemini's watt output will result in a shutdown due to undervoltage.

    b. Decreasing capacitance gradually to zero will result in a commutation failure shutdown when the var production is less than 10% of the pre-island var requirement.

c. Increasing inductance gradually will result in a continued sustained island with a higher frequency. Increasing inductance in large steps (50% of vars being produced in the island at the time) can result in shutdown due to a transient undervoltage condition.

The simulation results indicate that the Gemini inverter without overvoltage and over/under frequency protection will allow a sustained island to be formed for a fairly wide range of cases. The proposed lab experiments include a balanced case, $\pm$10% and $\pm$50% variations in watt and var load cases. These cases should be run in both modes of current operation. This range of tests should demonstrate the indefinite run-on cases and immediate shutdown associated with commutation failure and undervoltage detection.

2.4 Analytical Results for Combinations of TESLACO and Gemini Static Power Converters.

Computer simulations were run that modelled islanding in which combinations of TESLACO and Gemini SPC designs were in the island. The results of these simulations are given in Table 2.4-1. The focus of these studies was to determine if the two types of SPCs could somehow support each other during islanding and create longer duration islands. In single-converter TESLACO simulations the longest run on time was 2.3 sec. In single converter Gemini simulations, there were cases that ran on indefinitely.

The results of the multiple unit simulation were much as expected. In one of the cases (G.T.I.A.1), in which the watt load and watt generation in the island were balanced and no var support was provided, the Gemini unit shut down immediately. The TESLACO unit experienced a watt mismatch equal to the watts previously supplied by the Gemini and shut down in .007 sec.

In all of the remaining cases var support for the Gemini was provided in the local load. In these cases the TESLACO unit determined the initiation of shutdown for the island. Once the TESLACO sensed a phase error of a sufficient amount, it shut down. The Gemini was left with the entire load of the island. In all of our simulations, the island load was large enough that the island voltage dropped following the trip off of the TESLACO unit to a level at which the Gemini undervoltage circuit picked up. The Gemini tripped off in one cycle after the TESLACO in these cases.

Several cases were run, which are not reported in the table, to investigate the separation of PV generation and the distribution of load along a typical feeder. In the cases in which separation was studied, particular emphasis was placed on mismatching the load and generation at each PV site while maintaining a balance at the utility interface. The objective was to force a power transfer on the distribution feeder during the island. The results of these cases were not significantly different from those reported in Table 2.4-1 and did not result in longer run-on times.

The results of the combination tests indicated a maximum run-on time of 1.421 seconds for the TESLACO, which is less than the single-unit TESLACO simulations. In all cases, the Gemini shut down in the combination simulations due to undervoltage. Based on the single-unit simulations, the Gemini could run on indefinitely following the TESLACO shutdown if the island load were less than 130% of the Gemini's capability. This was demonstrated in the TVA field tests, which are reported in Section 4.4.

Table 2.4-1 Multiple SPC Islanding Simulations with Combinations of TESLACO and Gemini Converters

CASE	MISMATCH AT BOUNDARY WATT	MISMATCH AT BOUNDARY VAR	TESLACO OUTPUT WATT	TESLACO OUTPUT VAR	TESLACO RUN ON (SEC)	Gemini OUTPUT WATT	Gemini OUTPUT VAR	Gemini RUN ON (SEC)
G.T.I MULTIPLE SPC ISLANDING (1 Gemini, 1 TESLACO)								
A. PASSIVE TYPE LOADS CONNECTED TO SPC TERMINALS								
1. RESISTIVE LOAD MATCHED TO GENERATION	-25.05	-3526.	3444.	52.3	.007	2682.	-3688.	.000
2. RESISTIVE LOAD MATCHED TO GENERATION, REACTIVE LOAD MATCHED TO VAR REQUIREMENT	.002	.000	3444.	52.3	1.028	2682.	-3688.	1.039
3. RESISTIVE LOAD 10% LESS THAN GENERATION, REACTIVE LOAD MATCHED TO VAR REQUIREMENT	727.2	.003	3444.	54.1	.803	2811.	-3780.	.814
4. RESISTIVE LOAD 10% MORE THAN GENERATION, REACTIVE LOAD MATCHED TO VAR REQUIREMENT	-596.8	-.011	3444.	51.4	.819	2681.	-3694.	.830
5. RESISTIVE LOAD MATCHED TO GENERATION, REACTIVE 10% LESS THAN VAR REQUIREMENT	-.003	-368.3	3444.	49.2	.198	2676.	-3675.	.209
6. RESISTIVE LOAD MATCHED TO GENERATION, REACTIVE 10% MORE THAN VAR REQUIREMENT	.003	+j368.0	3444.	52.1	.176	2669.	-3723.	.186
G2.T.I MULTIPLE SPC ISLANDING (2 Geminis, 1 TESLACO)								
A. PASSIVE TYPE LOADS CONNECTED TO SPC TERMINALS								
2. RESISTIVE LOAD MATCHED TO GENERATION, REACTIVE LOAD MATCHED TO VAR REQUIREMENT	.002	-.002	3443.	65.8	1.385	2573	-3724.	1.398
						2964.	-4647.	1.398
GT2.I MULTIPLE SPC ISLANDING (1 Gemini, 2 TESLACOS)								
A. PASSIVE TYPE LOADS CONNECTED TO SPC TERMINALS								
2. RESISTIVE LOAD MATCHED TO GENERATION, REACTIVE LOAD MATCHED TO VAR REQUIREMENT	.00	+.058	3514	65.9	1.412	2695.	-3553.	1.422
			3191	35.9	1.412			

BLANK PAGE

III. LABORATORY EXPERIMENTS

The objectives of the laboratory experiments were to validate the SPC models and confirm the threshold values of the islanding windows as predicted by the detailed computer simulations. Furthermore, controlled conditions were attained in the laboratory to perform sensitivity analyses on the system parameters that may affect the static power converter islanding performance.

The laboratory experiments were performed at the Georgia Power Company's relay testing laboratory in Atlanta, Georgia, where the following experimental setup was designed and constructed.

3.1 Description of the Laboratory Setup

3.1.1 Construction of the Laboratory Setup

The intent of the laboratory setup was to provide a test environment that represented the "real world" as closely as possible. Figure 3.1-1 shows the detailed interconnections of the test fixture. The laboratory setup was designed so that two SPCs operating in parallel could be tested at the same time.

In the experiments, two different types of SPCs were employed: a TESLACO, 4-kW unit and a Gemini, 6-kW unit. There were two identical units of each type, and all of them were provided for testing by Sandia National Laboratories.

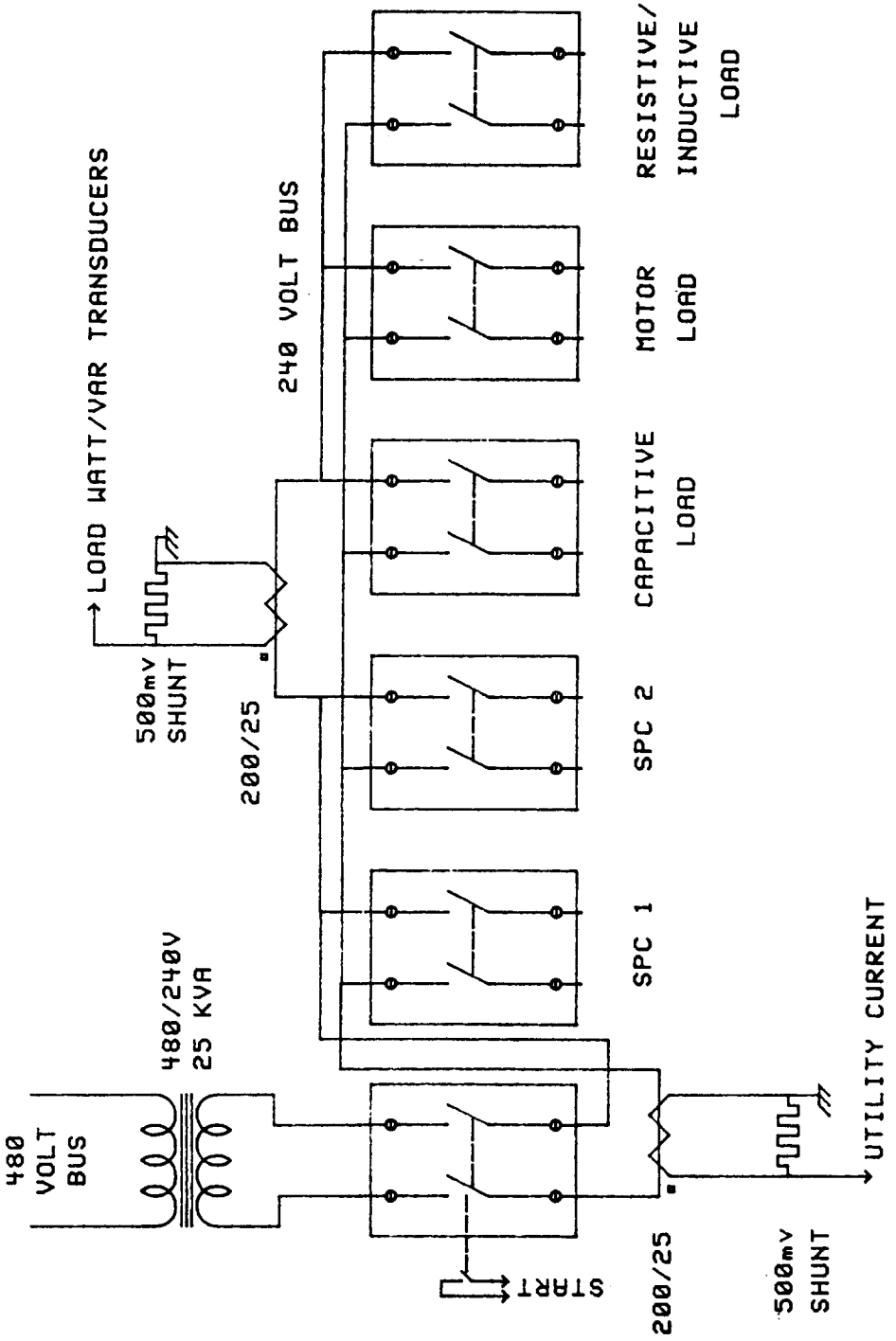

Figure 3.1-1. Test Board for Laboratory Experiments.

The input dc power to the SPCs was provided by means of controlled dc power supplies (0-300 Vdc). These dc power supplies were used to represent the photovoltaic arrays and were powered by a 50-kVA diesel generator to operate independent of the utility power.

The utility grid was one phase of the three-phase 480-Vac distribution system, which also supplied power to the building. The SPCs were connected to the utility grid through 480/240-V, 25-kVA transformers.

The loads used in the experiments included resistive, inductive, and capacitive loads as well as a dynamic load, which was a 1-HP, single-phase induction motor. The setup was designed so that the loads could easily be adjusted over a range of values changing from lagging to leading power factors.

Another independent 120-Vac source supplied power to the data acquisition system, which monitored the status of the island before and after the separation from the utility. The data collection system was composed of a test panel containing various switches, current transformers, voltage transformers, and transducers monitored by a 16-channel digital analyzer. The digital analyzer consisted of a Gould Recording Systems Model DASA 16-channel A/D data analyzer, an IBM PC/AT controller, and an Iomega Bernoulli 10-megabyte cartridge data storage unit.

The real-time display of variables within the test system or within the static power converter was done with a Nicolet Model 320 digital

oscilloscope. A complete list of the equipment used during the experiments is shown in Table 3.1-1.

After the test system was assembled, it was tested and calibrated by applying a potential of 240 Vac and a current of 25 amperes to the test panel and adjusting the calibration potentiometers of each transducer to their factory-recommended values. The system was recalibrated twice during the tests, and various portions were checked on numerous occasions to verify the accuracy of the data. The intent of the test system design was to provide highly accurate results, with the overall accuracy approaching 2 percent.

3.1.2 Test Procedures

The test procedures followed during the experiments were similar to those outlined in Reference [7]. These test procedures included detailed instructions for switching the utility, controlling the SPC, and adjusting the loads.

After analyzing the results of the initial computer simulations for the self- and line-commutated static power converters, a list of laboratory tests was proposed. These tests were single-unit and two-unit tests of each SPC plus one group of TESLACO-Gemini Cases. The details of the tests are provided later in the report.

Table 3.1-1 Test Equipment

A. Digital Data System:

Gould DASA 16 Channel Data Analyzer

IBM PC-AT Computer Iomega Bernoulli 10 Meg. Cartridge Storage Unit

B. Instruments:

Polymeter - Dranetz Model 325

Voltage, Current, Phase Angle

Phasemeter - Dranetz Model 314

Voltage, Current, Phase Angle

Power System Analyzer - Dranetz Model 3105

Power, Reactive power, Instantaneous Phase Angle, Harmonics

Oscilloscope - Nicolet Model 320

Multimeter - Keithley Model 175

C. Equipment:

Watt-Var Transducers - Scientific Columbus Model XLWV3-1K5-2.5A2

Current Transformers - Westinghouse Type C5B-10 Pearson Model 110

Current Shunts - Janco Model 8765

Potential Transformers - Westinghouse Type T6-A

For each of the laboratory tests, the desired operating point of the prospective island was set by the simultaneous adjustment of dc power supply, loads, and SPC controls according to the test procedures. The fine-tuning of the desired mismatch between the SPC power and load power was accomplished by adjusting the local load. The isolated operation was initiated by opening a switch that connected the utility to the SPCs and the loads. The switch was synchronized to the data acquisition system so that the switch system conditions were recorded both before and after the switch was opened.

The results of the experiments were recorded in the form of oscillograms and discrete data on a magnetic tape. The data include current flow on all energized circuit elements, total active and reactive power supplied by the SPCs, total active and reactive power delivered to the loads, system voltage, system frequency and duration of the island. Maintenance problems with both of the SPCs were frequent enough to prevent the performance of some two-unit tests, as both units were not operable at the same time.

3.2 TESLACO Static Power Convertor Laboratory Tests

Numerous laboratory tests were performed using a single TESLACO static power converter with varying load conditions. The types of tests performed were basically the same as those done in the computer simulations. The tests included resistive load only tests, resistive and inductive load tests, and tests with motor loads. One of the primary purposes for the lab tests was to provide verification for the computer simulations. This turned out to be difficult for several reasons. One reason was the switch that was used in the lab to interrupt the current to the utility to create the island. In the simulations, this switch was assumed to open at current zeroes. In the lab tests the switch did not wait for current zeroes. It chopped current and opened whenever it got a trip signal. As pointed out in the section describing simulation results, the point on the current wave that the switch opens makes a difference in run-on times. Therefore, the simulations had to be rerun and the switch set to open at the same time as it had for the lab tests in order to get comparable results. The switch used in the lab was able to interrupt at a current different from zero because it was operating in a 240-volt circuit. On a utility system, the breaker that opens to create a potential island will be operating at the utility's distribution voltage (on the order of 12 kV). It should interrupt only at current zeroes. Even if it does interrupt at a current other than zero, the run-on times given for the TESLACO should be conservative. Numerous simulations revealed that the maximum run-on times occurred for interruptions at current zeroes.

The second reason that it was difficult to verify the simulations with the lab tests was the way that watts and vars were measured in the lab tests.

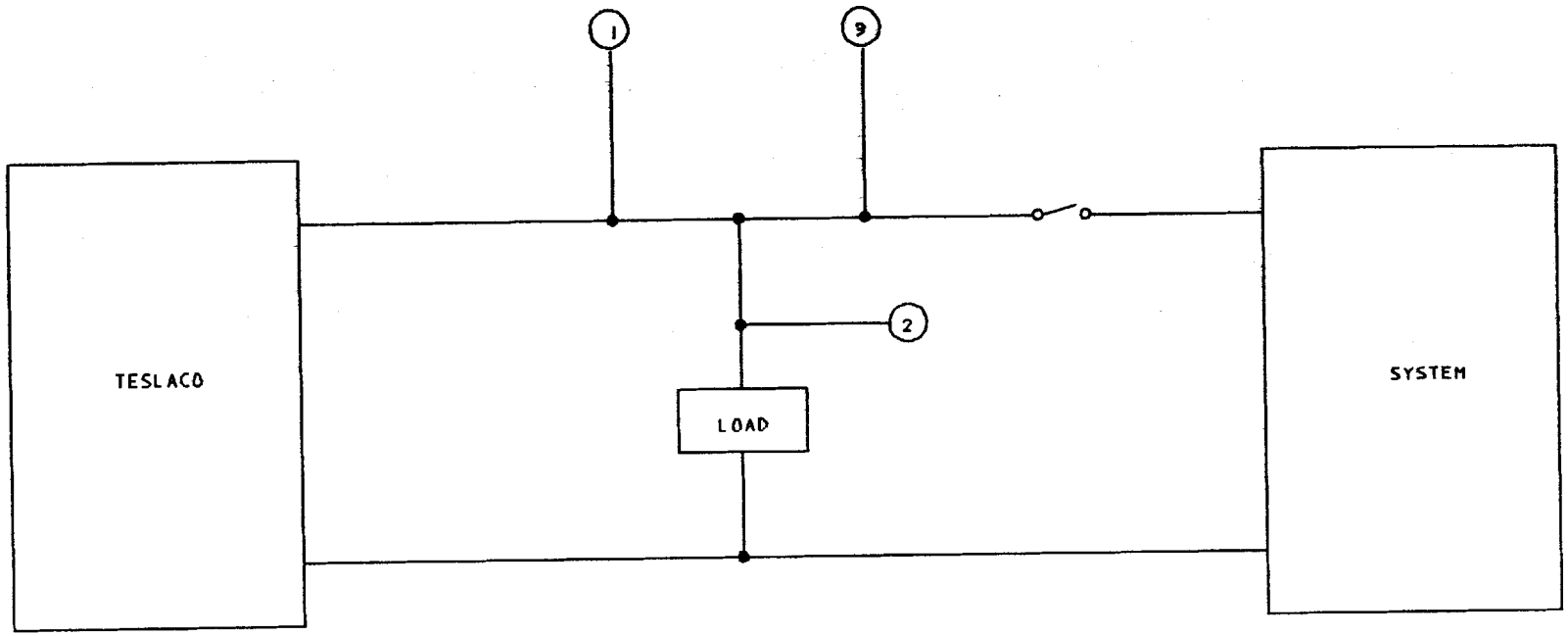

FIGURE 3.2-1 TYPICAL SET UP FOR A LAB TEST

Figure 3.2-1 shows a typical setup for a lab test. Watts and vars were measured at location 1 - out of the TESLACO and at location 2 - into the load. No watt and var measurement was made at location 3 - out to the system. It was assumed that the difference between the measurement at location 1 and the measurement at location 2 would equal the watts and vars out to the system. Ideally this would be true. However, the TESLACO operates at near unity power factor, and for a number of the tests the load was also near unity power factor. The transducer used to measure vars had its worst accuracy at near unity power factor conditions. It was estimated later that under these conditions the var measurements could have been off by as much as 40 vars. Therefore, the calculated vars out to the system could have been in error by as much as 80 vars. As pointed out in the section describing the computer simulations, the run-on time is very sensitive to the amount of var mismatch between load and generation within the island. When simulations were made in an attempt to match the lab tests, the vars flowing out to the system in the pre-island condition were treated as a variable.

A third reason that it was difficult to verify the simulations with the lab tests was that the initial simulations were made with a generic PV array model as input to the TESLACO. The lab tests were made with a dc power supply used as input to the TESLACO. The I-V curve for the array used in the simulations is shown in Figure 3.2-2a. The power supply had a current limit circuit, which had to be used to prevent it from increasing its power output during certain tests. This resulted in not being able to run the tests at the full power output level of the TESLACO at which the simulations had been made. Also, a .46-ohm resistor was used between the power supply and the TESLACO to limit current into the TESLACO when it was in its start-up

mode. One of the checks made by the TESLACO during start up is to short its input to see if enough current is available. Without this resistor, the current from the power supply is enough to damage some relay contacts on the TESLACO. When new simulations were made to match the lab tests, a simple power supply model was used instead of a PV array. The model had an I-V curve that looked like Figure 3.2-2b. It is not known how well the simple power supply model represented the actual device.

The results of the lab tests are summarized in Tables 3.2-1 and 3.2-2. The results of the simulations run to match selected lab test results are given in Table 3.2-3 and 3.2-4. These tables show how sensitive the run-on times are to small changes in the mismatch between vars generated and vars of load within the island. By varying the var mismatch within the island, run-on times were obtained from the simulations that are reasonably close (within .2 seconds most of the time) to the run-on times of the lab tests.

The comparison of test series IA1V to series IA2V in Table 3.2-1 illustrates why it was thought that the var measurements in the lab tests were in error. Test series IA1V had a resistive load that was matched to the generation of the TESLACO. Since the instruments showed the TESLACO to be producing between 44-116 vars, the resulting flow from the island to the system prior to disconnection was 0 watts and 44-116 vars. The run-on times were 1.0-1.3 seconds except for test IA1V-7, which will be discussed later. Test series IA2V used loads that supposedly matched the watts and vars generated within the island so that the net output from the island to the system was approximately 0 watts and 0 vars. These tests had run-on times ranging from .89 to .96 seconds. These results are counter to intuition and to computer

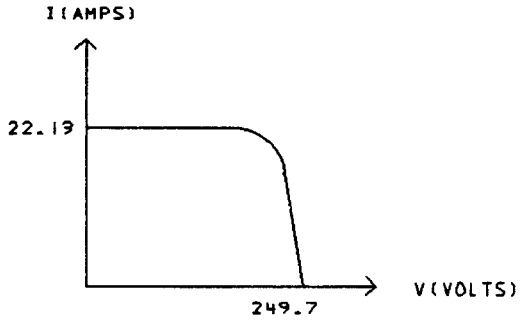

(A) ARRAY I-V CURVE USED IN ORIGINAL SIMULATIONS

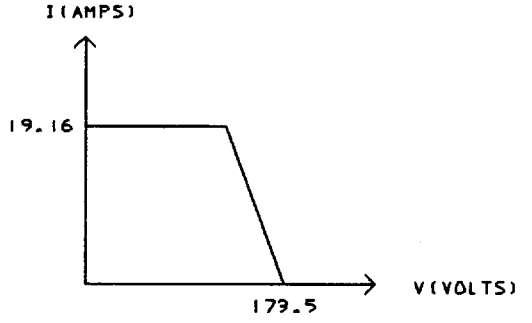

(B) POWER SUPPLY I-V CURVE USED IN SIMULATIONS OF LAB TESTS

FIGURE 3.2-2 COMPARISON OF ARRAY I-V CURVE
WITH POWER SUPPLY I-V CURVE

simulations. It seems reasonable to expect that the longer run-on time would occur for the more balanced test. This is what the computer simulations show. For a case with the watt and var load balanced within 1 watt and 1 var of the generation, the run-on time obtained was 1.5 seconds. When the var flow from the island to the system was approximately 50 vars, the run-on time was .7 seconds. Therefore, it appears that for test series IA2V, the vars were not really balanced. It appears that the var mismatch for this test series was more like 20-30 vars instead of being balanced. For test series IA1V, the var mismatch was probably more like 10-15 vars instead of 44-116 vars. Test IA1V-7 is exceptional in that its run-on time was 2.65 seconds. This result would be expected for a test in which the load was very closely matched to the generation. Because the reported var mismatch for this case was 94 vars, this test implies that the measured vars could have been off by as much as 94 vars.

In order to verify this conclusion some auxiliary tests were made at Sandia National Laboratories in Albuquerque. For these tests the watts and vars flowing from the island to the system were measured directly thereby allowing more accuracy in their determination. A series of tests was made in which the load watts matched the watts generated. The var mismatch ranged from -200 to 456. The results are plotted in Figure 3.2-3. This series showed that the longest run-on time was obtained when the var mismatch was near zero. Also plotted in this figure is a curve of simulation results made under similar conditions. The simulation run-on times are within .2 to .3 seconds of the lab run-on times; a reasonably good match. Therefore the conclusion is that most of the difference in run-on time between the

Table 3.2-1 Single TESLACO Lab Test Results

	SPC		Load		Net to System		System Voltage	Time of Interruption	Run-on Time
	Watts	Vars	Watts	Vars	Watts	Vars	(Volts)	(MS after Voltage Peak)	(Seconds)
1A1V	Resistive load only; watts load matched to watts generation.								
1	3000	72	2960	0	40	72	241.8	14	1.193
2	3040	56	3040	0	0	56	241.8	.6	1.339
3	3040	44	3040	0	0	44	241.8	11.7	1.195
4	3040	48	3040	0	0	48	242.4	12.1	1.212
5	3040	44	3040	0	0	44	242.4	13.6	1.277
6	3000	108	3000	6	0	102	241.8	13.0	1.103
7	3000	100	3000	6	0	94	241.8	.3	2.650
8	3000	116	3000	5	0	111	241.2	7.5	1.025
9	3000	108	3000	6	0	102	241.2	13.0	1.203
1A2X	Resistive load only; watts load 6.7% less than generation; vars balanced.								
1	3040	52	2840	52	200	0	243.0	13.0	.664
2	3040	60	2800	52	200	8	242.4	14.9	.662
3	3040	20	2840	24	200	-4	245.4	1.2	.482
4	3040	16	2840	16	200	0	245.4	.9	.400
5	3000	88	2800	108	200	-20	241.8	8.0	.775
6	3000	84	2800	102	200	-18	241.8	11.4	.773
7	3000	96	2800	108	200	-12	241.8	6.4	.777
1A3X	Resistive load only; watts load 6.7% more than generation; vars balanced.								
1	3040	24	3240	40	-200	-16	243.0	4.3	1.435
2	3040	36	3240	36	-200	0	243.6	8.4	1.581
3	3040	28	3240	44	-200	-16	243.6	1.2	1.605
4	3000	100	3200	108	-200	-8	241.8	16.2	1.647
5	3000	96	3200	112	-200	-16	241.2	16.2	1.765
6	3000	92	3200	108	-200	-16	241.2	9.9	1.553
1A4X	Resistive load only; watts load 13.3% less than generation; vars balanced.								
1	3040	28	2600	24	440	4	244.2	1.2	.175
2	3040	24	2640	24	400	0	244.2	1.5	.167
1A5X	Resistive load only; watts load 13.3% more than generation; vars balanced.								
1	3040	48	3400	44	-360	4	243.6	1.2	.772
2	3040	40	3400	40	-360	0	243.6	14.2	.692
1A6X	Resistive load only; watts load 20% less than generation; vars balanced.								
1	3040	60	2400	48	640	12	243.6	11.7	.115
2	3040	64	2440	64	600	0	243.6	11.7	.115
3	3040	76	2400	60	640	16	243.6	2.6	.117

Table 3.2-1 (cont'd) Single TESLACO Lab Test Results

	SPC		Load		Net to System		System Voltage (Volts)	Time of Interruption (MS after Voltage Peak)	Run-on Time (Seconds)
	Watts	Vars	Watts	Vars	Watts	Vars			
IA7X	Resistive load only; watts load 20% more than generation; vars balanced.								
1	3040	56	3680	64	-640	-8	241.8	11.1	.461
2	3040	64	3720	60	-680	4	241.8	6.8	.465
3	3040	72	3720	68	-680	4	242.4	9.9	.462
IA8X	Resistive load only; watts load 40% less than generation; vars balanced.								
1	3000	92	1800	84	1200	8	242.4	4.9	.037
IA9X	Resistive load only; watts load 40% more than generation; vars balanced.								
1	3000	116	4240	92	-1240	24	240.0	6.2	.356
IA2V	Resistive and inductive load; watt and var load matched to generation.								
1	3040	60	3040	60	0	0	243.0	15.4	.960
2	3040	72	2960	68	80	4	240.6	9.3	.890
3	3040	64	3000	60	40	4	242.4	0	.959
4	3040	48	3000	56	40	-8	242.4	6.2	.904
IC2	Resistive and inductive load; watts load 6.7% less than generation; vars balanced.								
1	3040	56	2840	56	200	0	243.6	2.5	.691
2	3040	52	2840	52	200	0	243.6	5.6	.655
IC3	Resistive and inductive load; watts load 6.7% more than generation; vars balanced.								
1	3040	60	3200	52	-160	8	243.0	3.1	1.620
2	3040	56	3200	40	-160	16	242.4	6.2	1.717
IC6	Resistive and inductive load; watts load balanced; var load 400 more than generation.								
1	3040	80	3040	480	0	-400	241.2	4.2	.244
2	3040	64	3040	464	0	-400	241.2	14.2	.251
3	3040	56	3000	456	40	-400	241.2	14.2	.251
IC7	Resistive and inductive load; watts load balanced; var load 800 more than generation.								
1	3040	48	3000	856	40	-808	241.2	15.4	.034
2	3000	56	3000	856	0	-800	241.2	1.9	.031
ID1	Resistive and motor load; watt and var load matched to generation.								
1	3000	68	3000	80	0	-12	241.8	16.1	.958
2	3040	76	3000	76	40	0	241.8	4.2	.954
ID2	Resistive and motor load; watts load 6.7% less than generation; vars balanced.								
1	3040	61	2880	74	160	-13	242.4	4.9	.672
2	3040	52	2880	72	160	-20	241.8	5.9	.687

Table 3.2-1 (cont'd) Single TESLACO Lab Test Results

	SPC		Load		Net to System		System Voltage	Time of Interruption	Run-on Time
	Watts	Vars	Watts	Vars	Watts	Vars	(Volts)	(MS after Voltage Peak)	(Seconds)
ID3	Resistive and motor load; watts load 6.7% more than generation; vars balanced.								
1	3040	64	3240	32	-200	32	241.8	11.0	.795
2	3000	64	3240	80	-240	-16	241.8	4.9	1.085
ID4	Resistive and motor load; watts load balanced; var load 400 more than generation.								
1	3040	56	3040	472	0	-416	242.4	7.4	.274
2	3040	48	3040	472	0	-424	242.4	13.6	.317
ID5	Resistive and motor load; watts load balanced; var load 800 more than generation.								
1	3040	56	3040	-336	0	392	242.4	13.6	.357
2	3040	48	3040	-352	0	400	243.0	14.2	.373

Table 3.2-2 Double TESLACO Lab Test Results

	SPC #1		SPC #2		Load		Net-to-System		System Voltage	Time of Interruption	Run-On Times	
	Watts	Vars	Watts	Vars	Watts	Vars	Watts	Vars	(Volts)	(MS after Voltage Peak)	SPC #1	SPC #2
IIF1	Two TESLACO's separated by transformers; watt and var load matched to generation.											
1.	3040	-248	2080	-264	4960	-252	160	-260	241.8	14.8	.894	.878
2.	3040	-264	2080	-284	5040	-704	80	156	241.8	14.8	.608	.591
3.	3040	-272	2080	-276	5040	-648	80	100	241.8	14.1	.743	.726
IIF3	Two TESLACO's separated by transformers; watts load 10% less than generation; vars balanced.											
1.	3040	-280	2080	-288	4560	-656	560	88	243.0	14.8	1.289	.909
2.	3040	-256	2080	-280	4560	-664	560	128	242.4	11.1	1.305	.947
IIF4	Two TESLACO's separated by transformers; watts load 10% more than generation; vars balanced.											
1.	3040	-252	2080	-288	5600	-640	-480	100	241.2	1.2	.412	.403
2.	3040	-248	2080	-280	5520	-656	-400	128	241.8	9.0	.405	.396

Table 3.2-3 Comparison of Computer Simulations To Single TESLACO Lab Test Results

	Lab Tests		Computer Simulations 0		1		2		3	
	Net-To-System (W+jV)	Run-on Time (Sec.)	Net-to-System (W+jV)	Run-on Time (Sec.)	Net-to System (W+jV)	Run-on Time (Sec.)	Net-to System (W+jV)	Run-on Time (Sec.)	Net-to System (W+jV)	Run-on Time (Sec.)
IA1V										
2	0+j56	1.339	0+j56	.695	0+j16	1.062				
3	0+j44	1.195	0+j44	.701	0+j14	1.051				
5	0+j44	1.277	0+j44	.715	0+j14	1.065				
IA2X										
1	200+j0	.664	200+j0	.965	200+j70	.647	200-j50	.566		
2	200+j8	.662	200+j8	1.305	200+j78	.612	200-j42	.639		
3	200-j4	.482	200-j4	1.336	200+j66	.602	200-j54	.645		
4	200+j0	.400	200+j0	1.636	200+j70	.577	200-j50	.653		
IA3X										
1	-200-j16	1.435	-200-j16	.950	-200-j10	1.074	-200-j7	1.133	-200-j3	1.300
2	-200+j0	1.581	-200+j0	1.304	-200-j10	1.395	-200-j7	1.671		
3	-200-j16	1.605	-200-j16	1.036	-200-j10	1.153	-200-j7	1.252	-200-j3	1.544
IA6X										
1	640+j12	.115	640+j12	.709	640+j82	.799	640-j58	.021	640-j40	.426
2	600+j0	.115	600+j0	.626			600-j70	.055		
3	640+j16	.117	640+j16	.927			640-j54	.670	640-j70	.595
IA7X										
1	-640-j8	.461	-460-j8	.702	-640+j32	.022	-640+j20	.584	-640-j68	1.194
2	-680+j4	.465	-680+j4	1.356	-680+j44	.730	-680+j64	.605	-680-j56	.657
3	-680+j4	.462	-680+j4	.669	-680+j44	.452			-680-j56	1.395
IC6										
1	0-j400	.244	0-j400	.054	0-j350	.070				
2	0-j400	.251	0-j400	.060	0-j350	.110				
IC7										
1	40-j808	.034	40-j808	.010						
2	0-j800	.031	0-j800	.006						
ID1										
1	0-j12	.958	0-j12	1.104	0-j42	.755				
2	40+j0	.954	40+j0	1.616	40-j30	.841				
ID2										
1	160-j13	.672	160-j13	.990	160-j53	.658				
2	160-j20	.687	160-j20	.897	160-j60	.574				
ID3										
1	-200+j32	.795	-200+j32	.734						
2	-240-j16	1.085	-240-j16	1.023						

Table 3.2-4 Comparison of Computer Simulations To Double TESLACO Lab Test Results

	Lab Tests		Computer Simulations 0		1		2		3	
	Net-To-System (W+jV)	Run-on Time (Sec.)	Net-to-System (W+jV)	Run-on Time (Sec.)	Net-to System (W+jV)	Run-on Time (Sec.)	Net-to System (W+jV)	Run-on Time (Sec.)	Net-to System (W+jV)	Run-on Time (Sec.)
IIF1										
2	80+j156	.608	80+j156	.371	0+j156	.329	0+j80	.597		
		.591		.380		.338		.589		
3	80+j100	.743	80+j100	.447	0+j100	.421	0+j50	.714		
		.726		.438		.430		.706		
IIF3										
1	560+j88	1.289	560+j88	.572	560+j48	.806				
		.909		.572		.806				
2	560+j128	1.305	560+j128	.474	560+j78	.642	560+j48	.825		
		.947		.466		.642		.825		
IIF4										
1	-480+j100	.412	-480+j100	.502						
		.403		.502						
2	-400+j128	.405	-400+j128	.368						
		.396		.377						

FIGURE 3.2-3 COMPARISON OF LAB TEST AND SIMULATION RUN-ON TIMES VERSUS VAR MISMATCH AS WATT MISMATCH HELD AT 0

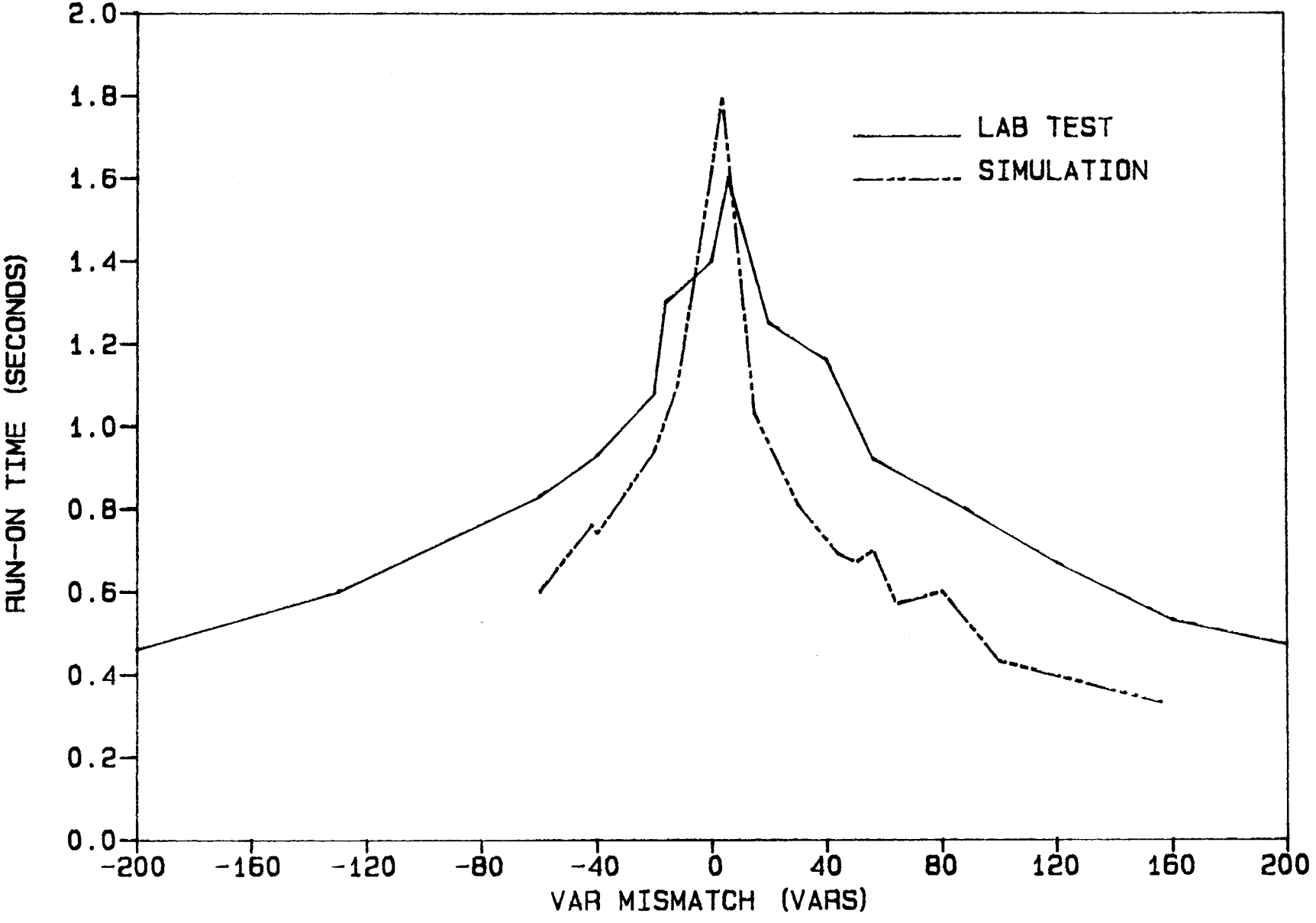

computer simulations and the original lab tests is due to var measurement error in the original lab tests.

One test made at Sandia was not plotted in Figure 3.2-3. A run-on time of 3.8 seconds was obtained for a test in which the watt and var mismatch was near zero. The test was repeated with the same load several times and the longest run-on time that could be achieved was only 1.6 seconds. Apparently, for one test the balance between load and generation was extremely good. The 3.8 second run-on was the longest achieved in any of the lab tests.

Summary of Lab Tests

The general trends seen in the lab test results were for the most part the same trends that were found in the simulations.

1. The lab test run-on times were found to vary with the point on the current wave that interruption took place. This effect was more pronounced when the load and generation were closer to being balanced.
2. The make-up of the load was not a significant factor. The net watt and var mismatch was the predominate factor in determining run-on times. This can be seen by comparing cases IA2X, IC2 and ID2. These cases all have 10% less load than generation but with different types of load. The run-on times are very similar.

3. The run-on times for the lab tests were more sensitive to mismatches in vars than to mismatches in watts.
4. When the mismatch between load watts and watts of generation becomes approximately 40% or larger, the TESLACO will shut down immediately (approximately two cycles). When the mismatch in load vars to vars generated is greater than approximately 800 vars (or 20% on the device's rating), the TESLACO will shut down immediately.
5. The run-on times were not significantly increased by having more than one TESLACO in the island.

One difference between the lab tests and the simulations was that no unfolder errors occurred for any of the lab tests. It has already been mentioned in the discussion of the simulations that unfolder errors were prevented in the simulations by having more inductance or capacitance in the load. The amount of vars that the TESLACO produced when connected to the utility in the lab tests implies that the unit had more internal inductance than is represented in the computer model. At rated conditions the computer model of the TESLACO will supply between 300 and 400 vars to the utility. In the lab tests the unit supplied anywhere from 0 to 100 vars. The implication is that there is internal inductance in the TESLACO that consumes vars. Part of this occurs in a circuit that supplies power to a fan. One measurement in the lab indicated that this fan consumed around 70 vars. This fan was not originally accounted for in the computer model. When the simulations were rerun to try to match the lab tests, an internal inductance was added to the computer to make the var output of the model equal to the var output measured in the lab. This internal inductance eliminated unfolder errors in most of the simulations.

3.3 Gemini Static Power Converter Laboratory Tests

The purpose of the laboratory experiments was to verify the EMTP computer model of the Gemini converter and aid in determining the cases that should be run in the field tests. The results of the lab tests are given in Table 3.3-1.

Comparison of Resistive Only Load Cases

The simulations and lab tests are in agreement. The Gemini unit shut down in less than one cycle in all cases. As discussed earlier, the Gemini requires var support from a net capacitive load to sustain islanding. Figures 3.3-1 and 3.3-2 give a comparison of lab and simulation shutdown for this type of loading case.

Comparison of Cases with Varying Watt Load Mismatch

The simulation and lab test results are not in exact agreement. Table 3.3-2 compares the original simulations with lab tests for cases with the resistive load being varied and the reactive load held constant equal to the Gemini's reactive requirement. One reason for this discrepancy is the method used in the lab test to determine a balanced case. In the lab tests watt and var meters were located on the output of the Gemini and the input to the load as shown in Figure 3.2-1. The case was determined to be "balanced" when the two watt and var readings were equal. This procedure resulted in loads that were too large when the island was formed. The reason is due to the harmonics produced by the Gemini. The transducer on the output of the Gemini was reading a power level that included the effects of the harmonics. The

TABLE 3.3-1 Single Gemini Laboratory Tests Results

CASE	OUT OF SYSTEM AMPS	STATIC POWER CONVERTER OUTPUT AMPS	VOLTS	WATTS	VARS	FREQ	LOCAL LOAD WATTS	VARS	DC ARRAY VOLTS	AMPS	RUN ON (CYCLES)
G-I Single Unit Gemini Static Power Converter											
A. Local Load only at the Power Converter Terminals											
1. Continuous Current Mode											
a. Resistive load matched to generation, no reactive load											
	34.56/-33.6	35.20/-35.84	345.6/-340.8	3520	-4640	60	3520	0	264	15.36	1
b. Resistive load matched to generation, capacitive load matched to supply Gemini var requirement											
	10.56/-10.88	35.84/-35.84	345.6/-340.8	3520	-4720	60	3520	-4720	264	15.29	INDEF.
	0	35.20/-40.96	331.2/-307.2	3520	-4720	63.5	3520	-4720	264	15.29	
c. Vary resistive load vs. generation, capacitive load matched to supply Gemini var requirement											
4. Resistive load 10% less than generation											
	12.16/-13.76	35.84/-36.48	345.6/-340.8	3520	-4800	60	3200	-4720	264	15.39	INDEF.
	0	35.84/-40.96	345.6/-326.4	3520	-5120	63.5	3520	-5200	264	15.22	
5. Resistive load 50% less than generation											
	18.24/-17.60	35.84/-36.48	345.6/-340.8	3520	-4800	60	1760	-4800	264	15.40	INDEF.
	0	43.52/-67.20	451.2/-412.8	3360	-8080	68.7	3280	-8640	264	15.27	
9. Resistive load 10% more than generation											
	10.56/-10.88	35.84/-36.48	345.6/-340.8	3520	-4720	60	3840	-4720	264	15.38	INDEF.
	0	34.56/-41.6	312.0/-288.0	3520	-4240	63.5	3520	-4320	264	15.37	
10. Resistive load 50% more than generation											
	15.04/-15.36	35.2/-35.84	340.8/-340.8	3520	-4640	60	5280	-4640	264	15.4	4
	0	37.12/-37.76	283.2/-273.6			63.1					
d. Resistive load matched to generation, vary capacitive load vs. Gemini var requirement											
4. Capacitive load 10% less than Gemini var requirement											
	10.56/-9.60	35.20/-35.84	340.8/-240.8	3520	-4640	60	3520	-4160	264	15.40	INDEF.
	0	33.92/-37.76	326.4/-307.2	3760	-4320	67.8	3600	-4240	264	15.07	
9. Capacitive load 10% more than Gemini var requirement											
	13.76/-12.80	35.84/-36.48	345.6/-340.8	3600	-4720	60	3520	-5200	264	15.41	INDEF.
	0	35.84/-46.08	326.4/-302.4	3520	-4960	61.1	3520	-5120	264	15.43	
10. Capacitive load 50% less than Gemini var requirement											
	21.12/-20.16	35.52/-35.84	345.6/-340.8	3480	-4680	60	3520	-2360	264	15.4	1

TABLE 3.3-1 (cont'd.) Single Gemini Laboratory Tests Results

CASE	OUT OF SYSTEM AMPS	STATIC POWER CONVERTER OUTPUT AMPS	VOLTS	WATTS	VARS	FREQ	LOCAL LOAD WATTS	VARS	DC ARRAY VOLTS	AMPS	RUN ON (CYCLES)
G-1 Single Unit Gemini Static Power Converter (cont.)											
A. Local Load at the Power Converter Terminals (cont.)											
2. Discontinuous Current Mode											
a. Resistive load matched to generation, no reactive load											
	25.92/-24.32	26.24/-26.88	345.6/-340.8	2120	-3400	60	2120	0	276	9.3	1/2
b. Resistive load matched to generation, capacitive load matched to supply Gemini var requirement											
	7.2/-6.08	26.24/26.88	345.6/340.8	2120	-3400	60	2120	-3400	268.8	9.3	11
	0	26.24/-28.48	340.8/-302.4			64					
c. Vary resistive load vs. generation, capacitive load matched to supply Gemini's var requirement											
4. Resistive load 10% less than generation.											
	8.64/-6.72	26.56/-26.88	345.6/340.8	2080	-3440	60	1880	-3440	268.8	9.3	10
	0	27.52/-28.16	355.2/-331.2			62.5					
9. Resistive load 10% more than generation.											
	6.56/-5.6	26.24/-26.88	345.6/-340.8	2080	-3400	60	2320	-3400	268.8	9.3	13
	0	26.24/-26.56	331.2/-312.0			61.2					
d. Resistive load matched to generation, vary capacitive load vs. Gemini var requirement											
4. Capacitive load 10% less than Gemini var requirement.											
	7.68/-5.12	26.56/-26.88	345.6/-340.8	2080	-3440	60	2080	-3080	268.8	9.3	12
	0	24.64/-24.64	336.0/-312.0			62.5					
9. Capacitive load 10% more than Gemini var requirement											
	10.24/-7.84	26.56/-26.88	345.6/-340.8	2080	-3480	60	2080	-3840	268.8	9.3	10
	0	28.8/-30.08	355.2/-312.0			60.6					
D. Local Load (including motor load) at the Power Converter Terminals											
1. Continuous Current Mode											
b. Resistive load matched to generation, capacitive load matched to Gemini var requirement											
	10.24/-12.96	35.84/-36.48	345.6/-340.8	3520	-4800	60	3520	-4800	264	15.36	INDEF.
	0	36.16/-40.8	340.8/-297.6	3480	-4880		3480	-4960	264	15.25	

Table 3.3-2 Comparison of Laboratory Tests and Simulations for Cases Where the Watt Mismatch is Varied and the Capacitive Load is Held Constant.

Case	Original Simulations			Laboratory Tests			Revised Simulations		
	Change in Term. Volt.	Change in Freq.	Run-on	Change in Term. Volt.	Change in Freq.	Run-on	Change in Term. Volt	Change in Freq.	Run-on
G-I Single Unit Gemini static power converter									
A. Local Load only at the Power Converter Terminals									
1. Continuous Current Mode									
b. Resistive load matched to generation, capacitive load matched to supply Gemini's var requirement.									
	No Change	-.4Hz	INDEF.	.93	+3.5Hz	INDEF.			
c. Vary resistive load vs. generation, capacitive load matched to supply Gemini's var requirement.									
4. Resistive load 10% less than generation.	1.046	+.7Hz	INDEF.	.97	+3.5Hz	INDEF			
5. Resistive load 50% less than generation.	1.363	-4.5Hz	INDEF.	1.26	+8.7Hz	INDEF.			
9. Resistive load 10% more than generation.	.95	-.7Hz	INDEF.	.87	+3.5Hz	INDEF			
10. Resistive load 50% more than generation.			1cycle	.81	+3.1Hz	4 cycles			
2. Discontinuous Current Mode									
b. Resistive load matched to generation, capacitive load matched to supply Gemini's var requirement.	1.0	+1.0Hz	INDEF.	.94	+4Hz	11	decreased	+7.5Hz	22
c. Vary resistive load vs. generation, capacitive load matched to supply Gemini's var requirement.									
4. Resistive load 10% less than generation.	1.042	+.3Hz	INDEF.	1.0	+2.5Hz	10	decreased	+7.5Hz	28
9. Resistive load 10% more than generation.	.97	+1.0Hz	INDEF.	.94	+1.2Hz	13	decreased	+7.5Hz	28

FIGURE 3.3-1 SIMULATION CASE G_I.A.1.A.

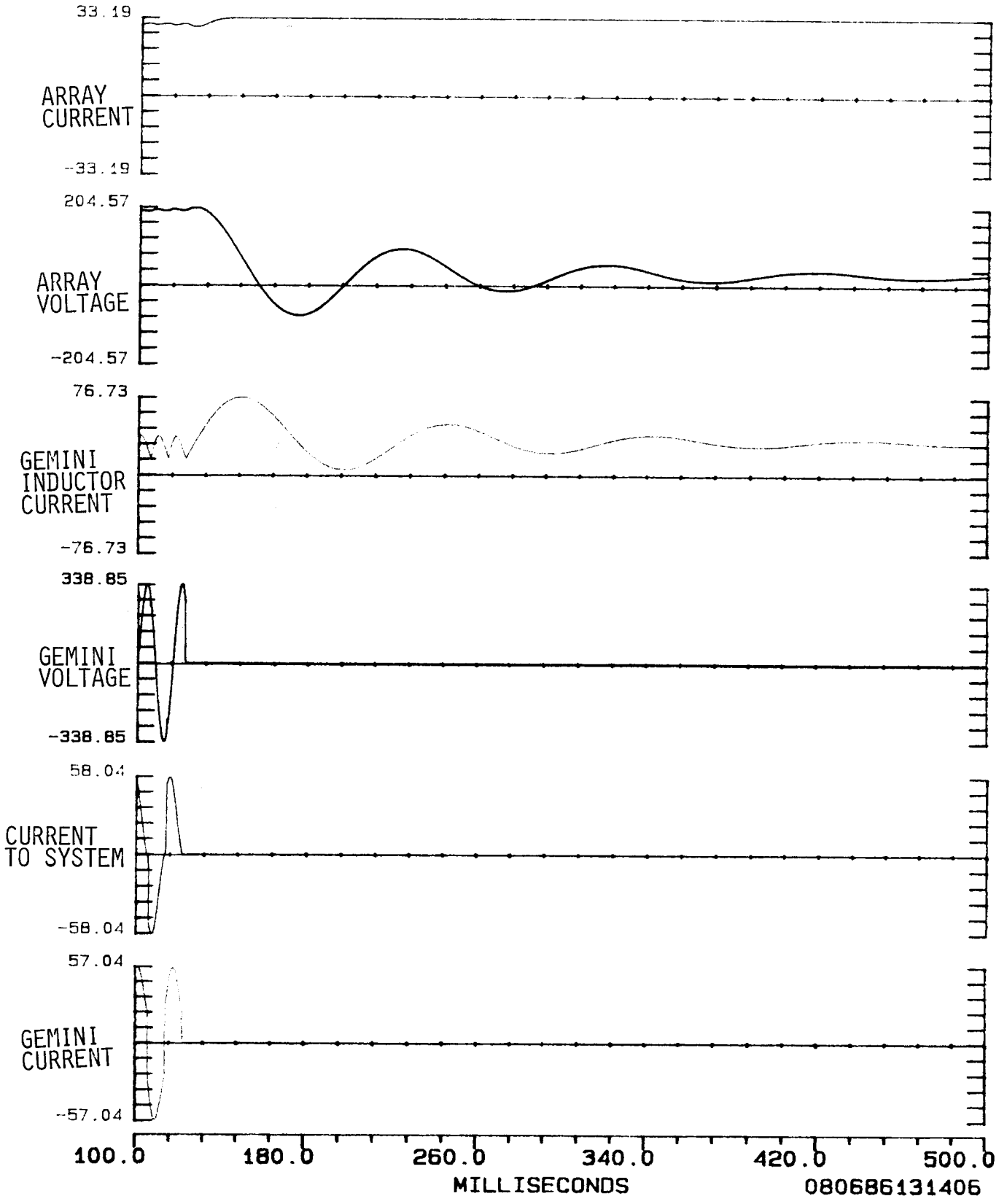

FIGURE 3.3-2 LAB TEST I.A.1.A

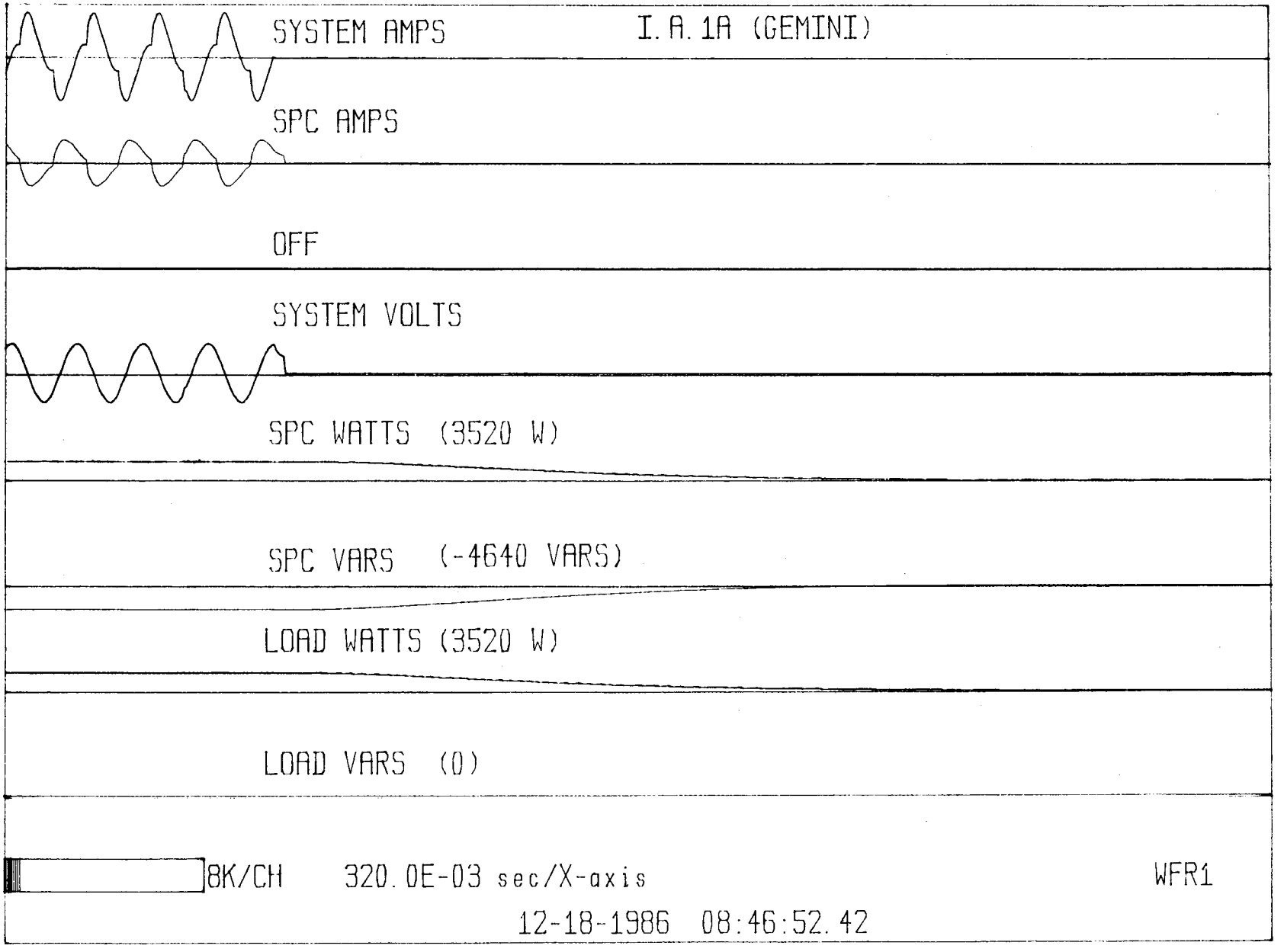

transducer on the load was measuring a power level that did not have as much harmonic content. As a result there was a significant watt and var mismatch at the utility switch when it was opened.

The results of the islanding tests in the lab varied a great deal between the continuous and discontinuous current mode cases. Therefore, the two will be discussed separately. In the continuous current mode, the lab tests indicated that the Gemini would island indefinitely as predicted by the simulations. The change in terminal voltage magnitude and frequency when the island reached a steady-state condition was not the same as predicted by the simulations. The laboratory balanced case terminal voltage dropped following the opening of the utility disconnect switch, which indicates that the local watt load was not matched. A similar result was noted in the simulations but the drop was not as great. The terminal voltage in the lab experiments also dropped when the island load was 10% less than generation, which indicates that the error caused by this measurement method was greater than 10%. Our calculations, based on the change in terminal voltage, estimate that the island load was actually 15% larger than a balanced load should have been. The results in Table 3.3-2 Case G-I.A.1.b for the lab tests indicate a drop in terminal voltage to 93% of the pre-island value, and the simulations did not demonstrate a change in voltage. If the drop in voltage of .07 pu is assumed for all of the simulation results as a constant offset, the change in voltage results match those measured in the lab. The simulations indicated that for a "balanced load" case the frequency in the island should not change much from the 60-Hz pre-island value. The simulations further indicated that changes in the watt load (watt mismatches) did not cause the frequency to vary significantly from 60 Hz when islanding. In the lab test balanced case, the frequency changed to 63.5 Hz, which

indicates that the vars were not balanced in the lab tests. However, the frequency for the ±10% load cases also changed to 63.5 Hz, which demonstrates that watt mismatches do not affect frequency significantly. It is very difficult to balance and maintain a balance of vars in the laboratory. Instead of rerunning the laboratory tests, a watt and var transducer was modeled with EMTP. The EMTP watt meter was also tricked by the harmonics, thus demonstrating the problems experienced in the lab.

The laboratory tests for the discontinuous current mode show the same difficulty in determining a balanced case. The resolution of these discrepancies between lab test and simulations is the same as described for the continuous current mode cases. However, the discontinuous current mode cases gave an unexpected result. The Gemini shut down after a run-on time much like the TESLACO's. The reason for this appears to be due to the saturation characteristics of the 350/240V step-down transformer and a presumed mismatch of impedances in the Gemini's SCRs. When the Gemini is connected to the utility system, the utility source forces the terminal voltage to be symmetrical 60 Hz. When the island is formed, this is no longer true and the Gemini's output voltage contains a dc offset that is most pronounced in the discontinuous mode of operation. The output current is offset and this causes the transformer to become further and further saturated during one half-cycle of the voltage, while operating in the linear region on the other half-cycle. The source of the dc offset is not known. One possibility is an unbalance in the SCR impedances of the Gemini. In our revised simulations we modeled both the unbalanced SCR impedances that could produce the initial dc offset and the saturation characteristic for the step-down transformer. Figures 3.3-3 and 3.3-4 are a comparison between a discontinuous current mode lab test that shut down and an EMTP simulation.

FIGURE 3.3-3 SIMULATION G_I.A.2.b

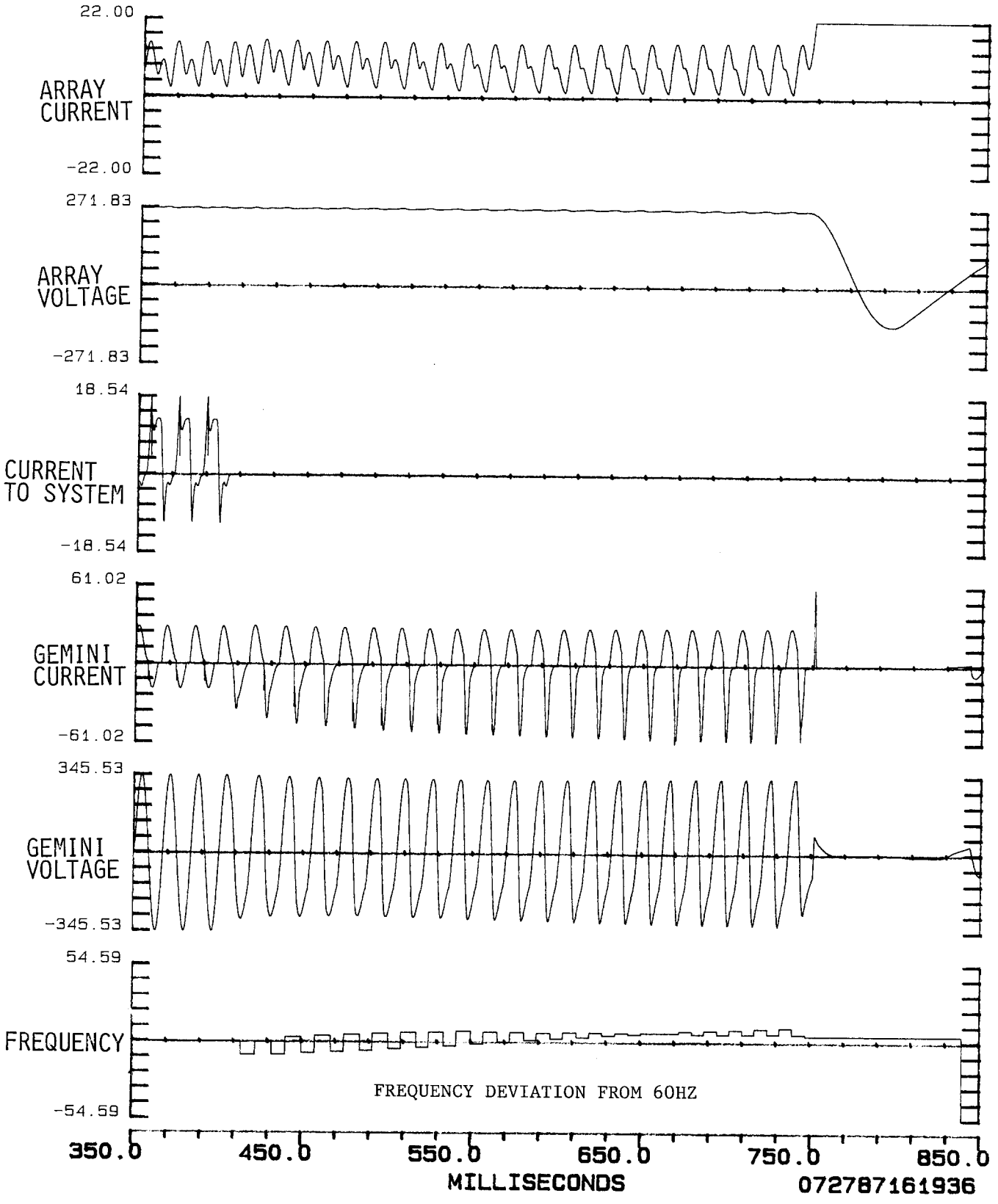

FIGURE 3.3-4 LAB TEST I.A.2.B

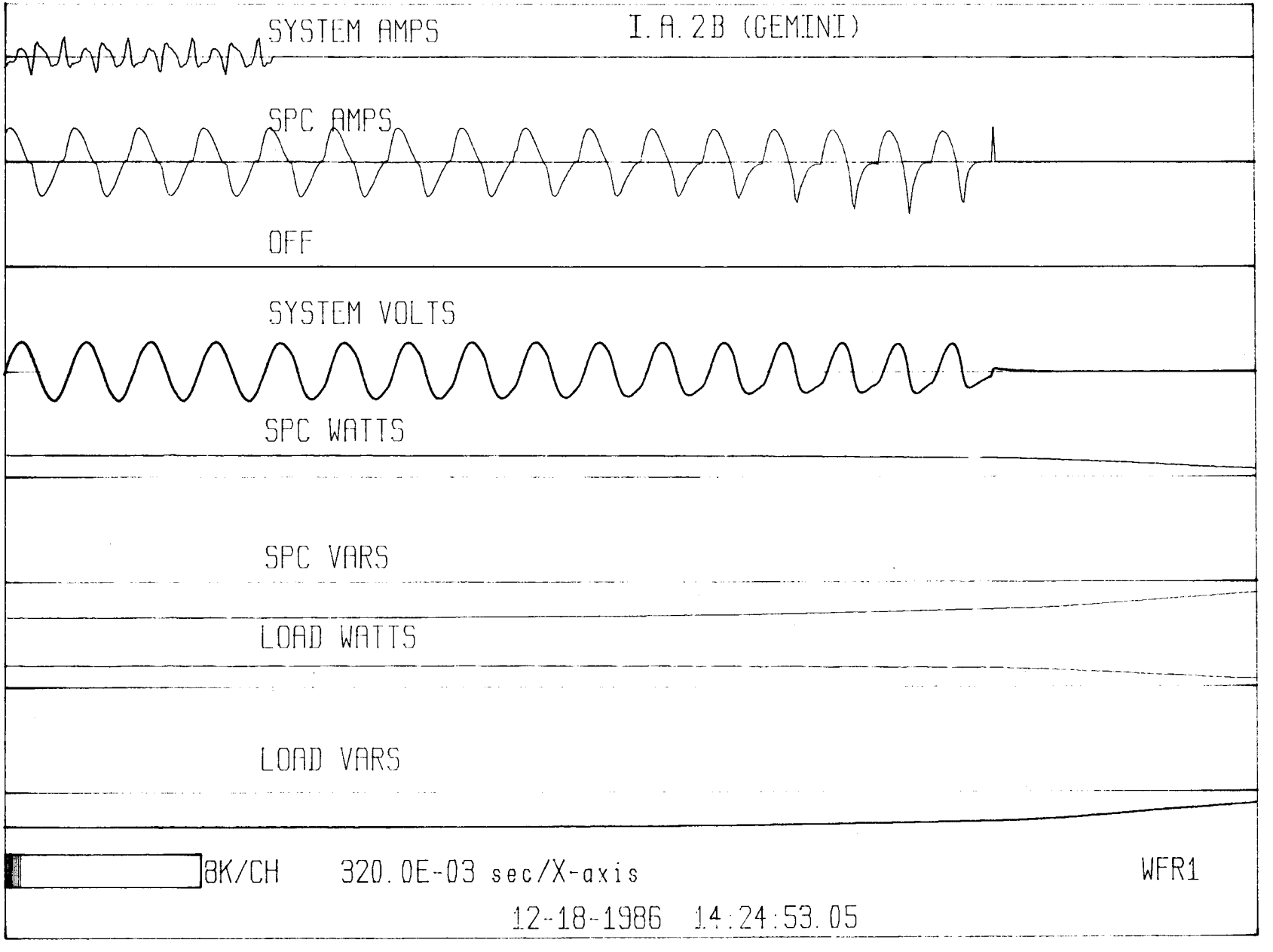

The EMTP simulation shut down in a similar manner with a longer run-on time.

The run-on time is dependent on whatever is producing the dc offset and the transformer saturation characteristic, which would vary from unit to unit. Therefore, we did not expend any more effort to exactly match the lab result. Although the lab tests imply that the Gemini must be in the continuous current mode of operation for indefinite runon to occur, the result may not apply to all Geminis. It is speculated that some Gemini units would not produce enough dc offset to cause a shutdown.

Comparison of Varying Var Load Mismatch Cases

A comparison between lab tests and simulations of balanced local watt load with variations in the local var load is given in Table 3.3-3. The simulations predicted that the var mismatches would cause changes in frequency from 60 Hz after islanding. The simulations also indicated that the terminal voltage magnitude would not change significantly after the island was allowed to reach steady state. However, a transient voltage change occurred when the island was created. If the vars available from the local load are a great deal less than the Gemini's var requirement, the transient voltage dip may be enough to cause the low voltage control circuitry to trip the unit. This occurred in our 50% less vars case in the simulations and lab test. A series of lab tests was run which indicated that local loads providing more than approximately 50% to 75% of the var requirement resulted in indefinite run-on for the continuous current mode cases. The simulations indicated these same trends. If "balanced load" error corrections to the steady-state values are assumed similar to those for the watt mismatch cases, the simulation and lab results are in agreement.

Table 3.3-3 Comparison of Laboratory Tests and Simulation for Cases Where the Var Mismatch is Varied and the Resistive Load is Constant

Case	Original Simulations			Laboratory Tests			Revised Simulations		
	Change in Term. Volt.	Change in Freq.	Run-on	Change in Term. Volt.	Change in Freq.	Run-on	Change in Term. Volt	Change in Freq.	Run-on
G-I Single Unit Gemini Static Power Converter									
A. Local Load only at the Power Converter Terminals									
1. Continuous Current Mode									
b. Resistive load matched to generation, capacitive load matched to supply Gemini's var requirement									
	1.0	No Change	INDEF.	.93	+3.5Hz	INDEF.			
d. Resistive load matched									
4. Capacitive load 10% less than Gemini's var requirement									
	1.0	+5.0Hz	INDEF.	.93	+7.8Hz	INDEF.			
5. Capacitive load 50% less than Gemini's var requirement									
	1.0		1 cycle			1 cycle			
9. Capacitive load 50% more than Gemini's var requirement									
	1.0	-4.3Hz	INDEF.	.92	+1.1Hz	INDEF.			
2. Discontinuous Current Mode									
b. Resistive load matched to generation, capacitive load matched to supply Gemini's var requirement									
	1.0	No change	INDEF.	.94	+4	11		+4.5Hz	22 cycles
d. Resistive load matched to generation, vary the capacitive load									
4. Capacitive load 10% less than Gemini's var requirement									
	.975	+7.1Hz	INDEF.	.94	+2.5	12		7.5Hz	20 cycles
9. Capacitive load 10% more than Gemini's var requirement									
	.983	-12.3Hz	INDEF.	.97	+.6	10			> 30 cycles

Conclusions from Gemini Laboratory Tests

The following conclusions were made when reviewing the lab results and comparing them to the computer simulations.

1. When operating in continuous current mode the lab results and simulations match very well.

2. When operating in discontinuous current mode in the lab the Gemini shut down after a short run-on time. This did not agree with initial simulations. The shutdown was the result of saturating the 350/240V step-down transformer. The computer model was revised and gave a similar shutdown.

3. The watt and var mismatch at the island boundary was calculated as the difference between Gemini output and load consumption. This method did not work well due to the harmonics being produced by the Gemini.

The technique used to determine a balanced case needs to be improved for the field tests. The field tests are expected to confirm that there are load/generation combinations in which the Gemini will island indefinitely, that local var support of 50% or less will cause the unit to shut down immediately, and that a real-world island can be sustained as the solar insolation and typical residential loads are varied.

3.4 Combinations of TESLACO and Gemini Static Power Converter Laboratory Tests

A limited number of lab tests were run using both a TESLACO and a Gemini static power converter. A summary of these tests is given in Table 3.4-1. These tests were chosen to be similar to the single TESLACO and single Gemini tests that were performed. The first test (G-T-IA1) had resistive load matched to generation but had no capacitive load to supply the var requirement of the Gemini. In the single Gemini simulations and tests, the Gemini shut down immediately if the load did not supply any vars. Also in the single TESLACO simulations and tests, the TESLACO shut down immediately whenever the mismatch between vars generated and var load exceeded 800 vars. Therefore, in the first combination test both units shut down immediately as expected.

The remainder of the tests had relatively small mismatches between watts and vars generated and watts and vars of the load. These tests ran on for short periods of time until the TESLACO reached 6° of phase error and shut down. After it shut down the watts load in the island was more than twice what the Gemini could supply. Therefore, the voltage dropped appreciably and the Gemini's low voltage sensing circuits shut it down approximately one cycle after the TESLACO did. Thus, the TESLACO controlled the duration of the island. Because of this, the comments made in Section 2.2 concerning the effect of watt and var mismatch on the run-on time of the TESLACO appear to hold true for islands with both a TESLACO and a Gemini. The amount of watts mismatch in the island determines what the voltage change will be when the island is formed. As described in Section 2.2, this voltage change produces

a phase error in the phase-locked loop of the TESLACO. The voltage change will modify the var requirement of the Gemini and thereby contribute to the var mismatch in the island. The var mismatch produces a phase shift in the terminal voltage of the TESLACO, which is also seen as a phase error in the phase-locked loop. These two errors can reinforce each other and result in a relatively short run-on time or they can cancel each other and result in a relatively long run-on time. If the results of tests G-T-IA2 through G-T-IA6 are compared to the corresponding single TESLACO tests (Table 3.2-1, tests IA1X through IA3X and IC6), the run-on times are not very different, considering the fact that the watt and var mismatches are only approximately the same for the corresponding tests.

Test G-T-IB1 included a 1-Hp motor as part of the load. For this test the watt and var mismatch in the island was supposed to be approximately zero. The measured mismatch was -200 watts and -24 vars. The island persisted for 1.9 seconds. Apparently the watt and var mismatches produced phase errors in the TESLACO phase-locked loop that tended to cancel and therefore produced a relatively long run-on time.

Simulations corresponding to the lab tests were run for only one of the combination TESLACO and Gemini tests. That was the test G-T-IA2, which had watt and var load matched to watt and var generation. The run-on times obtained in the simulation were 1.028 seconds for the TESLACO and 1.039 seconds for the Gemini. This compares very well with the lab test results.

Table 3.4-1 Multiple SPC Islanding Laboratory Test with a Combination of TESLACO and Gemini Converters

Case	Mismatch at Boundary Watts	Mismatch at Boundary Vars	TESLACO SPC Output Watts	TESLACO SPC Output Vars	TESLACO SPC Run-On (Sec)	GEMINI SPC Output Watts	GEMINI SPC Output Vars	GEMINI SPC Run-On (Sec)
G-T-I Multiple SPC Islanding Test								
A. Passive type loads connected to SPC terminals								
1. Resistive load matched to generation	120	-5050	3000	70	.002	2560	-5120	.004
2. Resistive load matched to generation, Reactive load matched to var requirement	-40	-116	3000	44	.994	2560	-5280	1.001
3. Resistive load 10% less than generation, Reactive load matched to var requirement	640	-32	3040	48	.219	2560	-5280	.235
4. Resistive load 10% more than generation, Reactive load matched to var requirement	-520	-24	3000	56	1.321	2560	-5200	1.339
5. Resistive load matched to generation, Reactive load 10% less than var requirement	0	-520	3000	40	.379	2520	-5360	.395
6. Resistive load matched to generation, Reactive load 10% more than var requirement	0	520	3000	40	.407	2520	-5440	.425
B. Island load includes motor load at SPC terminals								
1. Resistive load matched to generation, Reactive load matched to var requirement	-200	-24	2920	56	1.909	2560	-5520	1.928

BLANK PAGE

IV. FIELD EXPERIMENTS

The objective of the field experiments was to determine whether the islanding windows determined by simulations and lab tests were physically possible in a field environment wherein a photovoltaic array and normal house loads were used for the SPC testing.

4.1 Description of the Field Test Set-Up

Shenandoah Tests - To validate whether the results obtained in the laboratory experiments actually represent a real-world condition, the data acquisition system and test board were moved to the Solar Research Center at Shenandoah for single self-commutated SPC and single line-commutated SPC tests.

The tests were performed by using the two-axis tracking photovoltaic array which consists of 64 single-crystal photovoltaic modules. The photovoltaic array produces 4 kW at peak operating conditions. The modules were manufactured by Solec International Inc.

TVA Tests - The main field tests were performed at the TVA Energy Research Test Facility in Chattanooga, which includes four 4-kW photovoltaic arrays mounted on the roofs of four houses. The photovoltaic arrays are fixed flate-plate arrays and all of them are grid-interconnected by means of self-commutated SPCs. All of the houses are served from a single distribution transformer. The available array power is utilized to meet the

local loads of the residence on which the array is mounted. The local loads consist of HVAC, lighting, ranges, and attic fans.

The field tests were divided into two stages. Stage I tests were single-unit TESLACO, Gemini, and APCC SPCs, and Stage II tests were multiple-unit tests using four houses with different mixes of TESLACO and Gemini SPCs. Since the solar test facility at TVA had no means of disconnecting the houses from the utility supply other than the disconnect switch in each house, a test distribution system was created. This distribution system was a 480-volt bus fed with the same 25-KVA transformer used in the test system of the laboratory experiments.

4.1.1 Construction of the Field Test Set-Up

The test set up for the Shenandoah tests was the same as the set-up for the laboratory experiments. The connections for the single-unit tests conducted in Solar House #2 at Chattanooga are shown in the diagram of Figure 4.1-1 (Stage I). The distribution system and hook-up for the remaining experiments at TVA are shown in Figure 4.1-2 (Stage II).

4.1.2 Test Procedures

The calibration procedures, test procedures, and documentation practices were identical to those used in the laboratory experiments.

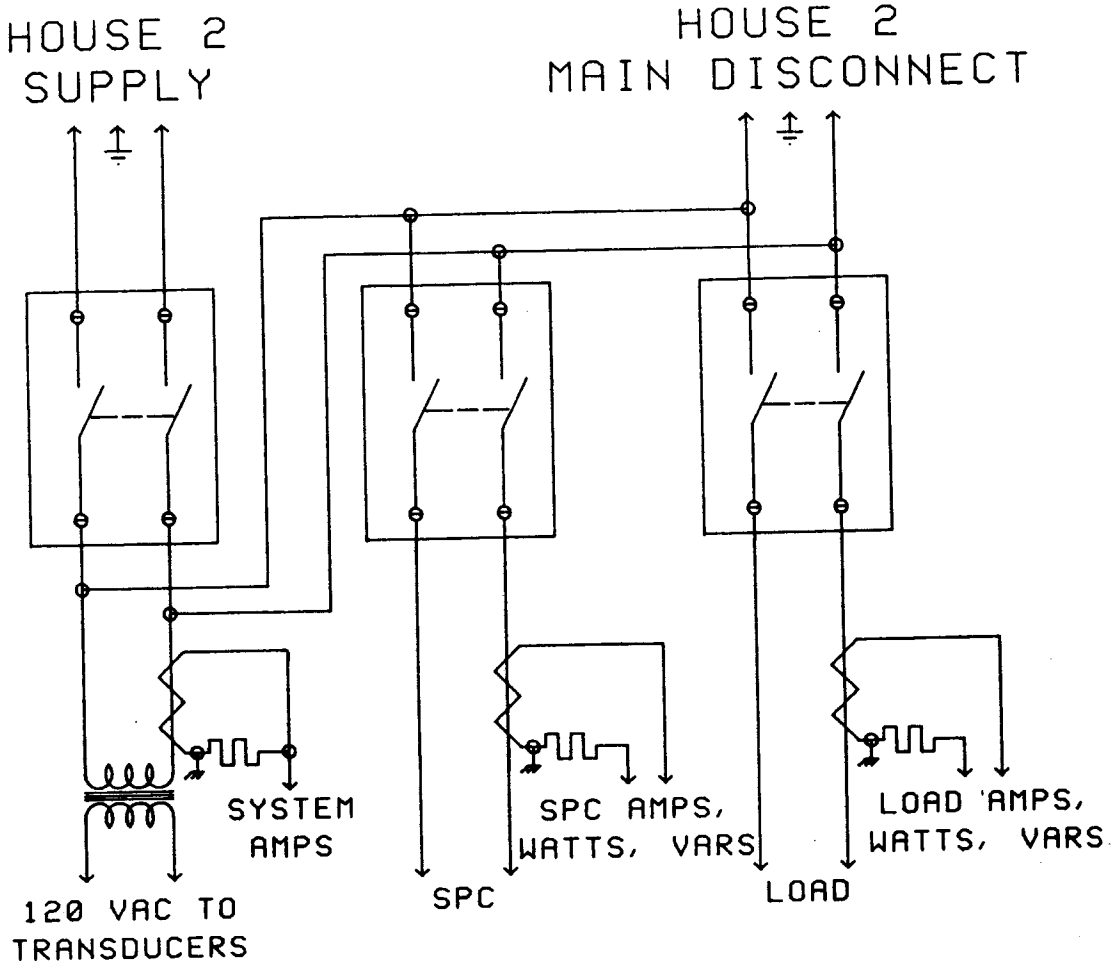

Figure 4.1-1. Test Board for Stage I Field Experiments.

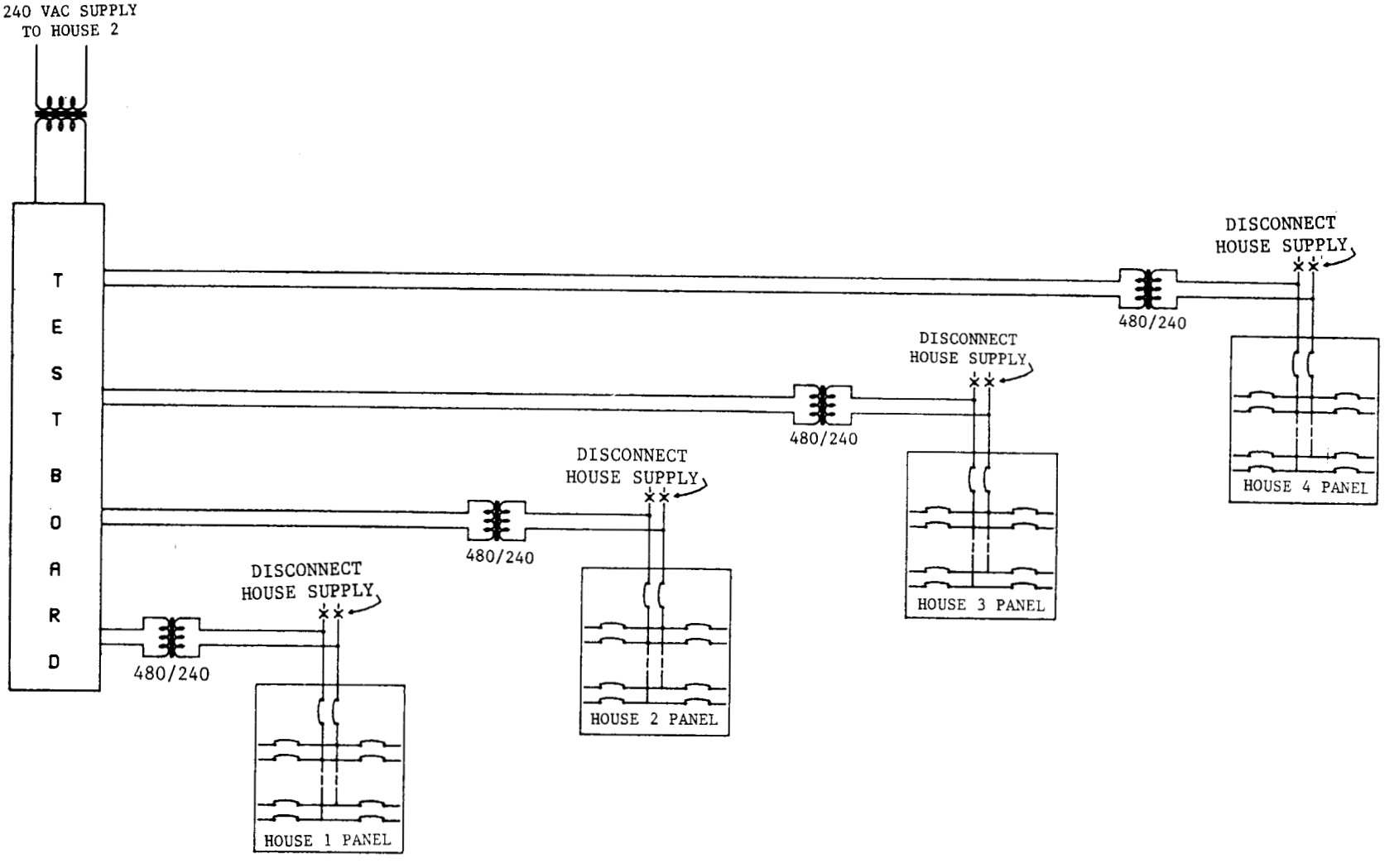

Figure 4.1-2. Distribution System for Stage II Field Experiments.

4.2 TESLACO Static Power Converter Field Tests

Several islanding field tests were performed with a TESLACO static power converter at Shenandoah and at Chattanooga. The types of tests performed were similar to those already made in the lab and similar to the computer simulations. The major difference between these field tests and the lab tests was that actual PV arrays were used in the field tests to supply dc input power to the SPC.

Table 4.2-1 gives the results of the single-unit field tests made at Shenandoah. These were resistive load only tests with only three basic types of tests: watts load matched to watts generated, watts load 10% less than watts generated, and watts load 10% more than watts generated. The load used for these tests was the same variable resistor that had previously been used in the lab tests. As was true in the lab tests, watts and vars were measured in two locations -- out of the TESLACO and into the load. For the same reasons given in Section 3.2, it was felt that the calculated vars flowing from the island to the system could have been in error by as much as 80-90 vars. More computer simulations were made to try to match the field test results. In these simulations the var output from the island to the system was treated as a variable. Also, the simulations were made with the switch opening to create the island at the same point on the current wave as the lab tests did. Table 4.1-2 gives the results of these simulations. From this table it can be seen that the simulated run-on times were very close to the field test run-on times when the calculated vars out to the system were varied by as much as 70 to 80 vars. The longest run-on time obtained for this series of tests was 1.2 seconds.

Several single TESLACO islanding field tests were also made at Chattanooga. These tests were resistive load only tests of the same three types as were done at Shenandoah: watts load matched to watts generated, watts load 10% less than watts generated and watts load 10% more than watts generated. The results of these tests are given in Table 4.2-3. Computer simulations were made to try to match these tests by varying the vars flowing from the island to the system. The results of these simulations are shown in Table 4.2-4. A good match of the field tests was obtained. The longest run-on time measured in these tests at Chattanooga was 1.0 second.

Also at Chattanooga several single TESLACO tests were made using the loads available in the PV houses where the tests were being made. The loads primarily used were resistive type such as incandescent lights, electric resistance heaters, and an electric range. One test was made with a window unit air conditioner (resistive and inductive type load). In all of these tests the total load within the island was balanced to the total generation by adding lab type resistance and capacitance to the loads in the PV house. The results of the tests are given in Table 4.2-3. In general these tests had shorter run-on times than the tests that utilized only lab type loads. The "real" loads tended to be more variable than the lab type loads, thereby making it harder to maintain a good match between load and generation.

Table 4.2-1 Single TESLACO Field Test Results at Shenandoah

	SPC		Load		Net to System		System Voltage (Volts)	Time of Interruption (MS after Voltage Peak)	Run-on Time (Seconds)
	Watts	Vars	Watts	Vars	Watts	Vars			
IA1V(s) Resistive load only. Watts load matched to watts generated.									
1.	2480	100	2280	0	200	100	231.6	8.3MS	1.232
2.	2600	96	2640	0	-40	96	234.6	6.5	.801
3.	2280	100	2600	0	-320	100	233.4	13.0	.392
4.	2560	100	2560	0	0	100	234.0	10.7	.845
5.	2920	100	2920	0	0	100	234.0	9.9	.731
6.	3040	100	3040	0	0	100	234.0	5.5	.817
IA2X(s) Resistive load only. Watts load 10% less than watts generated.									
1.	2960	90	2640	0	320	90	235.8	1.9	.906
2.	2800	95	2480	0	320	95	236.4	2.5	.857
3.	2560	100	2280	0	280	100	235.8	4.1	.807
IA3X(s) Resistive load only. Watts load 10% more than watts generated.									
1.	2560	130	2880	0	-320	130	228.6	0	.370
2.	2520	104	2800	0	-280	104	233.4	6.2	.433
3.	2760	112	3040	0	-280	112	233.4	15.0	.423

Table 4.2-2 Comparison of Computer Simulations To Single TESLACO Field Test Results at Shenandoah

	Field Tests		Computer Simulations					
			0		1		2	
	Net-To-System (W+jV)	Run-on Time (Sec.)	Net-to-System (W+jV)	Run-on Time (Sec.)	Net-to System (W+jV)	Run-on Time (Sec.)	Net-to System (W+jV)	Run-on Time (Sec.)
IA1V(s)								
1.	200+j100	1.232	200+j100	.436	200+j10	1.887	200+j20	1.104
2.	-40+j96	.801	-40+j96	.455	0+j50	.638	0+j30	.806
3.	-320+j100	.392	-320+j100	.281	-320+j70	.398	-280+j40	.515
4.	0+j100	.845	0+j100	.434	0+j30	.818		
5.	0+j100	.731	0+j100	.435				
6.	0+j100	.817	0+j100	.456				
IA2X(s)								
1.	320+j90	.906	320+j90	.476	320+j40	.709	360+j30	.818
2.	320+j95	.857	320+j95	.459				
3.	280+j100	.807	280+j100	.440				
IA3X(s)								
1.	-320+j130	.370	-320+j130	.397	-320+j60	.628	-280+j70	.594
2.	-280+j104	.433	-280+j104	.438				
3.	-280+j112	.423	-280+j112	.379				

Table 4.2-3 Single TESLACO Field Test Results at Chattanooga

	SPC		Load		Net to System		System Voltage (Volts)	Time of Interruption (MS after Voltage Peak)	Run-on Time (Seconds)
	Watts	Vars	Watts	Vars	Watts	Vars			
1A1V	Resistive load only; watts load matched to watts generation.								
1.	2720	50	2720	-14	0	64	241.0	9.9	.754
2.	2640	16	2640	-14	0	30	243.0	8.6	1.023
1A2X	Resistive load only; watts load 10% less than watts generated.								
1.	2640	10	2400	-14	240	24	243.2	0	.934
2.	2640	14	2400	-14	240	28	242.8	14.2	.953
1A3X	Resistive load only; watts load 10% more than watts generated.								
1.	2640	12	2920	-16	-280	28	242.8	8.6	.504
2.	2640	14	2880	-16	-240	30	242.6	4.9	.508
1A1VH	Resistive house loads; watts load matched to watts generation.								
1.	2626	-32	2537	-16	89	-17	242.8	4.9	.975
2.	2599	-36	2620	-57	-21	+21	243.0	0	.732
1A1VH	Resistive and inductive house loads; watts and var load matched to watts generation.								
1.	2479	-33	2337	-30	142	-3	242.4	16.0	.195
2.	2440	16	2375	141	66	-125	242.6	12.3	.266

Table 4.2-4 Comparison of Computer Simulations To Single TESLACO Field Test Results at Chattanooga

	Field Tests		Computer Simulations 0		Computer Simulations 1	
	Net-To-System (W+jV)	Run-on Time (Sec.)	Net-to System (W+jV)	Run-on Time (Sec.)	Net-to System (W+jV)	Run-on Time (Sec.)
IA1V						
1.	0+j64	.754	0+j64	.568	0+j44	.684
2.	0+j30	1.023	0+j30	.804	0+j15	1.004
IA2X						
1.	240+j24	.934	240+j24	.962		
2.	240+j28	.953	240+j28	1.147	240+j48	.822
IA3X						
1.	-280+j28	.504	-280+j28	.729	-280+j48	.570
2.	-240+j30	.508	-240+j30	.840	-240+j50	.690

4.3 Gemini Static Power Converter Field Tests

The purpose of the field tests was to verify the work done in the lab tests and simulations when the Gemini was operating with an actual PV array. The Gemini field tests were run in two locations. The first tests were at Georgia Power Company's Solar Research Center in Shenandoah, Georgia, where the Gemini was tested using the laboratory resistor boxes for loads. The second tests were at TVA's Energy Research Test Facility in Chattanooga, Tennessee, where the loads were normal home appliances and lighting. The results are given in Table 4.3-1. An effort was made to obtain a better "matched" case (for comparison with simulations) than had been achieved in the laboratory by trying to zero out the current transfer to the utility at the time the utility switch opened. This was done in two ways. First, a Dranetz 3105 power system analyzer was connected at the island/utility system interface and the load was adjusted to try to reduce the 60-Hz mismatch watts and vars to zero. There was also an oscilloscope connected to view the output current wave form to the system. The load was varied in an attempt to reduce the overall current magnitude including harmonics. The results in Table 4.3-1 indicate that these efforts were an improvement. In case G-I.A.1.b the voltage magnitude did not change and the frequency change was less than half of that seen in the lab.

Comparison of Field Tests and Lab Tests

The Gemini behaved in a similar manner in the field and lab tests. As explained earlier it is difficult to achieve an exact balanced condition with the Gemini SPC due to the harmonic current it produces. This was further complicated by the changing insolation conditions. The saturation of the step-down transformer was not as evident in the field tests. In the field tests the Gemini's reference voltage was set lower than it had been set in the lab due to a limited amount of power available from the PV array. This meant a good deal more dc current would need to be injected into the transformer before it began to saturate.

Table 4.3-1 Gemini Static Power Converter Field Test

CASE	OUT TO SYSTEM AMPS	STATIC POWER CONVERTER OUTPUT AMPS	VOLTS	WATTS	VARS	FREQ.	LOCAL LOAD WATTS	VARS	DC ARRAY VOLTS	AMTS	RUN-ON CYCLES
SHENANDOAH TESTS											
G-I Single Unit Gemini Static Power Converter											
A. Local Load at Power Converter Terminals											
1. Continuous Current Mode											
b. Resistive load matched to generation, capacitive load matched to supply Gemini's var requirement											
	4.48	24.8	234.0	2520	-5360	60	2520	-5360			INDEF.
	0	24.8	234.0	2480	-5200	61.2	2480	-5360			
c. Resistive load vs. generation, capacitive load matched to supply Gemini's var requirement											
4. Resistive load 10% less than generation											
	3.92	24.8	228.6	2520	-5120	60	2280	-5120			INDEF.
	0	25.4	239.4	2520	-5440	60.8	2480	-5500			
5. Resistive load 50% less than generation											
	6.8	25.2	238.8	2400	-5600	60	1240	-5600			INDEF.
	0	31.6	315.6	2280	-9120	63.1	2280	-9920			
d. Resistive load matched to generation, vary capacitive load vs. Gemini's var requirement											
5. Capacitive load 50% less than Gemini var requirement											
	14.4	24.8	228.6	2480	-5120	60	2480	-1600			1
TVA TESTS											
G-I Single Unit Gemini Static Power Converter											
A. Local Load at Power Converter Terminals											
1. Continuous Current Mode											
b. Resistive load matched to generation, capacitive load matched to supply Gemini's var requirement											
	5.0	-	235.6	2170	-6279	60.1	2197	-6271			INDEF.

Conclusions from Gemini Field Tests

The important results of the lab tests, which were confirmed in the field, are that the Gemini when operating in continuous current mode will run on indefinitely under certain load/generation conditions. Specifically, the tests show that the Gemini runs on if the watt load is equal to or less than generation and the local capacitive load can supply at least 60% of the vars that were required by the Gemini before the island was formed. Based on our knowledge of the Gemini control system the unit should also run on for loads greater than generation as long as the peak ac terminal voltage does not drop below 80% of its nominal value. A test was run to confirm this operation. A stable Gemini island was formed with the watt and var load approximately equal to the Gemini's watt output and var consumption. The Gemini was allowed to operate for several minutes. After this interval the watt and var loads were probably no longer matched to the generation. The load was then increased in 60-W light bulb increments and the Gemini shut down following the addition of the third bulb. Data were not being recorded during this part of the test, so no quantitative conclusions can be drawn. However, the test suggested that the Gemini can island when the load is initially greater than generation.

4.4 Combinations of TESLACO and Gemini Static Power Converter Field Tests

Several field tests were made involving combinations of TESLACO and Gemini static power converters at Chattanooga. Most of the tests involved only one TESLACO and one Gemini; however, one test included two TESLACOs and one Gemini and another test included two Geminis and one TESLACO. A summary of these tests is given in Table 4.4-1.

As indicated in Section 4.1 there are four houses with a PV array mounted on the roof at TVA's Energy Research Test Facility in Chattanooga. For these field tests TESLACO static power converters were located in houses 1 and 2 and Gemini static power converters were located in houses 3 and 4. All of the field tests were made with load and generation matched within the island. The loads used in these tests were mainly those located in the houses (incandescent lights, ranges, heaters), but some lab-type loads (variable resistor and capacitors) were used to balance load to generation more accurately. Tests 1A1 and 1A2 had the load at each house matched to the generation available at that house. Tests 1B1 and 1B2 had the load and generation at each house unbalanced, but had the load and generation within the island as a whole balanced. The run-on times for these four tests were very similar. They fell within the range of .86 seconds to 1.1 seconds.

As was true in the lab tests the TESLACO controlled the duration of the island. When it reached a 6° phase error and shut down, the Gemini was left connected to a load which was a little more than twice the power that it was

delivering. The voltage in the island therefore dropped and the Gemini shut down approximately one cycle after the TESLACO. All four of these tests had primarily resistive loads within the island. Tests 1C1 and 1C2 were similar to tests 1B1 and 1B2 except that some motor loads (attic fans) were included in the island. These tests ran on slightly longer than the resistive load tests. This could have been caused by having a different mismatch between load and generation because this mismatch could not be accurately controlled for these tests.

Test 4A was designed to have the load within the island (both real and reactive) matched to the output of the Gemini. The purpose was to see if the Gemini would continue to run on after the TESLACO shut down. This is exactly what happened. The initial load to total generation mismatch was so large that the TESLACO shut down in one cycle. The Gemini then ran on indefinitely.

Test 5A had two TESLACOs and one Gemini within an island with total load matched to total generation. Test 6A had two Geminis and one TESLACO within an island with total load matched to total generation. For both of these tests a TESLACO determined the duration of the island. When it shut down the load to generation mismatch became so large that the other static power converters shut within two cycles.

TABLE 4.4-1 Multiple SPC Islanding Field Tests With Both Teslaco and Gemini

CASE	DESCRIPTION	POWER OUT OF SPC (W+JV) HOUSE 1	HOUSE 2	HOUSE 3	HOUSE 4	NET TO SYSTEM (W+JV)	RUN-ON TIME (SEC) HOUSE 1	HOUSE 2	HOUSE 3	HOUSE 4
1A	ONE TESLACO, ONE GEMINI. WATT AND VAR OUTPUT OF EACH HOUSE MATCHED TO THE GENERATION OF ITS RESPECTIVE HOUSE. RESISTIVE TYPE LOADS.		2500 +J87	2290 -J6527		10 + J35		.861	.880	
			2440 +J89	2210 -J6415		-2 - J1		.975	.993	
1B	ONE TESLACO, ONE GEMINI. LOAD AT INDIVIDUAL HOUSES NOT MATCHED BUT TOTAL ISLAND LOAD MATCHED TO ISLAND GENERATION. RESISTIVE TYPE LOAD		2430 +J88	2210 -J6446		8 - J7		1.054	1.073	
			2420 +J109	2230 -J6431		-10 - J17		.966	.985	
1C	ONE TESLACO, ONE GEMINI. LOAD AT INDIVIDUAL HOUSES NOT MATCHED BUT TOTAL ISLAND LOAD MATCHED TO ISLAND GENERATION. INCLUDE MOTOR LOADS		2350 +J85	2170 -J6306		15 + J28		1.159	1.177	
			2360 +J81	2140 -J6309		-27 - J35		1.488	1.506	
4A	ONE TESLACO, ONE GEMINI. LOAD MATCHED TO GEMINI OUTPUT.		2280 +J40	2100 -J6351		2470 + J43		.015	RAN-ON	
5A	TWO TESLACOS, ONE GEMINI. LOAD MATCHED AT BOUNDARY.	2387 +J88	2100 +J33	1790 -J560		- 8 + J68	1.576	1.568	1.589	
6A	TWO GEMINIS, ONE TESLACO. LOAD MATCHED AT BOUNDARY.		2360 +J25	2040 -J1325	1580 -J198	87 - J114		1.074	1.091	1.100
			2360 +J25	2040 -J1325	1580 -J198	25 - J70		1.281	1.299	1.307

BLANK PAGE

V. Analysis of Results and Recommendations

The results obtained in the computer simulations and verified by lab and field tests can be used to assess the problems of islanding that a utility may have to face. There are several ways that potential islands may be formed. A breaker may be opened at a substation, which would isolate an entire distribution feeder network. A breaker may be opened out on a feeder, which would isolate a smaller section of distribution feeder. A disconnect switch or fuse may be opened, which would isolate a yet smaller section of feeder with anywhere from one to dozens of customers connected. A fourth way to form an island would be to open a fuse or disconnect switch on the primary side of a transformer serving one to four customers. The results of this research project are applicable to all four of these scenarios for forming an island. However, from a practical standpoint scenarios three and four would be of the most concern. For an island to form (not shut down immediately) there must be a reasonable balance between load and PV generation within the island. This implies that for scenarios one and two there is a very high penetration level of PV on a distribution feeder. This is not likely to happen in the near future. What is most likely to happen in the near future is a significant penetration on a localized basis. Therefore, the practical concern now would be for a small island.

If a breaker or fuse is opened to isolate a section of the distribution system because of a fault, and PV systems are connected to the faulted phase, the PV systems will be shut down by low voltage sensing circuits. If the PV system is connected to an unfaulted phase, the potential for islanding may

exist. Depending on the utility system conditions, the voltage on an unfaulted phase during a phase-to-ground fault can be higher than normal and may cause an immediate shutdown. Another method of creating a potential island would be for a breaker to open because of misoperation or a fuse to open because of aging. These would not be very likely occurrences. Probably the most common way for a potential island to be formed would be for a utility lineman to open the breaker switch or fuse in preparation for some kind of maintenance or construction activity. This would also be the case of maximum concern for personnel safety.

5.1 TESLACO Static Power Converter

The potential for having an indefinitely long islanding condition for a properly functioning TESLACO is nil. The device is designed to be unstable for the loss of utility condition and to shut itself down. All simulations, lab tests, and field tests support the fact that a properly functioning TESLACO will not island indefinitely. One of the TESLACOs tested in the lab was not functioning properly. One of the capacitors in the phase-locked loop had a capacitance at the boundary of its allowable range (-20% to +20%). This enabled the TESLACO to run on indefinitely in an island with a load that was matched fairly well to generation. When the circuit board with the phase-locked loop on it was replaced in the lab, the TESLACO behaved as the other TESLACOs did - no indefinite runon no matter how closely the load was matched to the generation. This experience suggests the need for manufacturers of static power converters to test the units for islanding as part of their factory testing.

Although the TESLACO will not island indefinitely, it can run on for a few seconds under certain conditions. The boundary conditions for run-on have been defined by the computer simulations made for this project in terms of watt and var mismatch between load and generation within the island. If the watt mismatch within a potential island is greater than 40% of the amount of PV generation, the TESLACOs will shut down within about two cycles. Another way of stating this is that if the amount of PV generation (with TESLACO static power converters) is not within 70% to 170% of the amount of load within the potential island, then the PV generation will be shut down within about two cycles. If the PV generation is within these boundaries, then the run-on time can be anywhere from a few cycles to a few seconds (less than four).

If the var mismatch within a potential island is greater than approximately 800 vars per TESLACO within the island, then the units will shut down in approximately two cycles. Since a TESLACO can supply as much as 100 vars to the system (for some operating conditions), this means that if the net var load within a potential island is greater than 900 times the number of TESLACO static power converters within the island, the units will shut down within about two cycles. If the net var load is less than this amount, the units may have run-on times that can range from a few cycles to a few seconds (less than four).

There are several factors that will affect where the run-on times will fall within this range. Smaller watt and var mismatches will tend to increase run-on time. Loads that are composed of a number of motors with a great deal of inertia will tend to produce longer run-on times. However, even if several

of these factors combine unfavorably to produce a long run-on time, this time will not exceed a few seconds. From a practical standpoint, the run-on time will be in the lower end of this range. Although one lab test had a 3.8 second run-on time, the longest run-on time that could be consistently achieved in the lab was around 1.6 seconds. It occurred when the load was intentionally matched to generation as closely as possible. This kind of balance between load and generation is just not likely to happen out on a utility system. Therefore, for the vast majority of potential islanding situations on a utility system, the run-on times will be less than 1.5 seconds.

From a safety standpoint, run-on times of a few seconds will not be a concern. If the island is initiated by a lineman opening a switch in preparation for performing maintenance, then the lineman need only wait a few seconds (approximately 10 seconds to be on the conservative side) before coming in contact with the circuit.

The other concern for islanding has been for the transients that may be produced upon reclosure of a feeder still energized by PV generation. Because reclosing times for distribution feeders can be on the order of 12 to 30 cycles, TESLACO static power converters could keep a circuit energized for some load conditions long enough for reclosure to take place. However, as pointed out earlier, the TESLACO's control circuitry shuts the unit down when its internal reference wave is out of phase with its terminal voltage by 6°. This means that if an island is sustained long enough for reclosure to occur, it will not be very far out of phase with the system. Therefore, the transients produced by reclosing will be of no concern.

5.2 Gemini Static Power Converter

The potential for having a sustained islanding condition for the Gemini converter is greater than that for the TESLACO. There are two requirements the local load must meet to produce a sustained island. The most critical element of the local load is capacitance. The local load must be able to supply at least 60% of the Gemini's pre-island reactive power requirement. If the load cannot supply any reactive power, the unit will shut down in one cycle due to a commutation failure. If the local load supplies less than 60% of the before-island reactive power the unit shuts down within three cycles due to a transient low-voltage condition. The second restriction is that the local load must not be greater than 130% of the PV generation in the island. Local loads greater than 130% will cause the unit to shut down in less than five cycles due to a low voltage condition. If these two conditions are satisfied the unit can run on indefinitely.

All of our original simulations ran on indefinitely regardless of the mode of current operation (continuous or discontinuous). For the lab and field tests in which the unit was in continuous mode of operation and satisfied the load restrictions given above, the unit ran on indefinitely. Small changes in insolation and loading did not affect the indefinite run on. In the lab and field tests the unit shut down in less than 15 cycles for all cases when operating in discontinuous mode. The shutdown was the result of a low-voltage condition that appears to be due to saturation of the output transformer caused by a dc offset in the output voltage. Several simulations were performed that indicated the time to shut down is dependent on two parameters unique to each individual unit: the amount of dc offset and the 350/240-V

step down transformer saturation characteristics. In the ideal case in which there is no dc offset, simulations predict that the discontinuous mode cases would result in long (at least several minutes) if not indefinite run-on times.

The load restrictions that result in indefinite run-on situations are realistic. Line-commutated converters have a fairly low power factor (around .5-.8). Most utilities will either install power-factor correcting capacitors on the distribution feeder or require the customers to install power-factor correcting capacitors that will satisfy their capacitive load requirement. Georgia Power Company has a requirement for cogenerators that the combined power factor for generation and load be .85 or greater. Therefore, it is realistic to consider capacitance within a potential island. In the field test with realistic house loads, it was not difficult to produce indefinite runon with the Gemini.

The window of loads that could result in islanding would be greatly reduced with the addition of two types of protective relaying circuits which are offered by the manufacturer but were not purchased for the units tested. The voltage magnitude was being checked for low voltage. If a high-voltage situation (greater than 10%) were also checked, it would provide shutdown for cases in which: the PV generation were large in comparison to the load; the local capacitance were large in comparison to the Gemini var requirement; and the unit were on an unfaulted phase during a single-phase fault on another phase of the feeder. The second check that should be made is frequency of the ac terminal voltage. The frequency of the island voltage will deviate

from 60 Hz based on the var mismatch when the island is formed. Over/under frequency relays are normally set to detect frequency variation of less than 1 Hz. Our simulations indicate that deviations of 1 Hz are achieved if the var mismatch is greater than $\pm$ 3% of the island var load. The use of a frequency relay would greatly reduce the probability of real-world islanding. It was difficult to control the var flow in the lab to obtain the $\pm$ 3% var mismatch. With the addition of these two features, the window of load/generation combinations that result in indefinite run-on conditions would be reduced to a near exact match of reactive power and $\pm$ 25% of real power.

From a safety standpoint, even with the additional protection described above, it would be theoretically possible for the unit to continue operating indefinitely in an island. Therefore, extreme caution should be used before making contact with the circuit.

The other concern for islanding is the transients, which might be produced following reclosure of a feeder that has remained energized by PV generation. Reclosing times for distribution feeders can be on the order of 12 to 30 cycles. Without the addition of over/under frequency relays the possibility of reclosing when the utility system and island voltages are very much out of phase is possible and might result in significant transients. If over/under frequency relays are used, the likelihood of reclosing out of phase is reduced, but may still exist for shorter reclosure times. It is common for the over/under frequency relays to be set so that the frequency must be out of range for 12 cycles before tripping the unit off. Therefore, the issue of reclosing may deserve some future consideration.

5.3 Combinations of TESLACO and Gemini Static Power Converters

The possibility exists for having a sustained islanding condition when both TESLACOs and Geminis are in the island. The TESLACOs will not run on indefinitely. Their behavior in an island with Geminis is very similar to their behavior in an island with only other TESLACOs. With their run-on times depending primarily on the load and generation mismatch within the island, the TESLACOs will always shut down. When they shut down, the resulting load-to-generation mismatch will determine what happens to the Geminis. At this point the behavior of the island becomes the same as has been described in Section 5.2 for only Geminis in an island. If the load vars can supply 60% or more of the reactive power requirement of the Geminis and the load watts are less than 130% of the power produced by the Geminis, then the island will be sustained indefinitely. Therefore, if a utility is concerned about the possibility of a sustained island that contains both TESLACOs and Geminis, the load and generation mismatches need to be checked in terms of the Geminis without regard to the TESLACOs. No evidence was found in simulations, lab tests, or field tests indicating that having a Gemini in an island with a TESLACO will make the TESLACO run on longer than it would without the Gemini. Also no evidence was found to indicate that having a TESLACO in an island with a Gemini would produce significantly different run-on times from those with only a Gemini.

The possibility of having a sustained island when both TESLACOs and Geminis are in the island can be greatly reduced by using over/under frequency relays and overvoltage relays with the Geminis. With these additions the boundary conditions for a sustained island would be reduced to those described in Section 5.2 for Gemini-only islands.

REFERENCES

[1] R. L. Das, J. W. Klein, T. W. Macie, Distributed Photovoltaic Systems: Utility Interface Issues and their Present Status, U.S. Department of Energy, September 1982.

[2] M. Hassan, J. Klein, Distributed Photovoltaic Systems: Utility Interface Issues and their Present Status, U.S. Department of Energy, September 1981.

[3] James B. Patton, Systems Control Inc., Interconnecting dc Energy Systems: Responses to Technical Issues, Systems Control Inc., June 1983.

[4] R. Bright, R. Leigh, T. Sills, Photovoltaic and Electric Utilities, Technology and Data Division Brookhaven National Laboratory, December 1981.

[5] D. P. Carroll. G.E. Gareis, P.C. Krause, C. M. Ong, R. J.Schwartz, O. Wasynczuk, Dynamic Simulation of Dispersed Grid-Connected Photovoltaic Power Systems: Task 1-Modeling and Control, SAND83-7108, Sandia National Laboratories, Albuquerque, 1983.

[6] O. Wasynczuk, D. P. Carroll, G. E. Gareis, P. C. Krause, C. M. Ong, R. J. Schwartz, Dynamic Simulation of Dispersed, Grid-Connected Photovoltaic Power Systems: System Studies, SAND83-7019, Sandia National Laboratories, Albuquerque, 1985.

[7] Islanding Experiments on Grid Connected Photovoltaic Systems - Part of a Sandia/Utilities Research Project, Georgia Power Company, February 1985.

[8] T. S. Key, Baseline Specification of a Utility-Interactive, Power-Conditioning Subsystem for residential Photovoltaic System Applications, SAND82-0290, Sandia National Laboratories, Albuquerque, 1982.

[9] T. S. Key, "Evaluation of Grid Connected Inverter Power Systems: The Utility Interface," IEEE Transactions on Industrial Applications, July/Aug., 1984.

[10] Ward Bower, Baron Brumley, Ben Petterson, Tom Key, Performance and Evaluation of Single-Phase Utility-Interactive Power Conditioners for Photovoltaic Applications, SAND83-1802, Sandia National Laboratories, Albuquerque, 1984.

[11] R. L. Steigerwald, et al., General Electric Company, Investigation of a Family of Power Conditioners Integrated Into the Utility Grid, Category 1-Residential Power Conditioner, SAND 81-7031, Sandia National Laboratories, Albuquerque, 1982.

[12] R. L. Steigerwald, et al., General Electric Company, Investigation of a Family of Power Conditioners Integrated Into the Utility Grid, Category 2-Intermediate Power Conditioner, SAND 81-7042, Sandia National Laboratories, Albuquerque, 1981.

[13] M. A. Slonim, E.K. Stanek, A. F. Imece, Analysis of Inverter Models and Harmonic Propagation Part 1: A Physical Simulator for Large Solar Cell Array, SAND83-7060/1 of 3, Sandia National Laboratories, Albuquerque, 1984.

[14] M. A. Slonim, E.K. Stanek, A. F. Imece, Analysis of Inverter Models and Harmonic Propagation, Part 2: Harmonic Propogation, SAND83-7060/2 of 3, Sandia National Laboratories, Albuquerque, 1984.

[15] M. A. Slonim, E.K. Stanek, A. F. Imece, Analysis of Inverter Models and Harmonic Propagation, Part 3: Transient Processes in Inverter Models, SAND83-7060/3 of 3, Sandia National Laboratories, Albuquerque, 1984.

[16] S.B. Dewan, A Straughen, Power Semiconductor Circuits, John Wiley & Sons, Inc., New York, 1975, pp 79-84.

[17] SCR MANUAL, 6th Ed., General Electric Company, 1979.

[18] Introduction to Solid State Power Electronics, Westinghouse Electric Corp., 1977.

[19] W. Bower, F. B. Brumley, B. Petterson, Engineering Evaluation Summary Reports for TESLACO Utility-Interactive Residential Photovoltaic Power Conditioning Subsystems, SAND 83-2602, Sandia National Laboratories, Albuquerque, 1985.

[20] W. Bower, F. B. Brumley, B. Petterson, Engineering Evaluation Summary Reports for APCC Utility-Interactive Residential Photovoltaic Power Conditioning Subsystems, SAND 83-2601, Sandia National Laboratories, Albuquerque, 1985.

[21] W. Bower, F. B. Brumley, B. Petterson, Engineering Evaluation Summary Reports for DECC Utility-Interactive Residential Photovoltaic Power Conditioning Subsystems, SAND 83-2317, Sandia National Laboratories, Albuquerque, 1984.

[22] EMTP Rule Book, EPRI, 1987.

[23] Donald G. Fink, Standard Handbook for Electrical Engineers, Section II, Mc Graw Hill, 1978, pp. 28-32.

[24] Alan Cocconi, Slobodan Cuk, "High Frequency Link 4 kW PV Inverter for Utility Interface," 4th PV Sys. Integ. Conf., 1983.

[25] Alan Cocconi, et al., "High-Frequency Isolated 4kW Photovoltaic Inverter for Utility Interface," Power Conversion International, May 1984.

[26] R. Best, Phase-Locked Loops: Theory, Design and Applications, AG Sandoz Ltd, 1984.

[27] O. Wasynczuk, P. C. Krause, Computer Modeling of the American Power Conversion Corporation Photovoltaic Power Conditioning System, SAND87-7006, Sandia National Laboratories, Albuquerque, 1987.

[28] Landsman, E. E., "Analysis and Test of Line-Commutated Inverter for Use in Residential Photovoltaic Power Systems," Proceedings of the 15th IEEE Photovoltaic Specialists Conference, pp. 627-635, Kissimmee, FL, May 12-15, 1981.

[29] Atmaram, G. H., Ayoub, A. H., Benton, J. and Bower, W., "Test Results of Islanding Experiments on Grid-Interactive Residential Power Conditioner," Proceedings of the 18th IEEE Photovoltaic Specialists Conference, pp. 1326-1335, Las Vegas, NV, October 21-25, 1985.

BLANK PAGE

A. APPENDIX A - PHOTOVOLTAIC ARRAY MODEL

The smallest unit of a photovoltaic array is the solar cell. Its output current-voltage characteristics depend on the operating temperature and the amount of solar insolation. The circuit shown in Figure A-1 was used to model a single solar cell. The current source and the diode in the model represent the photocurrent and the solar pn junction characteristics, respectively. Series and shunt resistances, which are sometimes shown in solar cell models, were assumed negligible and are not included in the model. Furthermore, the solar-cell series inductance and shunt capacitance were neglected since they produce PV array transient time constants that are extremely small when compared to the predicted system time constants.

The equations modeling a single solar cell in terms of cell voltage (V_{SC}) and the cell current (I_{SC}) are shown below [11,13].

$$I_{SC} = I_L - I_o\{\exp[qV_{SC}/(AKT)] - 1\}; \qquad \text{(A-1)}$$

$$I_o = I_{or}(T/T_R)^3\exp\{[E_g/(BK)][T-T_R]/[TT_R]\}; \text{ and} \qquad \text{(A-2)}$$

$$I_L = [I_{SCR} + K_1(T_C - 28.)]P_I/100, \qquad \text{(A-3)}$$

where

I_{SC} = Solar cell current [A]

V_{SC} = Solar cell voltage [V]

I_L = Light generated current [A]

I_o = Saturation current [A]

T = Solar-cell temperature [°K]

T_C = Solar-cell temperature [°C]

$K/q = 8.62 \times 10^{-5}$ eV/°K

P_I = Solar radiation [mW/cm^2]

I_{SCR} = Short-circuit current at 28°C and $100 mW/cm^2$
= 2.52 A

E_g = Band gap for silicon = 1.11 eV

T_R = Reference temperature = 301.18°K

I_{or} = Saturation current at $T_R = 19.963 \times 10^{-6}$ A

$A = B$ = Ideality factor = 1.92

K_1 = Short circuit current temperature coefficient
= 0.0017 A/°K.

For a fixed temperature, the saturation current I_o is constant. Assuming $T = T_R$,

$$I_o = I_{or} = 19.9693 \times 10^{-6} \text{ A};$$

$$\frac{q}{AKT} = \frac{1}{(8.62 \times 10^{-5})(301.18)(1.92)} = 20.06.$$

Thus,

$$I_{SC} = I_L - 19.9693 \times 10^{-6}[\exp(20.06 V_{SC}) - 1]; \qquad \text{(A-4)}$$

$$I_L = 2.52 P_I / 100. \qquad \text{(A-5)}$$

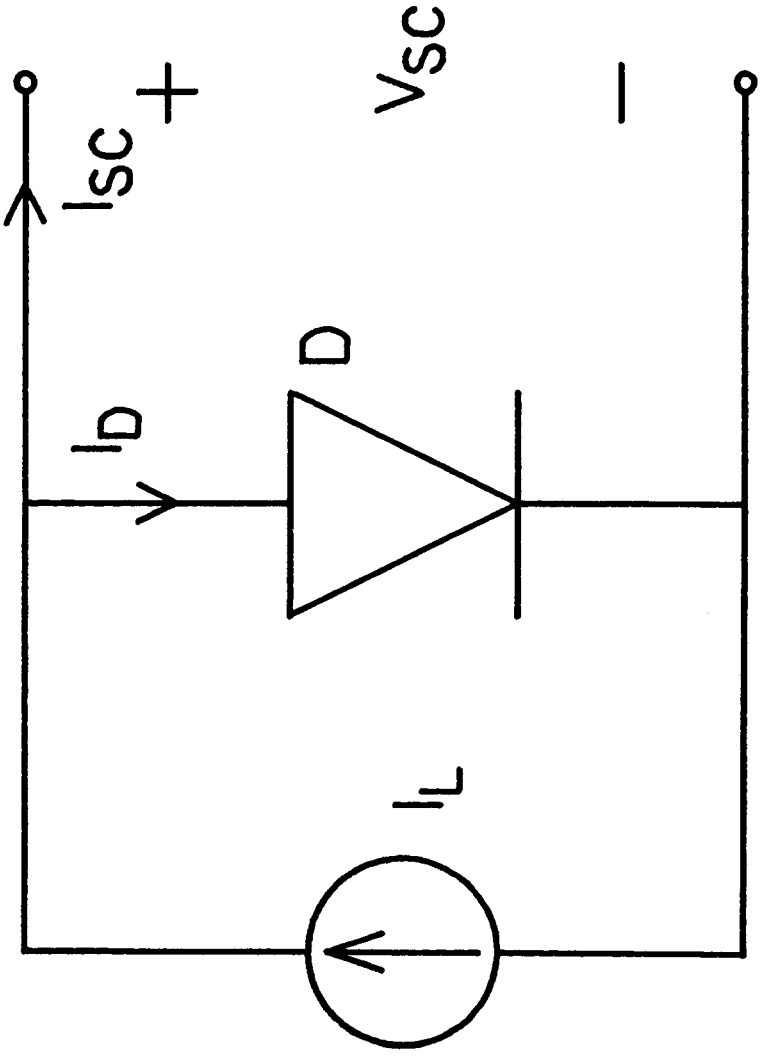

Figure A-1. Equivalent Model for a Solar Cell.

For P_I = 100 mW/cm^2, the voltage and current are 0.469 volts and 2.277 amperes at a maximum power of 1.068 watts. The corresponding short-circuit current is 2.52 amperes and the open circuit voltage is 0.585 volts. In order for the array to produce 4 kW at 200 Vdc and P_I = 100 mW/cm^2, the array must be composed of N_p number of parallel strings, where

$$N_p = 4000/200/2.277 = 8.78$$

and N_s number of series solar cells, where

$$N_s = 200/0.469 = 426.4$$

for a total of 3744 solar cells. The fact that N_s and N_p are not integers is of little consequence for the analytical studies. The photovoltaic array current-voltage characteristics may be approximated by aggregating the previous cell characteristics (Figure A-2). From Equation (A-1),

$$I_{PVA} = N_p I_{SC}$$

$$= N_p([I_L - I_o\{\exp[qV_{PVA}/N_s/(AKT)] - 1\}), \qquad \text{(A-6)}$$

where

I_{PVA} = Photovoltaic Array current [A], and

V_{PVA} = Photovoltaic Array voltage [V].

Therefore at $T = T_R$, $N_s = 426.4$, $N_p = 8.78$,

$$I_{PVA} = 22.12P_I/100 - 1.753x10^{-4}[\exp(V_{SC}/21.26) - 1]. \qquad (A-7)$$

It can easily be verified that at $P_I = 100$ mW/cm^2, the peak power voltage and current are 200 volts and 20 amperes, respectively. The open circuit array voltage is 249.5 volts.

When performing validation tests, the actual array current-voltage characteristics can be obtained by the method described in Carroll et al. [5].

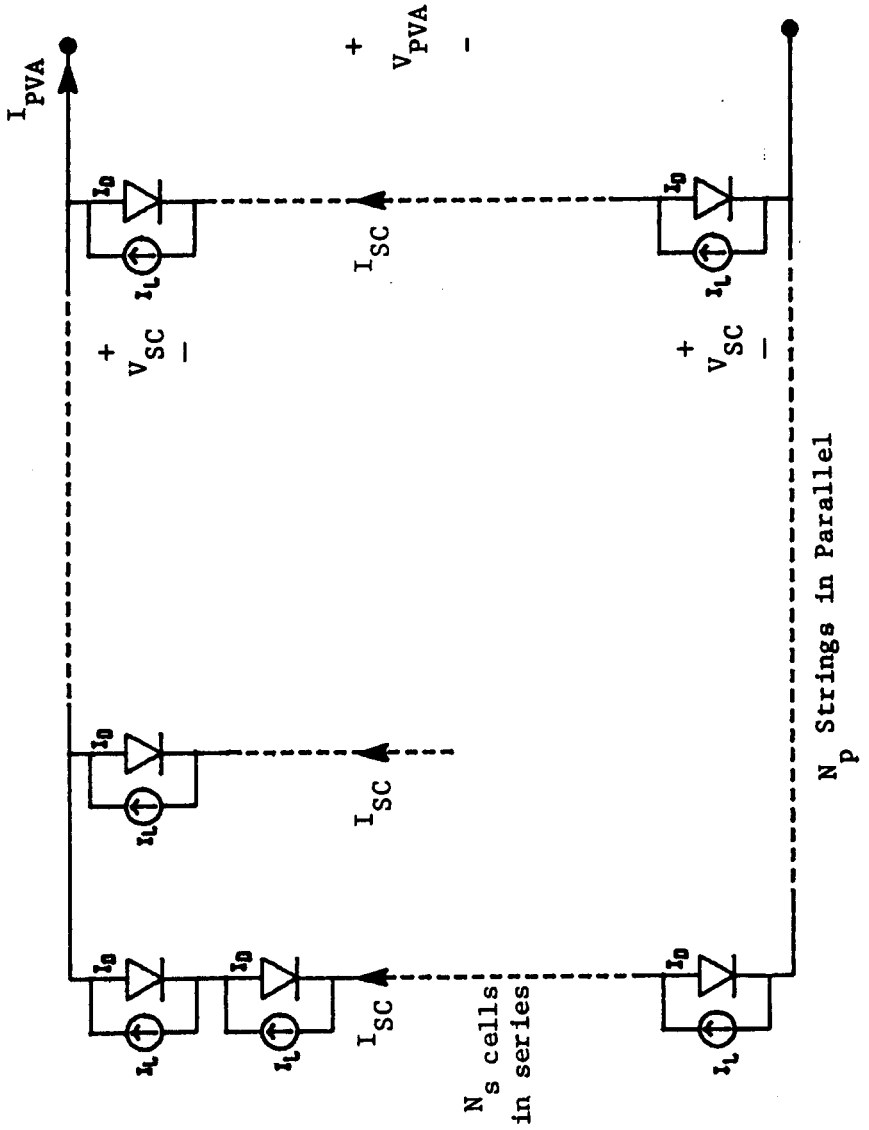

Figure A-2. Equivalent Model for a Photovoltaic Array.

B. APPENDIX B - TESLACO STATIC POWER CONVERTER MODEL

B.1. Description of the Model

The static power converter (SPC) is a single-phase, 240-V, 4-kW residential unit manufactured by the TESLACO company [24,25]. The operating principle is based on the high-frequency link approach in which the PV array voltage is pulse-width modulated and converted to high-frequency ac. The modulation on the voltage is such that after passing through a high-frequency transformer and full-wave diode rectifier, the waveform is a full-wave rectified sinewave at 2*60=120 Hz. The unfolder then inverts every other half cycle to form a full sine-wave voltage at the output terminals of the SPC [19]. Figure B.1-1 shows the power stage and control block diagram of the SPC and the expected waveforms at the critical points of the system. To simulate the operational performance of the SPC, the equivalent circuit shown in Figure B.1-2 was utilized. The analytical equations were developed for each section of the equivalent circuit and put into a form that could be implemented on the Electromagnetic Transients Program (EMTP). The model and the parameters for the model were supplied by Paul Krause and Associates. The parameters were based primarily on data obtained from the manufacturer. The detailed description of the model and the corresponding equations are provided in this section of Appendix B.

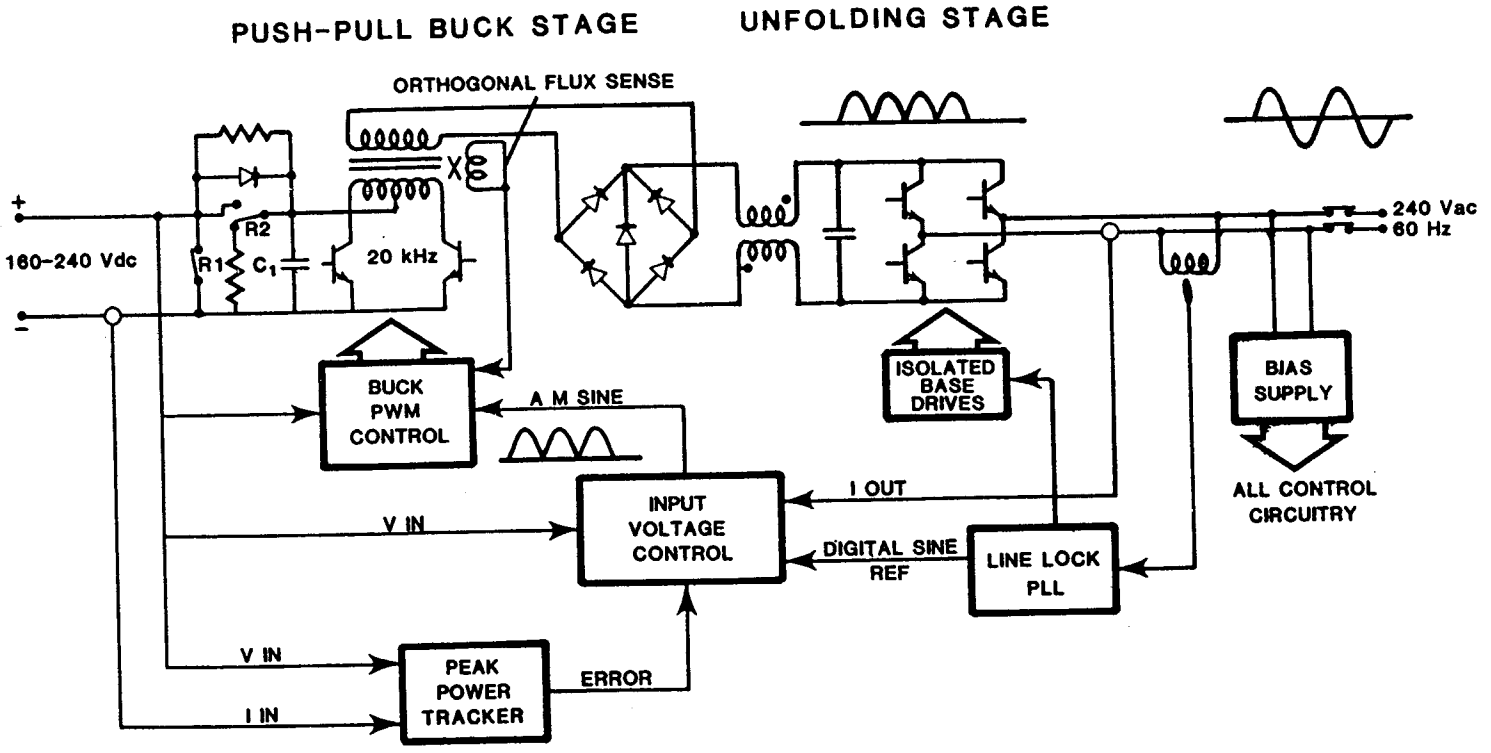

Figure B.1-1. Power Stage and Control Block Diagram for TESLACO High Frequency Link Static Power Converter.

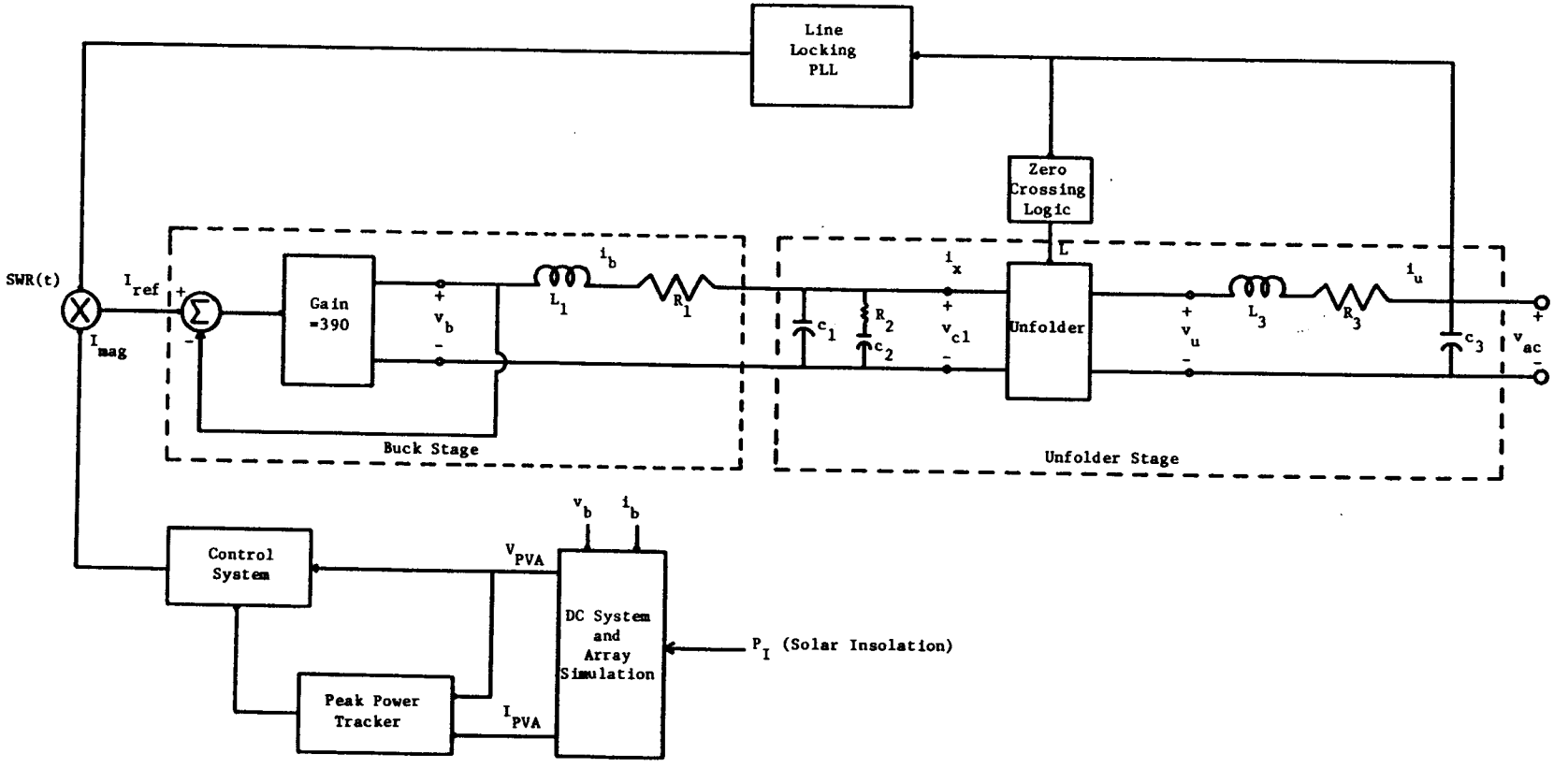

Figure B.1-2. Equivalent Circuit for the TESLACO Static Power Converter.

Buck Stage

The operation of the push-pull buck stage, including the high-frequency transformer and rectifier, is represented by a gain only. An equivalent block diagram of the buck stage, along with pertinent parameters is provided below (Figure B.1-3).

$$v_b = G(I_{ref} - 0.031*i_b)$$

$$= v_{c1} + L_1 di_b/dt + R_1 i_b; \qquad \text{(B.1-1)}$$

$$di_b/dt = (v_b - v_{c1} - R_1 i_b)/L_1, \qquad \text{(B.1-2)}$$

where

$G = 390$

$R_1 = 0.02$ ohms

$L_1 = 600$ uH.

Unfolder Stage

Figure B.1-2 shows the circuit diagram of the unfolder stage where L is a logic signal determined by a voltage zero crossing detector described later. In essence, L is high whenever $v_{ac} > 0$ and low when $v_{ac} < 0$. The action of the unfolder may be described by the following equations:

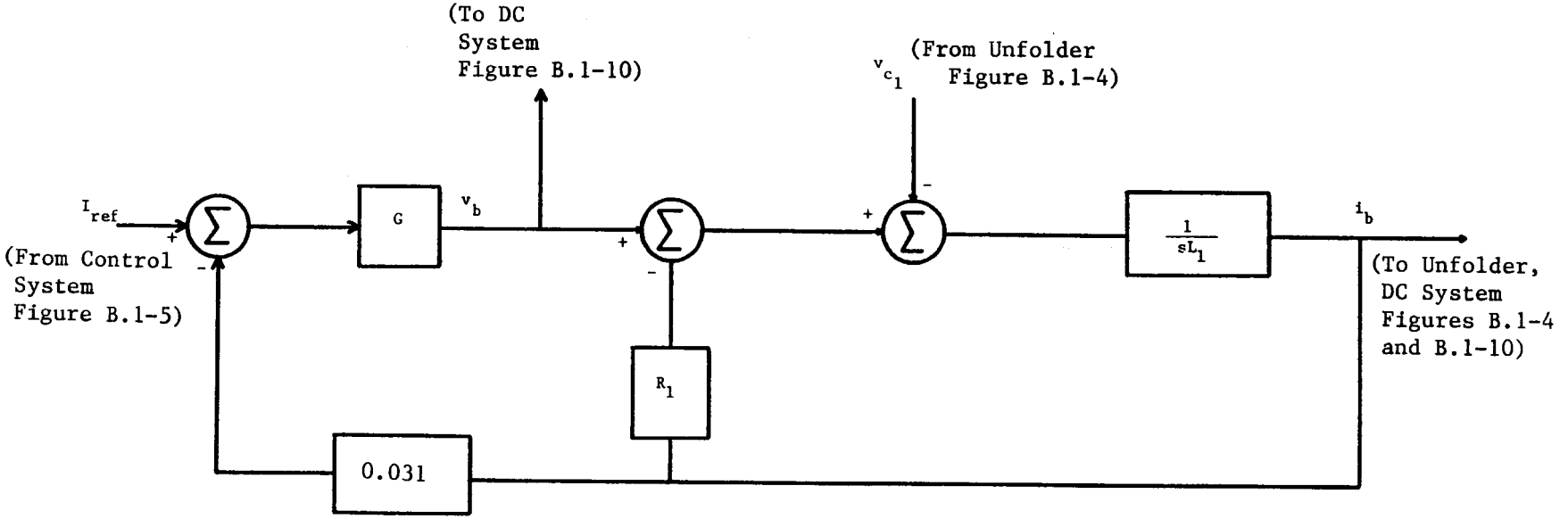

Figure B.1-3. Equivalent Block Diagram of Buck Stage.

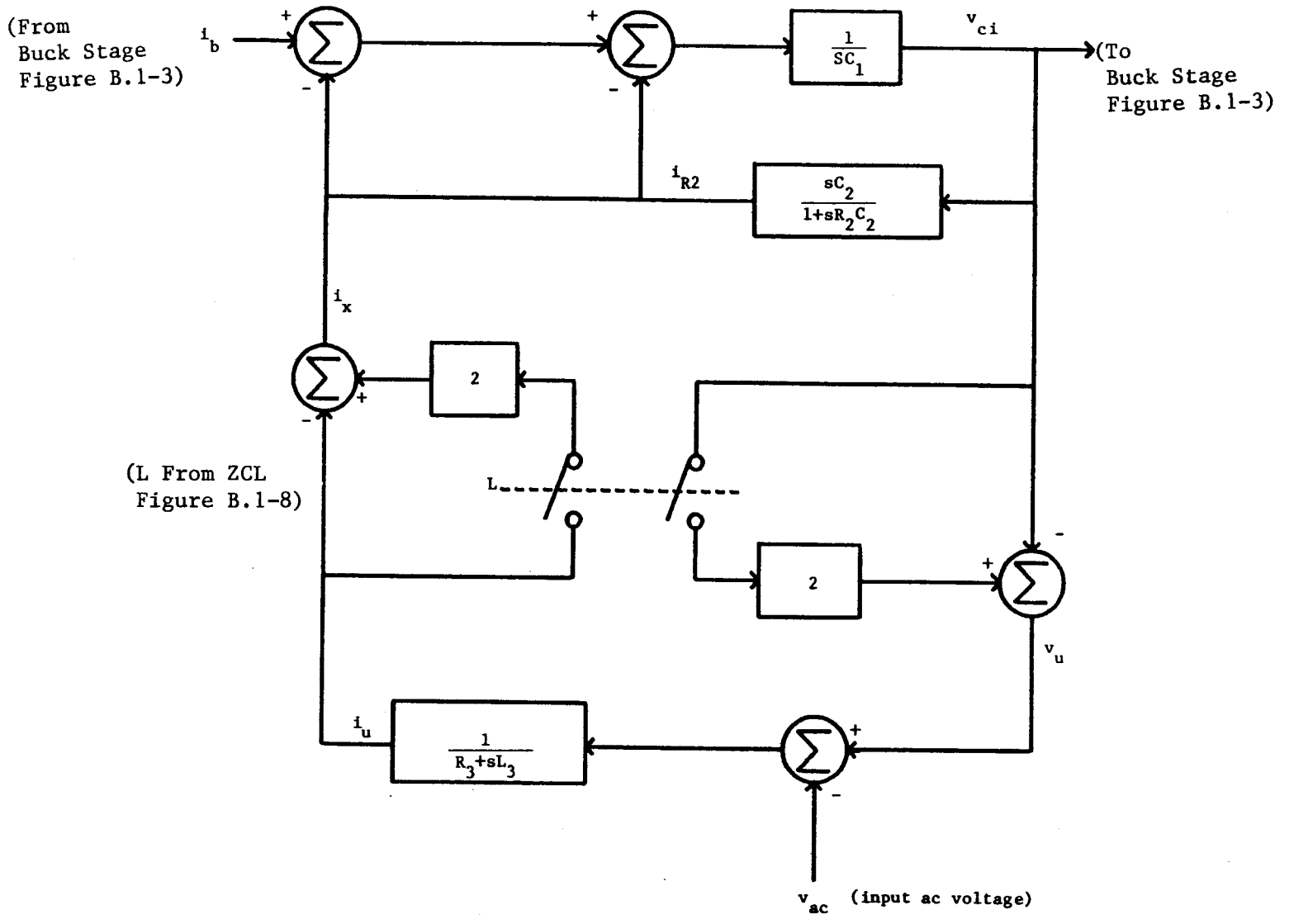

Figure B.1-4. Equivalent Block Diagram of Unfolder Stage.

When L = 1, $i_x = i_u$, and $v_{c1} = v_u$. (B.1-3)

When L = 0, $i_x = -i_u$, and $v_{c1} = -v_u$. (B.1-4)

An equivalent block diagram of the unfolder is provided in Figure B.1-4. The corresponding element values are shown below:

C_1 = 4.7 uF R_2 = 30 ohms

C_2 = 2.2 uF R_3 = 0.0075 ohms

C_3 = 1.0 uF L_3 = 200 mH

Control System

A functional equivalent model of the control system is presented in Figure B.1-5. Note that this diagram does not include the ac overcurrent and dc under/over voltage controls, which are not likely to be active during normal operation. During the experimental tests, the operating points were selected so that the operation was within the rating of the inverter which represents the common operating mode.

Line-Locking Phase-Locked Loop

A block diagram of the line-locking phase-locked loop (PLL) is depicted in Figure B.1-6.

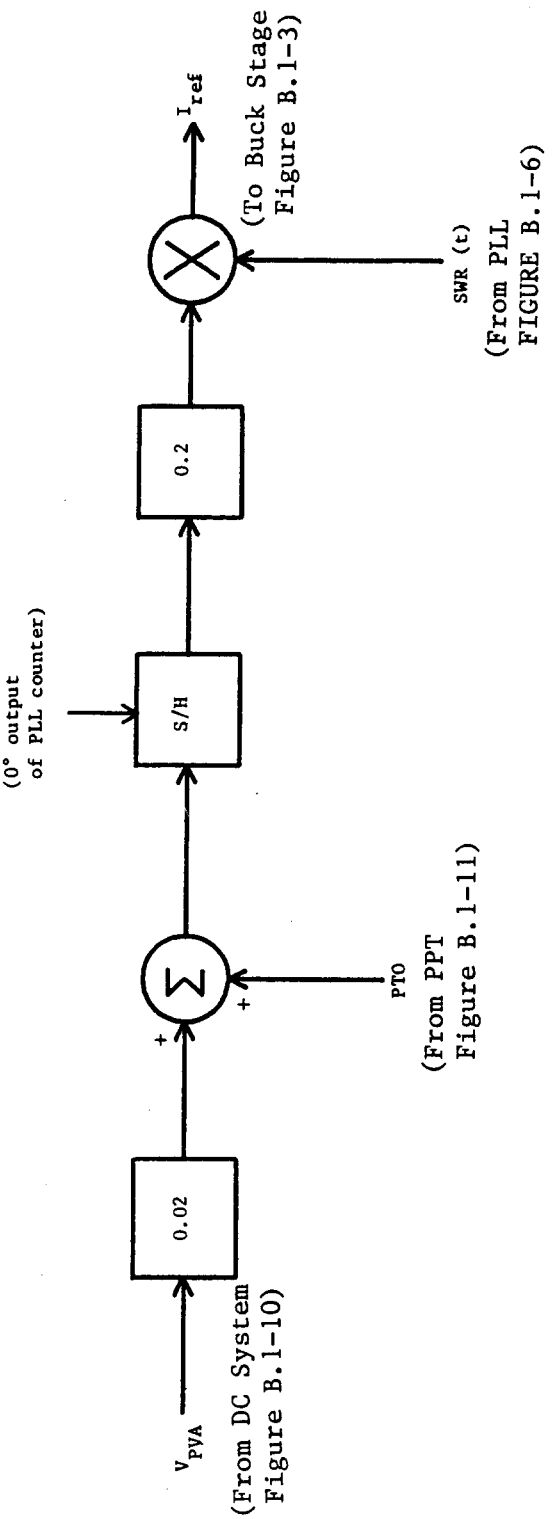

Figure B.1-5. Control System Block Diagram.

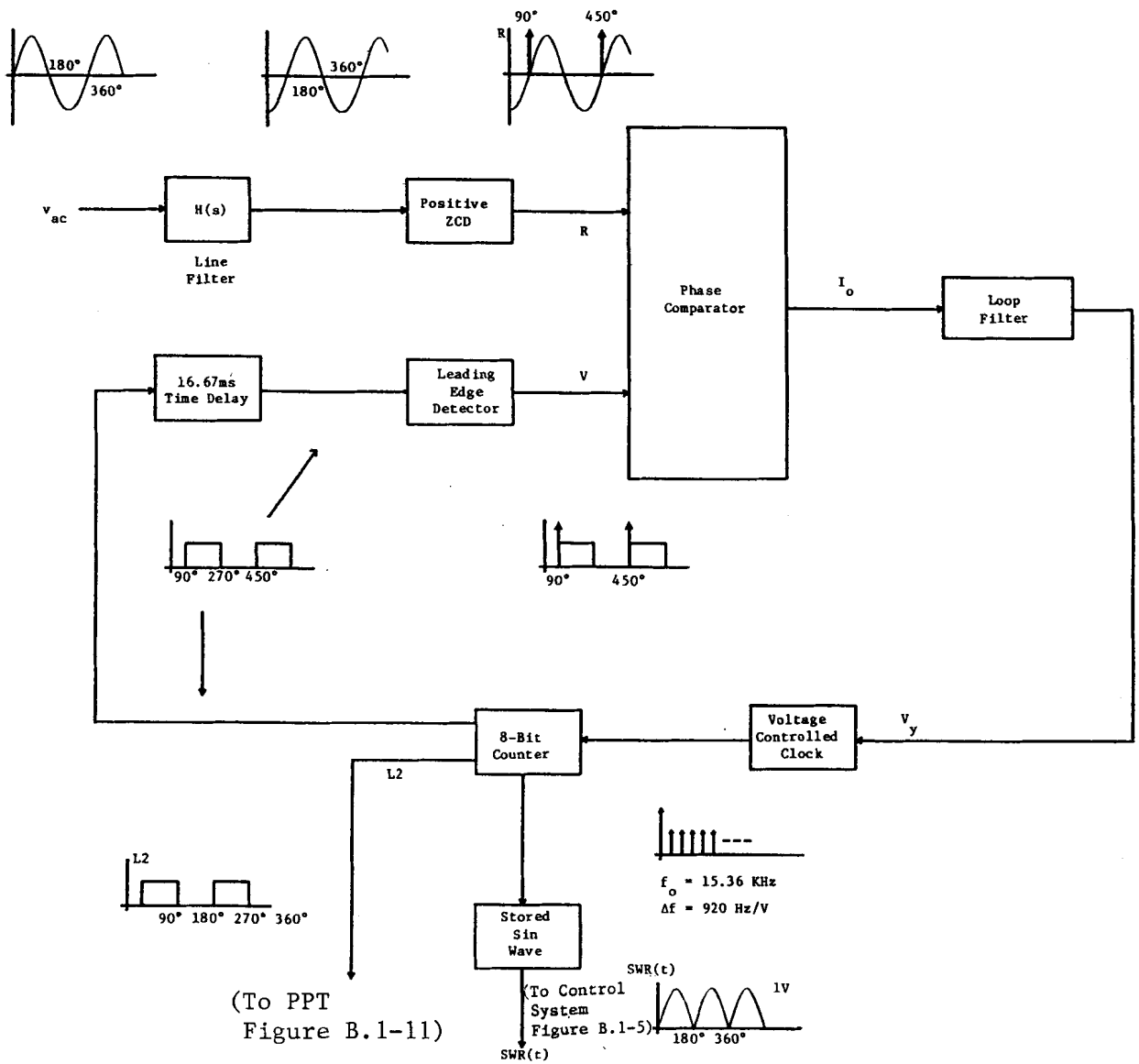

Figure B.1-6. Line Locking PLL Block Diagram.

Line Filter

The line filter transfer function is

$$H(s) = \frac{200.}{(s+5)} \times \frac{16119.}{(s+16119.)} \times \frac{s}{(s+4.26)} \quad . \qquad \text{(B.1-5)}$$

Note that $\underline{/H(j377)} = -90°$ (output lags input by 90°), and the magnitude of H(jw) is irrelevant since the output feeds a zero crossing detector.

Phase Comparator

The output of the phase comparator, I_o, is equal to +0.227 mA (-0.227 mA) during the period of time when the reference pulse, R, leads (lags) the pulse, V, and is zero otherwise. During steady-state operation at 60 Hz, R and V are in phase so that I_o is zero. An illustrative example follows (Figure B.1-7).

Loop Filter

The loop filter transfer function is

$$\frac{V_y(s)}{I_o(s)} = \frac{1.47 \times 10^5}{S} + \frac{33 \times 10^5}{(.00726S + 1)} \quad . \qquad \text{(B.1-6)}$$

Voltage-Controlled Clock (VCC)

If V_y = 0 volts, the VCC produces a pulse train at 15.36 kHz (60Hzx256). A non-zero V_y will produce a frequency deviation of delta f = 920 Hz x V_y volts, which represents an increase (decrease) if V_y is positive (negative). The action of the PLL is easily explained. If R leads V, the output of the phase comparator, I_o, becomes positive causing V_y to increase. This increases the frequency of the VCC, which causes the pulse, V, to occur earlier, as desired. The opposite situation occurs if R lags V.

Counter and Time Delay

The counter is an eight-bit (0-to-255) counter whose output increments by 1 at each input clock pulse. It is convenient to define a VCC angle as the angular equivalent of the counter output, i.e.,

$$Q_{VCC}(t) = \frac{\text{count}}{256} \times 360^\circ. \qquad \text{(B.1-7)}$$

In reality, $Q_{VCC}(t)$ changes at discrete increments of 360°/256 = 1.4°; however, this is small enough that $Q_{VCC}(t)$ can be considered a continuous variable for modeling purposes. In any case, the output of the counter defines the sine-wave reference, SWR, (stored in digital read only memory). In particular,

$$SWR(t) = \sin[Q_{VCC}(t)] \; . \qquad \text{(B.1-8)}$$

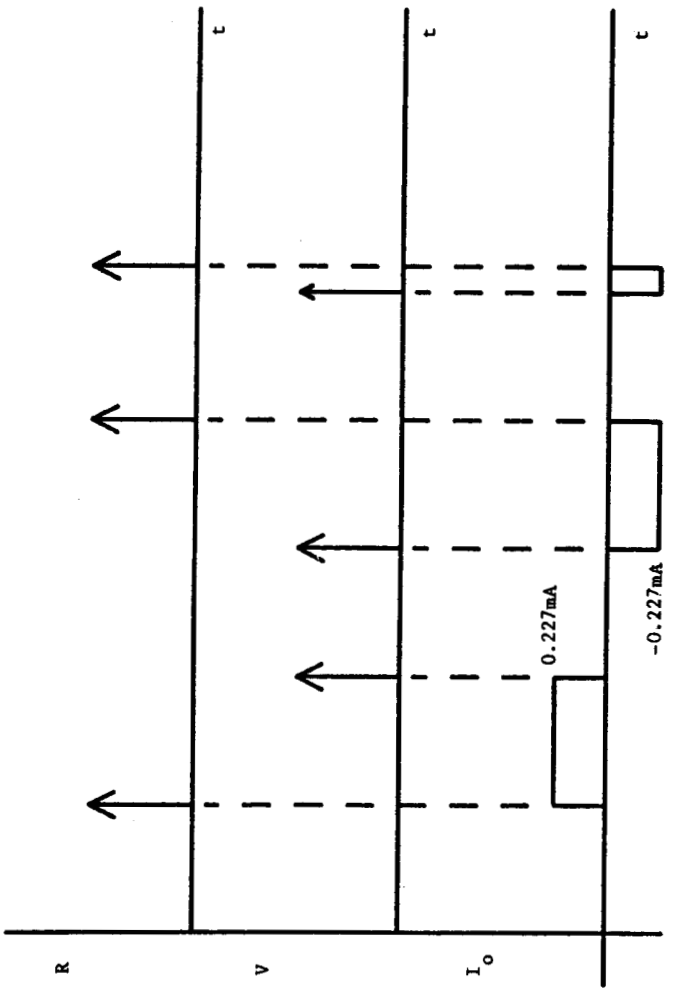

Figure B.1-7. Phase Comparator Input and Output Relationship.

A second output is provided that is equal to a logic "1" whenever 90° < Q_{VCC} (t) < 270°. This output is fed into a 16.667 mS time delay whose output at a given time, t, is equal to its input at t-16.667 mS. During steady-state operation at 60 Hz, this time delay is transparent since the phase shift between input and output is precisely one cycle. However, during isolated operation, when the system frequency may deviate from 60 Hz, the time delay is no longer transparent, with a frequency dependent phase shift occuring between the input and output. This phase shift is important since it serves to "destabilize" the system during isolated operation.

Zero Crossing Logic (ZCL)

A block diagram of the zero crossing logic used to control the unfolder is depicted in Figure B.1-8. All flip-flops (FF) are assumed to be edge triggerred. That is, the output changes state only on positive (0 to logic 1) transitions of the S and R inputs. By design, the positive transitions of S and R do not occur simultaneously.

As v_{ac} goes from negative to positive, the output of comparator 1 changes from 0 to 1, setting FF_1. The output of FF_1, in turn, sets L (FF_3) to 1. FF_1 is reset when v_{ac} falls below -4V thus preventing L from "bouncing" near the voltage zero crossings due to noise or harmonics. As v_{ac} goes from a positive to negative value, the output of comparator 3 goes high setting FF_2 which, in turn, resets FF_3 causing L to go to zero. FF2 is reset when v_{ac} exceeds +4V.

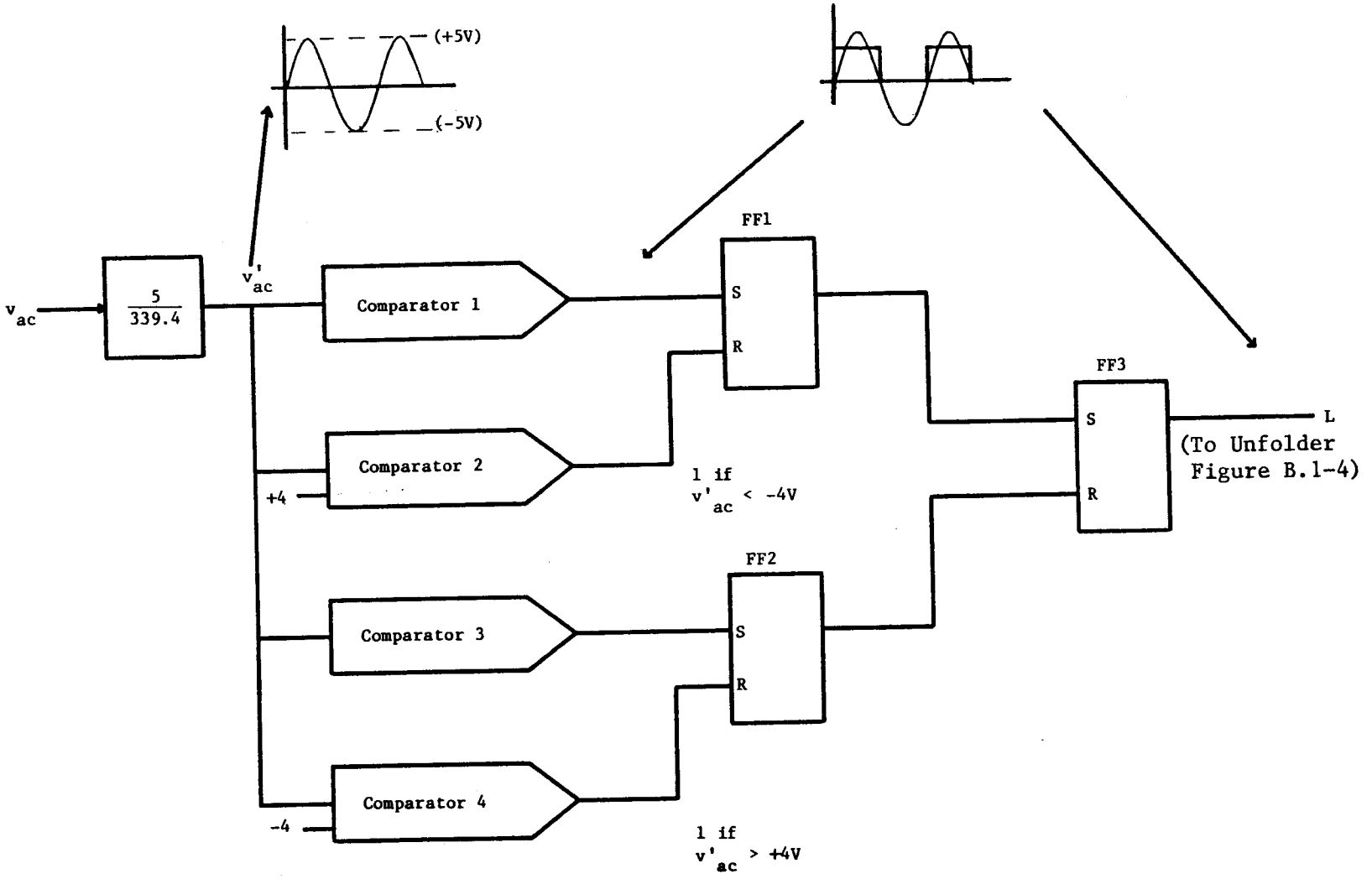

Figure B.1-8. Block Diagram of Zero Crossing Logic.

DC System

A circuit diagram of the dc system is shown in Figure B.1-9. Figure B.1-10 illustrates the corresponding simulation block diagram.

Peak Power Tracker (PPT)

Figure B.1-11 shows a block diagram of the peak power tracker, where, i_{PVA}, v_{PVA} represent the ripple components of I_{PVA}, V_{PVA}, respectively. The high pass filters used to extract the ripple components have the transfer function

$$HP(s) = \frac{s^2}{s_2+200s+40000} \times \frac{s}{s+5}$$
$$= \frac{s^3}{s^3+205s^2+41000s+20000} . \qquad \text{(B.1-9)}$$

A shared multiplier is used to calculate $I_{PVA}\ v_{PVA}$ and $V_{PVA}\ i_{PVA}$. The output of the multiplier is equal to $I_{PVA}\ v_{PVA}$ 50% of the time and $V_{PVA}\ i_{PVA}$ for the remaining 50%. The switching rate between these values is 4 kHz.

The output of the multiplier is connected to an automatic gain controlled (AGC) amplifier, which controls the gain so that the peak output voltage is 1.5 V. A possible computer representation of the AGC amplifier is depicted in Figure B.1-12.

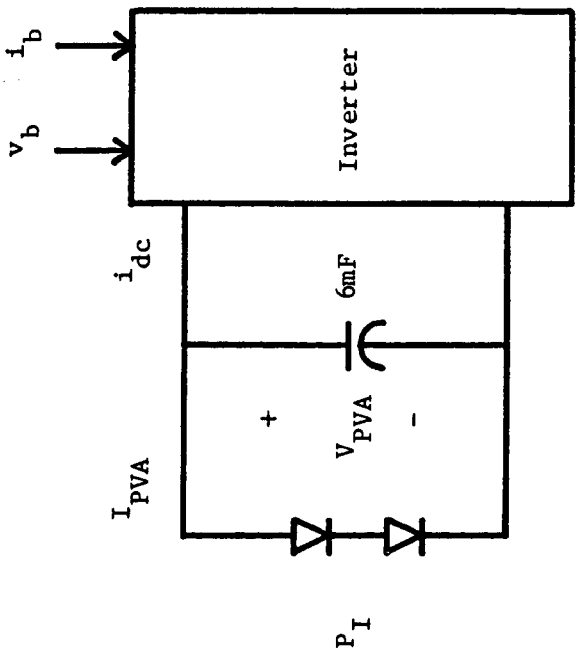

Figure B.1-9. Circuit Block Diagram of DC System.

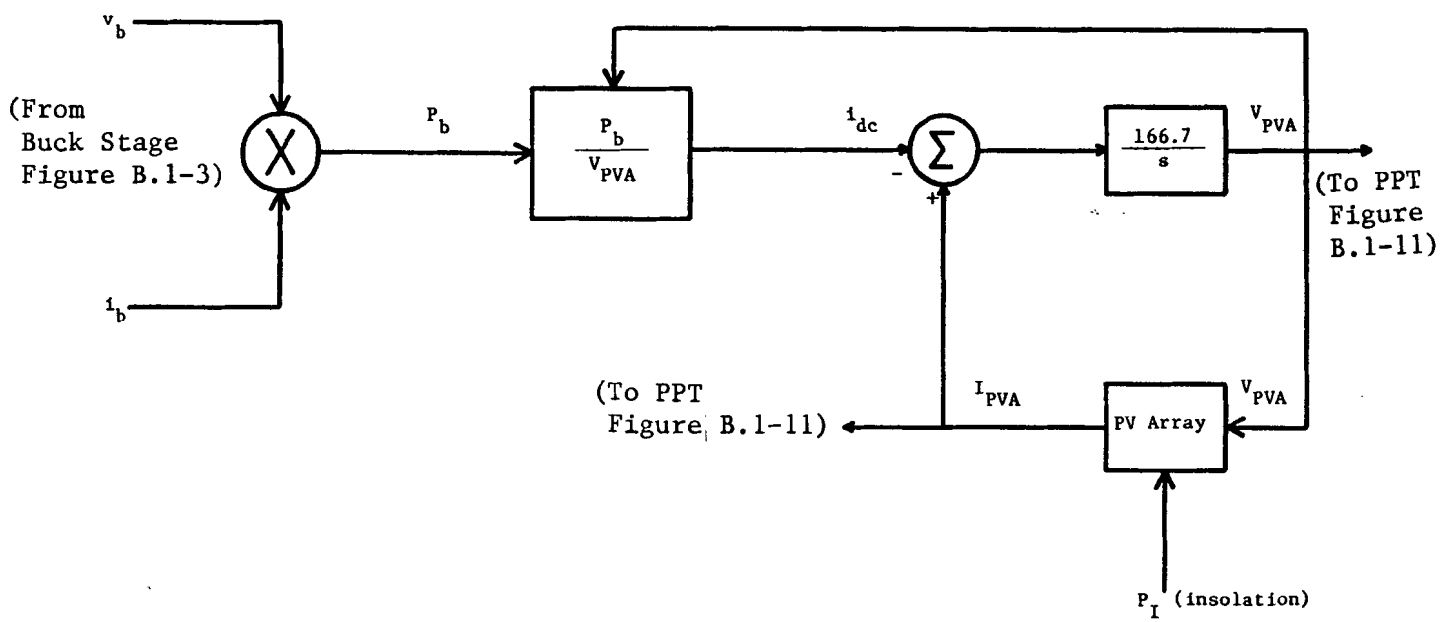

Figure B.1-10. Simulation Block Diagram of DC System.

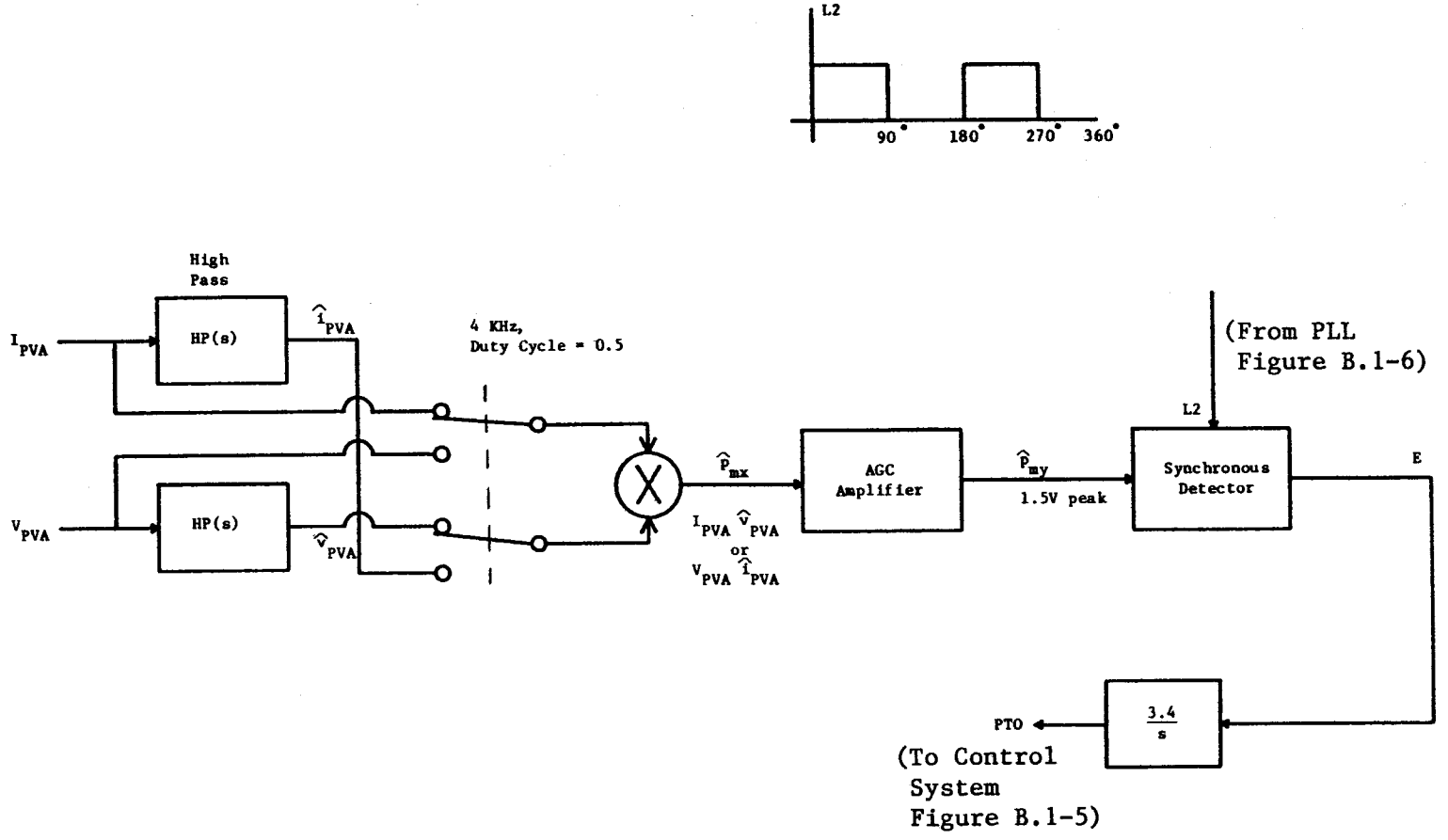

Figure B.1-11. Block Diagram of Peak Power Tracker.

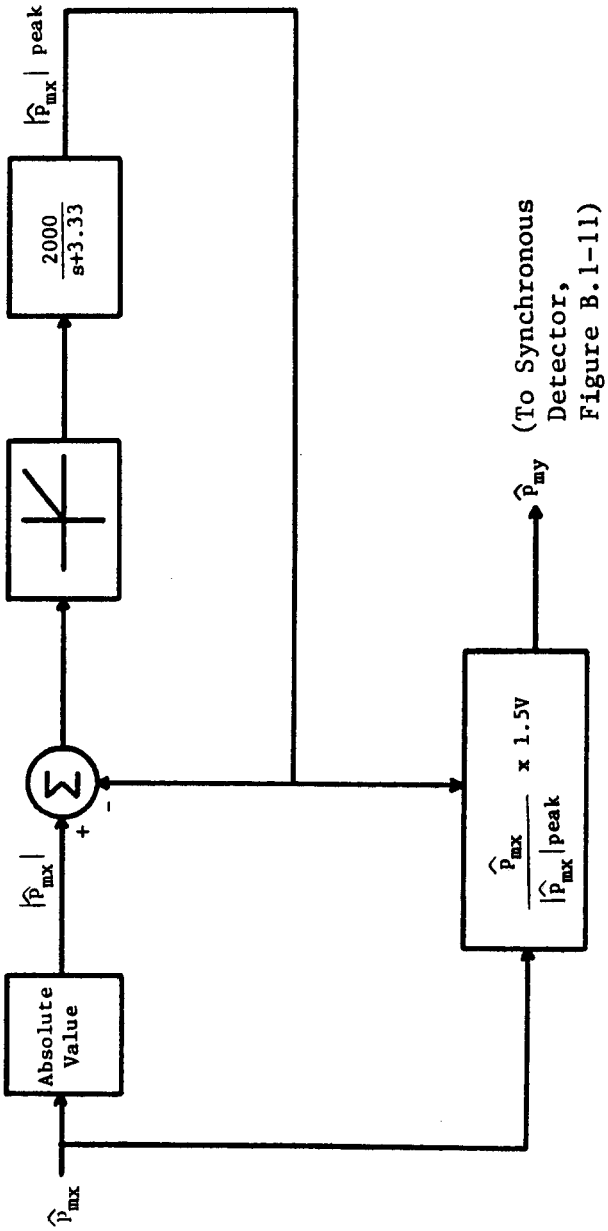

Figure B.1-12. Computer Representation of AGC Amplifier.

In the steady state, p_{mx} and p_{my} appear identical except that p_{my} is scaled so that its peak value is 1.5 V. This signal is then fed into a synchronous detector (Figure B.1-11). Basically, the output of the synchronous detector, E, is equal to $+p_{my}$ whenever the logic signal L_2 is high and $-p_{my}$ when L_2 is low. L_2 is determined by the counter associated with the PLL, (Figure B.1-6) i.e.,

$$L_2 = 1 \quad \text{when} \quad 0° < Q_{VCC}^{(t)} < 90°$$

$$\text{or} \quad 180° < Q_{VCC}^{(t)} < 270°; \qquad \text{(B.1-10)}$$

$$L_2 = 0 \quad \text{otherwise.}$$

The output of the synchronous detector, E, is then integrated to give PTO, which, in turn, controls the current reference, I_{ref} (Figure B.1-5).

It should be noted that the computer representation of the AGC amplifier is approximate. The actual circuit is highly nonlinear and depends upon a transistor 'beta' which is not well controlled. Although the performance of the actual AGC amplifier may be somewhat different, the difference is not likely to be important since the output of the AGC feeds a relatively slow integrator whose output is not likely to change significantly during the time of interest.

B.2 EMTP Implementation

The TESLACO static power converter model given in the previous section was implemented on EMTP. This was not always a straightforward process. Most of the model (the control circuitry) was represented using the transient analysis of control systems (TACS) portions of EMTP. The rest of the model involved in the conversion of PV array dc power to ac power was represented in a normal EMTP electrical network. Figure B.2-1 indicates the overall flow of signals between the EMTP network and the various components of the model represented in TACS. Figures B.2-2 through B.2-11 give details of the implementation of each component of the model.

The TACS portion of EMTP has predefined "devices" with which the user can model typical control functions. Most of the blocks in the figures contain a number, an "S", or an "F" in the upper right-hand corner. A number refers to the number of the TACS supplemental device used (see EMTP Rule Book [22]). An "F" indicates that a Fortran expression was used to accomplish the function described in the block. An "S" indicates that the block represents a transfer function. Some of the device blocks contain signals pointing to a triangle containing letters. These triangles indicate control of the block as follows: R-reset, RV-reset value, S-sample. A small box with a shaded arrow containing a signal name indicates this signal is an interface variable between the EMTP electrical network and TACS.

The most complicated portions of the EMTP implementation of the TESLACO model are shown in Figures B.2-7 and B.2-8. They were the phase comparator and

loop filter implementations in which two signals within the phase locked loop are compared, a current pulse with duration equal to the phase error is generated, and the current pulse is applied to a loop filter to generate a voltage error signal to the voltage controlled oscillator. The reason this implementation was so complicated is that the solution time step used for the EMTP model was 46.296 usec or 1° of 60 Hz. The phase error measured in the phase locked loop needed to be more accurate than just to within 1°. Therefore, an elaborate model was implemented that interpolated zero crossings of the compared signals to times within a time step, determined the duration of the current pulse, and charged and discharged the capacitors of the loop filter as needed within a time step. Figures B.2-12 and B.2-13 help to explain this. Figure B.2-13 shows the situation when both signals crossed zero between the last time step and the present one. The times T1 and T2 are calculated by interpolation. Therefore, a pulse of current with duration T1-T2 should be applied to the loop filter for only a portion of the time between the last time step and the present one. Figure B.2-12 shows the circuit of the loop filter and how the voltage changes on the two capacitors that make up the filter. For the portion of the time step before signal U#VACF crossed zero (Δt-T1), the current pulse was zero and only VC2 changed. For the portion of the time step after U#VACF crossed and before U#VPVT crossed zero (T1-T2), the current pulse was applied to the filter and both VC1 and VC2 changed. For the portion of the time step after U#VPVT crossed zero (T2), the current was zero and only VC2 changed. The EMTP implementation will include the effect of all three of these intervals when determining a value for Vin at time t. The implementation was general enough to cover all possible combinations of zero crossings, whether they occurred within the same time step or on different time steps.

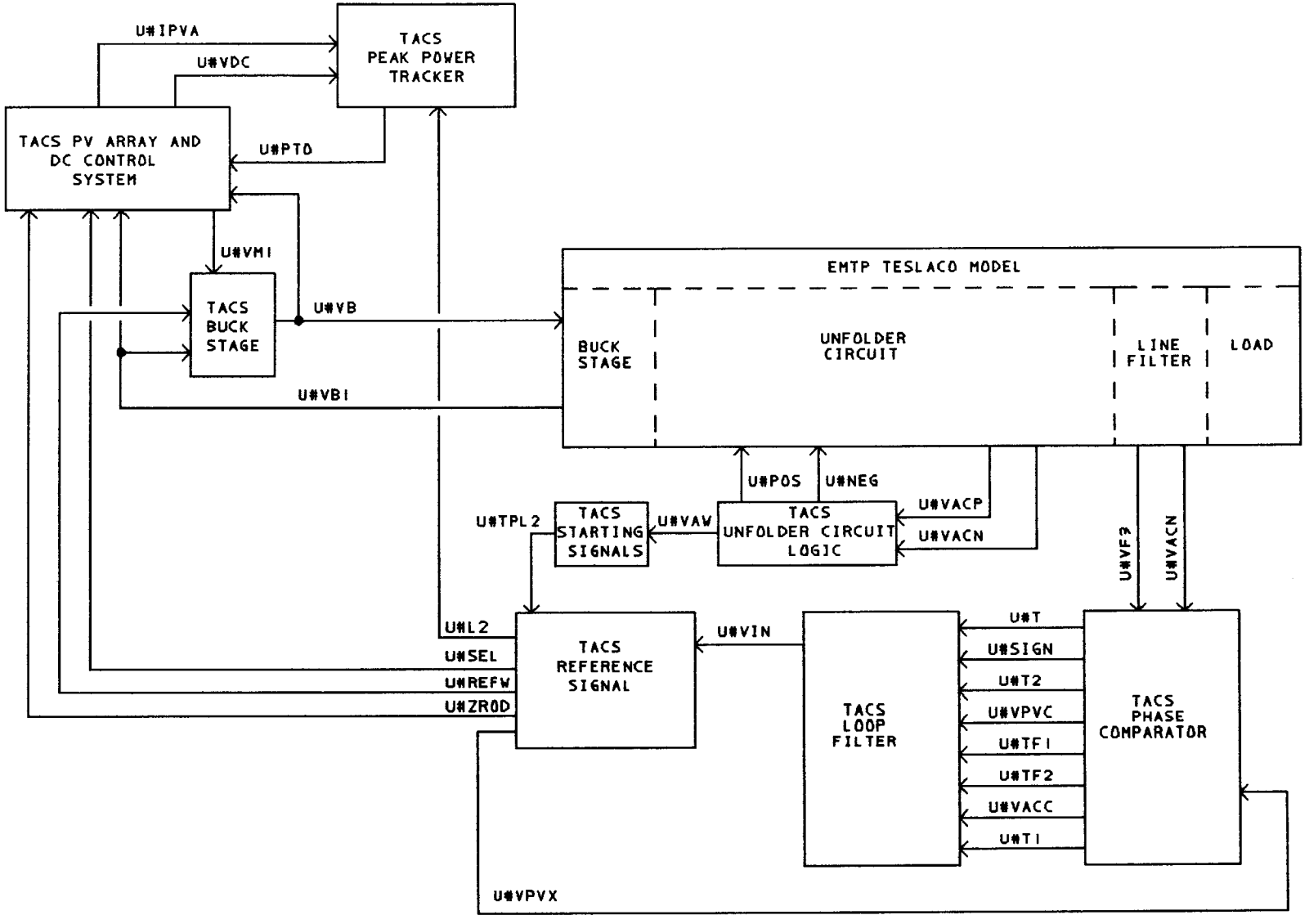

FIGURE B.2-1 SIGNAL FLOW DIAGRAM FOR TESLACO MODEL

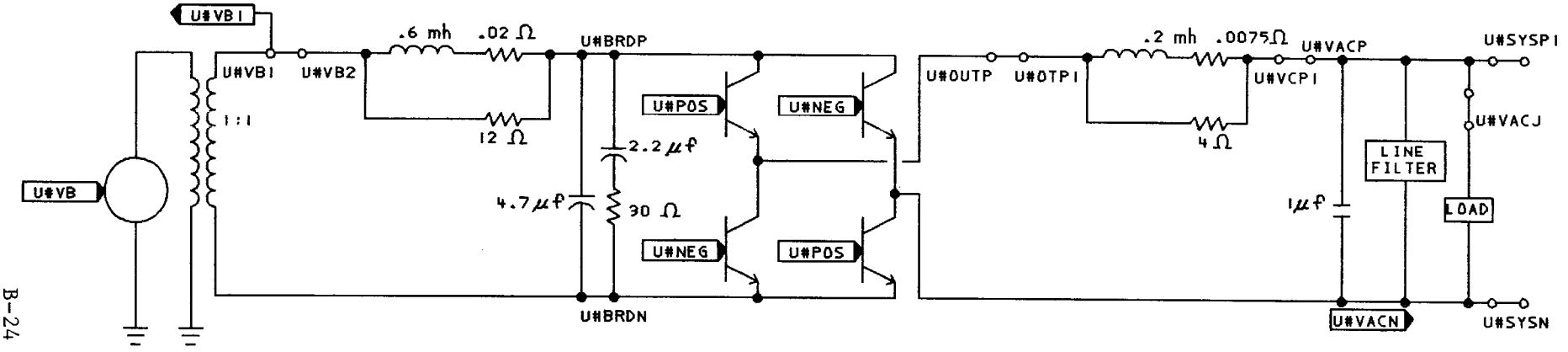

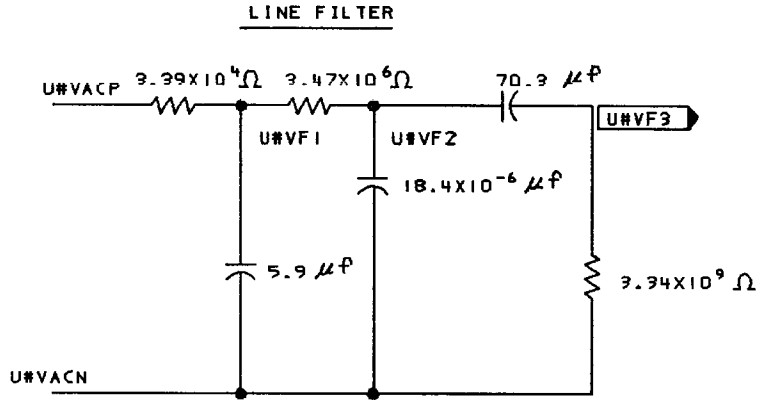

FIGURE B.2-2 EMTP TESLACO MODEL

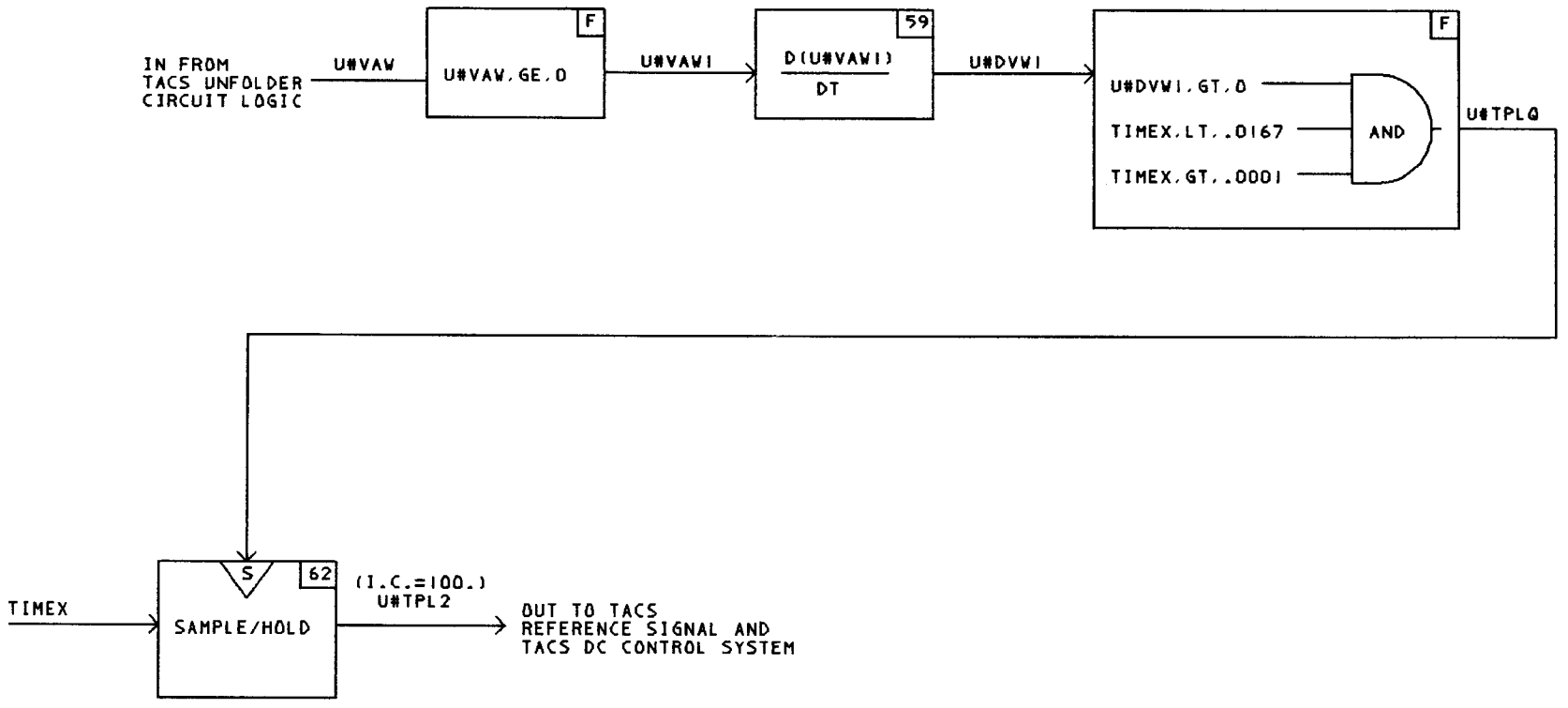

FIGURE B.2-3 TACS STARTING SIGNALS

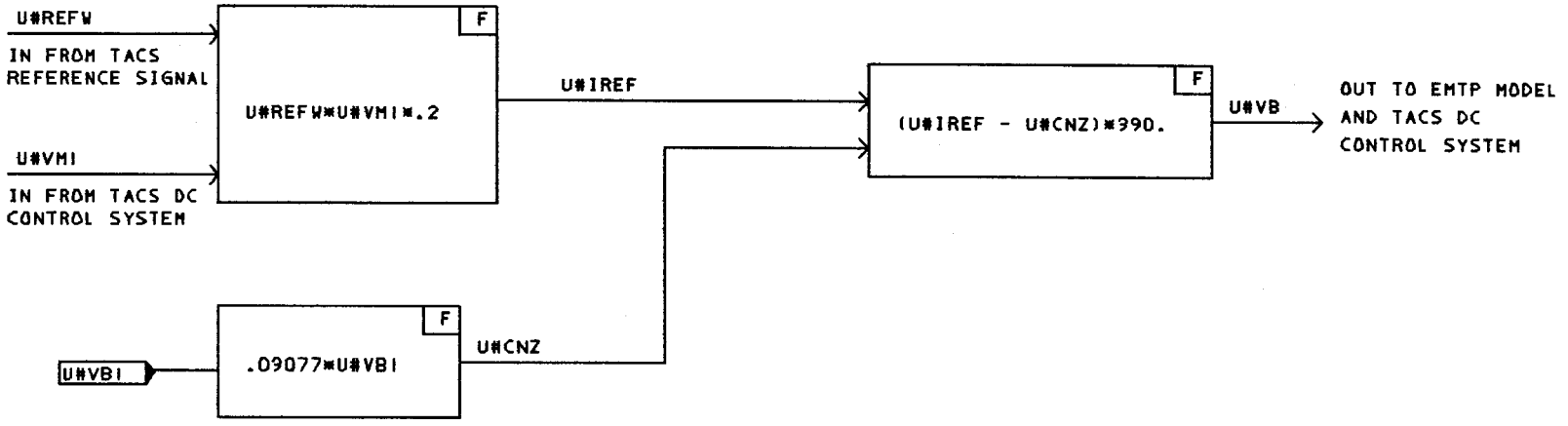

FIGURE B.2-4 TACS BUCK STAGE

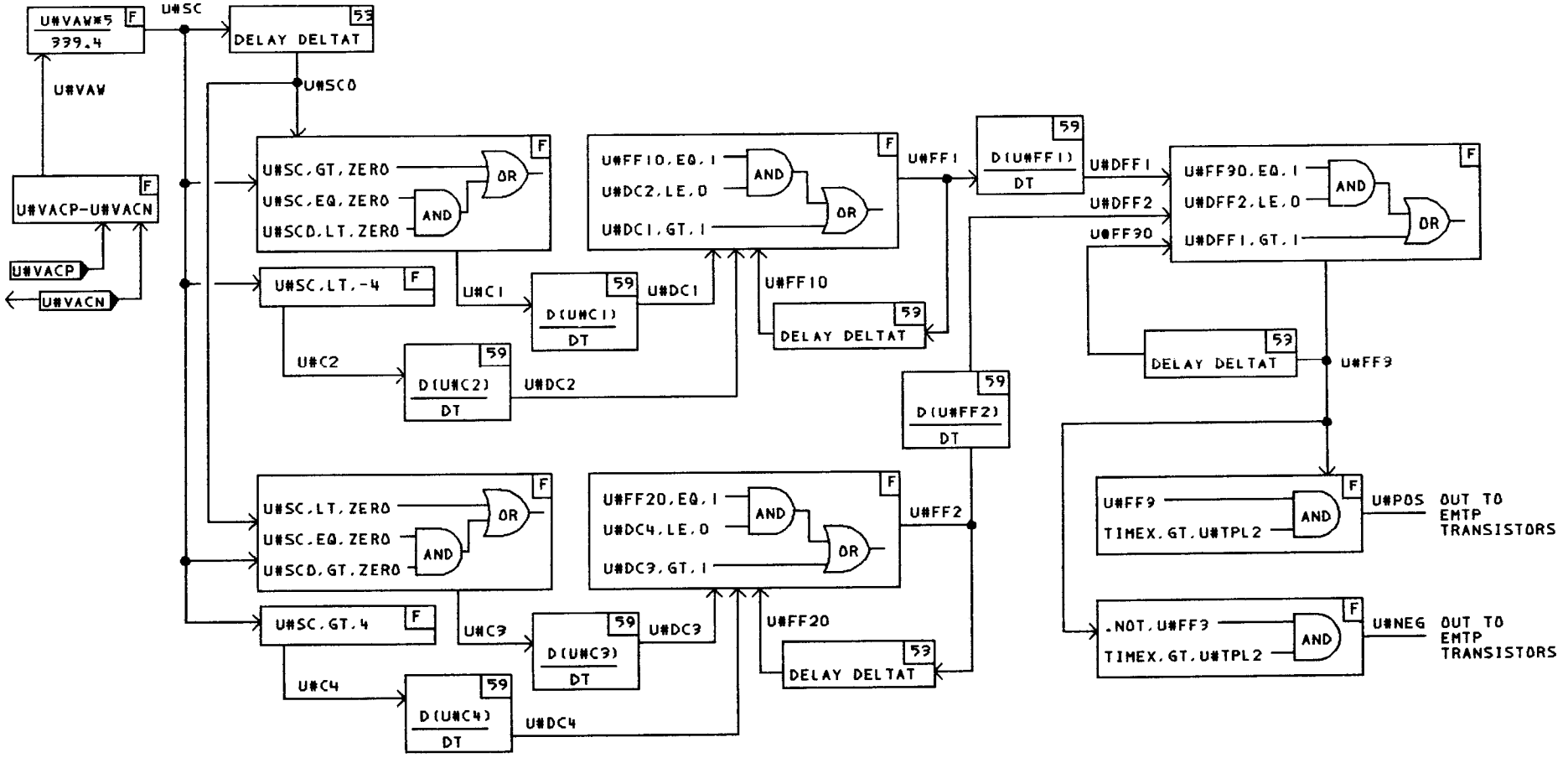

FIGURE B.2-5 TACS UNFOLDER CIRCUIT LOGIC

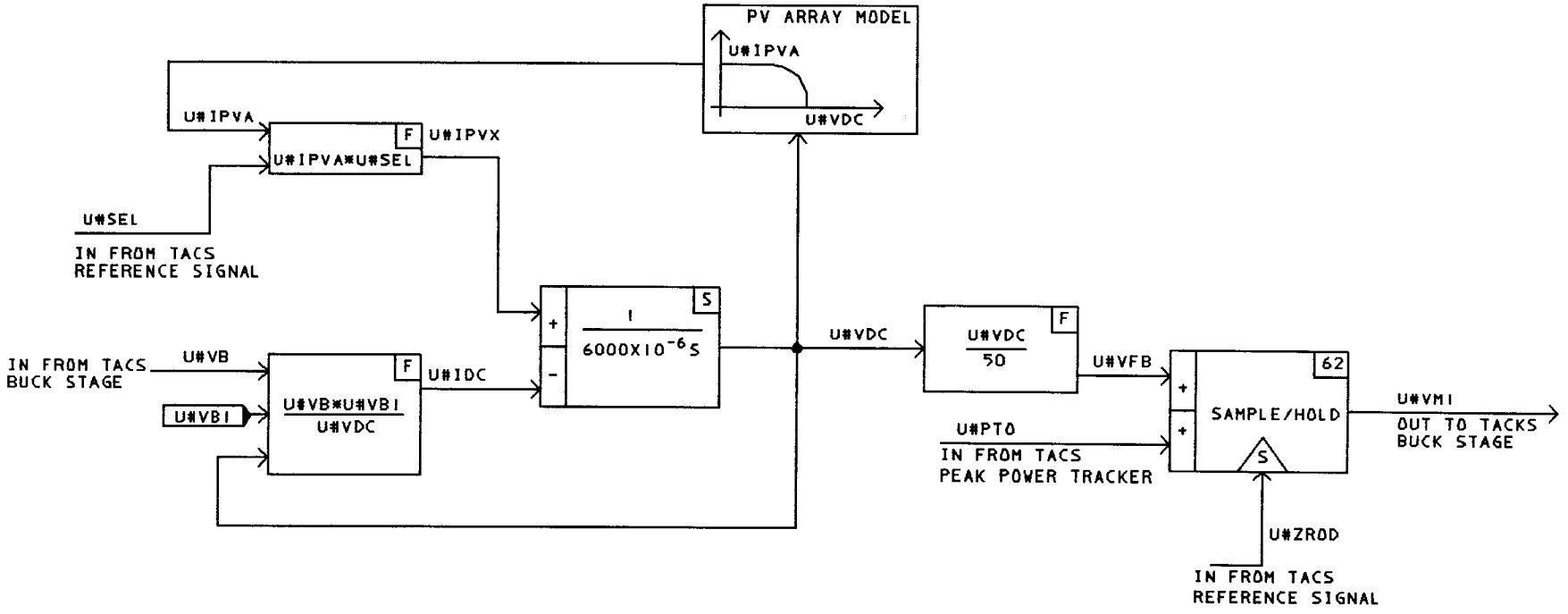

FIGURE B.2-6 TACS PV ARRAY AND DC CONTROL

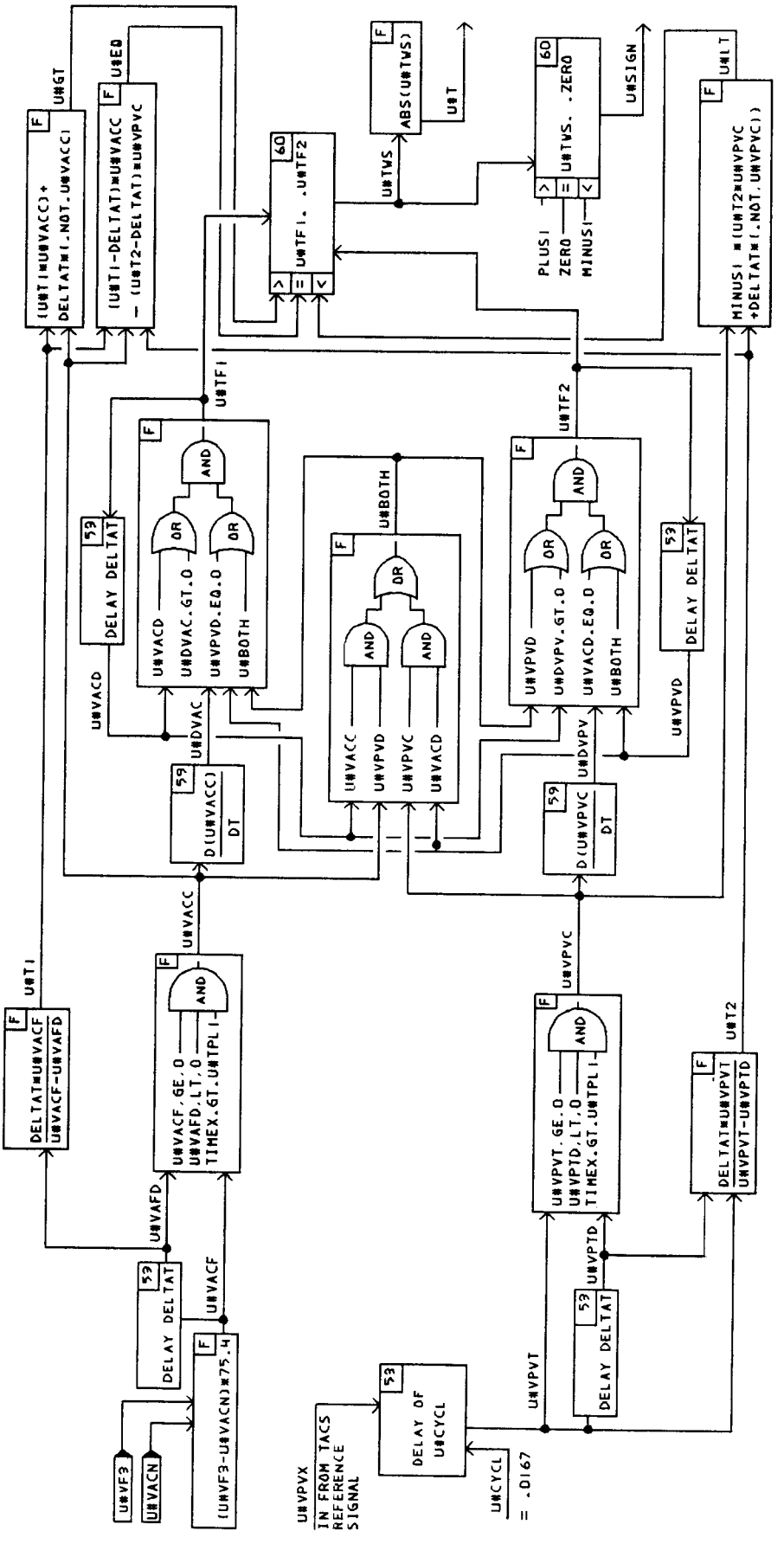

FIGURE B.2-7 TACS PHASE COMPARATOR

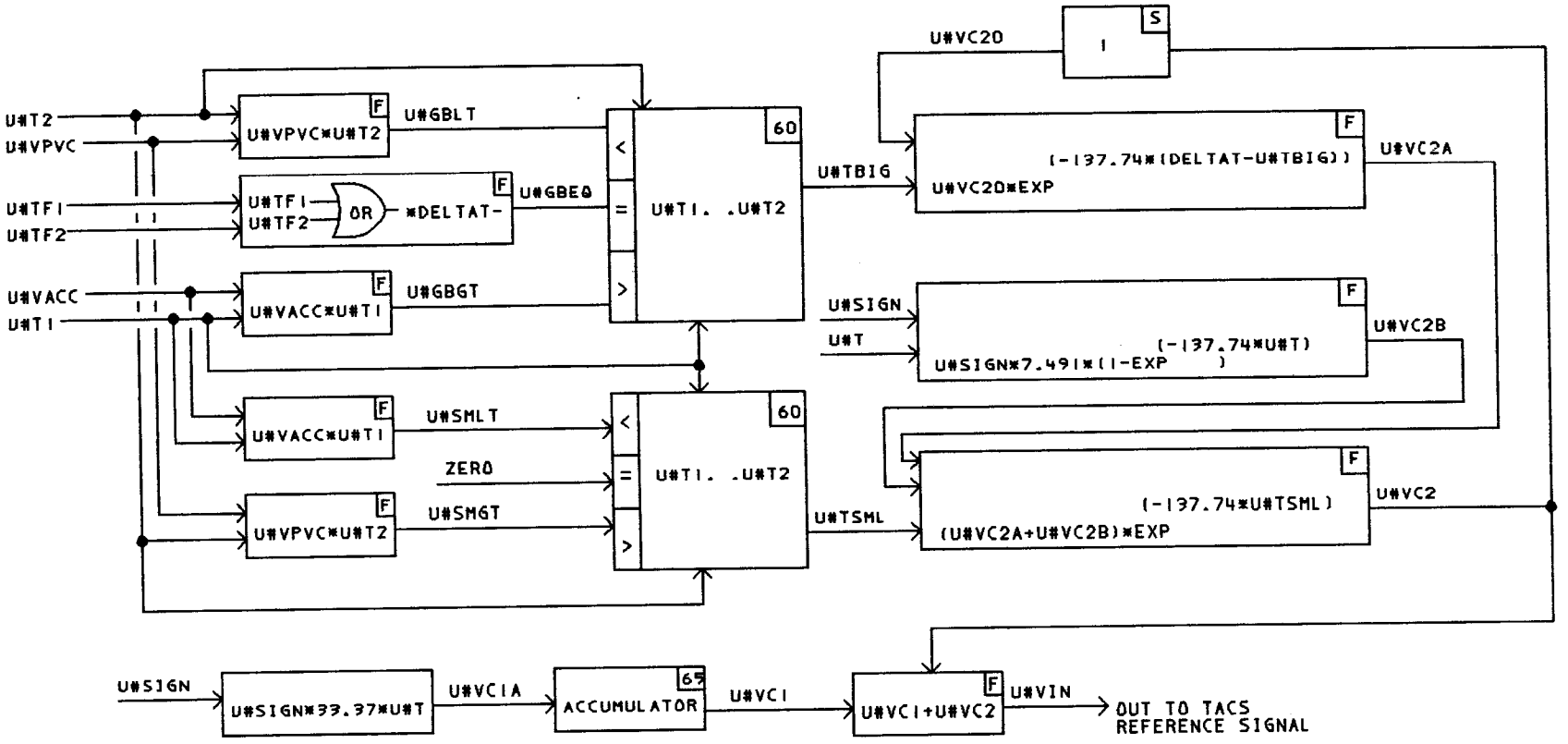

FIGURE B.2-8 TACS LOOP FILTER

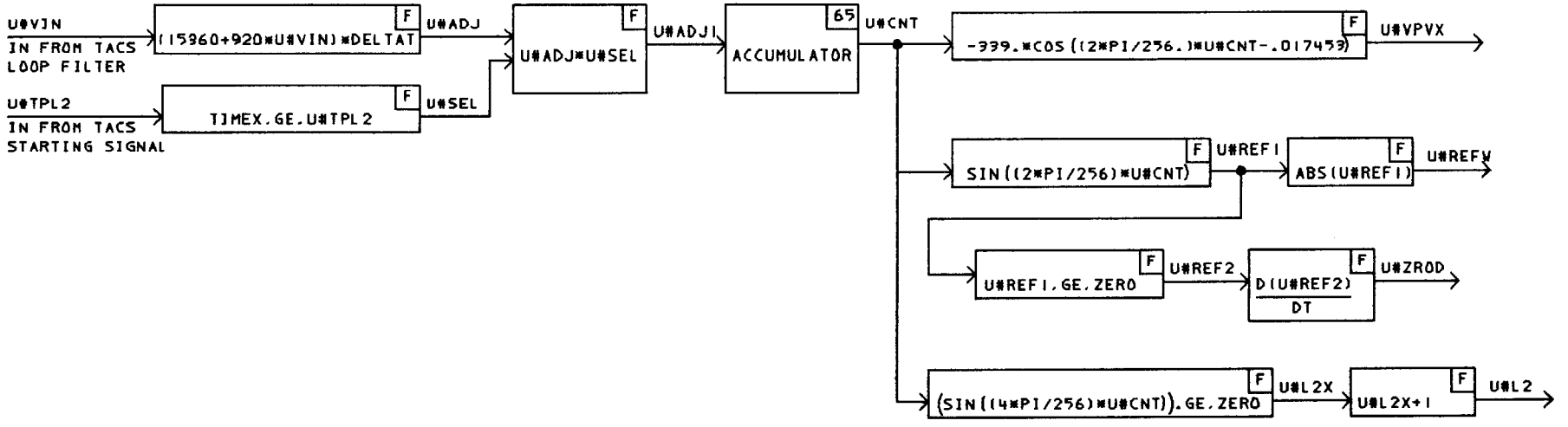

FIGURE B.2-9 TACS REFERENCE SIGNAL

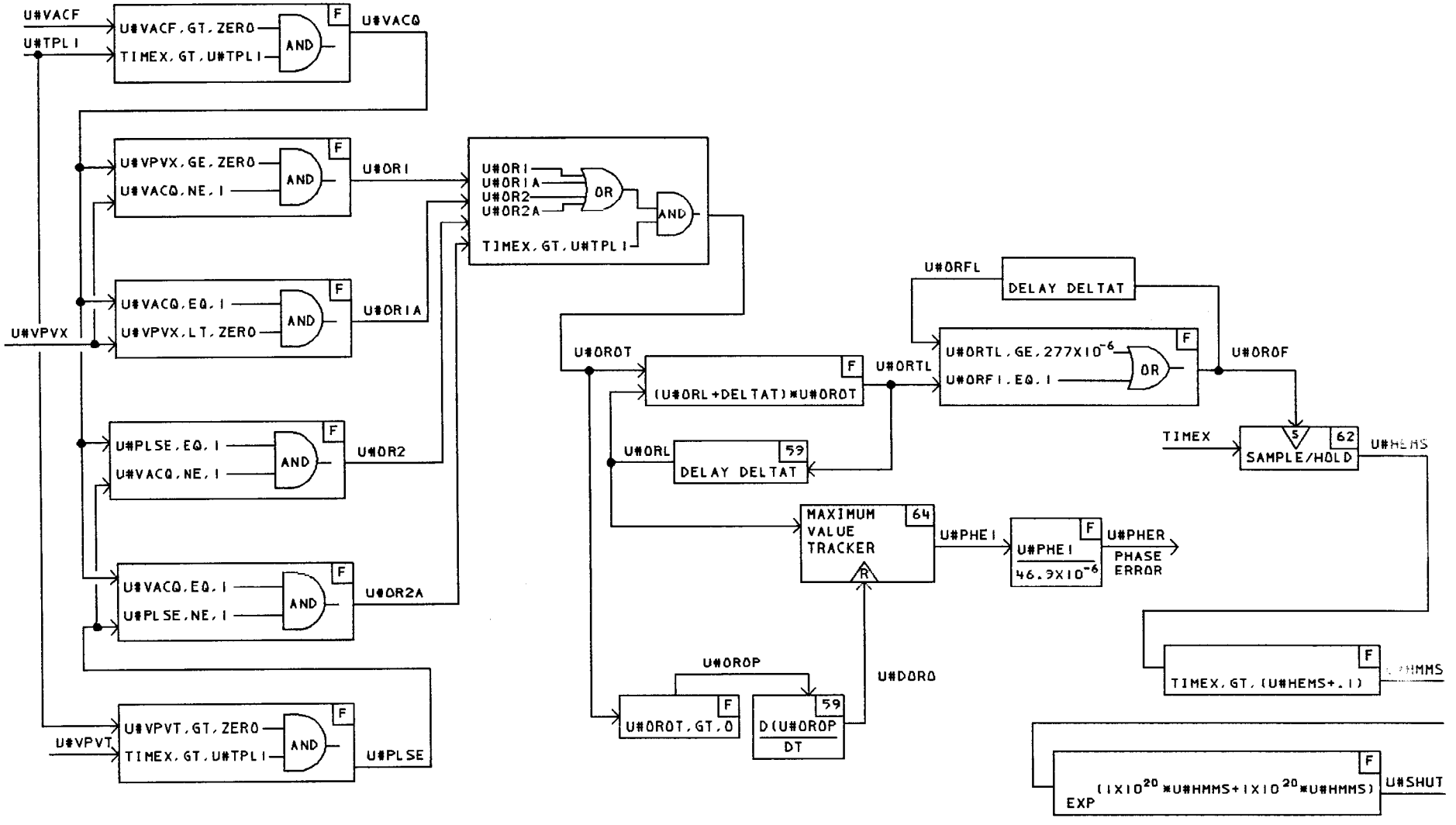

FIGURE B.2-10 TACS PHASE ERROR SHUT DOWN LOGIC

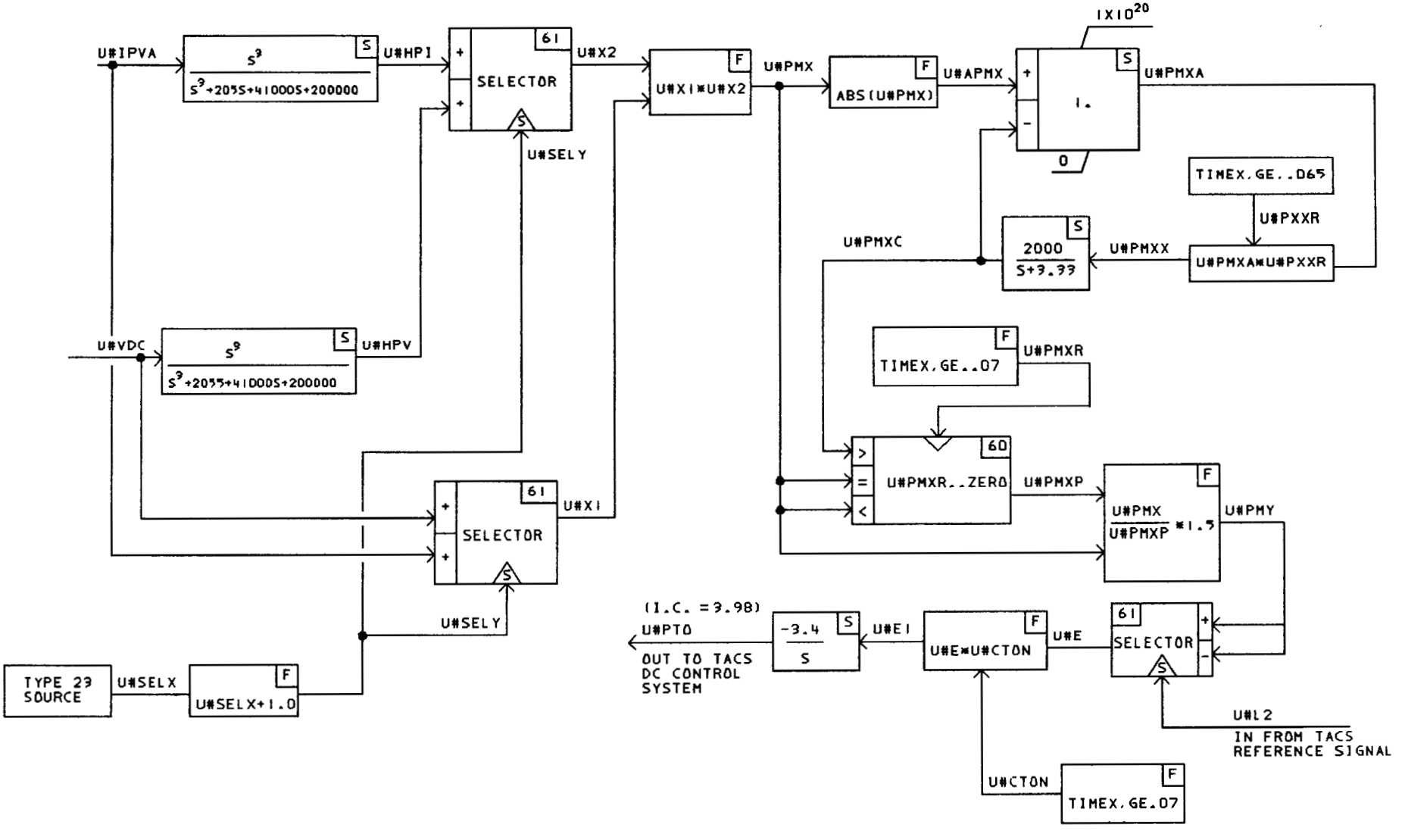

FIGURE B.2-11 TACS PEAK POWER TRACER

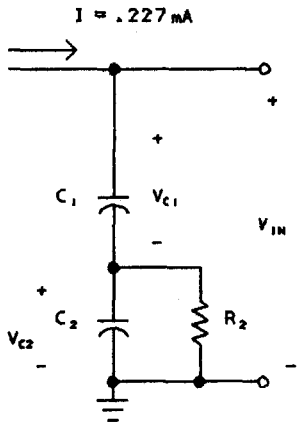

$R_2 = 33000\ \Omega$
$C_1 = 6.8\ \mu f$
$C_2 = .22\ \mu f$
FOR I = 0: V_{c1} IS UNCHANGED
$V_{c2} = V_{C2OLD}E^{-197.74T}$
FOR I ≠ 0: $V_{c1} = V_{C1OLD}+39.98T$
$V_{c2} = V_{C1OLD}+7.491\ (1-E^{-197.74T})$

FIGURE B.2-12 LOOP FILTER IN PHASE LOCKED LOOP

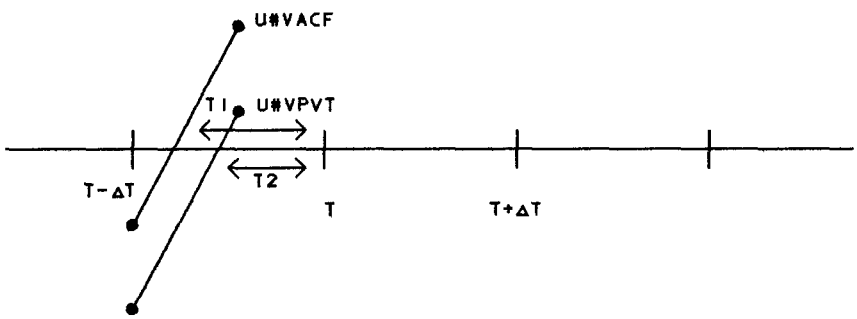

FIGURE B.2-13 EXAMPLE OF PHASE COMPARATOR OPERATION

TESLACO Model Data File Listing

A listing of the EMTP/TACS data file follows. The file is divided into two sections with the TACS section treated as an INSERT file to the EMTP file. This file is the base file used for the islanding study. The study was performed on the M39 Apollo version of EMTP.

```
BEGIN NEW DATA CASE
C
C DATA FILE NAME = SHEN12_1V1A
C                                        CASE NO.        CALCULATION NO.
C
C
C                              TITLE :
C
C
C
C
C
C                      ORIGINATING ENG.:                  DATE:
C
C                        REVIEWING ENG.:                  DATE:
C
C
C  REVISED LINE FILTER BASED ON ACTUAL TESLACO
ABSOLUTE TACS DIMENSIONS
      15      90      95      30     200    3600    2000     200
46.296-63000.E-3      0.      0.  1.0E-8
       1       5       1       3       1      -1               2
      25    1000
TACS HYBRID
C
$INCLUDE,TESLACO_UNIT
33U1VDC U1IPVAU1POWRU1PTO U1VIN U1PHERU1FREQ
33U1VPVXU1VPVTU1VACF
C
99OPEN    =(TIMEX.LT..39997)-.5
C

C BRANCH CARDS
  U1VCP1U1VACN                           1.0                                  2
C ADD INTERNAL LOAD TO SOAK UP  76 VARS (NET 100 VARS)
  U1VACNU1VCP1                        1872.1
C
C OUTPUT LOAD     ( 2280W+J494.4V ) (V=231.6)
  U1VACJU1VACN            22.46912.924                                        2
C                 (   -J404.4
  U1VACNU1VACJ                          20.0
C
C INDUCTOR DISSIPATION RESISTORS
  U1VB2 U1BRDP             12.00
  U1OTP1U1VCP1              4.00
C LINE FILTER (REVISED - ZERO PHASE SHIFT)
  U1VACPU1VF1             3.39E4
  U1VF1 U1VACN                             5.9
  U1VF1 U1VF2             3.47E6
  U1VF2 U1VACN                          18.4-6
  U1VF2 U1VF3                           70.3-6
  U1VF3 U1VACN            3.34E9
C UNFOLDER CIRCUIT PARAMETERS
  U1VB2 U1BRDP               .02     .6
```

```
  U1BRDPU1BRDN                              4.7
  U1BRDPU1BRDN                 30.          2.2
  U1OTP1U1VCP1               .0075    .2
C ISOLATION TRANSFORMER TO ALLOW GROUNDED SOURCE
  TRANSFORMER                              U1TRNS
            9999
 1U1VB                              1.0E-3     1
 2U1VB1 U1BRDN                      1.0E-3     1
C 50KVA DISTRIBUTION TRANSFORMER
  TRANSFORMER                              TRAND
            9999
C  1VSYS                          .001  .001 7200.
C  2SYSP1                         .036 .0955  120.
C  3      SYSN                    .036 .0955  120.
 1VSYS                              .0001 7200.
 2SYSP1                             .0001  120.
 3      SYSN                        .0001  120.

C SWITCH CARDS
C SWITCH TO SEND BUCK STAGE OUTPUT CURRENT TO TACS
  U1VB1 U1VB2          -1.  1E4
C SWITCH TO SEND UNFOLDER STAGE OUTPUT CURRENT TO TACS
  U1OUTPU1OTP1         -1.  1E4                                                  1
  U1BRDPU1BRXP         -1.  1E4                                                  1
  U1VCP1U1VACP         -1.  1E4                                                  1
  U1VACPU1VACJ         -1.  1E4                                                  1
C SWITCH TO MONITOR THE LOAD CURRENT FROM THE SYSTEM
C U1VACPSYSP1          -1. .130                                                  1
C U1VACNSYSN           -1. .130
13U1VACPSYSP1                                          CLOSED          OPEN    11
13U1VACNSYSN                                           CLOSED          OPEN    11
C UNFOLDER TRANSISTORS
13U1BRXPU1OUTP                                                         U1POS
13U1BRXPU1VACN                                                         U1NEG
13U1OUTPU1BRDN                                                         U1NEG
13U1VACNU1BRDN                                                         U1POS

C SOURCE CARDS
C VOLTAGE OUTPUT OF BUCK STAGE FROM TACS
60U1VB                                                          -1.
C SYSTEM SOURCE
14VSYS         9825.9        60.    -180.00                    -1.

  U1VB

C PLOT CARDS
  FOURIER ON                    5
 182100 23. 24.           U1VCP1U1VACN
 192100 23. 24.           U1VCP1U1VACP
 192100 23. 24.           U1VACPSYSP1
  FOURIER OFF

BEGIN NEW DATA CASE
```

```
C ************************************************************************
C
C  MODEL FOR TESLACO 4.0KW INVERTER
C
C ************************************************************************
C
$LISTOFF
C
C
C ************************************************************************
C TACS STARTING SIGNAL
C ************************************************************************
C
11U#TPL1       .10000
C
99U#VAW1  =U#VAW.GE.0
88U#DVW159+U#VAW1
88U#TPLQ  =(U#DVW1.GT.0.).AND.(TIMEX.LT..0167).AND.(TIMEX.GT..0001)
88U#TPL262+TIMEX                                                    U#TPLQ
C
77U#TPL2         100.
C
C ************************************************************************
C TACS BUCK STAGE  (12 OHM MODEL)
C ************************************************************************
C
91U#VB1                                                        -1.      1.E4
99U#CNZ   =.03077*U#VB1
88U#IREF  =U#REFW*U#VM1*.2
99U#VB    =(U#IREF-U#CNZ)*390.
C
C ************************************************************************
C  TACS UNFOLDER CIRCUIT LOGIC
C ************************************************************************
C
90U#VACP
99U#VAW   =U#VACP-U#VACN
99U#SC    =U#VAW*5./339.4
99U#SCO 53+U#SC                                              .00050DELTAT
C COMPARATOR #1 - SET SIGNAL TO FLIP FLOP #1
99U#C1    =(U#SC.GT.0.).OR.((U#SC.EQ.0.).AND.(U#SCO.LT.0.))
C COMPARATOR #2 - RESET SIGNAL TO FLIP FLOP #1
99U#C2    =U#SC.LT.-4.
C COMPARATOR #3 - SET SIGNAL TO FLIP FLOP #2
99U#C3    =(U#SC.LT.0.).OR.((U#SC.EQ.0.).AND.(U#SCO.GT.0.))
C COMPARATOR #4 - RESET SIGNAL TO FLIP FLOP #2
99U#C4    =U#SC.GT.4.
C FLIP FLOP #1 - SET SIGNAL FOR FLIP FLOP #3
99U#DC1 59+U#C1
99U#DC2 59+U#C2
99U#FF1O53+U#FF1                                             .00050DELTAT
99U#FF1   =((U#FF1O.EQ.1).AND.(U#DC2.LE.0)).OR.(U#DC1.GT.1)
C FLIP FLOP #2 - RESET SIGNAL FOR FLIP FLOP #3
99U#DC3 59+U#C3
```

```
99U#DC4 59+U#C4
99U#FF2053+U#FF2                                                    .00050DELTAT
99U#FF2   =((U#FF20.EQ.1).AND.(U#DC4.LE.0)).OR.(U#DC3.GT.1)
C FLIP FLOP #3
99U#DFF159+U#FF1
99U#DFF259+U#FF2
99U#FF3053+U#FF3                                                    .00050DELTAT
99U#FF3   =((U#FF30.EQ.1).AND.(U#DFF2.LE.0)).OR.(U#DFF1.GT.1)
C OUTPUT TO EMTP TACS CONTROLLED SWITHES - UNFOLDER TRANSISTORS
99U#POS   =U#FF3.AND.(TIMEX.GT.U#TPL2)
99U#NEG   =(.NOT.U#FF3).AND.(TIMEX.GT.U#TPL2)
C
C ***************************************************************************
C TACS DC CONTROL
C ***************************************************************************
C
88U#IPVX  =U#IPVA*U#SEL
88U#IDC   =(U#VB*U#VB1)/U#VDC
 1U#VDC   +U#IPVX -U#IDC                              1.0
        1.         0.
        0.       .006
88U#VFB   =U#VDC/50.
88U#VM1 62+U#VFB  +U#PTO                                              U#ZROD
C
C ***************************************************************************
C TACS PV ARRAY MODEL
C ***************************************************************************
C
11U#CLTC       28.00
11U#ISRT        2.52
11U#AIDL        1.92
11U#BIDL        1.92
11U#NP          8.78
11U#NS         426.4
99U#CLTK  =U#CLTC+273.18
99U#ILG   =U#NSOL/100.*(U#ISRT+.0017*(U#CLTC-28.))
99U#IOS   =7.31E-13*U#CLTK**3*EXP(12886./U#BIDL*(.00332-1./U#CLTK))
88U#IPVA  =U#NP*U#ILG-U#NP*U#IOS*(EXP(11601.*U#VDC/U#NS/U#AIDL/U#CLTK)-1.0)
C
77U#NSOL      100.00
C
C ***************************************************************************
C TACS PHASE COMPARATOR
C ***************************************************************************
C
90U#VF3                                                                -1.
90U#VACN                                                               -1.
99U#VACF  =(U#VF3-U#VACN)*75.4
11U#CYCL   .01666656
88U#VPVT53+U#VPVX                                                   .01667U#CYCL
99U#VAFD53+U#VACF                                                   .00050DELTAT
99U#VPTD53+U#VPVT                                                   .00050DELTAT
99U#VACC  =(U#VACF.GE.0).AND.(U#VAFD.LT.0).AND.(TIMEX.GT.U#TPL1)
99U#T1    =(DELTAT*U#VACF)/(U#VACF-U#VAFD)
```

```
99U#VPVC  =(U#VPVT.GE.0).AND.(U#VPTD.LT.0).AND.(TIMEX.GT.U#TPL1)
99U#T2    =(DELTAT*U#VPVT)/(U#VPVT-U#VPTD)
99U#BOTH  =(U#VACC.AND.U#VPVD).OR.(U#VPVC.AND.U#VACD)
99U#DVAC59+U#VACC
99U#TF1   =(U#VACD.OR.(U#DVAC.GT.0)).AND.((U#VPVD.EQ.0).OR.U#BOTH)
99U#VACD53+U#TF1                                                .00050DELTAT
99U#DVPV59+U#VPVC
99U#TF2   =(U#VPVD.OR.(U#DVPV.GT.0)).AND.((U#VACD.EQ.0).OR.U#BOTH)
99U#VPVD53+U#TF2                                                .00050DELTAT
99U#LT    =MINUS1*((U#T2*U#VPVC)+(DELTAT*(.NOT.U#VPVC)))
99U#EQ    =((U#T1-DELTAT)*U#VACC)-((U#T2-DELTAT)*U#VPVC)
99U#GT    =(U#T1*U#VACC)+(DELTAT*(.NOT.U#VACC))
99U#TWS 60+U#LT   +U#EQ   +U#GT                                 U#TF1 U#TF2
99U#SIGN60-PLUS1  +ZERO   +PLUS1                                U#TWS ZERO
99U#T     =ABS(U#TWS)
C
C ***************************************************************************
C TACS LOOP FILTER
C ***************************************************************************
C
99U#GBLT  =U#VPVC*U#T2
99U#GBEQ  =(U#TF1.OR.U#TF2)*DELTAT
99U#GBGT  =U#VACC*U#T1
99U#TBIG60+U#GBLT +U#GBEQ +U#GBGT                               U#T1  U#T2
99U#SMLT  =U#VACC*U#T1
99U#SMGT  =U#VPVC*U#T2
99U#TSML60+U#SMLT +ZERO   +U#SMGT                               U#T1  U#T2
99U#VC2A  =(U#VC2O*(EXP(-137.74*(DELTAT-U#TBIG))))
99U#VC2B  =U#SIGN*7.491*(1-EXP(-137.74*U#T))
  U#VC2O  +U#VC2
99U#VC2   =(U#VC2A+U#VC2B)*EXP(-137.74*U#TSML)
99U#VC1A  =U#SIGN*33.37*U#T
99U#VC1 65+U#VC1A
99U#VIN   =U#VC1+U#VC2
C
C ***************************************************************************
C TACS REFERENCE SIGNAL
C ***************************************************************************
C
88U#ADJ   =(15360.+(920*U#VIN))*DELTAT
88U#SEL   =TIMEX.GE.U#TPL2
88U#ADJ1  =U#ADJ*U#SEL
88U#CNT 65+U#ADJ1
88U#VPVX  =-339.*COS((2*PI/256.)*U#CNT-.017453)
88U#REF1  =SIN((2*PI/256.)*U#CNT)
88U#REFW  =ABS(U#REF1)
88U#REF2  =(U#REF1.GE.ZERO)
88U#ZROD59+U#REF2
88U#L2X   =(SIN((4*PI/256.)*U#CNT)).GE.ZERO
88U#L2    =U#L2X+1.0
C
C ***************************************************************************
C TACS PHASE ERROR SHUT DOWN LOGIC
C ***************************************************************************
```

```
C
88U#PLSE  =(U#VPVT.GT.ZERO).AND.(TIMEX.GT.U#TPL1)
99U#VACQ  =(U#VACF.GT.ZERO).AND.(TIMEX.GT.U#TPL1)
88U#OR1   =((U#VPVX.GE.0).AND.(U#VACQ.NE.1))
88U#OR1A  =((U#VACQ.EQ.1).AND.(U#VPVX.LT.0))
88U#OR2   =((U#PLSE.EQ.1).AND.(U#VACQ.NE.1))
88U#OR2A  =((U#VACQ.EQ.1).AND.(U#PLSE.NE.1))
88U#OROT  =((U#OR1.OR.U#OR1A).OR.(U#OR2.OR.U#OR2A)).AND.(TIMEX.GT.U#TPL1)
88U#ORL 53+U#ORTL                                                .00050DELTAT
88U#ORTL  =(U#ORL+DELTAT)*U#OROT
88U#ORFL53+U#OROF                                                .00050DELTAT
88U#OROF  =(U#ORTL.GE.(277.E-6)).OR.(U#ORFL.EQ.1)
88U#HEMS62+TIMEX                                                          U#OROF
88U#HMMS  =TIMEX.GT.(U#HEMS+.100)
88U#SHUT  =EXP((10E20*U#HMMS)+(10E20*U#HMMS))
88U#OROP  =U#OROT.GT.0.
88U#DORO59+U#OROP
88U#PHE164+U#ORL                                          1.     0.U#DORO
88U#PHER  =U#PHE1/46.3E-6
C
C ***************************************************************************
C  TACS PEAK POWER TRACKER
C ***************************************************************************
C
 3U#HPI   +U#IPVA                                        1.
        0.         0.         0.         1.
   200000.     41000.       205.         1.
 3U#HPV   +U#VDC                                         1.
        0.         0.         0.         1.
   200000.     41000.       205.         1.
23U#SELX          1.0   500.E-6   250.E-6                        0.
99U#SELY  =U#SELX+1.0
88U#X1  61+U#VDC  +U#IPVA                                          U#SELY
88U#X2  61+U#HPI  +U#HPV                                           U#SELY
88U#PMX   =U#X1*U#X2
88U#APMX  =ABS(U#PMX)
 0U#PMXA  +U#APMX -U#PMXC                                 0. 1.E20
99U#PXXR  =TIMEX.GE..065
99U#PMXX  =U#PMXA*U#PXXR
 1U#PMXC  +U#PMXX                                        1.
     2000.         0.
      3.33         1.
99U#PMXR  =(TIMEX.GE..07)
88U#PMXP60+U#PMX  +U#PMX  +U#PMXC                                  U PMXR
88U#PMY   =U#PMX/U#PMXP*1.5
88U#E   61-U#PMY  +U#PMY                                                  U#L2
99U#CTON  =TIMEX.GE..070
99U#E1    =U#E*U#CTON
 1U#PTO   +U#E1                                         -1.
       3.4         0.
        0.         1.
C
77U#PTO          2.55
C
```

```
C ***************************************************************************
C   TACS  FREQUENCY METER
C ***************************************************************************
C
99U#FREQ50+U#VAW
C
C ***************************************************************************
C   INITIAL CONDITIONS
C ***************************************************************************
C
77U#IPVA          0.
77U#VDC         200.0
77U#IDC           0.
77U#VM1           5.
77U#VFB           5.
77U#PMX         2.0
77U#X1          1.0
77U#X2          1.0
77U#CNT         0.0
77U#HEMS        100.0
C
$LISTON
C
```

B.3 Model Validation

After the model of a TESLACO static power converter was implemented on EMTP, it was necessary to check the accuracy of the implementation. Along with the original model, P. C. Krause and Associates supplied five simulations using this model as implemented on an analog computer at Purdue University. The simulations were for a single TESLACO in an island with passive load consisting of a 288 ohm resistor in parallel with an RL series branch of 16.87 ohms and 16.61 mh. The only differences among the five simulations were in the amount of solar insolation and therefore in the output power of the TESLACO. Figures B.3-1, B.3-3, B.3-5, B.3-7, and B.3-9 give the results obtained on the analog computer. Figures B.3-2, B.3-4, B.3-6, B.3-8, and B.3-10 give the corresponding results which were obtained with EMTP. Plots for Io and Ppva are not shown in the EMTP results. Otherwise, the EMTP plots correspond one for one with the Purdue plots.

FIGURE B.3-1 ANALOG COMPUTER MODEL RESULTS OF TESLACO SPC WITH INSOLATION = 60 MW/CM^2

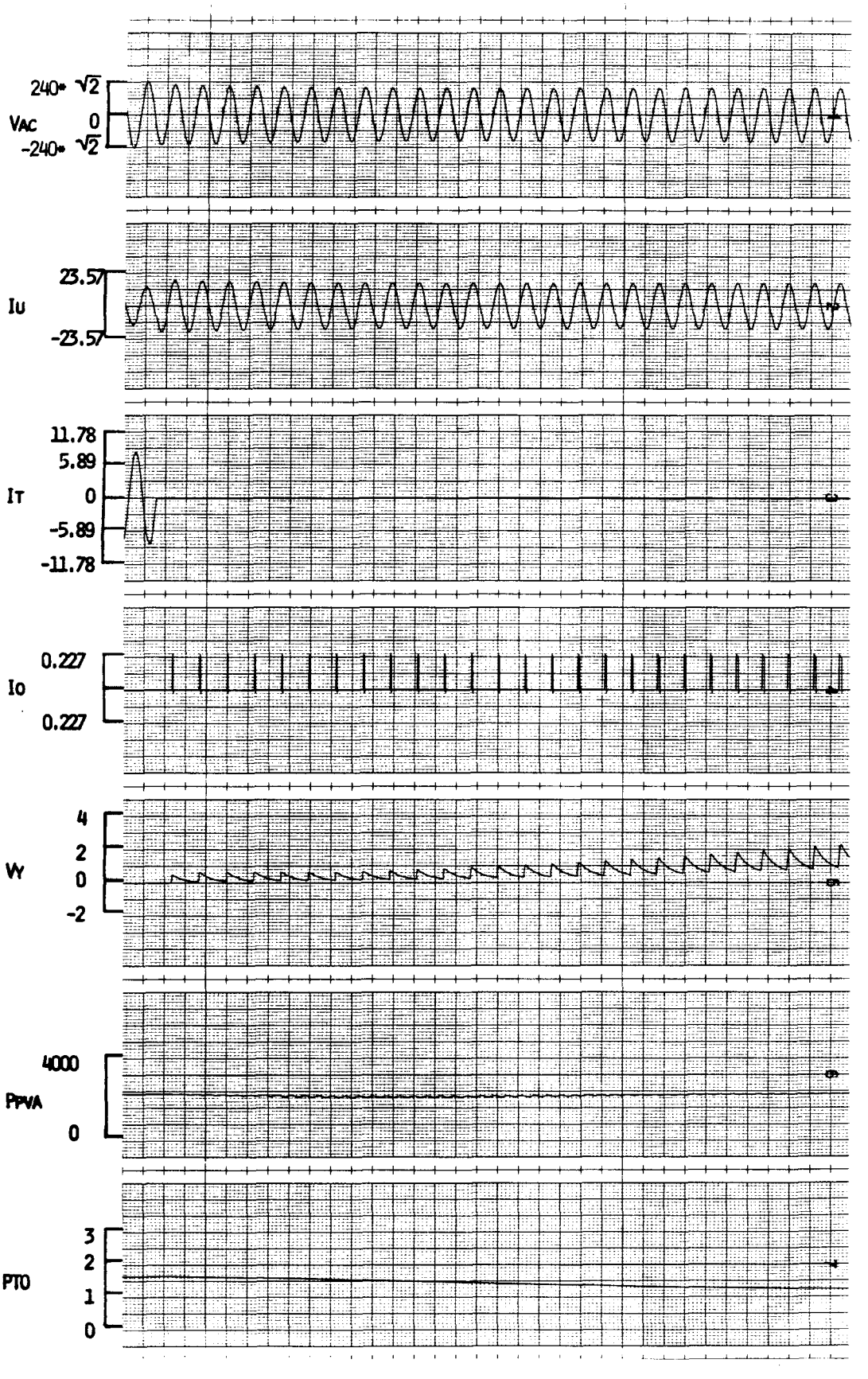

FIGURE B.3-2 EMTP COMPUTER MODEL RESULTS OF TESLACO SPC WITH INSOLATION = 60 MW/CM^2

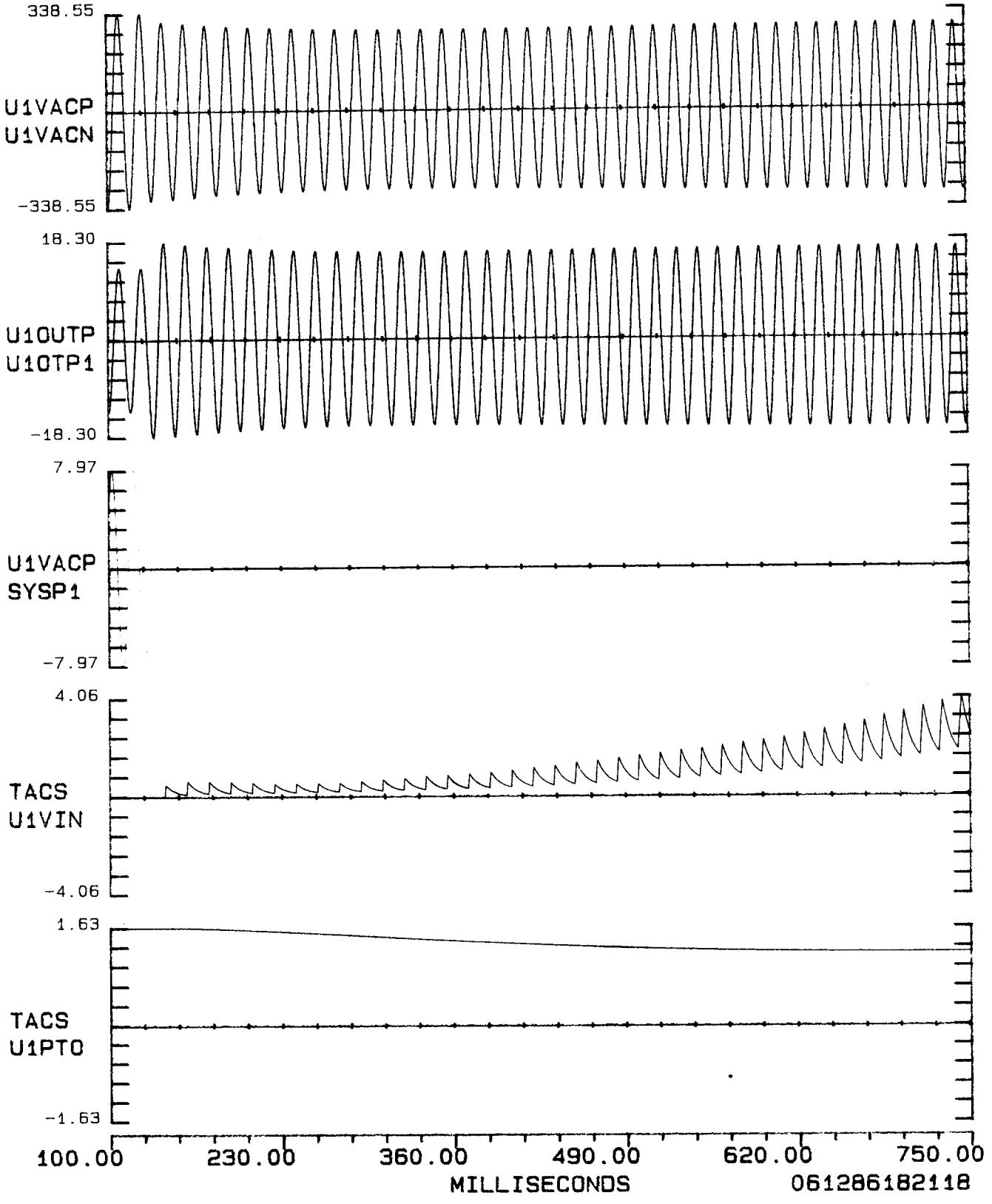

FIGURE B.3-3 ANALOG COMPUTER MODEL RESULTS OF TESLACO SPC WITH INSOLATION = 70 MW/CM^2

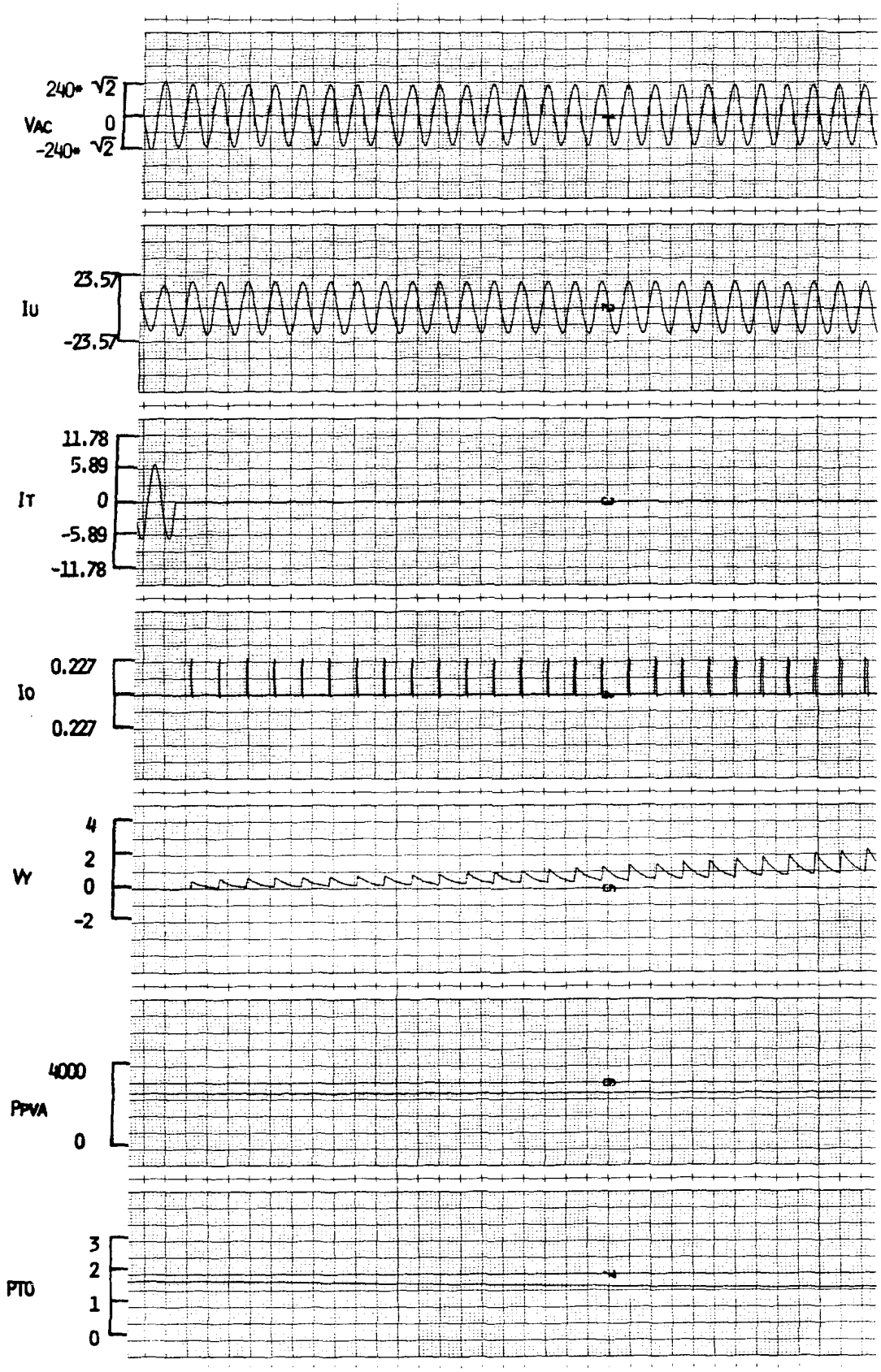

← 450 MILLISECONDS →

FIGURE B.3-4 EMTP COMPUTER MODEL RESULTS OF TESLACO SPC WITH INSOLATION = 70 MW/CM^2

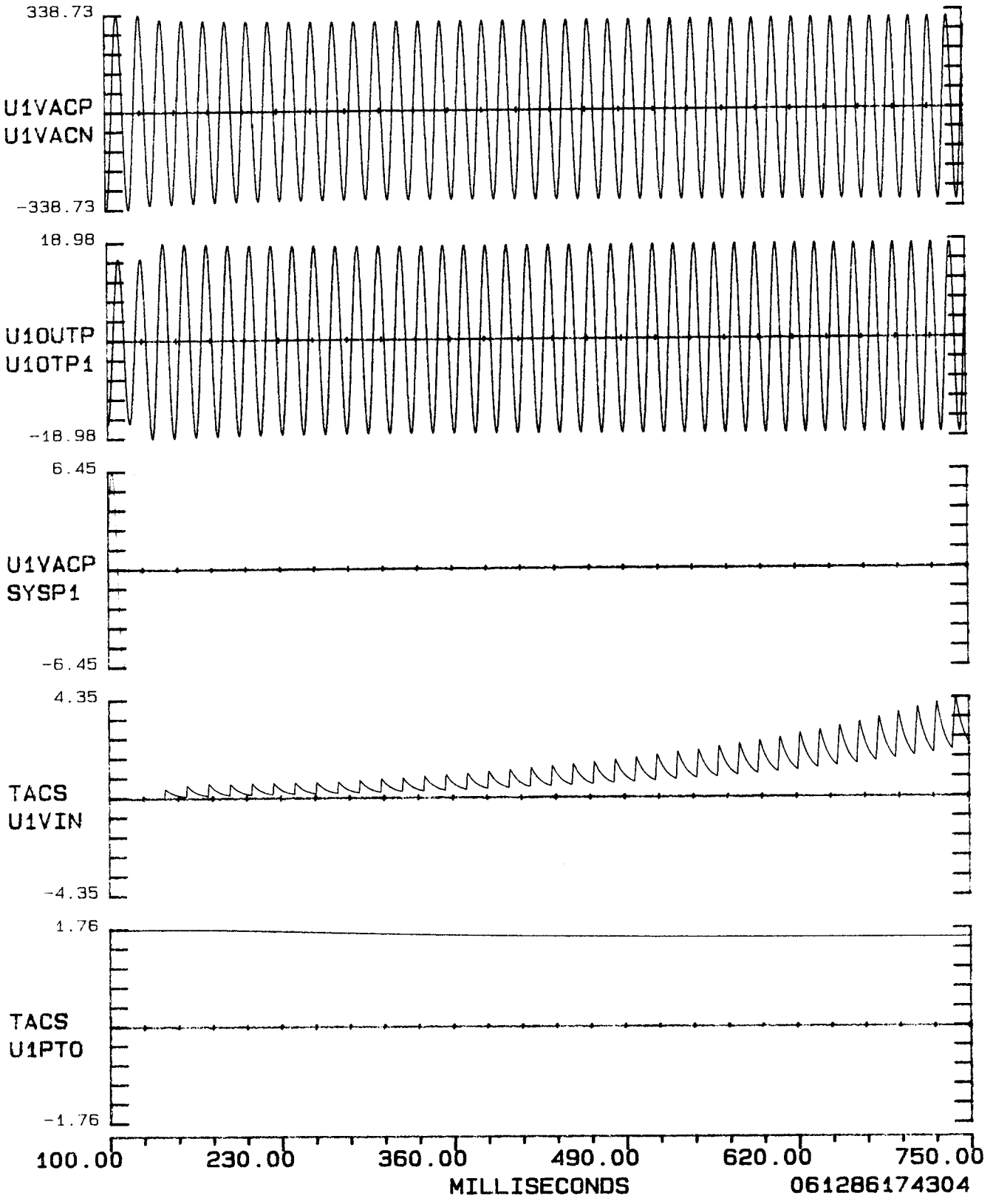

FIGURE B.3-5 ANALOG COMPUTER MODEL RESULAT OF TESLACO SPC WITH INSOLATION = 80 MW/CM^2

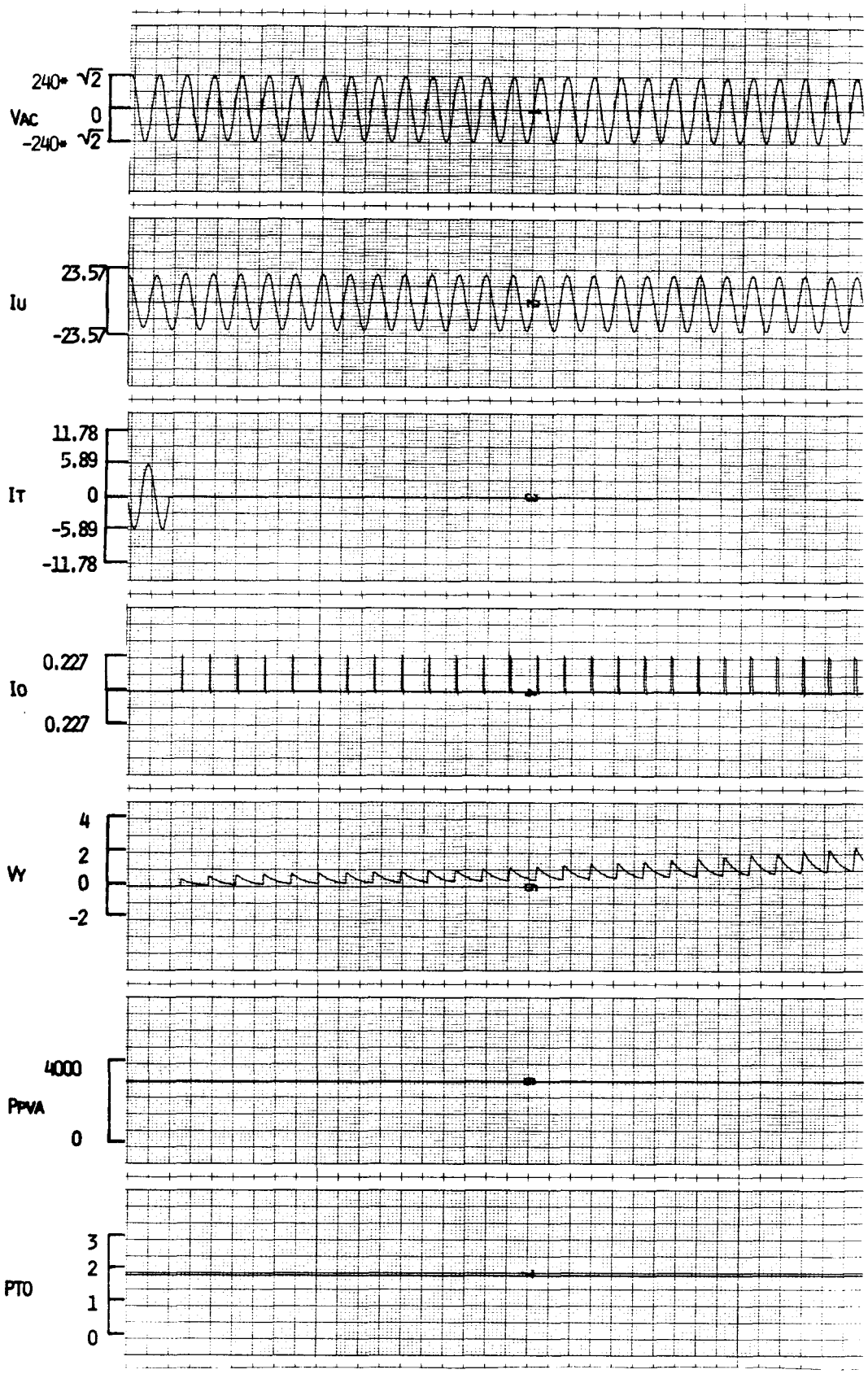

FIGURE B.3-6 EMTP COMPUTER MODEL RESULTS OF TESLACO SPC WITH INSOLATION = 80 MW/CM2

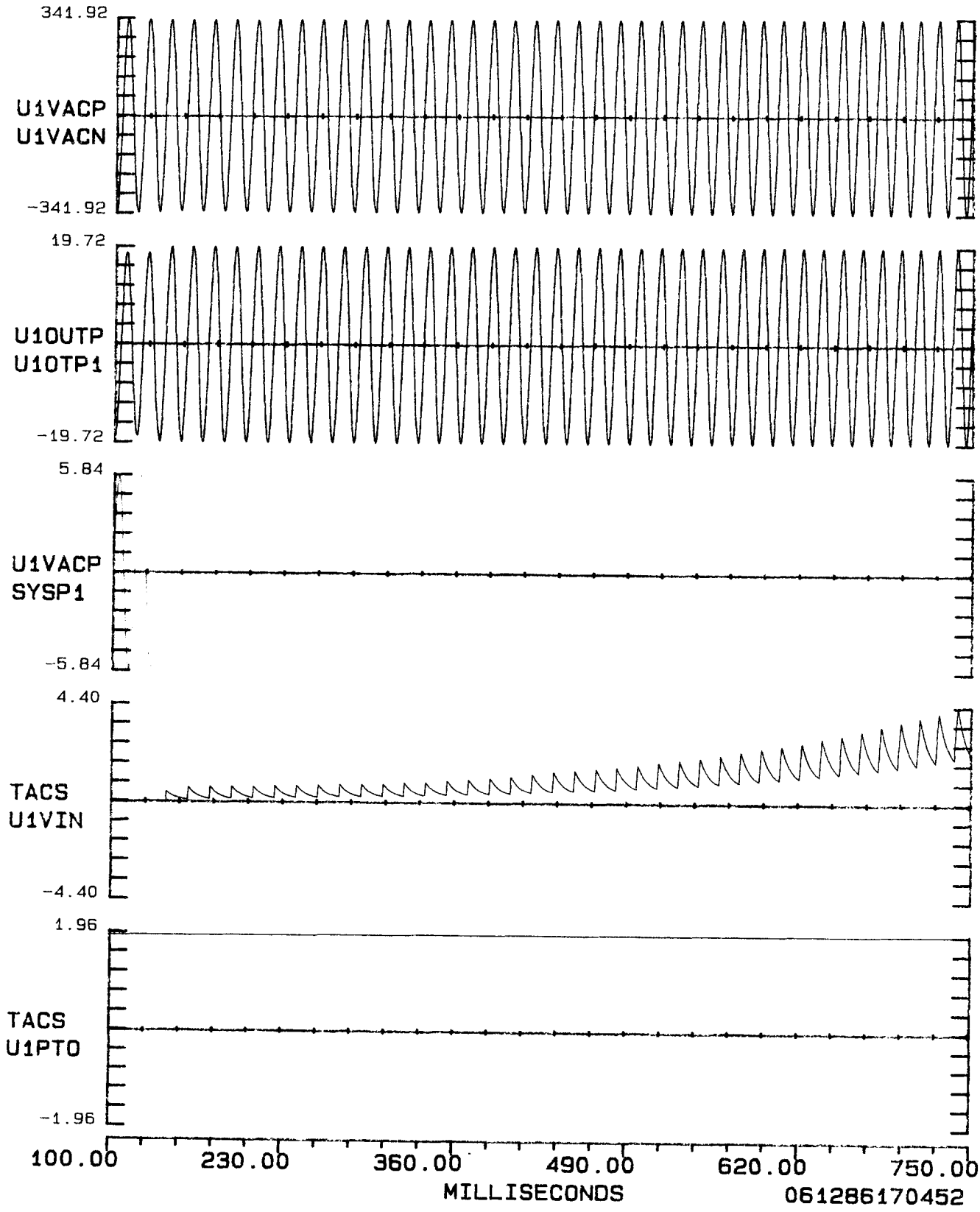

FIGURE B.3-7 ANALOG COMPUTER MODEL RESULTS OF TESLACO SPC WITH INSOLATION = 90 MW/CM^2

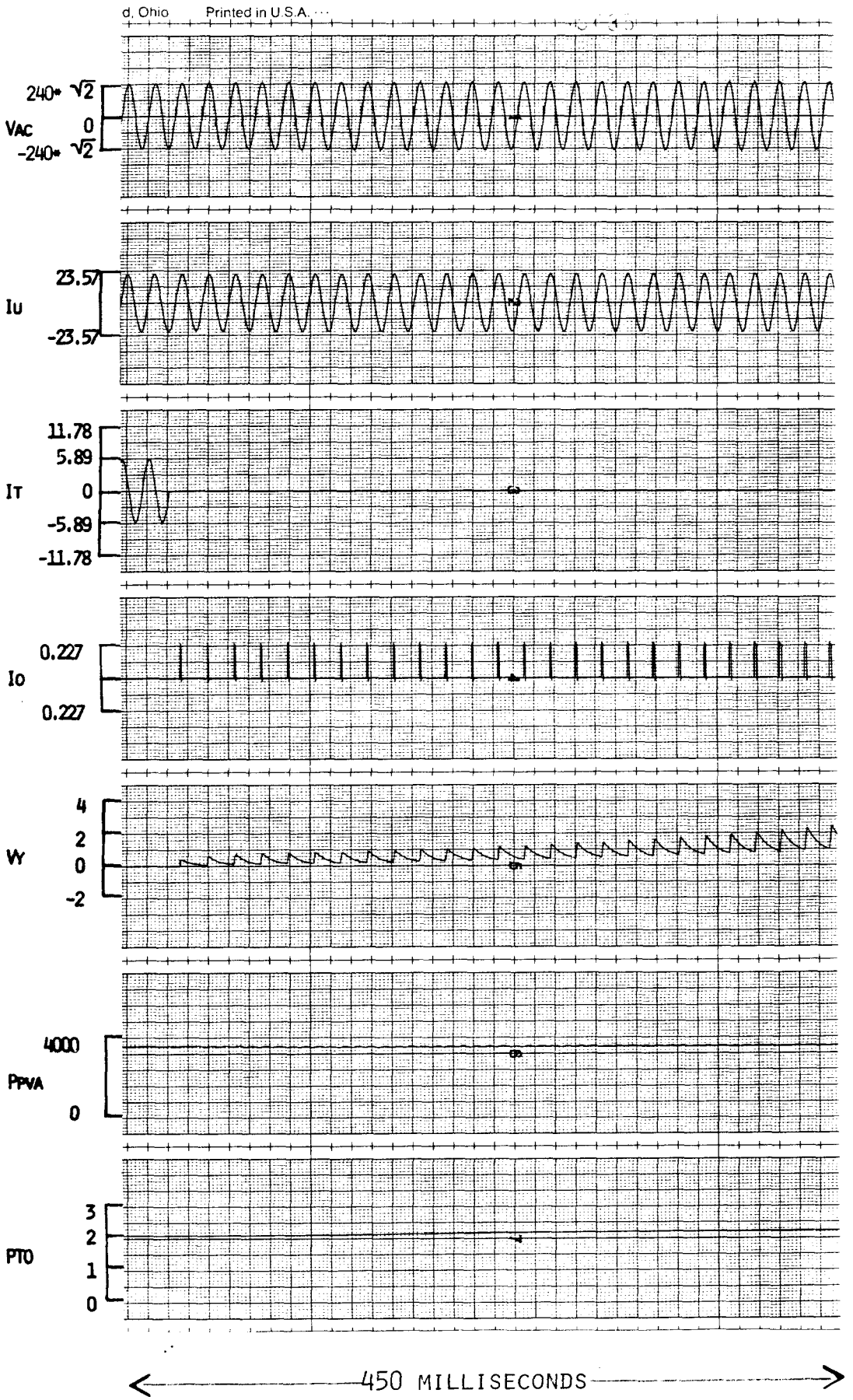

FIGURE B.3-8 EMTP COMPUTER MODEL RESULTS OF TESLACO SPC WITH INSOLATION = 90 MW/CM^2

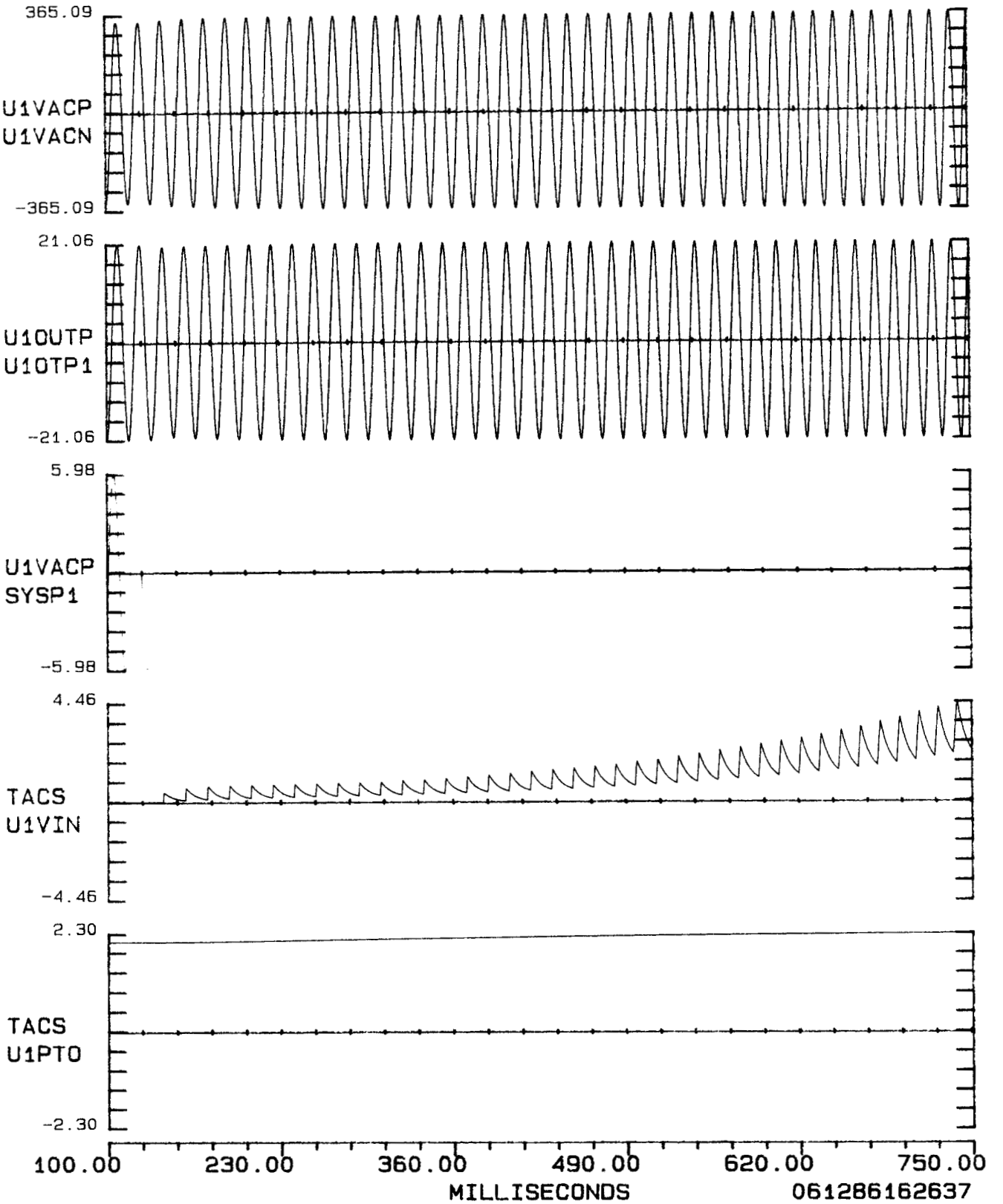

FIGURE B.3-9 ANALOG COMPUTER MODEL RESULTS OF TESLACO SPC WITH INSOLATION = 100 MW/CM^2

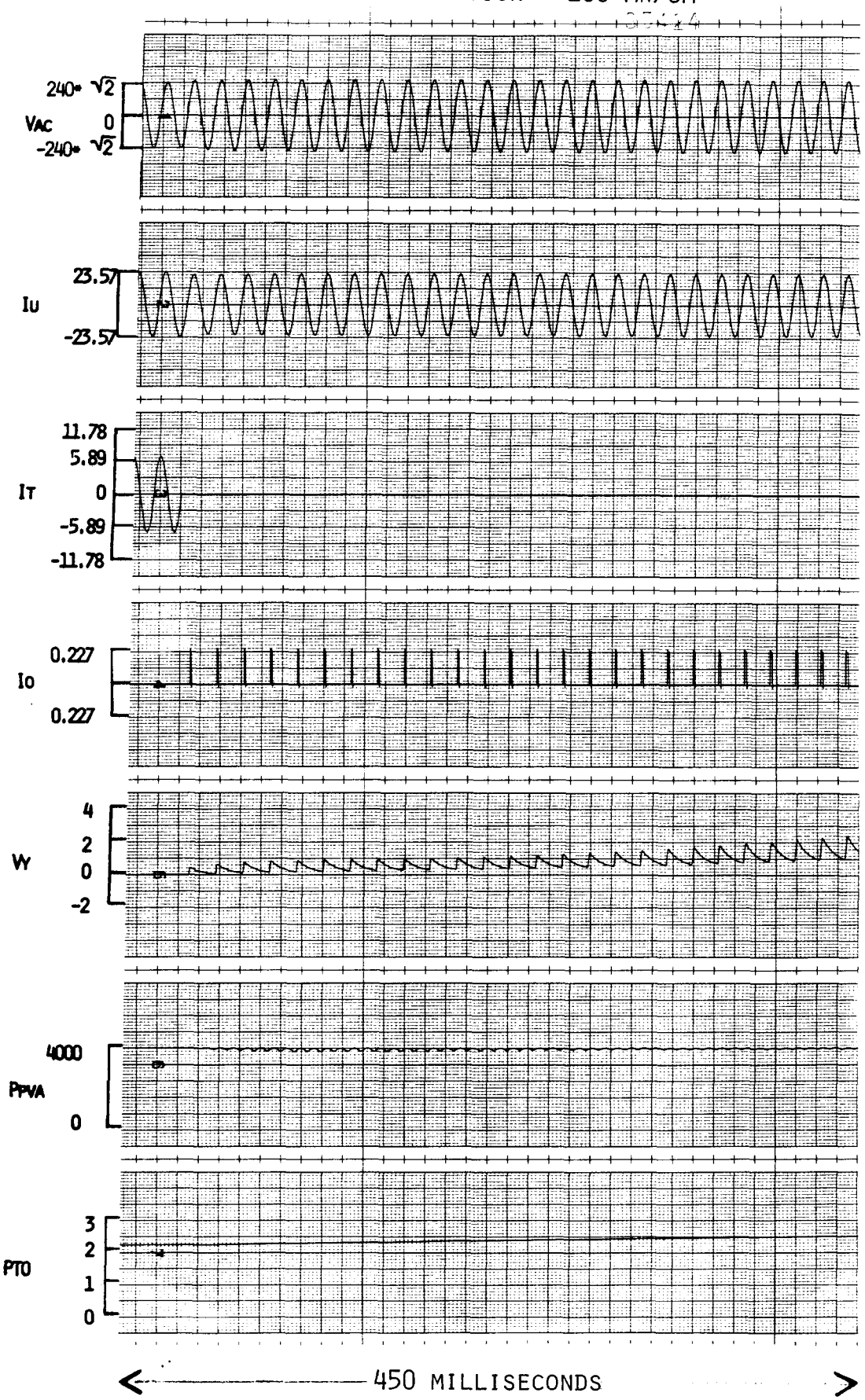

FIGURE B.3-10 EMTP COMPUTER MODEL RESULTS OF TESLACO SPC WITH INSOLATION = 100 MW/CM^2

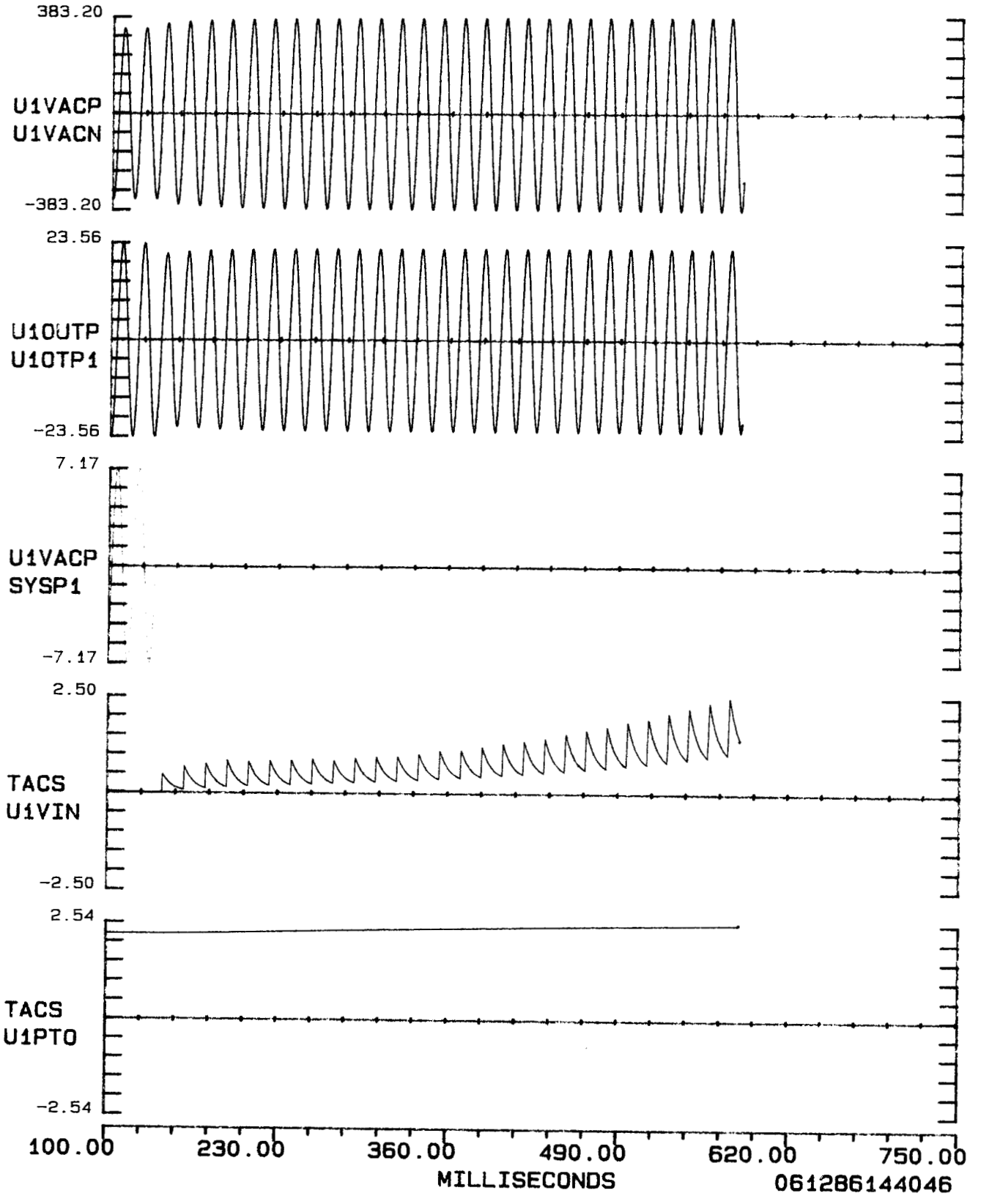

B.4 Simplified Model

Because of the complexity of the SPC models and the EMTP program itself, the time involved in computer simulations is quite long. A simplified model that can be used to make an initial screening calculation could decrease the simulation time substantially and eliminate the need for some of the detailed EMTP simulations. In this section the development and islanding performance of a simple model for a commercially available self-commutated SPC is described.

The SPC is the TESLACO whose operating principle is based on the high-frequency link approach as described before (Figure B.1-1).

The aim of the simplified model is to determine the response of the SPC in terms of dc or rms values of system variables instead of instantaneous time domain waveforms. The results of the simulations are given in terms of the "run-on time" which is defined as the time elapsed between the utility power interruption and the disconnection of SPC from the line. The model should predict the run on times optimistically under all operating conditions and indicate the problem areas sufficiently close.

Using the detailed model of EMTP computer simulations and considering the effects of SPC control algorithm during isolated operation, simplifying assumptions were established and an equivalent circuit was obtained. The equivalent circuit is composed of four sections: Converter, Phase-Locked Loop, Control System, and Photovoltaic Array. The details of each section are provided below.

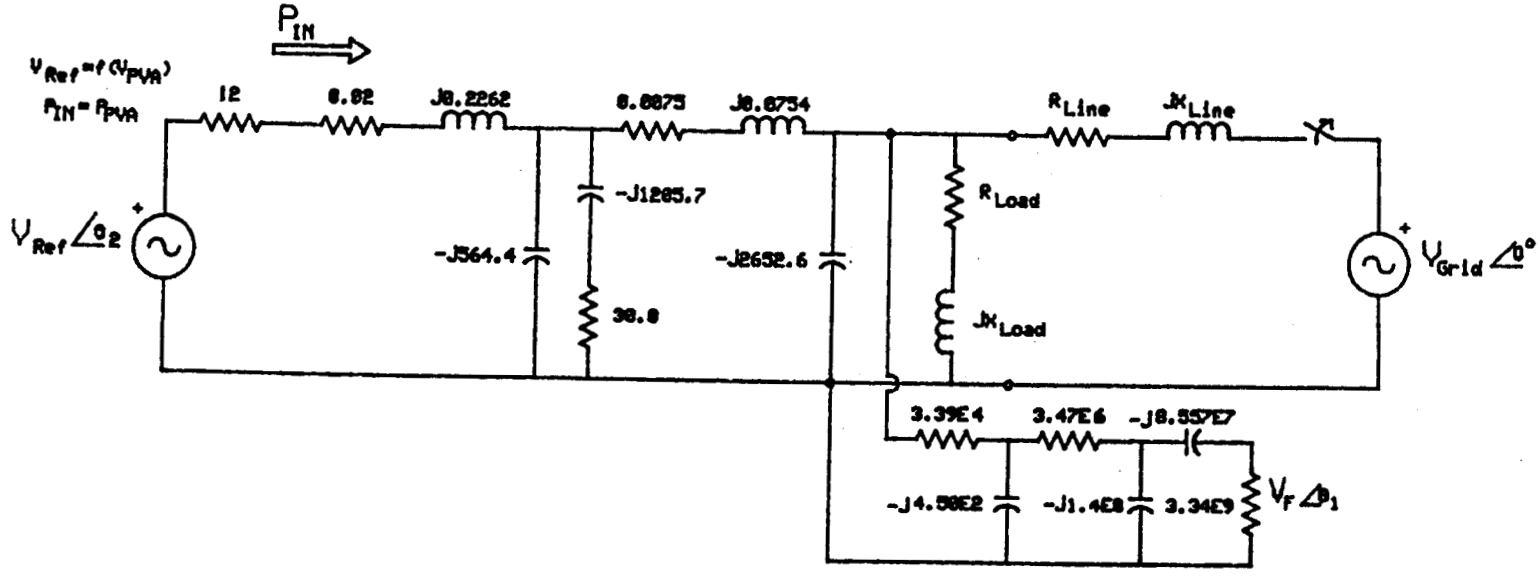

Figure B.4-1. Simplified Circuit Diagram for the Converter.

Converter

The converter part of the equivalent circuit characterizes the dc-ac conversion process, and includes the rectifier, unfolder, filters, line filter, utility and load (Figure B.4-1). In the equivalent circuit, the effects of the voltage feedforward and current feedback controls are represented by a synthesized non-dissipative internal resistance and shown as the 12.0 ohm resistor in Figure B.4-1. The transients due to the operation of the unfolder are neglected since the SPC operates around unity power factor.

The utility power interruption is simulated by the operation of the switch shown in Figure B.4-1. Before the switch opens, the SPC is in the pre-islanding mode and its operation can be described by the following equations:

$$\bar{I}_R = (K_{1r} + jK_{1i})\bar{V}_{Ref} + (K_{2r} + jK_{2i})\bar{V}_{Grid}, \qquad \text{(B.4-1)}$$

$$\bar{V}_F = (K_{3r} + jK_{3i})\bar{V}_{Ref} + (K_{4r} + jK_{4i})\bar{V}_{Grid}, \qquad \text{(B.4-2)}$$

where $\bar{V}_F = V_F \angle\theta_1$, $\bar{I}_R = I_R \angle\theta_3$,

$\bar{V}_{Ref} = V_{Ref} \angle\theta_2$, $\bar{V}_{Grid} = V_{Grid} \angle\theta°$,

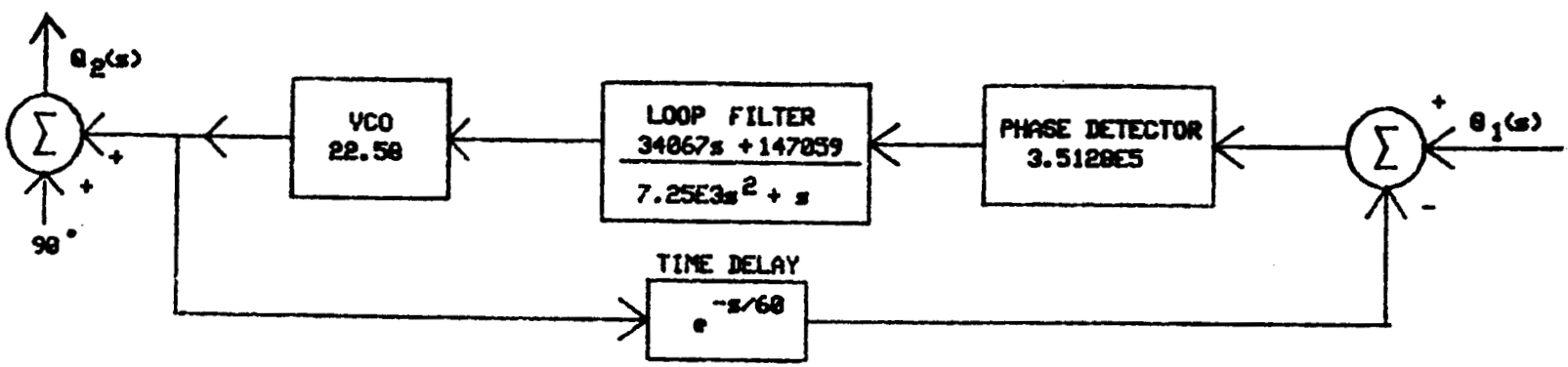

Figure B.4-2. Simplified Block Diagram for the Phase-Locked Loop.

and K_{1r}, K_{1i}, K_{2r}, K_{2i}, K_{3r}, K_{3i}, K_{4r} and K_{4i} can be determined from the circuit diagram.

After the utility switch opens, the converter goes into the islanding mode, and the following equations describe the converter operation.

$$\bar{I}_R = (K_{5r} + jK_{5i})\bar{V}_{Ref}, \tag{B.4-3}$$

$$\bar{V}_F = (K_{6r} + jK_{6i})\bar{V}_{Ref}. \tag{B.4-4}$$

The constants K_{5r}, K_{5i}, K_{6r} and K_{6i} can be determined from the converter equivalent circuit diagram.

Phase-Locked Loop

The phase-locked loop (PLL) is responsible for synchronizing the SPC control system to the utility grid for unity power factor operation. In terms of the equivalent model, the PLL sets the angle of the converter reference voltage (i.e., θ_2) depending upon the angle of the line filter voltage (i.e., θ_1). At steady-state the PLL operation is described by the following equation:

$$\theta_2 = \theta_1 + 90°. \tag{B.4-5}$$

During islanding, the dynamics of the PLL operation are described by

$$\theta_2(s) = PLL(s)*\theta_1(s) + 90./s, \qquad (B.4\text{-}6)$$

where PLL(s) is the closed-loop transfer function of the PLL equivalent model shown in Figure B.4-2 [26].

The PLL utilized in TESLACO is an RCA 4046, which is a digital-analog PLL. The PLL equivalent model shown in Figure B.4-2 was obtained using the procedure outlined in Best [26]. In the actual system, the loop filter input is a pulse whose duty cycle is proportional to phase error. In this analysis the average value of the pulse waveform is assumed to be proportional to the phase error.

Control System

The control system of the TESLACO SPC is based on feedforward voltage control, and includes a maximum power point tracker (MPPT). The controller adjusts the magnitude of the internal reference voltage (i.e., V_{Ref}) of the converter so that at steady-state, the PV array operates at its maximum power point (MPP). Due to the slow response time of the MPPT, the PV array may not operate at its MPP during isolated operation but at another point as determined by the circuit configuration. Also during isolated operation, the MPPT can only decrease the run-on time since it continuously perturbs the operating point. For these reasons the MPPT operation can be neglected; that

is, its effect can be characterized by a constant (CMPPT) during the isolated operation of the SPC.

$$V_{Ref} = 1.56*V_{PVA} + 78.0*CMPPT, \qquad (B.4\text{-}7)$$

where

CMPPT = The output voltage of the maximum power point tracking controller.

Photovoltaic Array

A linear equation is utilized to describe the output characteristics of the PV array (Equation B.4-8). The coefficients are determined from a specified maximum power level and the corresponding maximum power point voltage.

$$V_{PVA} = V_{oc\ PVA} - R_{PVA}*I_{PVA}, \qquad (B.4\text{-}8)$$

where

V_{PVA} = photovoltaic array voltage (V)

I_{PVA} = photovoltaic array current (A)

$V_{oc\ PVA}$ = photovoltaic array open-circuit voltage for linearized output characteristics (V)

R_{PVA} = photovoltaic array equivalent internal resistance for linearized output characteristics (ohms).

The open-circuit voltage of the linearized equation is equal to twice the maximum power point voltage, and the equivalent internal resistance can be determined from the specified maximum power and voltage levels. This linearized PV array equation gives reasonably satisfactory results for operating points around the maximum power voltage; however, exact equations can be used if necessary.

The power equations are obtained by assuming that the PV array power is converted to ac power without any losses; that is,

$$P_{PVA} = P_{IN}$$

$$= V_{Ref}*I_R*\cos(\theta_2-\theta_3) - 12*I_R*I_R \qquad \text{(B.4-9)}$$

or

$$V_{PVA}*I_{PVA} = V_{Ref}*I_R*\cos(\theta_2-\theta_3) - 12*I_R*I_R, \qquad \text{(B.4-10)}$$

where

P_{PVA} = photovoltaic array output power (W)

P_{IN} = The average ac input power to the SPC after the synthesized resistance as shown in Figure B.4-1.

Solution Method

To find the isolated operation performance of the SPC, one method of analysis is to solve the converter, PLL, control system, and PV array equations simultaneously. Note that the transients are only included in the PLL equations, whereas converter equations are complex-ac. Therefore a full-blown EMTP solution is not required. The program "PVISL" in Fortran 77 was developed to solve the problem. The structure of the program is such that the nonlinear equations of the converter, control system, and PV array are solved to compute the input (i.e., θ_1) for the PLL state variables for each step of the differential equation solution. Then, the output of the PLL (i.e., θ_2) is used to update the corresponding coefficients of the nonlinear equations. The process continues until the phase error (input to the phase detector) exceeds the trip setting of the TESLACO SPC (which is 6 degrees) and the time elapsed is the SPC run-on time for the specified load and utility-grid parameters. More detail is provided below.

As the first step in the program, initial array operating voltage and power, grid voltage, load and line impedance values are specified. The initial conditions on the PLL equations and the MPPT controller output are determined by assuming that the system is initially phase-locked. To find these pre-islanding conditions, Equations (B.4-1), (B.4-2), (B.4-5), (B.4-7) and (B.4-9) are solved simultaneously for the variables V_F, V_{Ref}, I_R, θ_1, θ_2, θ_3, and CMPPT.

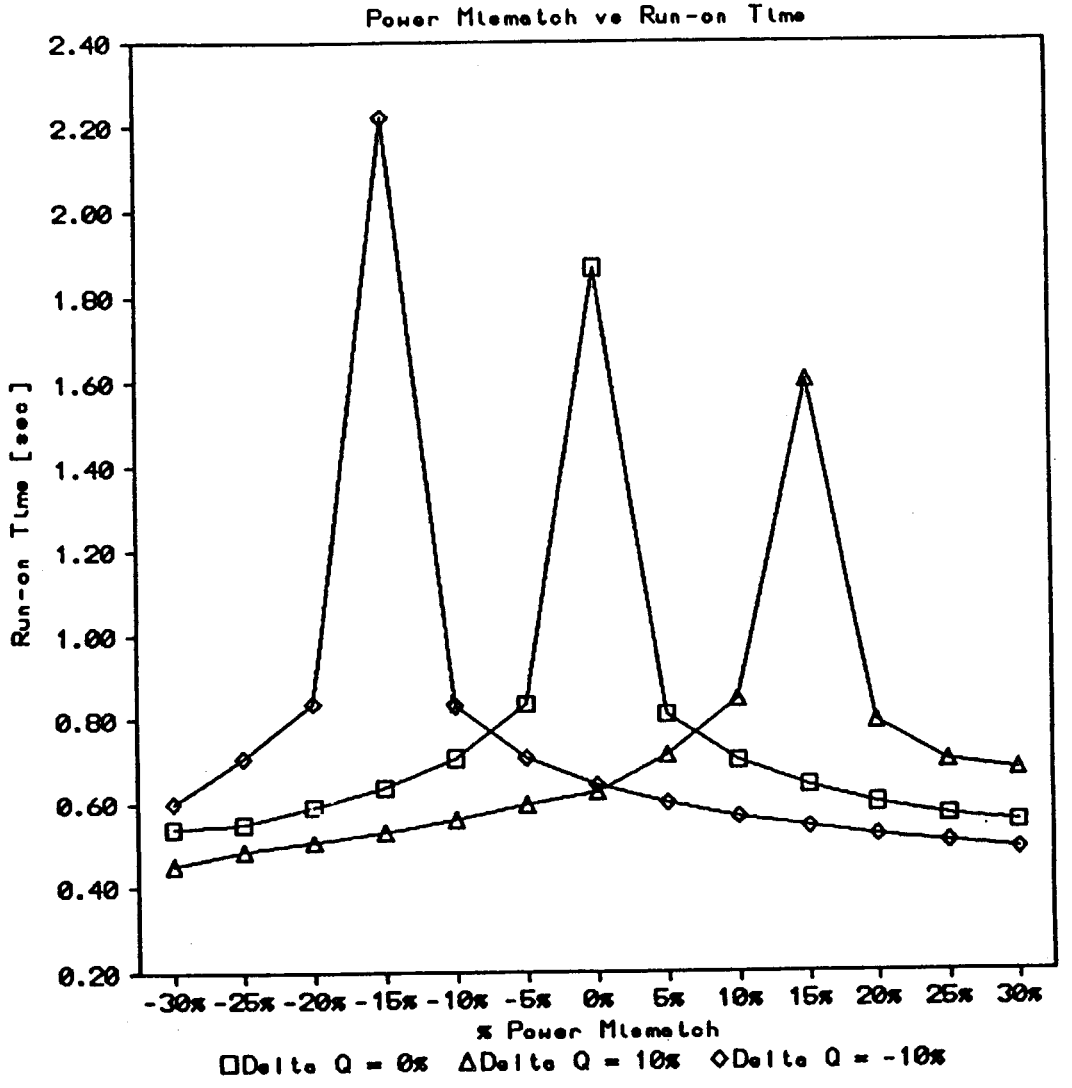

Figure B.4-3. Simplified Static Power Converter Model Run-on Times.

After the isolation, the MPPT output, CMPPT, and the PLL output, θ_2, are assumed to stay constant, and the angle of output filter voltage, θ_1, undergoes a step change as determined by the circuit parameters. To calculate θ_1, the islanding equations, Equations (B.4-3), (B.4-4), (B.4-7), (B.4-8) and (B.4-10), are solved simultaneously for the variables V_F, V_{Ref}, I_R, θ_1, θ_3, V_{PVA}, and I_{PVA}. The new value of θ_1 is the step input to the PLL, and PLL response, θ_2, is calculated for the next time step. After substituting the calculated value of θ_2 into the islanding equations a new set of equations is obtained, which is solved simultaneously to determine the next value of θ_1. The simulation continues, and if the SPC does not reach its trip setting within the predetermined simulation time, the program terminates with a message; otherwise the run-on time is output with the corresponding system parameters.

Computer Simulation Results

The results of computer simulations are shown in Figure B.4-3, where the islanding performance of the SPC is characterized in terms of run-on times as a function of both real and reactive power mismatch between generation and the load. These results will accurately and optimistically predict the islanding performance of the self-commutated TESLACO SPC. This is shown in Figure B.4-4 where the lab tests performed at Sandia (see Section 3.2) are compared with EMTP simulations and with the results of the simplified model.

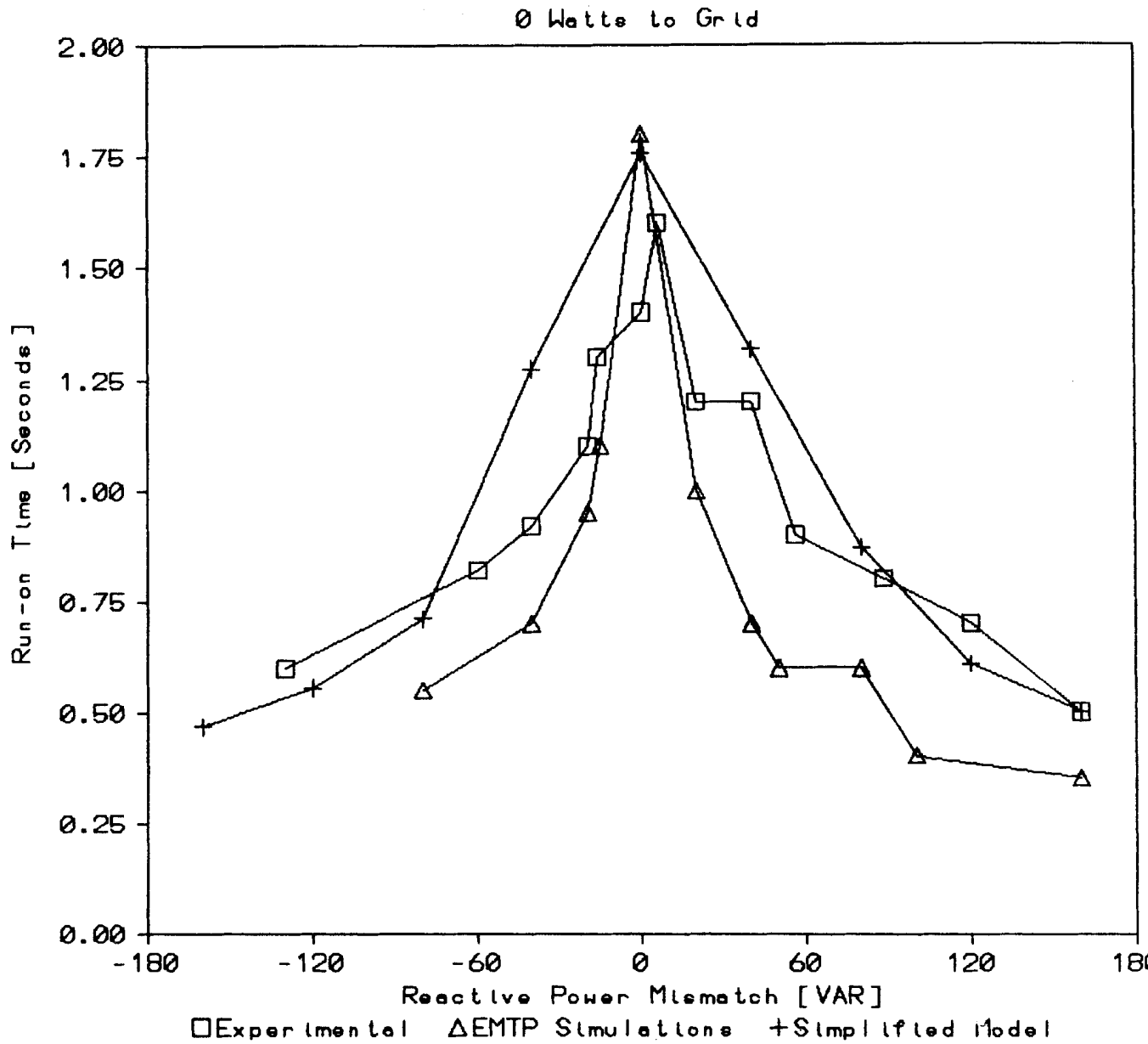

FIGURE B.4-4 COMPARISON OF SIMPLIFIED MODEL RESULTS WITH EMTP AND LAB TEST RESULTS.

Simplified Model Fortran Source Code

```
C
C               SIMULATION OF TESLACO STATIC POWER CONVERTER
C
C                              A SIMPLIFIED MODEL
C
C
      DIMENSION XINIT(15),ALPHA(15,15),BETA(15),INDX(15),Y(10),
     *DYDX(10),TH2D(1500)
      CHARACTER*50,TITLE
      COMMON/PREISL/A1,B1,C1,D1,E1,F1,G1,H1
      COMMON/ISL/A2,B2,E2,F2
      COMMON/SYSTEM/RLINE,XLINE,RLOAD,XLOAD
      COMMON/VP/VUTIL,PPVA,RDCONV
      COMMON/CONSTANT/TH2,CON1,CON2,CON3,CON4,PPT
      COMMON/INPUT/THE
C                     INITIALIZATION
      OPEN(UNIT=10,FILE='TESLAIN.DAT',STATUS='OLD')
      READ(10,*)
      READ(10,*)TITLE
        PRINT*,TITLE
      READ(10,*)
      READ(10,*)DT
        PRINT*,DT
      READ(10,*)
      READ(10,*)TMAX
      READ(10,*)
      READ(10,*)M
      READ(10,*)
      READ(10,*)RLINE
      READ(10,*)
      READ(10,*)XLINE
      READ(10,*)
      READ(10,*)RLOAD
      READ(10,*)
      READ(10,*)XLOAD
      READ(10,*)
      READ(10,*)VUTIL
      READ(10,*)
      READ(10,*)PPVA
      READ(10,*)
      READ(10,*)VPVA
        PRINT*,VPVA
      CLOSE(UNIT=10)
      OPEN(UNIT=20,FILE='TESLAOUT.DAT',STATUS='UNKNOWN')
 999     PRINT*, 'ENTER TITLE'
      READ*, TITLE
      PRINT*, 'ENTER PLL GAIN; "TO STOP ENTER A NEGATIVE #"'
      READ*,GAIN
        PRINT*,GAIN,'GAIN'
      IF(GAIN.LE.0.0)GOTO 998
      PRINT*,'ENTER PBASE'
      READ*,PBASE
```

```
      PRINT*,'ENTER PDELTA'
      READ*,PDELTA
      PRINT*,'ENTER PMAX'
      READ*,PMAX
      MAXPN=(PMAX-PBASE)/PDELTA
      PRINT*,'ENTER QBASE'
      READ*,QBASE
      PRINT*,'ENTER QDELTA'
      READ*,QDELTA
      PRINT*,'ENTER QMAX'
      READ*,QMAX
      MAXQN=(QMAX-QBASE)/QDELTA
C
         DO  11 MNP=1,MAXPN+1
         PLOAD=PBASE+(MNP-1)*PDELTA
         DO  12 NMQ=1,MAXQN+1
         QLOAD=QBASE+(NMQ-1)*QDELTA
            RLP=VUTIL*VUTIL/PLOAD
         IF(QLOAD.EQ.0.0)QLOAD=0.1
            XLP=VUTIL*VUTIL/QLOAD
         RLOAD=RLP*XLP*XLP/(RLP*RLP+XLP*XLP)
         XLOAD=RLP*RLP*XLP/(RLP*RLP+XLP*XLP)
C

C       PRINT*,'INITIALIZING THE SIMULATION'
C
C           FIND EQUIVALENT CIRCUIT CONSTANTS (A1,B1,,,,)
C           FROM GIVEN LOAD AND LINE DATA
C
      CALL INITIAL
C
C
C             FIND PRE-ISLANDING CONDITIONS BY ASSUMING
C             STEADY STATE OPERATION
C
      RDCONV=180./3.1415927
      NTRIAL=10
C                 VF,TH1,VB,CB,TH3,TH2
      XINIT(1)=3.0
      XINIT(2)=-90.0/RDCONV
      XINIT(3)=350.
      XINIT(4)=20.0
      XINIT(5)=0.0
      XINIT(6)=0.0
      N=6
      TOLX=5.E-2
      TOLF=5.E-2
C      PRINT*,'SOLVING PRE-ISLANDING CONDITIONS'
      CALL MNEWT(NTRIAL,XINIT,N,TOLX,TOLF)
C
C
C      CALCULATE THE CONSTANT FOR NEGLECTING THE MPPT
C      OPERATION FOR GIVEN PVA VOLTAGE
C
      PPT=XINIT(3)/390./0.2-VPVA/50.
      TH2=XINIT(6)
```

```
C
C
C       CALCULATE THE CONSTANTS FOR PVA USING THE MPP
C       VOLTAGE AND POWER
C                          VPVA=CON1-CON2*CPVA
C
        CON1=VPVA*2.
        CON2=VPVA*VPVA/PPVA
C
C                     OUTPUT PRE-ISLANDING CONDITIONS
C
        WRITE(20,100)TITLE,DT,TMAX,M
  100   FORMAT('1',10X,'*** TESLACO STATIC POWER CONVERTER
     *SIMULATION ***'//' ',10X,A50
     *//' ',15X,'*** SIMULATION PARAMETERS ***'/
     *' ',1X,'TIME INCREMENT=',F10.5,3X,'SIMULATION TIME=',
     *F10.5,3X,'OUTPUT FREQ.=',I4)
        WRITE(20,110)RLINE,XLINE
  110   FORMAT('0',15X,'  *** SYSTEM PARAMETERS ***'/
     *' ',10X,'RLINE=',F10.6,5X,'XLINE=',F10.6)
        WRITE(20,120)RLOAD,XLOAD
  120   FORMAT(' ',10X,'RLOAD=',F10.5,5X,'XLOAD=',F10.5)
        WRITE(20,121)PLOAD,QLOAD
  121   FORMAT(' ',10X,'PLOAD=',F10.5,5X,'QLOAD=',F10.5)
        WRITE(20,125)VUTIL,PPVA
  125   FORMAT(' ',10X,'VUTIL=',F10.2,5X,' PPVA=',F10.2)
        WRITE(20,130)CON1,CON2,GAIN
  130   FORMAT(' ',10X,' CON1=',E12.5,3X,' CON2=',E12.5/' ',
     *10X,'PHASE-LOCKED LOOP GAIN = ',E12.5)
        WRITE(20,140)XINIT(1),XINIT(2)*RDCONV,XINIT(3),
     *XINIT(6)*RDCONV,XINIT(4),XINIT(5)*RDCONV
  140   FORMAT('0',13X,'*** PRE-ISLANDING CONDITIONS ***'/
     *' ',10X,' VF=',E12.5,3X,'TH1=',E12.5/
     *' ',10X,' VB=',E12.5,3X,'TH2=',E12.5/
     *' ',10X,' CB=',E12.5,3X,'TH3=',E12.5)
        WRITE(20,150)VPVA,PPVA/VPVA,PPVA,PPT
  150   FORMAT(' ',9X,'VPVA=',E12.5,2X,'CPVA=',E12.5/
     *' ',9X,'PPVA=',E12.5,2X,' PPT=',E12.5)
C
C
C       FIND INITIAL CONDITIONS FOR ISLANDING, SPECIFICALLY
C       CALCULATE THE CHANGE IN TH1 AFTER UTILITY IS
C       DISCONNECTED, ASSUME THAT TH2 HAS NOT CHANGED
C
C        PRINT*,'FINDING INITIAL CONDITIONS FOR ISLANDING'
C
        NTRIAL=10
C                 VF,TH1,VB,CB,TH3,VPVA,CPVA
        XINIT(1)=5.
        XINIT(2)=-90./RDCONV
        XINIT(3)=350.
        XINIT(4)=20.
        XINIT(5)=0.
        XINIT(6)=200.
        XINIT(7)=20.
```

```
      N=7
      TOLX=5.E-2
      TOLF=5.E-2
      CALL MNEWT(NTRIAL,XINIT,N,TOLX,TOLF)
      TH1=XINIT(2)
C
C      PRINT*,'INITIAL CONDITIONS FOUND'
C
C      MO=TMAX/DT/M
      NR=3
      NDELAY=1./60./DT+1
      DO 40 I=1,NDELAY
 40   TH2D(I)=TH2
      THE=TH1+90./RDCONV-TH2D(1)
      YCON1=8.1578125E-4*GAIN
      YCON2=34067.647
      YCON3=147058.82
      YCON4=7.26E-3
      Y(1)=TH2/YCON1/YCON3
      Y(2)=0.
      Y(3)=0.
      T=0.
      ISHUT=0
      WRITE(20,200)
 200  FORMAT(//' ',15X,'*** ISLANDING CONDITIONS ***'
     */' ',4X,'TIME',10X,' VF',10X,'TH1',10X,' VB',10X,'TH2'
     */' ',12X,'CB',10X,'TH3',9X,'VPVA',9X,'PPVA')
      WRITE(20,210)T,XINIT(1),XINIT(2)*RDCONV,XINIT(3),
     *TH2*RDCONV,XINIT(4),XINIT(5)*RDCONV,XINIT(6),
     *XINIT(6)*XINIT(7)
 210  FORMAT(' ',5(1X,E12.5)/' ',6X,4(1X,E12.5))
C      PRINT*,'SOLVING ISLANDING'
      NTRIAL=20
 30   DO 10 I=1,M
         IF(T.GT.TMAX) GOTO 20
         CALL RK4(Y,DYDX,NR,T,DT,Y)
         TH2=YCON1*(YCON3*Y(1)+YCON2*Y(2))
               DO 50 J=1,NDELAY-1
 50            TH2D(J)=TH2D(J+1)
      TH2D(NDELAY)=TH2
         CALL MNEWT(NTRIAL,XINIT,N,TOLX,TOLF)
      TH1=XINIT(2)
      THE=TH1+90./RDCONV-TH2D(1)
      T=T+DT
      IF(ABS(THE*RDCONV).GE.6.)ISHUT=1
      IF(ISHUT.EQ.1)GOTO 55
 10   CONTINUE
 55   WRITE(20,210)T,XINIT(1),XINIT(2)*RDCONV,XINIT(3),
     *TH2*RDCONV,XINIT(4),XINIT(5)*RDCONV,XINIT(6),
     *XINIT(6)*XINIT(7)
      IF(ISHUT.EQ.1)GO TO 20
      GOTO 30
 20   CONTINUE
C      PRINT*,'ISLANDING SOLVED'
      PRINT*,' '
      PRINT*,'PLOAD=',PLOAD,'QLOAD=',QLOAD
```

```
      IF(ISHUT.EQ.1) PRINT*,'TESLACO SHUT-DOWN IN
     *',T,' SECONDS'
      IF(ISHUT.EQ.0) PRINT*,'TESLACO DID NOT SHUT-DOWN IN',
     *TMAX,'SECONDS'
      IF(ISHUT.EQ.1) WRITE(20,220)T
 220  FORMAT(' '///5X,'TESLACO SHUT-DOWN IN',F10.5,' SEC.'/)
      IF(ISHUT.EQ.0) WRITE(20,225)TMAX
 225  FORMAT(' '///5X,'TESLACO DID NOT SHUT-DOWN IN ',F10.5,
     *' SEC.'/)
  12  CONTINUE
  11  CONTINUE
      GO TO 999
 998    CLOSE(UNIT=20)
      STOP
      END
C
C
      SUBROUTINE INITIAL
      COMMON/PREISL/A1,B1,C1,D1,E1,F1,G1,H1
      COMMON/ISL/A2,B2,E2,F2
      COMMON/SYSTEM/RLINE,XLINE,RLOAD,XLOAD
      COMPLEX Z1,Z2,Z3,Z4,Z5,ZF1,ZF2,ZF3,ZF4,ZF5,ZF6,
     *ZLOAD,ZLINE,CMPLX
      COMPLEX ZF,ZF3456,ZDUM1,ZDUM2,ZDUM3,ZDUM4,ZDUM5,ZDUM6,
     *ZDUM7,ZDUM8,ZDUM9,ZDUM10,A1B1,C1D1,E1F1,G1H1,A2B2,E2F2
C
      Z1=(12.02,0.2262)
      Z2=(0.0,-564.379)
      Z3=(30.0,-1.2057193E3)
      Z4=(0.0075,0.0754)
      Z5=(0.0,-2.65258E3)
      ZF1=(3.39E4,0.0)
      ZERO=0.0
      PI=3.1415927
      ZF22=-1./2/PI/60./5.9E-6
      ZF2=CMPLX(ZERO,ZF22)
      ZF3=(3.47E6,0.0)
      ZF44=-1./2/PI/60./19.E-12
      ZF4=CMPLX(ZERO,ZF44)
      ZF55=-1./2/PI/60./31.E-12
      ZF5=CMPLX(ZERO,ZF55)
      ZF6=(3.34E9,0.0)
      ZLOAD=CMPLX(RLOAD,XLOAD)
      ZLINE=CMPLX(RLINE,XLINE)
C
      ZF3456=ZF4*(ZF5+ZF6)/(ZF4+ZF5+ZF6)+ZF3
      ZF=ZF1+ZF2*ZF3456/(ZF2+ZF3456)
      ZDUM1=Z5*ZLOAD*ZF/(Z5*ZLOAD+ZF*ZLOAD+ZF*Z5)
      ZDUM2=Z2*Z3/(Z2+Z3)
      ZDUM3=Z4+ZDUM1*ZLINE/(ZDUM1+ZLINE)
      ZDUM4=ZDUM2*ZDUM3/(ZDUM2+ZDUM3)
      A1B1=1./(ZDUM4+Z1)
      ZDUM5=Z1+ZDUM2*(Z4+ZDUM1)/(ZDUM2+Z4+ZDUM1)
      A2B2=1./ZDUM5
      C1D1=-ZDUM4*ZDUM1/ZDUM3/(ZDUM4+Z1)/(ZDUM1+ZLINE)
```

```
C
      ZDUM1=Z5*ZLOAD/(Z5+ZLOAD)
      ZDUM3=Z1*ZDUM2/(Z1+ZDUM2)
      ZDUM4=ZDUM3+Z4
      ZDUM5=ZDUM1*ZDUM4/(ZDUM1+ZDUM4)
      ZDUM6=ZF1+ZDUM5
      ZDUM7=ZDUM6*ZF2/(ZDUM6+ZF2)
      ZDUM8=ZF3+ZDUM7
      ZDUM9=ZDUM8*ZF4/(ZDUM8+ZF4)
      ZDUM10=ZDUM3*ZDUM5*ZDUM7*ZDUM9/ZDUM4/ZDUM6/ZDUM8/Z1
      E2F2=ZF6*ZDUM10/(ZDUM9+ZF5+ZF6)
C
      ZDUM1=Z5*ZLOAD*ZLINE/(Z5*ZLOAD+ZLOAD*ZLINE+ZLINE*Z5)
      ZDUM3=Z1*ZDUM2/(Z1+ZDUM2)
      ZDUM4=ZDUM3+Z4
      ZDUM5=ZDUM1*ZDUM4/(ZDUM1+ZDUM4)
      ZDUM6=ZF1+ZDUM5
      ZDUM7=ZDUM6*ZF2/(ZDUM6+ZF2)
      ZDUM8=ZF3+ZDUM7
      ZDUM9=ZDUM8*ZF4/(ZDUM8+ZF4)
      ZDUM10=ZDUM3*ZDUM5*ZDUM7*ZDUM9/ZDUM4/ZDUM6/ZDUM8/Z1
      E1F1=ZF6*ZDUM10/(ZDUM9+ZF5+ZF6)
C
      ZDUM3=Z4+Z1*ZDUM2/(Z1+ZDUM2)
      ZDUM5=ZDUM1*ZDUM3/(ZDUM1+ZDUM3)
      ZDUM6=ZF1+ZDUM5
      ZDUM7=ZDUM6*ZF2/(ZDUM6+ZF2)
      ZDUM8=ZF3+ZDUM7
      ZDUM9=ZDUM8*ZF4/(ZDUM8+ZF4)
      ZDUM10=ZDUM5*ZDUM7*ZDUM9/ZDUM6/ZDUM8/ZLINE
      G1H1=ZF6*ZDUM10/(ZDUM9+ZF5+ZF6)
C
C
      A1=REAL(A1B1)
      B1=AIMAG(A1B1)
      C1=REAL(C1D1)
      D1=AIMAG(C1D1)
      E1=REAL(E1F1)
      F1=AIMAG(E1F1)
      G1=REAL(G1H1)
      H1=AIMAG(G1H1)
C
      A2=REAL(A2B2)
      B2=AIMAG(A2B2)
      E2=REAL(E2F2)
      F2=AIMAG(E2F2)
C
      RETURN
      END
C
      SUBROUTINE USR(X,ALPHA,BETA)
      COMMON/PREISL/A1,B1,C1,D1,E1,F1,G1,H1
      COMMON/VP/VUTIL,PPVA,RDCONV
      DIMENSION X(15),ALPHA(15,15),BETA(15)
      VF=X(1)
```

```
      TH1=X(2)
      VB=X(3)
      CB=X(4)
      TH3=X(5)
      TH2=X(6)
      BETA(1)=-(PPVA+CB*CB*12.0-VB*CB*COS(TH2-TH3))
      BETA(2)=-(A1*VB*COS(TH2)-B1*VB*SIN(TH2)+C1
     **VUTIL-CB*COS(TH3))
      BETA(3)=-(B1*VB*COS(TH2)+A1*VB*SIN(TH2)+D1
     **VUTIL-CB*SIN(TH3))
      BETA(4)=-(E1*VB*COS(TH2)-F1*VB*SIN(TH2)+G1
     **VUTIL-VF*COS(TH1))
      BETA(5)=-(F1*VB*COS(TH2)+E1*VB*SIN(TH2)+H1
     **VUTIL-VF*SIN(TH1))
      BETA(6)=-(TH1-TH2+90.0/RDCONV)
      ALPHA(1,1)=0.0
      ALPHA(1,2)=0.0
      ALPHA(1,3)=-CB*COS(TH2-TH3)
      ALPHA(1,4)=-VB*COS(TH2-TH3)+2.*12.0*CB
      ALPHA(1,5)=-VB*CB*SIN(TH2-TH3)
      ALPHA(1,6)=VB*CB*SIN(TH2-TH3)
      ALPHA(2,1)=0.0
      ALPHA(2,2)=0.0
      ALPHA(2,3)=A1*COS(TH2)-B1*SIN(TH2)
      ALPHA(2,4)=-COS(TH3)
      ALPHA(2,5)=CB*SIN(TH3)
      ALPHA(2,6)=-A1*VB*SIN(TH2)-B1*VB*COS(TH2)
      ALPHA(3,1)=0.0
      ALPHA(3,2)=0.0
      ALPHA(3,3)=B1*COS(TH2)+A1*SIN(TH2)
      ALPHA(3,4)=-SIN(TH3)
      ALPHA(3,5)=-CB*COS(TH3)
      ALPHA(3,6)=-B1*VB*SIN(TH2)+A1*VB*COS(TH2)
      ALPHA(4,1)=-COS(TH1)
      ALPHA(4,2)=VF*SIN(TH1)
      ALPHA(4,3)=E1*COS(TH2)-F1*SIN(TH2)
      ALPHA(4,4)=0.0
      ALPHA(4,5)=0.0
      ALPHA(4,6)=-E1*VB*SIN(TH2)-F1*VB*COS(TH2)
      ALPHA(5,1)=-SIN(TH1)
      ALPHA(5,2)=-VF*COS(TH1)
      ALPHA(5,3)=F1*COS(TH2)+E1*SIN(TH2)
      ALPHA(5,4)=0.0
      ALPHA(5,5)=0.0
      ALPHA(5,6)=-F1*VB*SIN(TH2)+E1*VB*COS(TH2)
      ALPHA(6,1)=0.0
      ALPHA(6,2)=1.0
      ALPHA(6,3)=0.0
      ALPHA(6,4)=0.0
      ALPHA(6,5)=0.0
      ALPHA(6,6)=-1.0
      RETURN
      END
C
C
      SUBROUTINE USRFUN1(X,ALPHA,BETA)
```

```
      COMMON/ISL/A2,B2,E2,F2
      COMMON/CONSTANT/TH2,CON1,CON2,CON3,CON4,PPT
      DIMENSION X(15),ALPHA(15,15),BETA(15)
      VF=X(1)
      TH1=X(2)
      VB=X(3)
      CB=X(4)
      TH3=X(5)
      VPVA=X(6)
      CPVA=X(7)
      BETA(1)=-(VPVA*CPVA+CB*CB*12.0-VB*CB*COS(TH2-TH3))
      BETA(2)=-(A2*VB*COS(TH2)-B2*VB*SIN(TH2)-CB*COS(TH3))
      BETA(3)=-(B2*VB*COS(TH2)+A2*VB*SIN(TH2)-CB*SIN(TH3))
      BETA(4)=-(E2*VB*COS(TH2)-F2*VB*SIN(TH2)-VF*COS(TH1))
      BETA(5)=-(F2*VB*COS(TH2)+E2*VB*SIN(TH2)-VF*SIN(TH1))
      BETA(6)=-(VPVA-CON1+CON2*CPVA)
      BETA(7)=-(VB-1.56*VPVA-78.*PPT)
      ALPHA(1,1)=0.0
      ALPHA(1,2)=0.0
      ALPHA(1,3)=-CB*COS(TH2-TH3)
      ALPHA(1,4)=-VB*COS(TH2-TH3)+2.*12.0*CB
      ALPHA(1,5)=-VB*CB*SIN(TH2-TH3)
      ALPHA(1,6)=CPVA
      ALPHA(1,7)=VPVA
      ALPHA(2,1)=0.0
      ALPHA(2,2)=0.0
      ALPHA(2,3)=A2*COS(TH2)-B2*SIN(TH2)
      ALPHA(2,4)=-COS(TH3)
      ALPHA(2,5)=CB*SIN(TH3)
      ALPHA(2,6)=0.0
      ALPHA(2,7)=0.0
      ALPHA(3,1)=0.0
      ALPHA(3,2)=0.0
      ALPHA(3,3)=B2*COS(TH2)+A2*SIN(TH2)
      ALPHA(3,4)=-SIN(TH3)
      ALPHA(3,5)=-CB*COS(TH3)
      ALPHA(3,6)=0.0
      ALPHA(3,7)=0.0
      ALPHA(4,1)=-COS(TH1)
      ALPHA(4,2)=VF*SIN(TH1)
      ALPHA(4,3)=E2*COS(TH2)-F2*SIN(TH2)
      ALPHA(4,4)=0.0
      ALPHA(4,5)=0.0
      ALPHA(4,6)=0.0
      ALPHA(4,7)=0.0
      ALPHA(5,1)=-SIN(TH1)
      ALPHA(5,2)=-VF*COS(TH1)
      ALPHA(5,3)=F2*COS(TH2)+E2*SIN(TH2)
      ALPHA(5,4)=0.0
      ALPHA(5,5)=0.0
      ALPHA(5,6)=0.0
      ALPHA(5,7)=0.0
      ALPHA(6,1)=0.0
      ALPHA(6,2)=0.0
```

```
      ALPHA(6,3)=0.0
      ALPHA(6,4)=0.0
      ALPHA(6,5)=0.0
      ALPHA(6,6)=1.0
      ALPHA(6,7)=CON2
      ALPHA(7,1)=0.0
      ALPHA(7,2)=0.0
      ALPHA(7,3)=1.0
      ALPHA(7,4)=0.0
      ALPHA(7,5)=0.0
      ALPHA(7,6)=-1.56
      ALPHA(7,7)=0.0
      RETURN
      END
C
C
      SUBROUTINE MNEWT(NTRIAL,X,N,TOLX,TOLF)
      PARAMETER (NP=15)
      DIMENSION X(NP),ALPHA(NP,NP),BETA(NP),INDX(NP)
      DO 13  K=1,NTRIAL
        IF(N.EQ.6)CALL USR(X,ALPHA,BETA)
        IF(N.EQ.7)CALL USRFUN1(X,ALPHA,BETA)
        ERRF=0.
        DO 11 I=1,N
          ERRF=ERRF+ABS(BETA(I))
11      CONTINUE
        IF(ERRF.LE.TOLF)RETURN
        CALL LUDCMP(ALPHA,N,NP,INDX,D)
        CALL LUBKSB(ALPHA,N,NP,INDX,BETA)
        ERRX=0.
        DO 12 I=1,N
          ERRX=ERRX+ABS(BETA(I))
          X(I)=X(I)+BETA(I)
12      CONTINUE
        IF(ERRX.LE.TOLX)RETURN
13    CONTINUE
      PRINT*,'NEWTON-RAPHSON DID NOT CONVERGE'
      RETURN
      END
C
C
      SUBROUTINE LUDCMP(A,N,NP,INDX,D)
      PARAMETER (NMAX=100,TINY=1.0E-20)
      DIMENSION A(NP,NP),INDX(N),VV(NMAX)
      D=1.
      DO 12 I=1,N
        AAMAX=0.
        DO 11 J=1,N
          IF (ABS(A(I,J)).GT.AAMAX) AAMAX=ABS(A(I,J))
11      CONTINUE
        IF (AAMAX.EQ.0.) PAUSE 'Singular matrix.'
        VV(I)=1./AAMAX
12    CONTINUE
      DO 19 J=1,N
        IF (J.GT.1) THEN
          DO 14 I=1,J-1
```

```
            SUM=A(I,J)
            IF (I.GT.1)THEN
              DO 13 K=1,I-1
                SUM=SUM-A(I,K)*A(K,J)
13            CONTINUE
              A(I,J)=SUM
            ENDIF
14        CONTINUE
        ENDIF
        AAMAX=0.
        DO 16 I=J,N
          SUM=A(I,J)
          IF (J.GT.1)THEN
            DO 15 K=1,J-1
              SUM=SUM-A(I,K)*A(K,J)
15          CONTINUE
            A(I,J)=SUM
          ENDIF
          DUM=VV(I)*ABS(SUM)
          IF (DUM.GE.AAMAX) THEN
            IMAX=I
            AAMAX=DUM
          ENDIF
16      CONTINUE
        IF (J.NE.IMAX)THEN
          DO 17 K=1,N
            DUM=A(IMAX,K)
            A(IMAX,K)=A(J,K)
            A(J,K)=DUM
17        CONTINUE
          D=-D
          VV(IMAX)=VV(J)
        ENDIF
        INDX(J)=IMAX
        IF(J.NE.N)THEN
          IF(A(J,J).EQ.0.)A(J,J)=TINY
          DUM=1./A(J,J)
          DO 18 I=J+1,N
            A(I,J)=A(I,J)*DUM
18        CONTINUE
        ENDIF
19    CONTINUE
      IF(A(N,N).EQ.0.)A(N,N)=TINY
      RETURN
      END
C
C
      SUBROUTINE LUBKSB(A,N,NP,INDX,B)
      DIMENSION A(NP,NP),INDX(N),B(N)
      II=0
      DO 12 I=1,N
        LL=INDX(I)
        SUM=B(LL)
        B(LL)=B(I)
        IF (II.NE.0)THEN
          DO 11 J=II,I-1
```

```
            SUM=SUM-A(I,J)*B(J)
11        CONTINUE
        ELSE IF (SUM.NE.0.) THEN
          II=I
        ENDIF
        B(I)=SUM
12    CONTINUE
      DO 14 I=N,1,-1
        SUM=B(I)
        IF(I.LT.N)THEN
          DO 13 J=I+1,N
            SUM=SUM-A(I,J)*B(J)
13        CONTINUE
        ENDIF
        B(I)=SUM/A(I,I)
14    CONTINUE
      RETURN
      END
C
C
      SUBROUTINE RK4(Y,DYDX,N,X,H,YOUT)
      PARAMETER (NMAX=10)
      DIMENSION Y(N),DYDX(N),YOUT(N),YT(NMAX),DYT(NMAX),
     *DYM(NMAX)
      HH=H*0.5
      H6=H/6.
      XH=X+HH
      DO 11 I=1,N
        YT(I)=Y(I)+HH*DYDX(I)
11    CONTINUE
      CALL DERIVS(XH,YT,DYT)
      DO 12 I=1,N
        YT(I)=Y(I)+HH*DYT(I)
12    CONTINUE
      CALL DERIVS(XH,YT,DYM)
      DO 13 I=1,N
        YT(I)=Y(I)+H*DYM(I)
        DYM(I)=DYT(I)+DYM(I)
13    CONTINUE
      CALL DERIVS(X+H,YT,DYT)
      DO 14 I=1,N
        YOUT(I)=Y(I)+H6*(DYDX(I)+DYT(I)+2.*DYM(I))
14    CONTINUE
      RETURN
      END
C
C
      SUBROUTINE DERIVS(T,Y,DY)
      COMMON/INPUT/THE
      DIMENSION Y(15),DY(15)
      DY(1)=Y(2)
      DY(2)=Y(3)
      DY(3)=(-Y(1)+THE)/7.25E-3
      TD=T
      RETURN
      END
```

APPENDIX C - GEMINI STATIC POWER CONVERTER MODEL

C.1 Description of the Model

The Gemini line-commutated static power converter (SPC) is a single-phase, 240-Vac, 6000-watt residential unit. The SPC utilizes silicon-controlled rectifiers (SCRs) as the power-switching devices, which are connected in single-phase bridge configuration. The general circuit diagram of the SPC and interconnections to the utility and the photovoltaic (PV) array are shown in Figure C.1-1 [14]. The model and the parameters for the model were supplied by Paul Krause and Associates. The parameters were based primarily on data obtained from the manufacturer.

The utility interconnection is accomplished through an isolation transformer, which is a step-down transformer with a voltage ratio of 350/240 Volts. In the circuit diagram, the isolation transformer is modeled by a resistor, R_T, in series with an inductor, L_T. The component values are shown below.

$$R_T = 0.04 \text{ ohms.}$$

$$L_T = 1.06 \text{ mH.}$$

The filter at the dc side is composed of an inductor and a capacitor (L_L and C_F), and the series resistor (R_L) represents the internal resistance of the filter inductor.

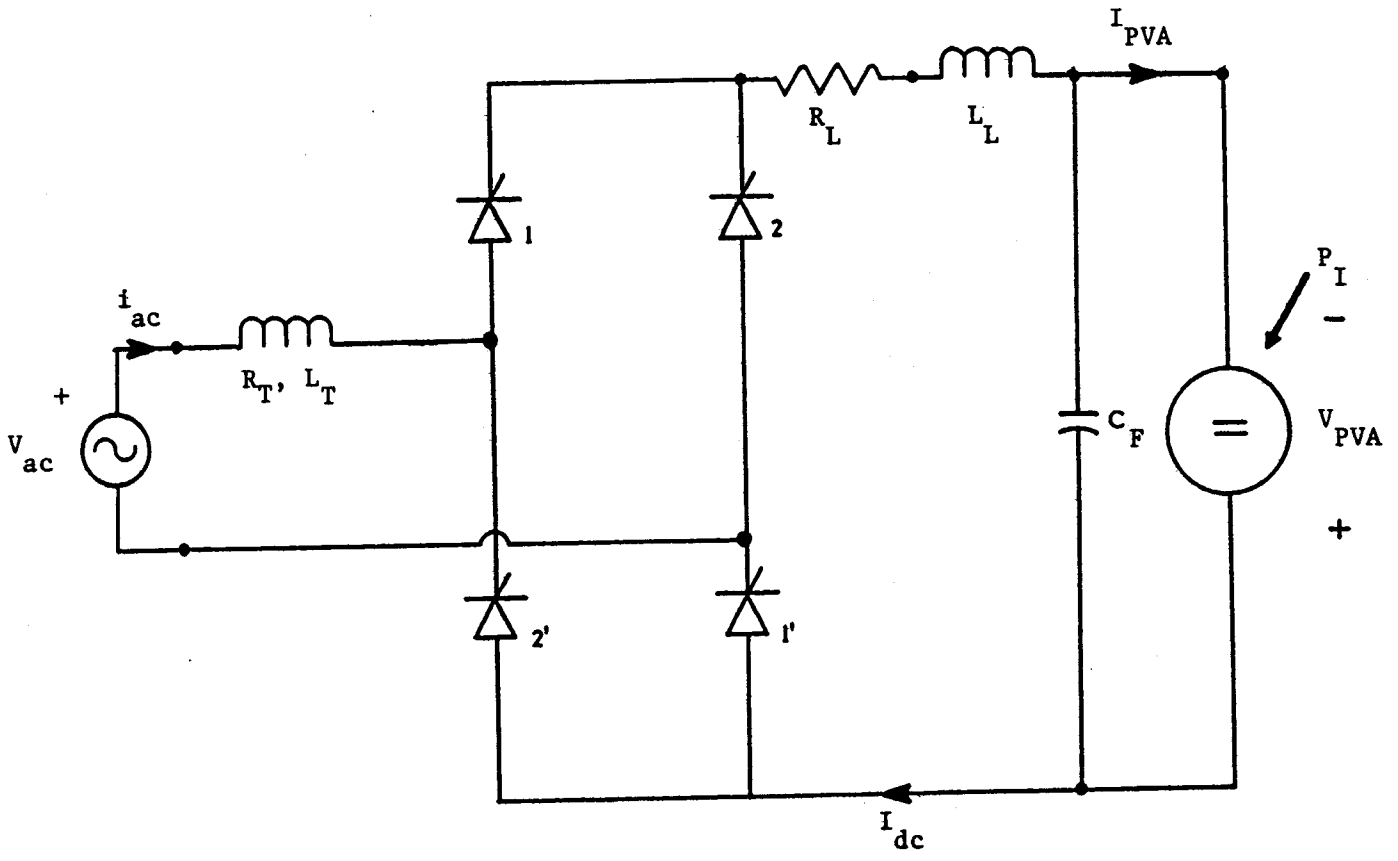

Figure C.1-1. Single-Phase, Line-Commutated Static Power Converter Circuit Diagram.

R_L = 0.9 ohms,

L_L = 48 mH, and C_F = 4.8 mF.

The operating principles of the single-phase line-commutated SPCs are discussed in detail in the literature and will not be repeated here. Only a brief description helpful in understanding the results of this report is provided.

According to the operation principle of the SPC, during the positive half-cycle of the ac voltage waveform, SCRs 1 and 1' must be turned on, and 180° later, during the negative half-cycle, 2 and 2' must be turned on. A gating signal synchronized to the ac voltage is supplied to the gates of the SCRs to turn them on. Figures C.1-2 and C.1-3 show the circuit diagram when SCRs 1-1', and 2-2' are in conduction, respectively [14,16-18].

The instant the gating signal is applied to the gate of the SCR, with respect to the the zero crossing of the ac voltage waveform, is defined as the firing angle(α). For inverter operation of the SPC, that is, dc-ac conversion, the firing angle of the SCRs must be between 90° and 180°.

The line-commutated inverter, as viewed from dc terminals, can be considered as a variable dc voltage source, where the level of the dc voltage source depends on the firing angles of the SCRs. At constant atmospheric conditions, the PV array output current depends on the inverter voltage across the array. By varying this voltage, the array current varies

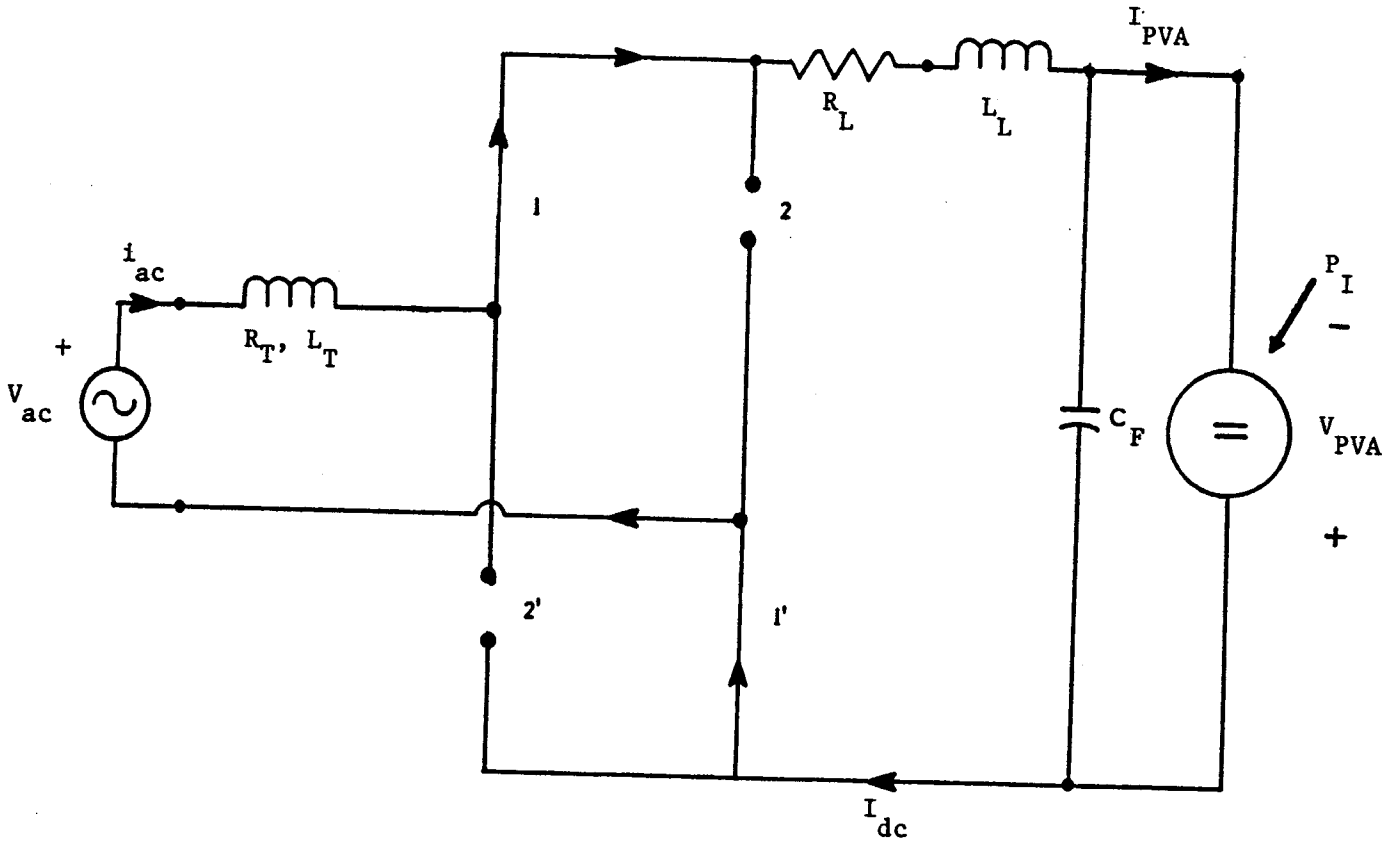

Figure C.1-2. Single-Phase, Line-Commutated Static Power Converter Circuit Diagram when SCR's 1 and 1' are Conducting.

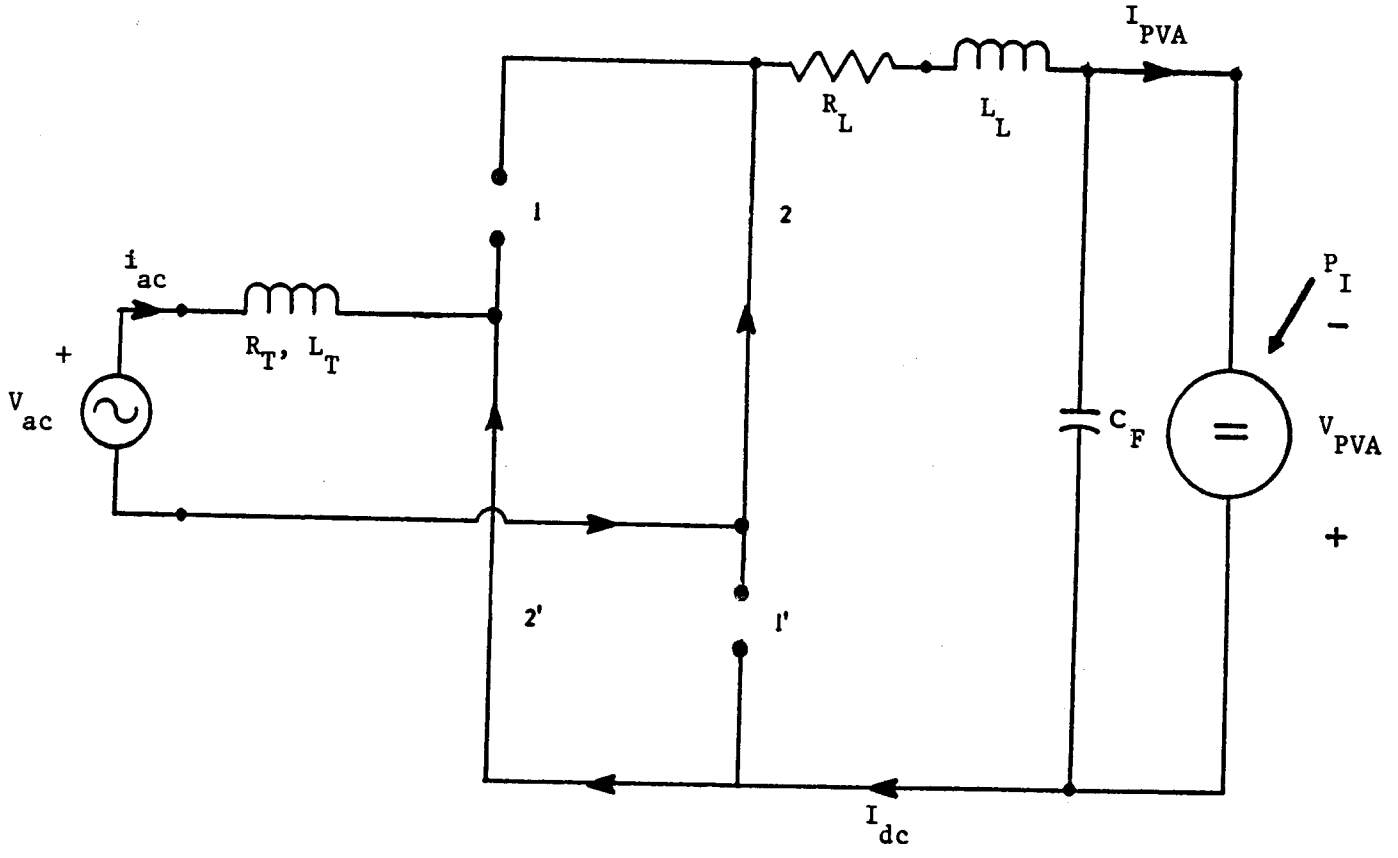

Figure C.1-3. Single-Phase, Line-Commutated Static Power Converter Circuit Diagram when SCR's 2 and 2' are Conducting.

correspondingly; that is, the magnitude of the power flow from the dc side to the ac side can be adjusted by changing the firing angle of the SCRs.

In normal operation of the SPC, the firing angles are controlled so that the array operating voltage is fixed under all atmospheric conditions. Depending upon the operating voltage and available array power, there are two possible modes of operation; discontinuous dc current and continuous dc current. The discontinuous mode of the dc current occurs when the conduction period of the SCR's pair is less than 180°. Figure C.1-4 illustrates the ac voltage, firing pulses, dc and ac current waveforms for the SPC during the discontinuous mode of operation.

If the SCR pairs conduct more than 180° the SPC is in continuous current mode of operation, and the corresponding waveforms are depicted in Figure C.1-5. Note that, due to the finite amount of the transformer inductance the SCR current cannot commutate from one pair to the other instantenously, and a short-circuit occurs at the converter terminals during commutation intervals.

The SCR model in the Electromagnetic Transients Program (EMTP) is used in modeling the power circuit of the line-commutated SPC. The power circuit is represented component by component and discussed in detail in Section C.2. The photovoltaic array is selected so that its rating at the chosen reference voltage of 248V is 4.33 kW. The analytical equation showing the corresponding PV array current-voltage characteristics was obtained by the procedure described in Appendix A [Equation (C.1-1)].

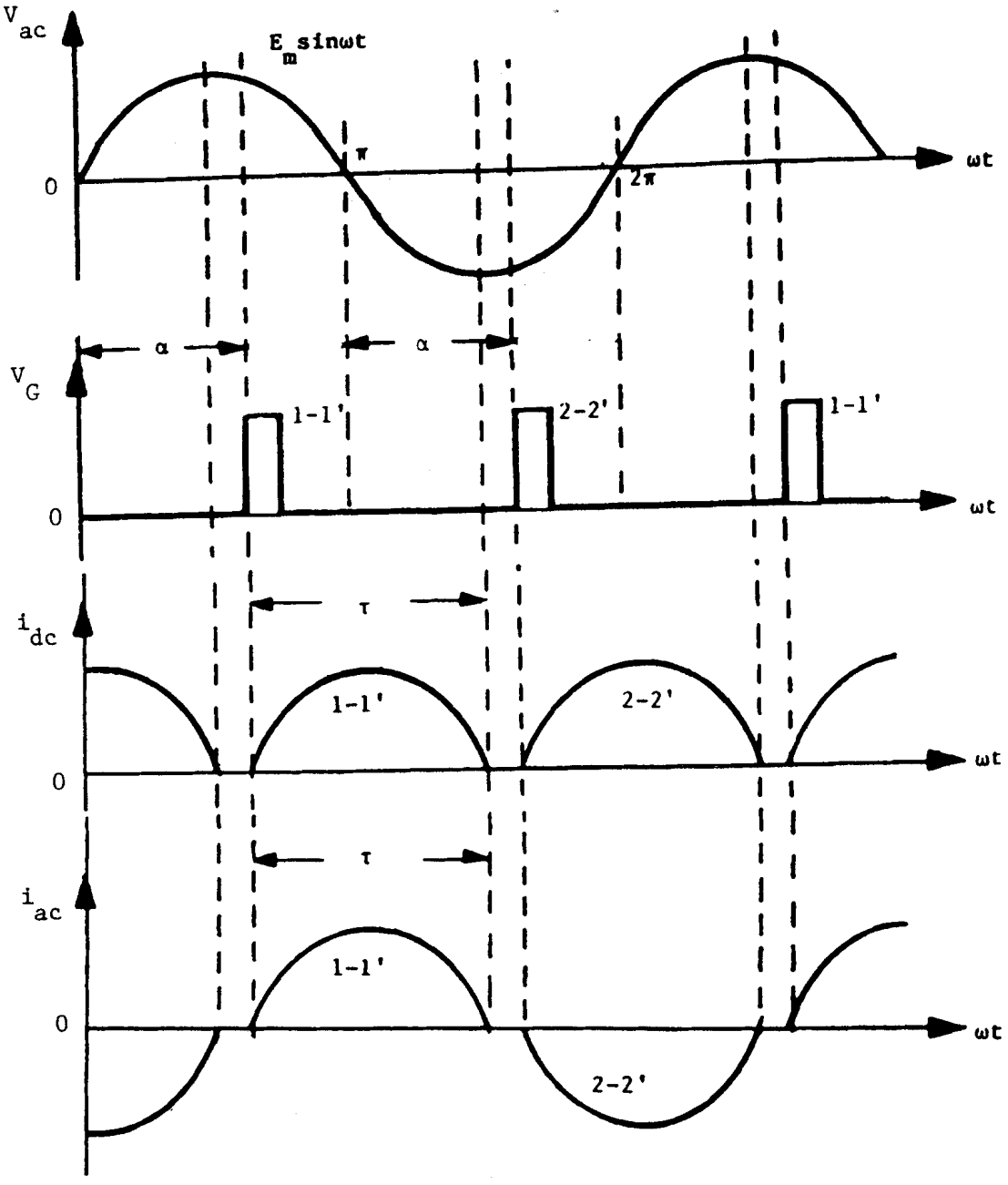

Figure C.1-4. Current and Voltage Waveforms During Discontinuous Current Mode.

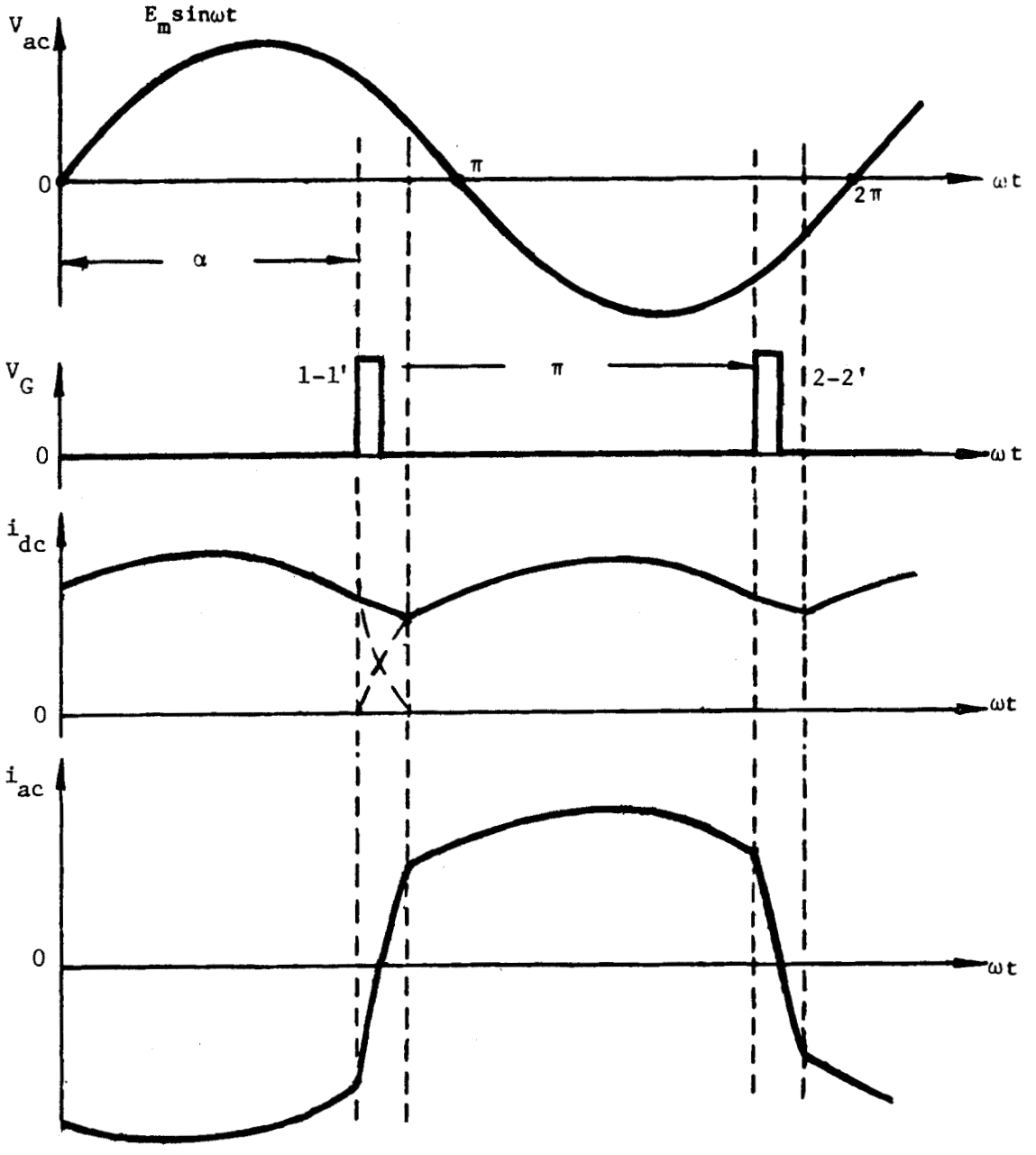

Figure C.1-5. Current and Voltage Waveforms During Continuous Current Mode.

$$I_{PVA} = 17.64P_I/100 - 1.398\times10^{-4}[\exp(V_{PVA}/34.12) - 1]. \qquad (C.1\text{-}1)$$

The equivalent models for the control circuit and firing logic are developed and put into a form that can be implemented on EMTP. A detailed description of these sections is provided below.

Control System and Firing Logic

The objective of the SPC control system is to regulate the array operating voltage at the reference voltage level.

The block diagram of the control system is shown in Figure C.1-6. Note that the voltage, V_{PVA}, is regulated at V_{ref}; however current is not regulated at I_{ref}. I_{ref} is a signal within the control loop that is compared to I_{PVA}.

The limits on I_{ref} and e_c (control signal) are non-windup limits. Whenever I_{ref} (e_c) is at a limit, the steady-state value of V_e (I_e) in Figure C.1-6 is zero and the limit value will appear at the output of the integrator. The limit values on the output of the control system, e_c, were selected so that the gating of the SCRs occur at 90° when e_c=-4V, and at 165° when e_c=+0.5V.

The block diagram of the firing circuit is shown in Figure C.1-7 where the gains (264 and 384) were determined by considering the limit values on the firing angle. The line filter and zero crossing detector (ZCD) shown in Figure C.1-8 are used to obtain a reference signal for the firing angle

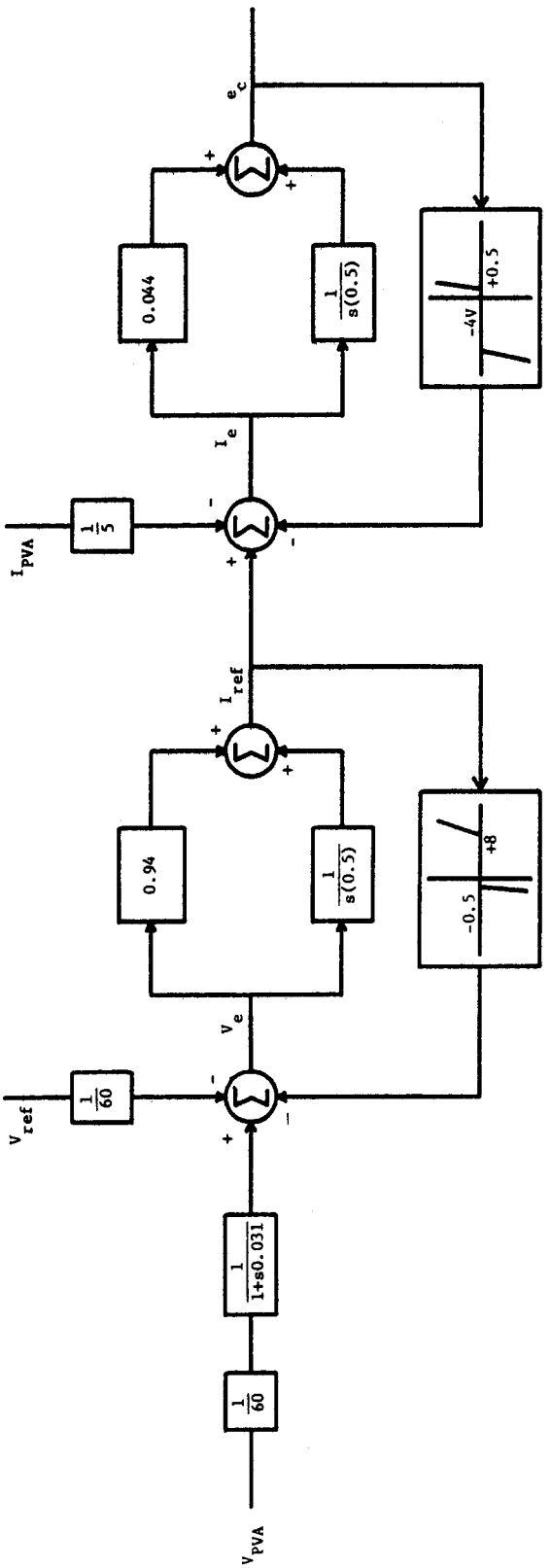

Figure C.1-6. Voltage and Current Regulator.

control. Actually, ZCD is developed but not used directly in the simulation; instead, the outputs of comparators C_1 and C_2 are used in synchronizing the firing angles to the utility grid. Note that in Figure C.1-7 the integrators are reset to zero depending on the state of C1 and C2 in Figure C.1-8. The outputs of the AND gates, FF1 and FF2, are directly used to trigger the SCRs of the power circuit.

Using the block diagrams of the control system and firing circuit, a complete model for the single-phase, line-commutated SPC was implemented on EMTP and its islanding performance was simulated as discussed in Section 2.3.

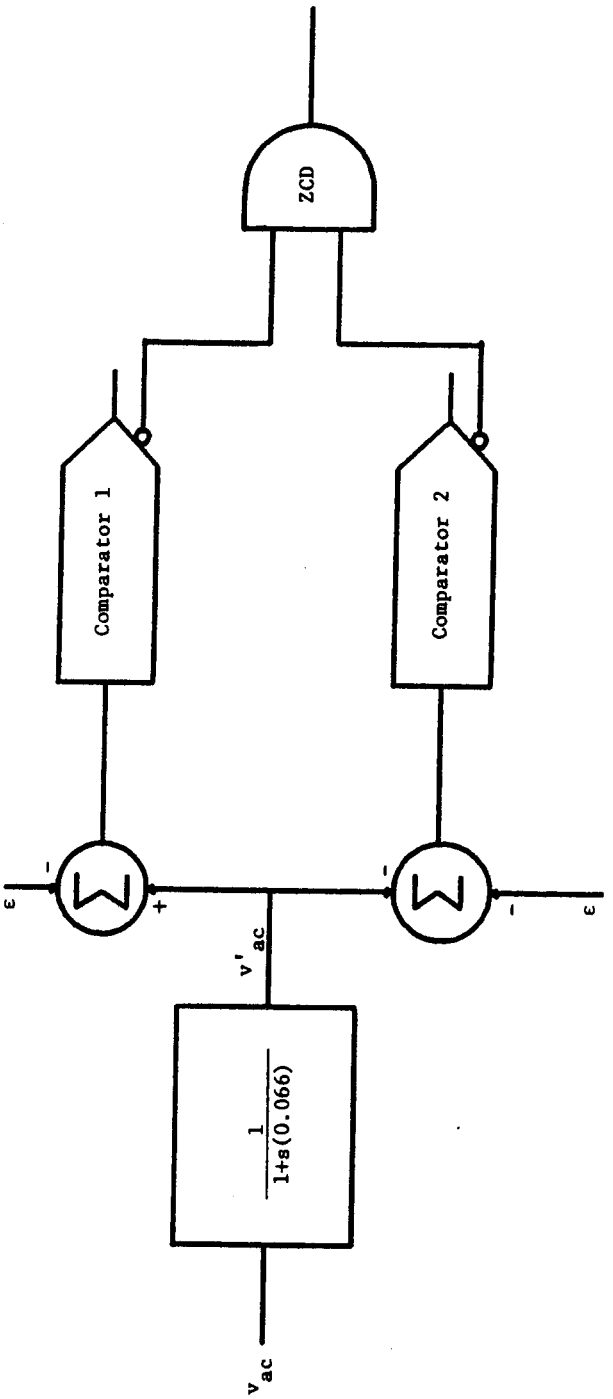

Figure C.1-7. Line Filter and Zero Crossing Detector (ZCD).

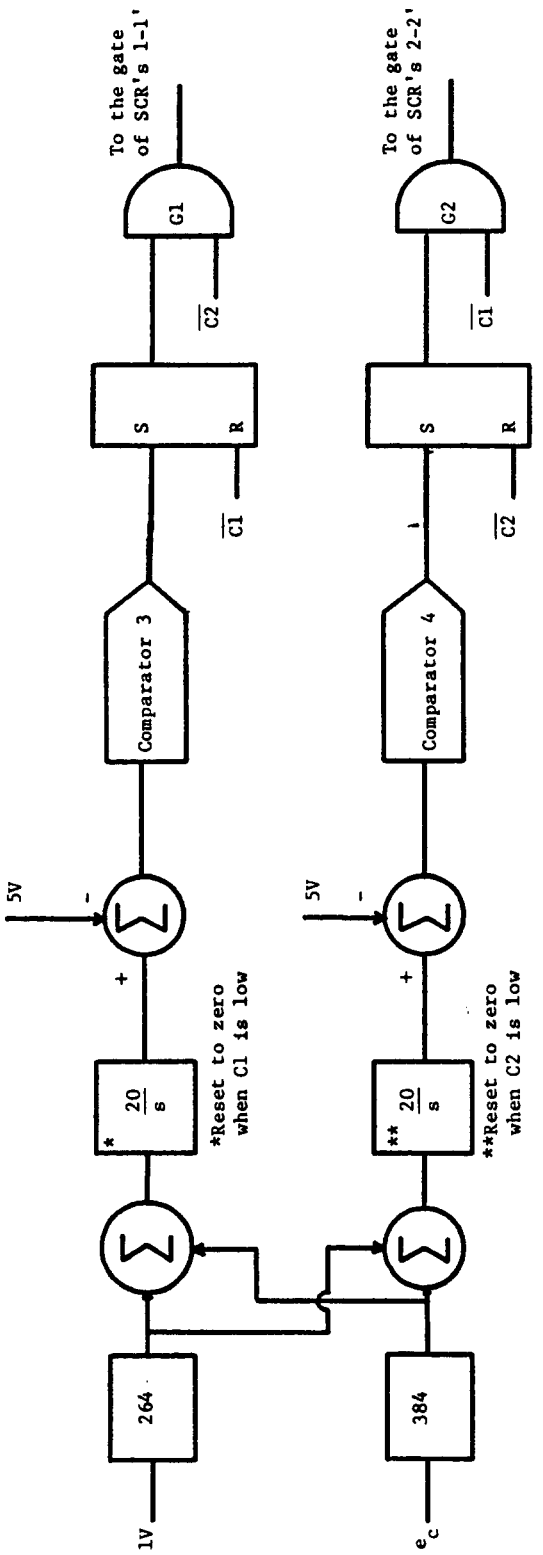

Figure C.1-8. Firing Control Circuit Diagram.

BLANK PAGE

C.2 EMTP Implementation

A diagram of the Gemini model as implemented is shown in Figure C.2-1. The model is divided into two portions. The EMTP network models the actual Gemini SPC components that are involved in the conversion of PV array dc power to output ac power. The TACS portion models the Gemini's control circuitry.

The EMTP portion (Figure C.2-3) and the TACS PV array model (Figure C.2-4), voltage and current regulator (Figure C.2-7), zero crossing detector (Figure C.2-8) and firing control (Figure C.2-11) very closely follow the block diagrams described in the last section. The remaining TACS sections are described following this introduction. The TACS portion of EMTP has predefined "DEVICES" with which the user can model typical control system functions. Most of the blocks in the control block diagrams contain a number, an "S", or an "F" in the upper right-hand corner. This number references the TACS device that was used in the model. A listing of the devices used in the Gemini model are given below; for more details see the EMTP Rule Book[22].

Device	Function
50	frequency meter
53	transport delay
58	controlled integrator
59	simple derivative
62	sample and track
64	minimum/maximum tracking
65	accumulator and converter
66	rms meter

The "F" indicates that a Fortran expression was used to accomplish the function described in the block. The "S" indicates that the block represents a transfer function. Some of the device blocks contain signals pointing to a triangle containing letters. These triangles indicate control of the block as follows: R-reset, RV-reset valve, and S-sample.

A triangular box containing a node name with a shaded arrow indicates that this signal is either input from TACS to EMTP or vice versa. Timing graphs taken during steady-state operation are also included for some of the control signals to aid in understanding the control system model.

The TACS undervoltage shut-down logic (Figure C.2-13) is representative of actual control circuitry in the Gemini. The ac terminal voltage (G#VAC) is monitored during each cycle. The peak value (G#PEKP) is stored and compared to 271.5 (80% of 240 x $\sqrt{2}$) to determine if a shut-down signal (G#BRKR) should be sent to an EMTP switch, which would disconnect the Gemini.

The remaining blocks do not represent actual control circuitry but are included to monitor the operation of the model. The Alpha calculation provides the delay angle in degrees based on a 60-cycle degree (1 degree = 46.29 x 10^{-6} sec) as G#ALPH. The watt and var meters were included as discussed in Section 3.3 in order to run simulations to compare with lab tests. The TACS starting signals are used to enable sections of the model in a fashion that allows for fairly rapid starting (400 ms) to a steady-state condition in preparation for an islanding condition to occur.

The Gemini model does require some special attention if a smooth start is to be achieved. Some points to keep in mind are:

1. The values of G#VPVA and G#IPVA should be calculated for the desired G#VPVA condition (Equation C.1-1). The G#VPVA condition must be placed on all of the circuit elements in the EMTP circuit in the proper EMTP initial conditions section. The G#VPVA ÷ 60 operating point must also agree with the value of G#VREF.

2. The initial value of G#IREF must be G#IPVA (calculated in 1) ÷ 5.

3. The choice of an initial condition for G#EC is fairly critical. G#EC sets the firing angle for the SCRs. This value is set and not allowed to change during the first 80 ms of a simulation to give the rest of the system a chance to stabilize. If G#EC is chosen to be significantly different from its final value, too much or too little power may be removed from the array causing the array voltage to be in error and taking some time to recover. Finding the proper valve of G#EC may take some trial and error. A set-up case can be run for several hundred milliseconds, stopped, and restarted with the new value of G#EC equal to the previous simulation's final value until the right combination is found.

4. The final start-up feature, which only applies to the continuous mode cases, is getting the proper initial current in the dc filter inductor. This is achieved by locating a dc current source with the proper current to drive current through the inductor (see Figure C.2-3). The dc current

source is switched out by TACS signal G#GON at the same time the first pair of SCRs is fired. This can be a bit tricky and may require adjustment of the constant added to G#TPL2 to obtain the G#GO signal. G#TPL2 is the time of the first positive going zero crossing of the ac terminal voltage.

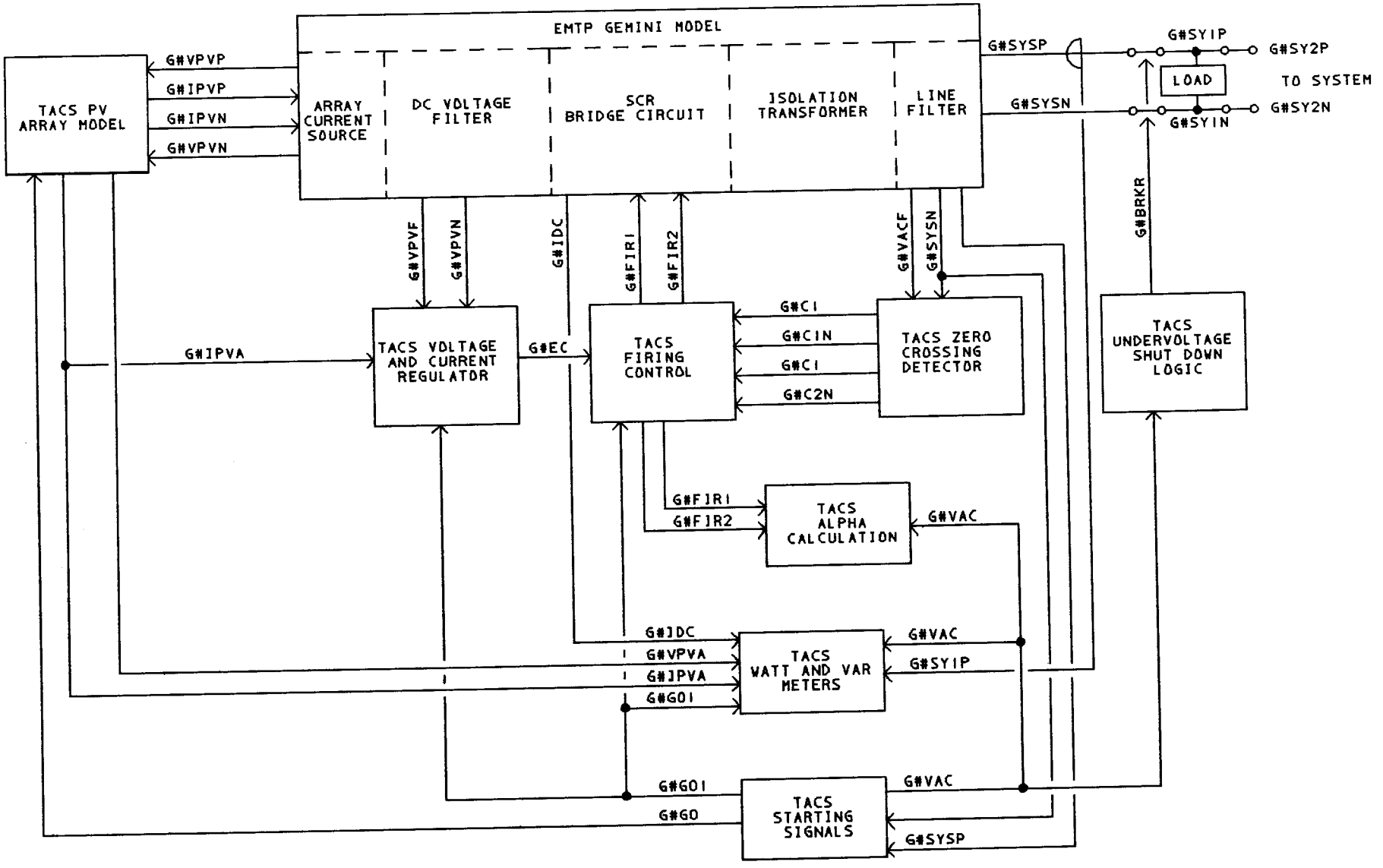

FIGURE C.2-1 GEMINI COMPUTER MODEL

FIGURE C.2-2 NETWORK SIGNALS

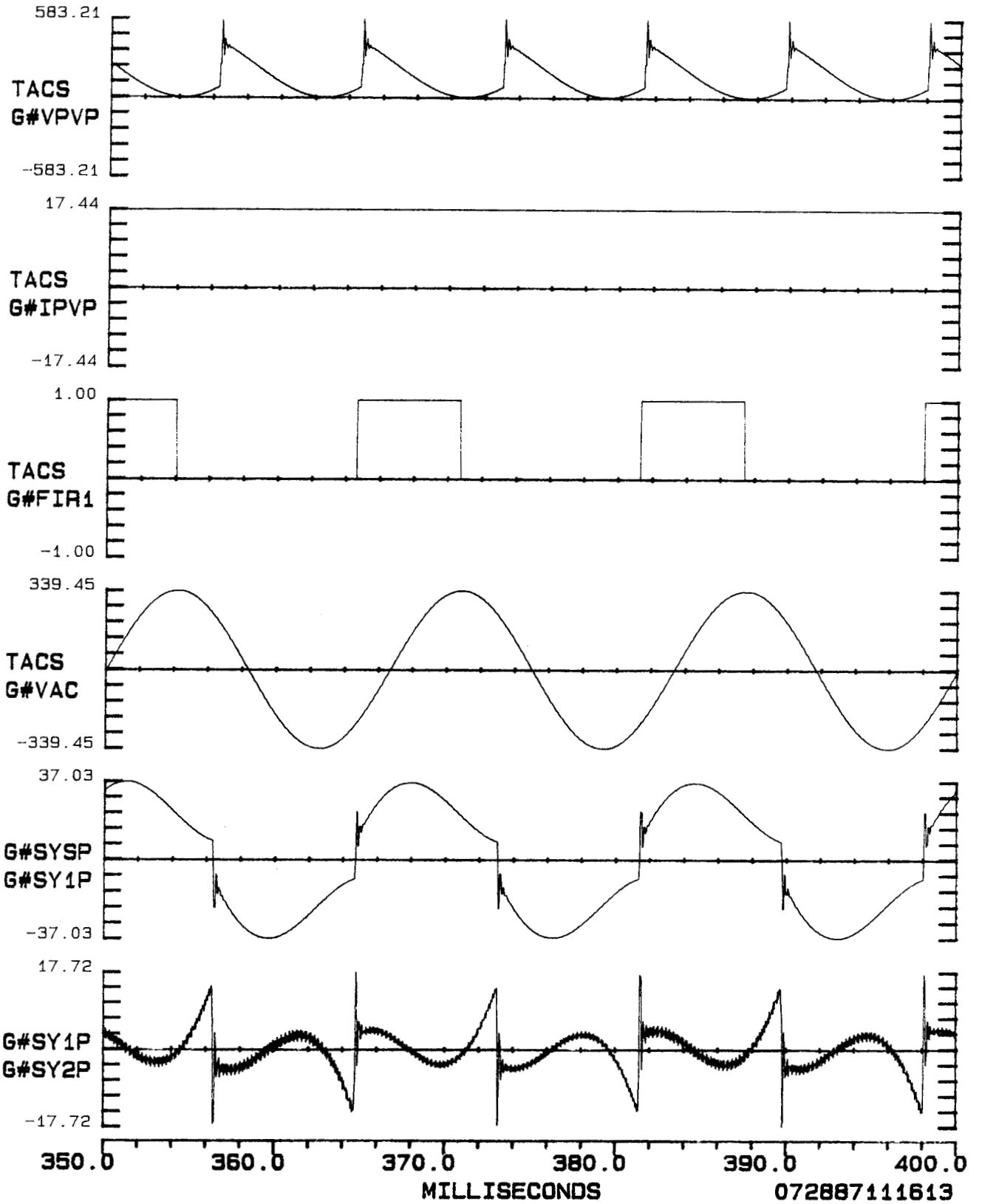

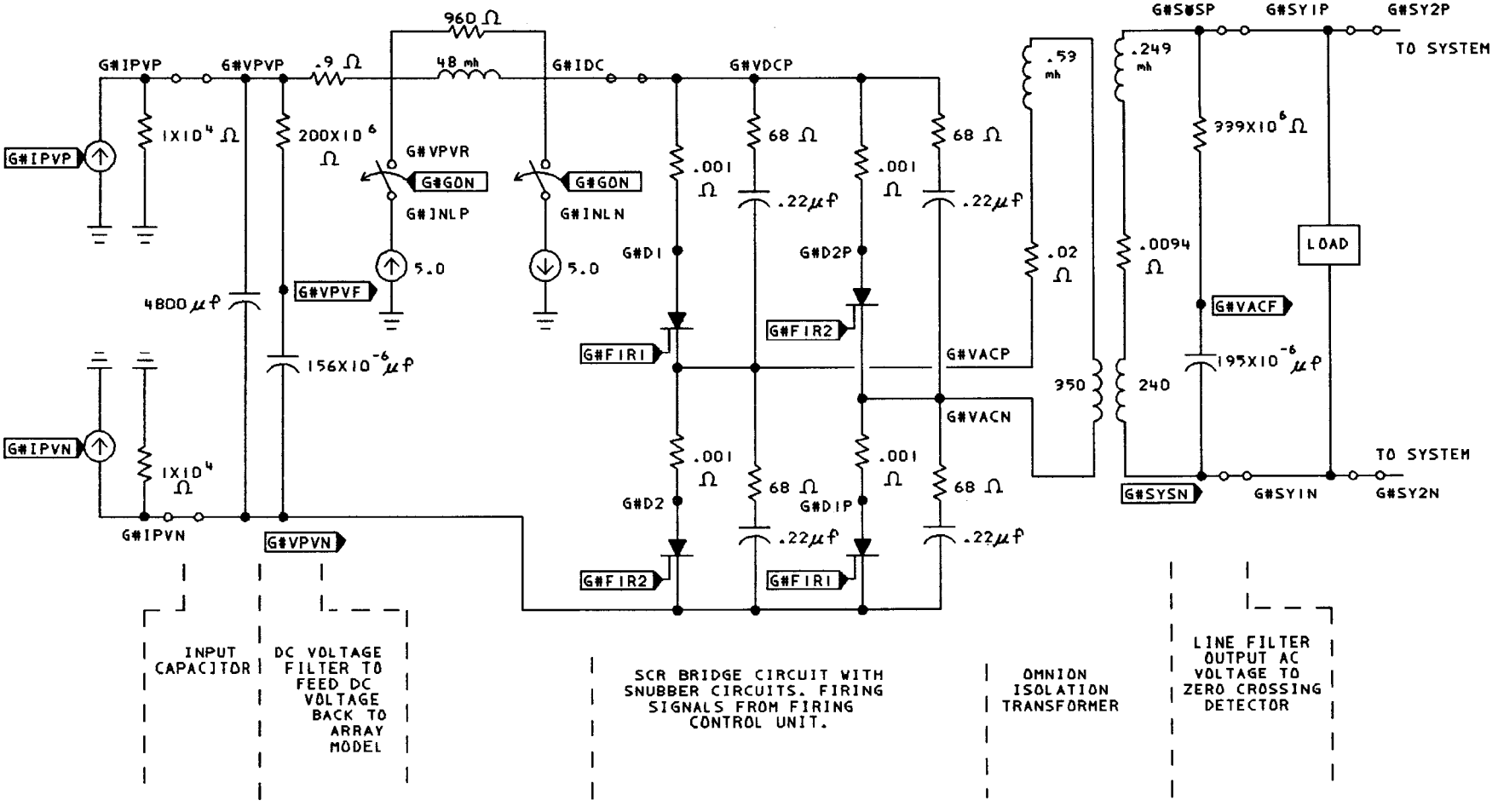

FIGURE C.2-9 EMTP NETWORK MODLE

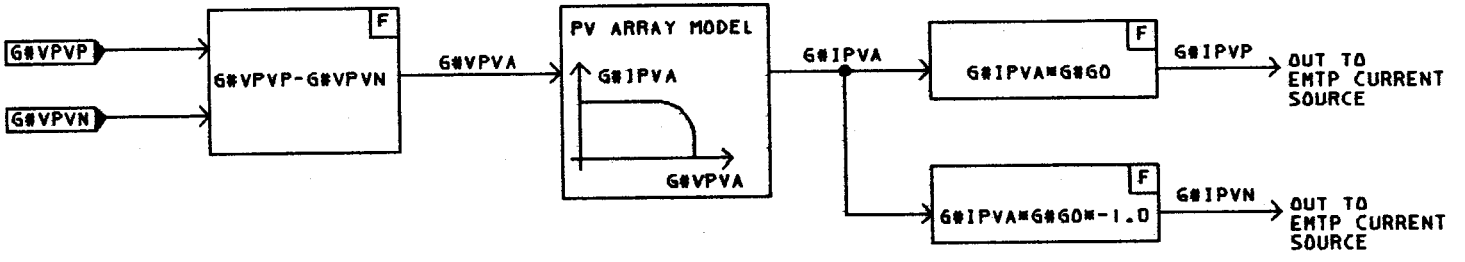

FIGURE C.2-4 TAC PV ARRAY MODEL

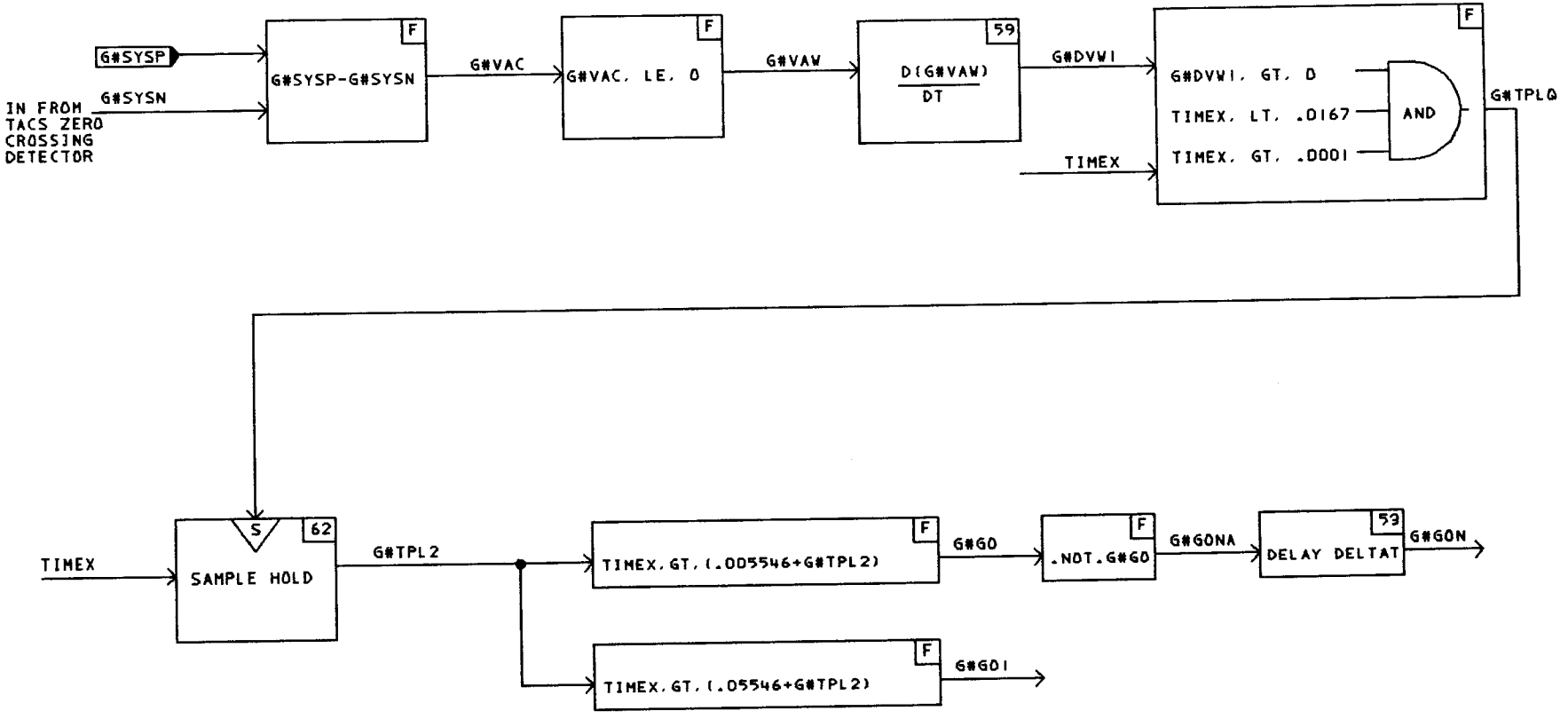

FIGURE C.2-5 TACS STARTING SIGNALS

FIGURE C.2-6 REGULATOR SIGNALS

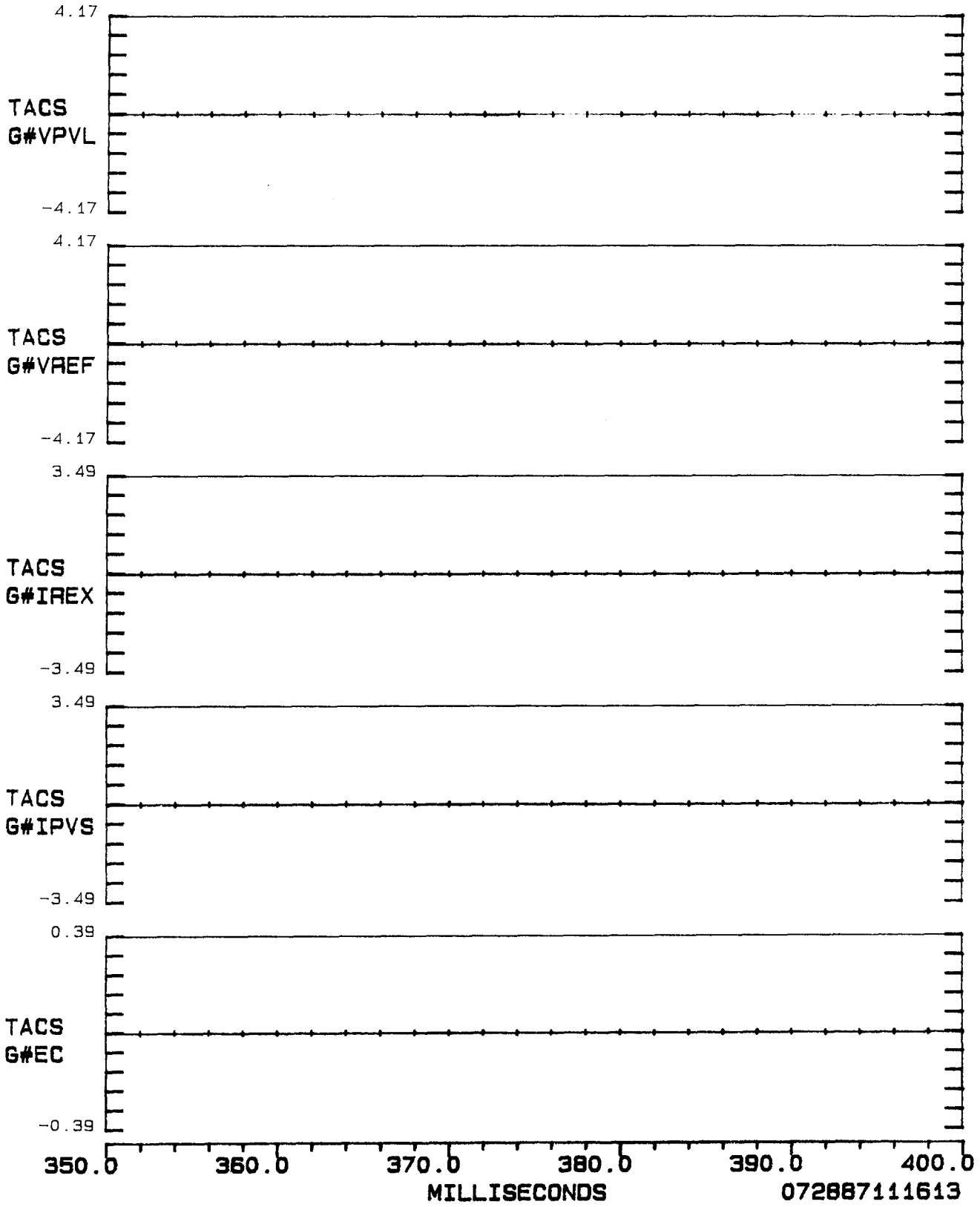

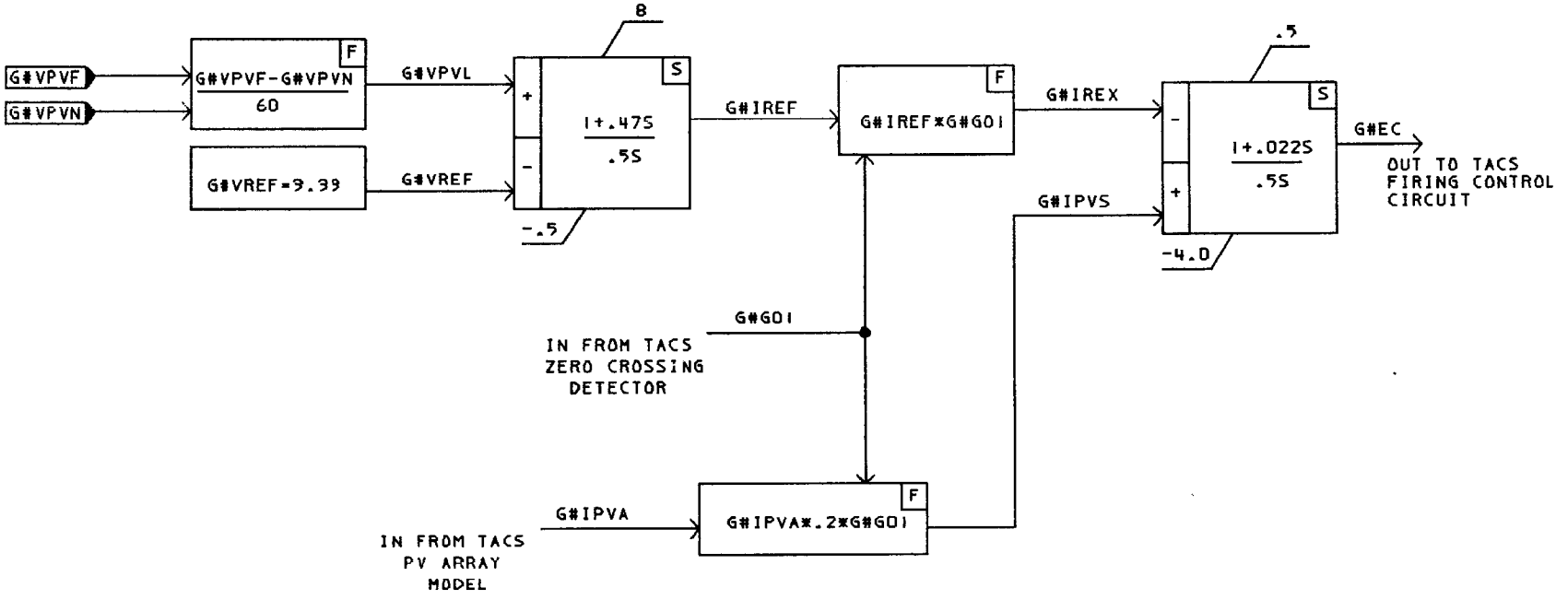

FIGURE C.2-7 TACS VOLTAGE AND CURRENT REGULATOR

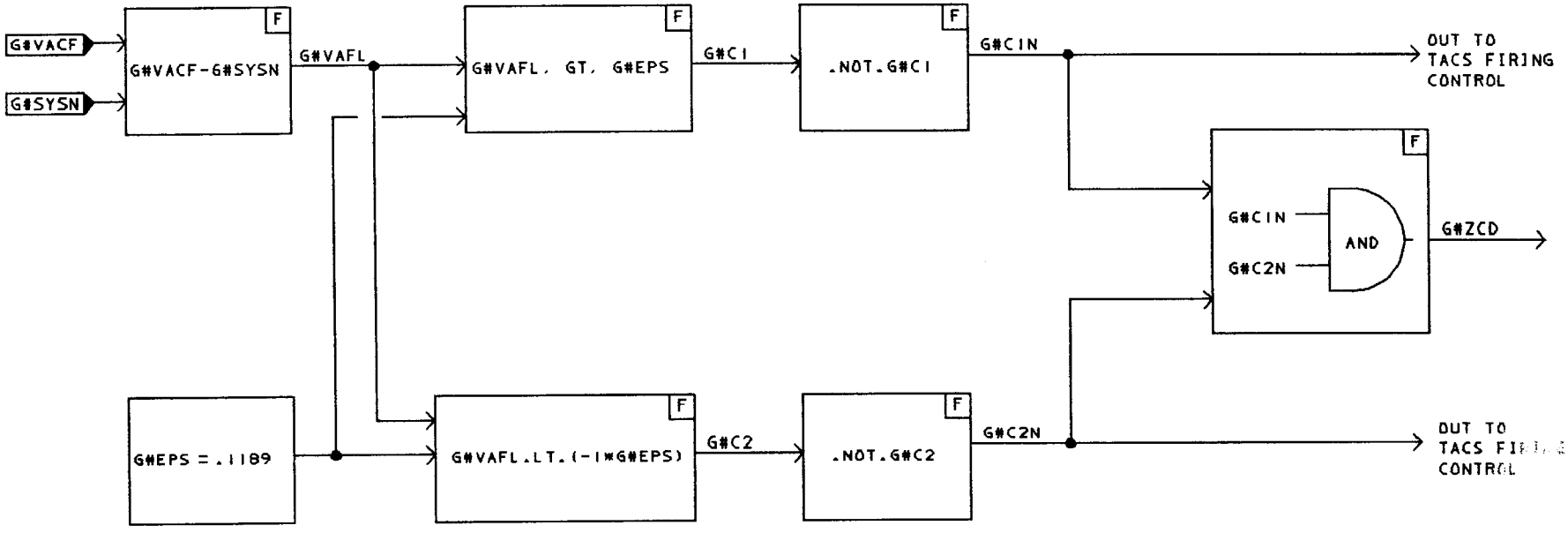

FIGURE C.2-8 TACS ZERO CROSSING DETECTOR

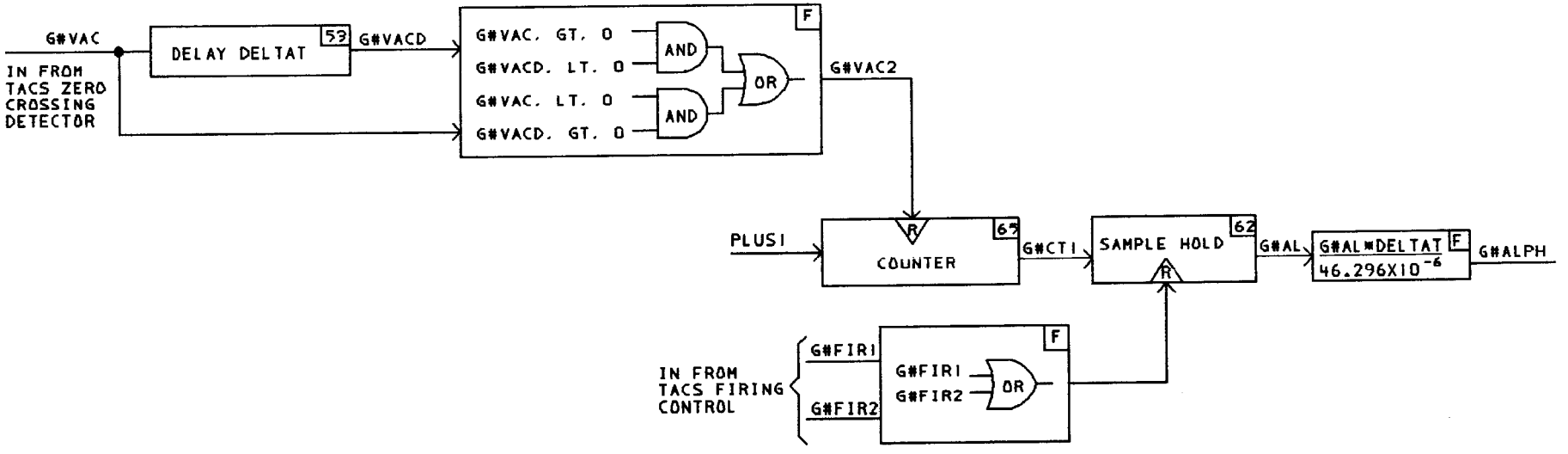

FIGURE C.2-9 TACS ALPHA

FIGURE C.2-10 FIRING SIGNALS

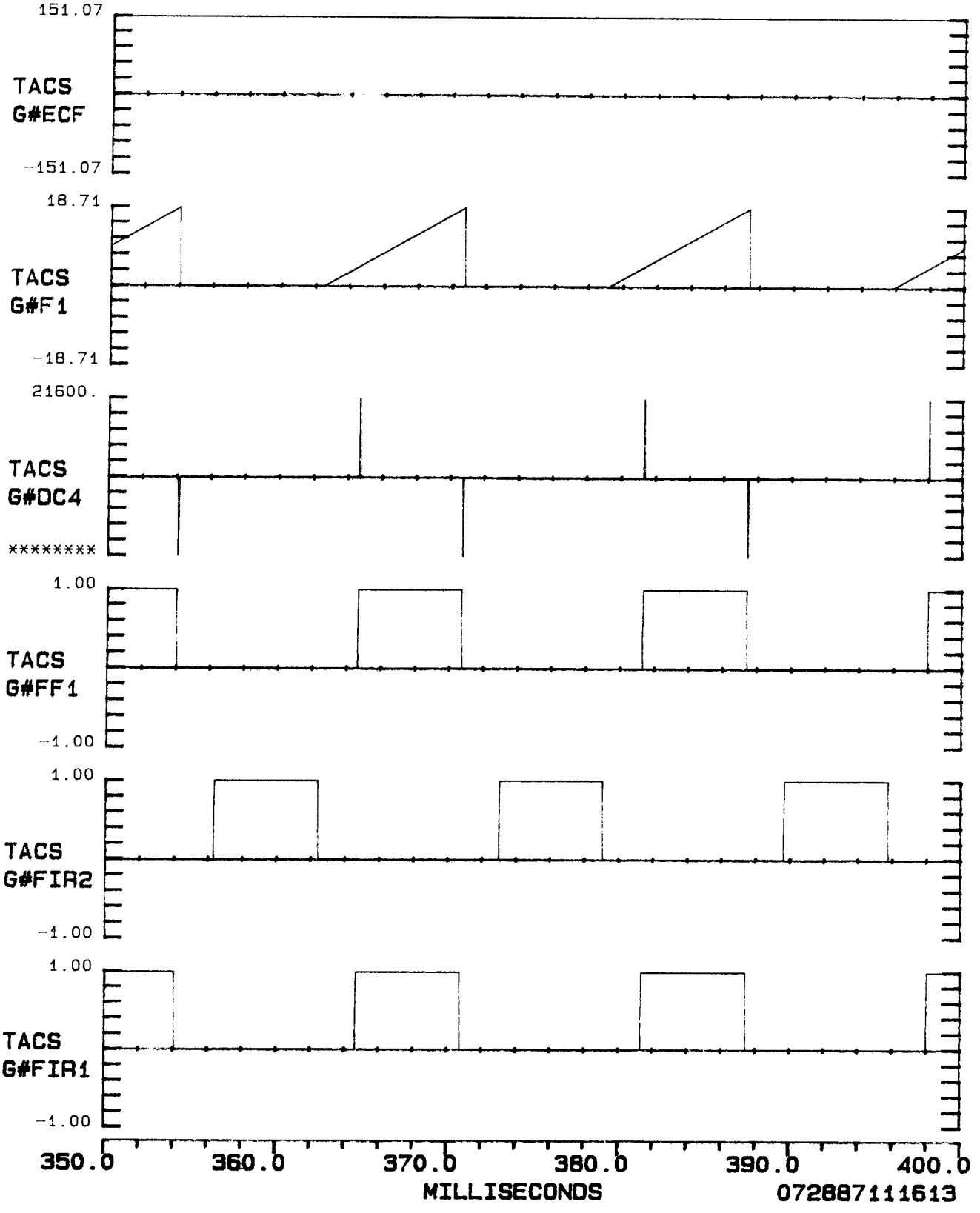

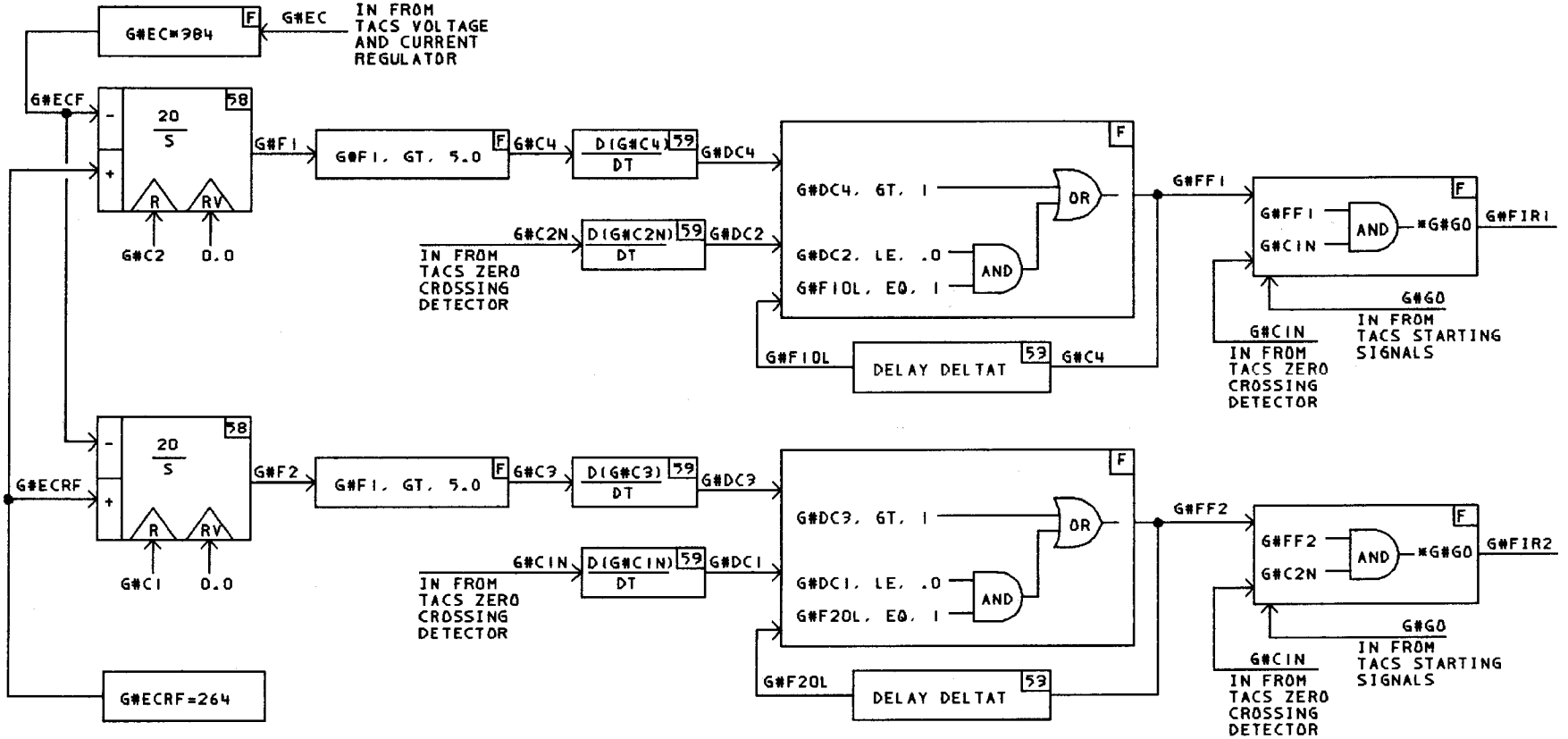

FIGURE C.2-11 TACS FIRING CONTROL

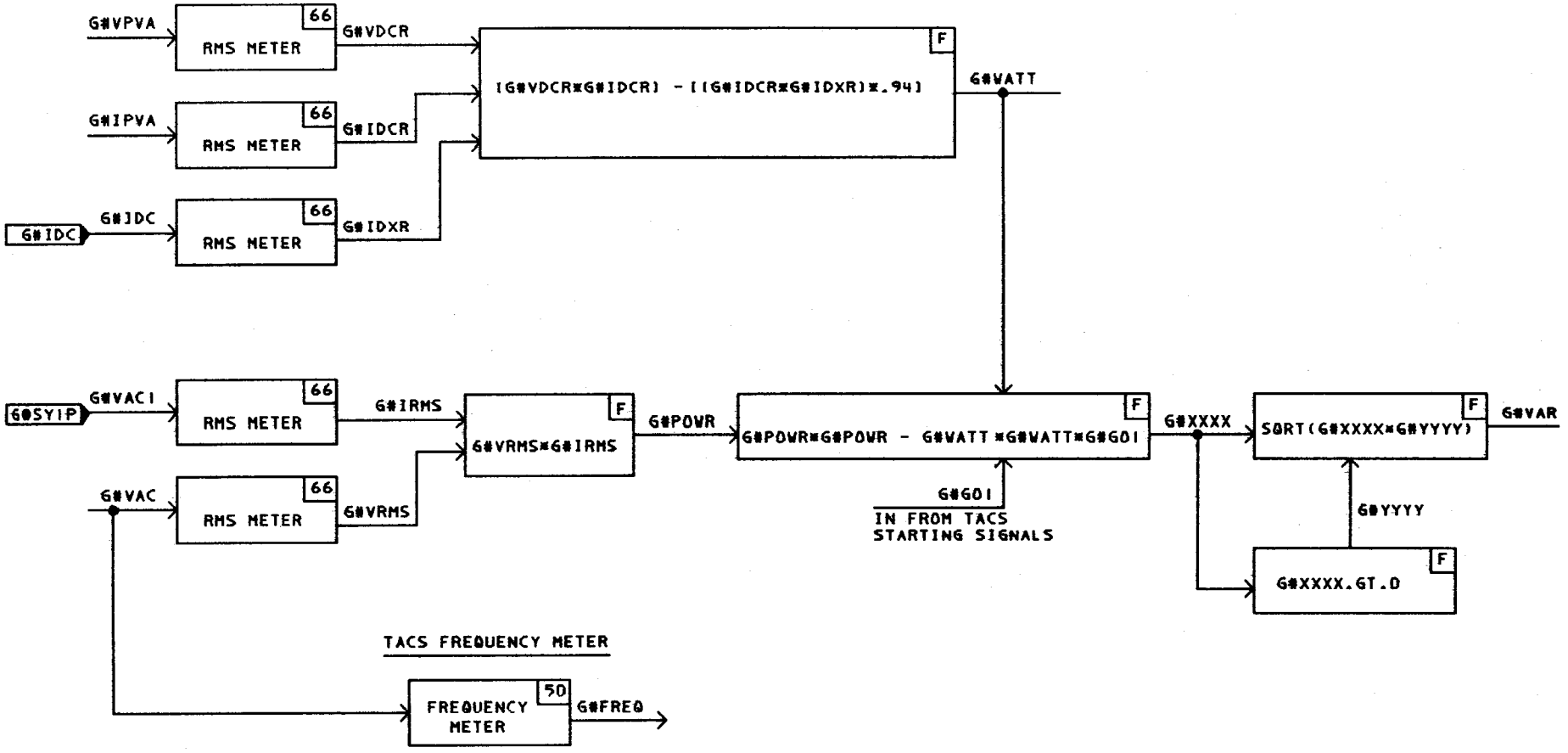

FIGURE C.2-12 TACS WATT,VAR AND FREQUENCY METERS

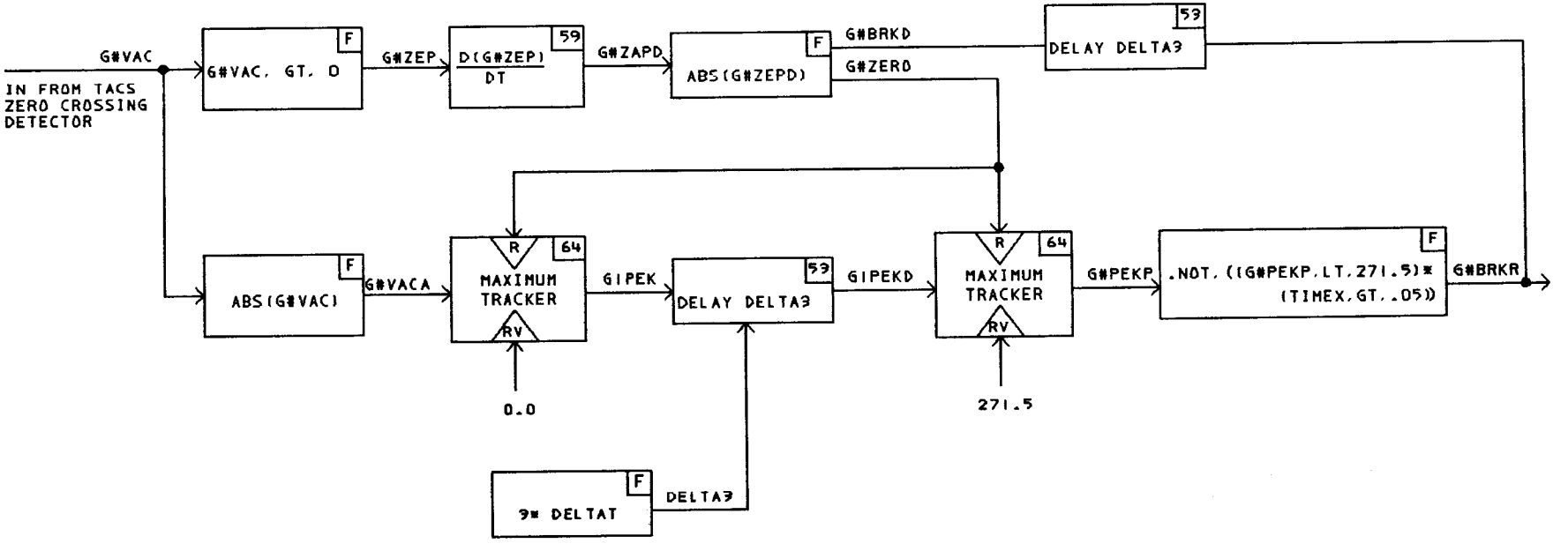

FIGURE C.2-13 TACS UNDERVOLTAGE SHUT DOWN LOGIC

Simulation Model Data File Listing

A listing of the EMTP/TACS data file follows. The file is divided into two sections, and the TACS section is treated as an INSERT file to the EMTP data file. This file is the base file used for the islanding study. The data file was used on the M39 version of EMTP on an Apollo computer system.

```
BEGIN NEW DATA CASE
C
C DATA FILE NAME = G_I.A.1.B
C
C                                        CASE NO.        CALCULATION NO.
C
C
C                              TITLE :
C
C
C
C
C
C                      ORIGINATING ENG.:    TRS            DATE:
C
C                        REVIEWING ENG.:                    DATE:
C
C
C
C      RESISTIVE  LOAD            CAPACITIVE LOAD
C     --------------------     --------------------
C        MATCHED                    MATCHED
C
C
C
ABSOLUTE TACS DIMENSIONS
     120      720      600      240     1600    24240    7600     1600
46.296-6 400.E-3       0.       0.  1.0E-8
       1        1        1        3        1       -1                2
      25     1000
TACS HYBRID
$INCLUDE,gemini_unit_cont
C
99OPEN     =(TIMEX.LT..40466)-.5
C
C
33G#FREQG#VAC G#ECF G#F1  G#DC4 G#FF1 G#FIR1G#FIR2
33G#VPVLG#VREFG#IREXG#IPVSG#EC  G#VPVPG#IPVPG#VAC
C

C BRANCH CARDS
C
C 10KVA FIELD TEST TRANSFORMERS
  TRANSFORMER                          TRAND2
             9999
 1TACSW                              .0001  480.
 2G#SY2P                             .0001  120.
 3       G#SY2N                      .0001  120.
C
C
  G#VPVPG#VPVN                              4800.
  G#VPVPG#VPVR                .900
  G#VPVRG#IDC                          48.
  G#VPVRG#IDC                1037.
```

```
C INVERTER CIRCUIT GROUND REFERENCE
  G#IPVP                    1.0E5
  G#IPVN                    1.0E5
C LOAD REFERENCE TO GROUND
  G#SY1P                    1.0E5
  G#SY1N                    1.0E5
C SCR SNUBBER CIRCUIT
  G#VDCPG#MID1               68.0
  G#MID1G#VACP                            .22
  G#VDCPG#MID2               68.0
  G#MID2G#VACN                            .22
  G#VACPG#MID3               68.0
  G#MID3G#VPVN                            .22
  G#VACNG#MID4               68.0
  G#MID4G#VPVN                            .22
C SCR RESISTORS TO SEPARATE SWITCHES
  G#VDCPG#D1                 .001
  G#VDCPG#D2P                .001
  G#VACPG#D2                 .001
  G#VACNG#D1P                .001
C ISOLATION TRANSFORMER
  TRANSFORMER                           G#TRNS
           9999
 1G#SYSPG#SYSN              .0094  .249   240
 2G#VACP                      .01  .265   175
 3      G#VACN                .01  .265   175
C LINE FILTER
  G#SYSPG#VACF             339.E6
  G#VACFG#SYSN                          195.-6
C FILTER TO REMOVE RIPPLE BEFORE SENDING TO TACS VOLTAGE AND CURRENT REGULATOR
  G#VPVPG#VPVF             200.E6
  G#VPVFG#VPVN                          156.-6
C ------------------------------------------------------
C OUTPUT LOAD
  G#SY1PG#SY1N               14.78
  G#SY1PG#SY1N                           229.0
C
C ------------------------------------------------------
C ------------------------------------------------------
C BOUNDARY LOAD FOR MATCHING
  TACSW                     64.0E3
  TACSW                                 .0753
C
C ------------------------------------------------------

C SWITCH CARDS
C SWITCH TO MONITOR THE LOAD CURRENT FROM THE SYSTEM
  VSYS  SYSSW         -1.   1E4
C SWITCH TO OPEN AND FORM ISLAND
13SYSSW TACSW                                        CLOSED          OPEN    11
C SWITCH TO SEND DC OUTPUT CURRENT TO TACS WATT AND VAR METERS
  G#IDC G#VDCP        -1.   1E4
C SWITCHES TO MONITOR DC CURRENT FROM ARRAY
  G#IPVPG#VPVP        -1.   1E4
```

```
  G#IPVNG#VPVN       -1.   1E4
C SWITCHES TO MONITOR OUTPUT CURRENT OF GEMINI UNIT
  G#SYSPG#SY1P       -1.   1E4                                                1
  G#SYSNG#SY1N       -1.   1E4
C SWITCHES TO MONITOR OUTPUT CURRENT OF GEMINI LOCAL ISLAND
  G#SY1PG#SY2P       -1.   1E4                                                1
  G#SY1NG#SY2N       -1.   1E4
C TACS CONTROLLED SWITCHES FOR STARTUP - NEEDED FOR PROPER INITIAL INDUCTOR
C CURRENT CONTROL FROM TACS STATRUP SIGNALS
13G#VPVRG#INLP                                          CLOSED          G#GON
13G#IDC G#INLN                                          CLOSED          G#GON
C UNFOLDER SCRS - FIRING SIGNALS FROM TACS FIRING CONTROL
11G#D1  G#VACP                                                      G#FIR1
11G#D2  G#VPVN                                                      G#FIR2
11G#D2P G#VACN                                                      G#FIR2
11G#D1P G#VPVN                                                      G#FIR1

C SOURCE CARDS
C
C OUTPUT CURRENT OF PV ARRAY FROM TACS PV ARRAY MODEL
60G#IPVP-1                                                             -1.
60G#IPVN-1                                                             -1.
C INDUCTOR INITIAL CONDITION SOURCE
11G#INLP-1       6.2                                                   -1.
11G#INLN-1      -6.2                                                   -1.
C SYSTEM SOURCE
14VSYS        678.82       60.    -91.00                               -1.

C EMTP CIRCUIT INITIAL CONDITIONS
 2G#VPVP           125.
 2G#VPVN          -125.
 2G#IDC            125.
 2G#VPVR           125.
 2G#VDCP           125.
 2G#D1             125.
 2G#D2P            125.
 2G#VPVF           125.
 3G#VPVPG#VPVN             0.          250.
 3G#VPVFG#VPVN             0.          250.
 3G#VPVRG#IDC              0.
C EMTP NODE VOLTAGE OUTPUT REQUESTS
  VSYS

C PLOT CARDS - FOURIER ANALYSIS OF SIGNALS
  FOURIER ON                 7
 192100 23. 24.         G#SYSPG#SY1P
 192100 23. 24.         G#SY1PG#SY2P
 192100 23. 24.         TACS  G#VAC
 192100 23. 24.         TACSW SYSSW
 192100 52. 53.         G#SYSPG#SY1P
 192100 52. 53.         TACS  G#VAC
 142100 23. 24.         VSYS
  FOURIER OFF
```

```
C
C ***************************************************************************
C
C  TACS PORTION OF OMNION 6.0KW INVERTER MODEL
C
C ***************************************************************************
$LISTOFF
C ***************************************************************************
C TACS PV ARRAY MODEL
C ***************************************************************************
C
90G#VPVP
99G#VPVA  =(G#VPVP-G#VPVN)
11G#NSOL      100.00
11G#CLTC       28.00
11G#ISRT        2.52
11G#AIDL        1.92
11G#BIDL        1.92
11G#NP            7.
11G#NS          680.
99G#CLTK  =G#CLTC+273.18
99G#ILG   =G#NSOL/100.*(G#ISRT+.0017*(G#CLTC-28.))
99G#IOS   =7.31E-13*G#CLTK**3*EXP(12886./G#BIDL*(.00332-1./G#CLTK))
88G#IPVA  =G#NP*G#ILG-G#NP*G#IOS*(EXP(11601.*G#VPVA/G#NS/G#AIDL/G#CLTK)-1.0)
88G#IPVP  =G#IPVA*G#GO
88G#IPVN  =(G#IPVA)*(-1.0)*G#GO
C
77G#NSOL      100.00
C
C ***************************************************************************
C  TACS STARTING SIGNALS
C ***************************************************************************
90G#SYSP
99G#VAC   =G#SYSP-G#SYSN
99G#VAW   =G#VAC.LE.0.
99G#DVW159+G#VAW
99G#TPLQ  =(G#DVW1.GT.0.).AND.(TIMEX.LT..0167).AND.(TIMEX.GT..0001)
77G#TPL2        100.
99G#TPL262+TIMEX                                                    G#TPLQ
C START UP TIME
99G#GO    =(TIMEX.GT.(.0025+G#TPL2))
99G#GO1   =(TIMEX.GT.(.05546+G#TPL2))
99G#GO2   =(TIMEX.GT.(.00634+G#TPL2))
99G#GONA  =.NOT.G#GO2
99G#GON 53+G#GONA                                          .00050DELTAT
C
C ***************************************************************************
C  TACS VOLTAGE AND CURRENT REGULATOR
C ***************************************************************************
C
90G#VPVF
90G#VPVN
99G#VPVL  =(G#VPVF-G#VPVN)/60.
11G#VREF       4.167
```

```
 1G#IREF  +G#VPVL -G#VREF                                    1.0   -.5   8.0
       1.0       .47
                  .5
99G#IPVS  =G#IPVA*.2*G#GO1
88G#IREX  =G#IREF*G#GO1
 1G#EC    +G#IPVS -G#IREX                                    1.0  -4.0    .5
       1.0      .022
                  .5
C SET TO G#VPVA/60.0
77G#VREF       4.167
77G#VPVL       4.167
C
C SET TO G#IPVA/5.0
77G#IREF       3.484
77G#EC           .39
C
C
C ***************************************************************************
C  TACS ZERO CROSSING DETECTOR
C ***************************************************************************
C
90G#VACF
90G#SYSN
99G#VAFL  =G#VACF-G#SYSN
11G#EPS        .1189
99G#C1    =(G#VAFL.GT.G#EPS)
99G#C2    =(G#VAFL.LT.(G#EPS*(-1)))
99G#C1N   =.NOT.G#C1
99G#C2N   =.NOT.G#C2
99G#ZCD   =(G#C1N.AND.G#C2N)
C
C ***************************************************************************
C TACS FIRING CONTROL
C ***************************************************************************
C
11G#ECRF        264.
99G#ECF   =G#EC*384
99G#F1  58+G#ECRF -G#ECF                                  20.0   0.0   1.0G#C2
99G#F2  58+G#ECRF -G#ECF                                  20.0   0.0   1.0G#C1
99G#C4    =(G#F1.GT.5.0)
99G#C3    =(G#F2.GT.5.0)
99G#DC1 59+G#C1N
99G#DC2 59+G#C2N
99G#DC3 59+G#C3
99G#DC4 59+G#C4
99G#F10L53+G#FF1                                                  .00050DELTAT
99G#F20L53+G#FF2                                                  .00050DELTAT
99G#FF1   =((G#F10L.EQ.1).AND.(G#DC2.LE.0)).OR.(G#DC4.GT.1)
99G#FF2   =((G#F20L.EQ.1).AND.(G#DC1.LE.0)).OR.(G#DC3.GT.1)
99G#FIR1  =(G#FF1.AND.(G#C1N))*G#GO
99G#FIR2  =(G#FF2.AND.(G#C2N))*G#GO
C
C
C ***************************************************************************
```

```
C TACS ALPHA CLACULATION
C ************************************************************************
C
99G#VACD53+G#VAC                                                .00050DELTAT
99G#VACZ  =((G#VAC.GT.0).AND.(G#VACD.LT.0)).OR.((G#VAC.LT.0).AND.(G#VACD.GT.0))
99G#ST    =G#FIR1.OR.G#FIR2
99G#CT1 65+PLUS1                                                  G#VACZ
99G#AL  62+G#CT1                                                       G#ST
99G#ALPH  =G#AL*DELTAT/46.296E-6
C
C
C ************************************************************************
C TACS WATT AND VAR METERS
C ************************************************************************
C
91G#SY1P
99G#VAC1  =G#SY1P
99G#VRMS66+G#VAC                                        60.
99G#IRMS66+G#VAC1                                       60.
99G#POWR  =G#VRMS*G#IRMS
99G#VDCR66+G#VPVA                                       60.
91G#IDC
99G#IDCR66+G#IPVA                                       60.
99G#IDXR66+G#IDC                                        60.
99G#WATT  =G#VDCR*G#IDCR-G#IDXR*G#IDXR*.94
99G#XXXX  =(G#POWR*G#POWR-G#WATT*G#WATT*G#GO1)
99G#YYYY  =G#XXXX.GT.0.
99G#VAR   =SQRT(G#XXXX*G#YYYY)
C
C ************************************************************************
C TACS  FREQUENCY METER
C ************************************************************************
C
C 99G#FREQ50+G#VAC                                        60.
99G#FREQ50+G#VACF                                       60.
33G#VACF
C
C ************************************************************************
C TACS UNDERVOLTGE SHUT DOWN LOGIC
C ************************************************************************
C
99G#BEGA  =TIMEX.GT.(G#TPLQ+.035)
99G#ZEP   =G#VAC.GT.0
99G#ZEPD59+G#ZEP
99G#ZERO  =ABS(G#ZEPD)*G#BRKD
99G#VACA  =ABS(G#VAC)
99G#PEK 64+G#VACA                                    1.     0.G#ZERO
99DELTA3  =3.0*DELTAT
99G#PEKD53+G#PEK                                        .00150DELTA3
99G#PEKP62+G#PEKD                                                G#ZERO
99G#BRKD53+G#BRKR                                       .00050DELTAT
99G#BRKR  =.NOT.((G#PEKP.LT.271.5)*(TIMEX.GT..050))
$LISTON
```

C.3 Model Validation

The EMTP digital computer program results were compared with analog computer results provided by Paul Krause and Associates. The analog computer results modeled four events that caused the Gemini controls to operate and adjust to a new steady-state operating condition. These events included decreasing and increasing the solar insolation, and increasing and decreasing the reference voltage. Plots of the EMTP results are given and then the corresponding analog computer results.

The EMTP model behaved as expected. The only event in which a significant difference occurred was the decrease in the VREF case. All four events were run in succession in the EMTP simulation just as they had been on the analog computer. The amount of actual time required to adjust to a new steady-state condition after VREF was stepped from 200 V to 260 V was several minutes, which was not practical to simulate. Our simulation was allowed to run long enough to demonstrate the first 1.5 seconds after the increase of VREF. VREF did not reach the final value of 260 V, which it had in the analog model. We decided to allow the value of VREF to be reduced to 200 V when it reached 240 V instead of 260 V. With this taken into account, the results matched.

FIGURE C3-1 EMTP COMPUTER MODEL RESULTS OF GEMINI SPC STEADY STATE OPERATION WITH SOLAR INSOLATION = 100 MW/CM^2

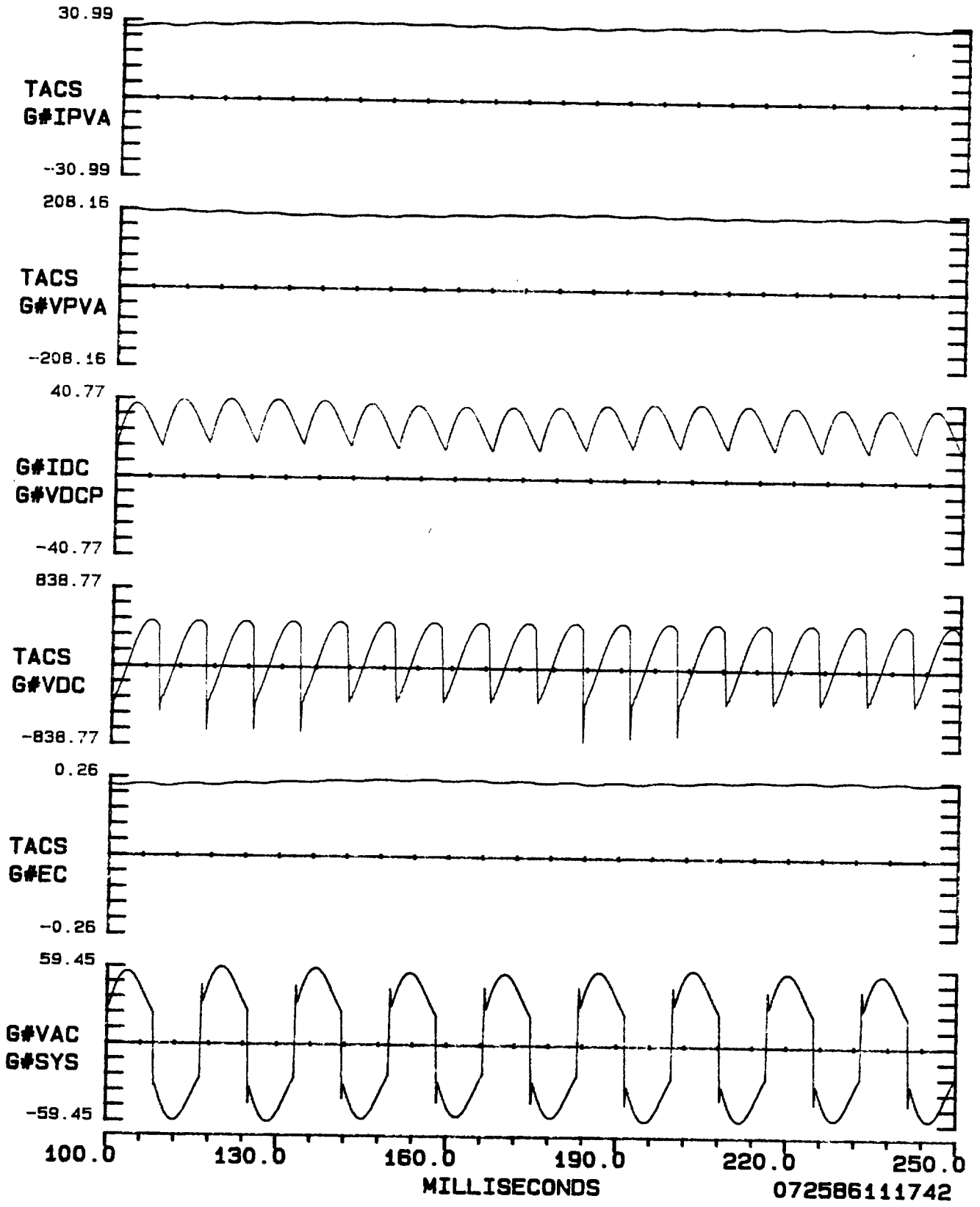

FIGURE C3-2 ANALOG COMPUTER RESULTS OF GEMINI SPC STEADY STATE OPERATION WITH SOLAR INSOLATION = 100 MW/CM^2

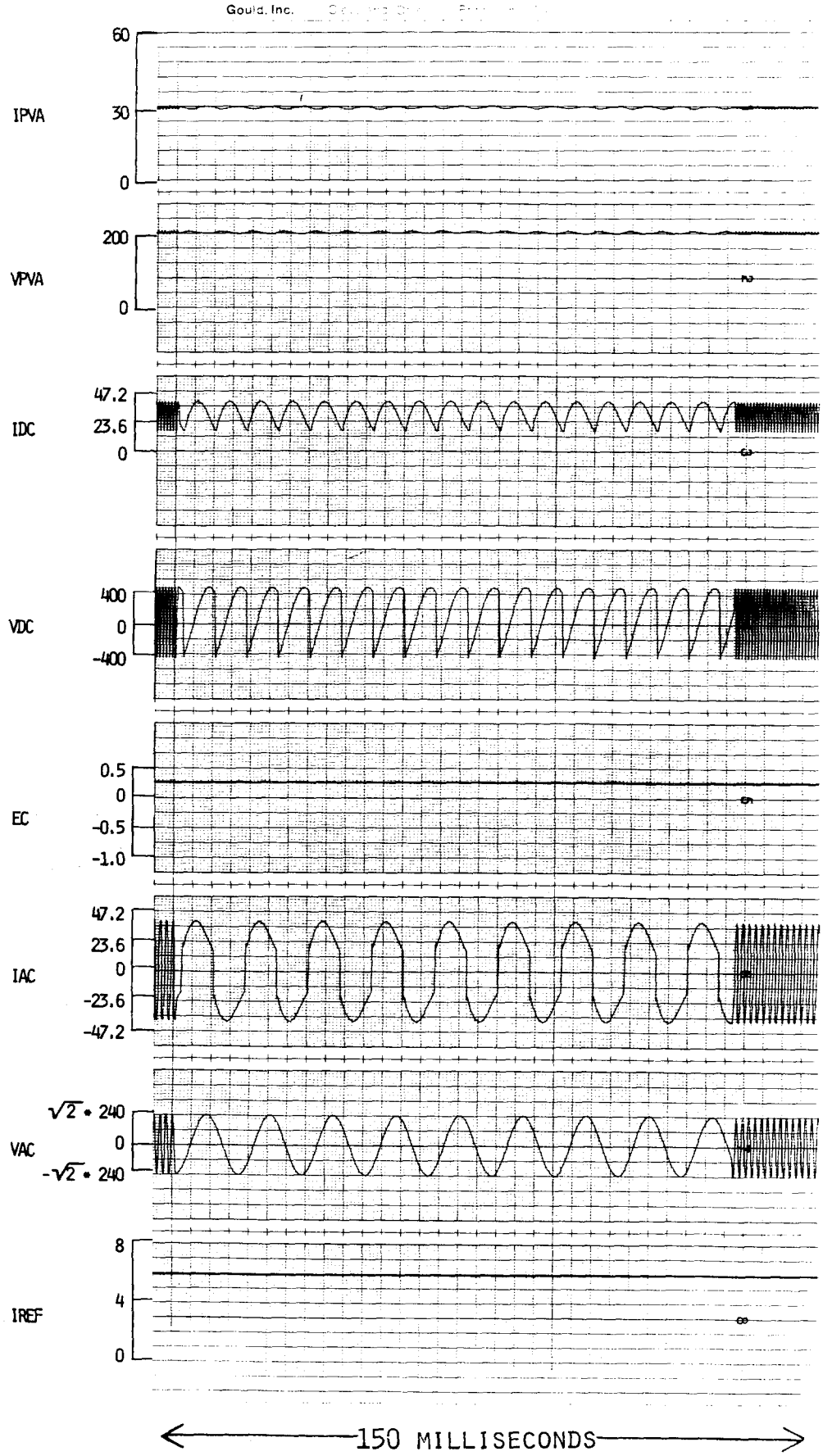

FIGURE C3-3 EMTP COMPUTER MODEL RESULTS OF GEMINI SPC WHEN SOLAR INSOLATION IS REDUCED FROM 100 MW/CM^2 TO 20 MW/CM2

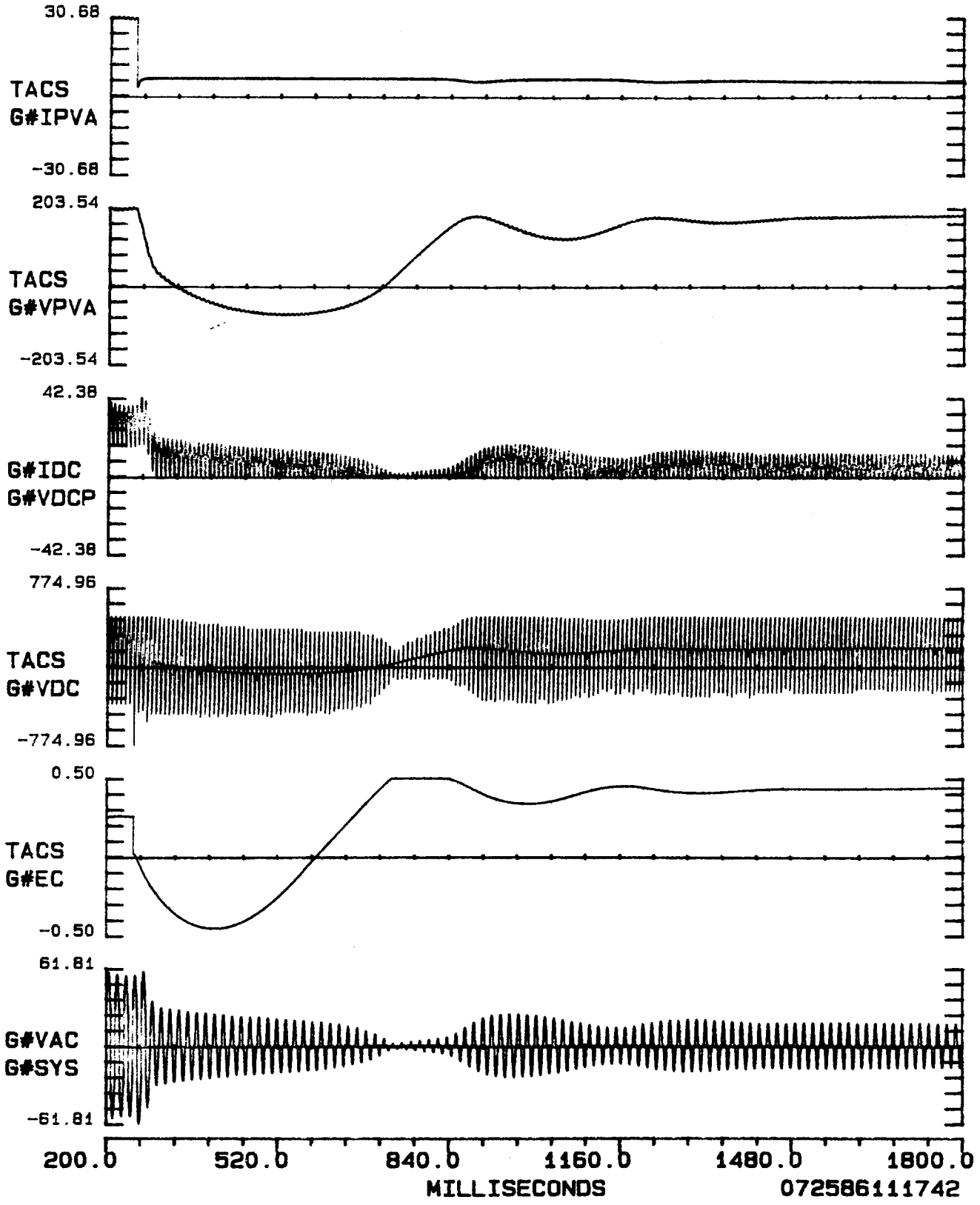

FIGURE C3-4 ANALOG COMPUTER RESULTS OF GEMINI SPC WHEN SOLAR INSOLATION IS REDUCED FROM 100 MW/CM^2 TO 20 MW/CM^2

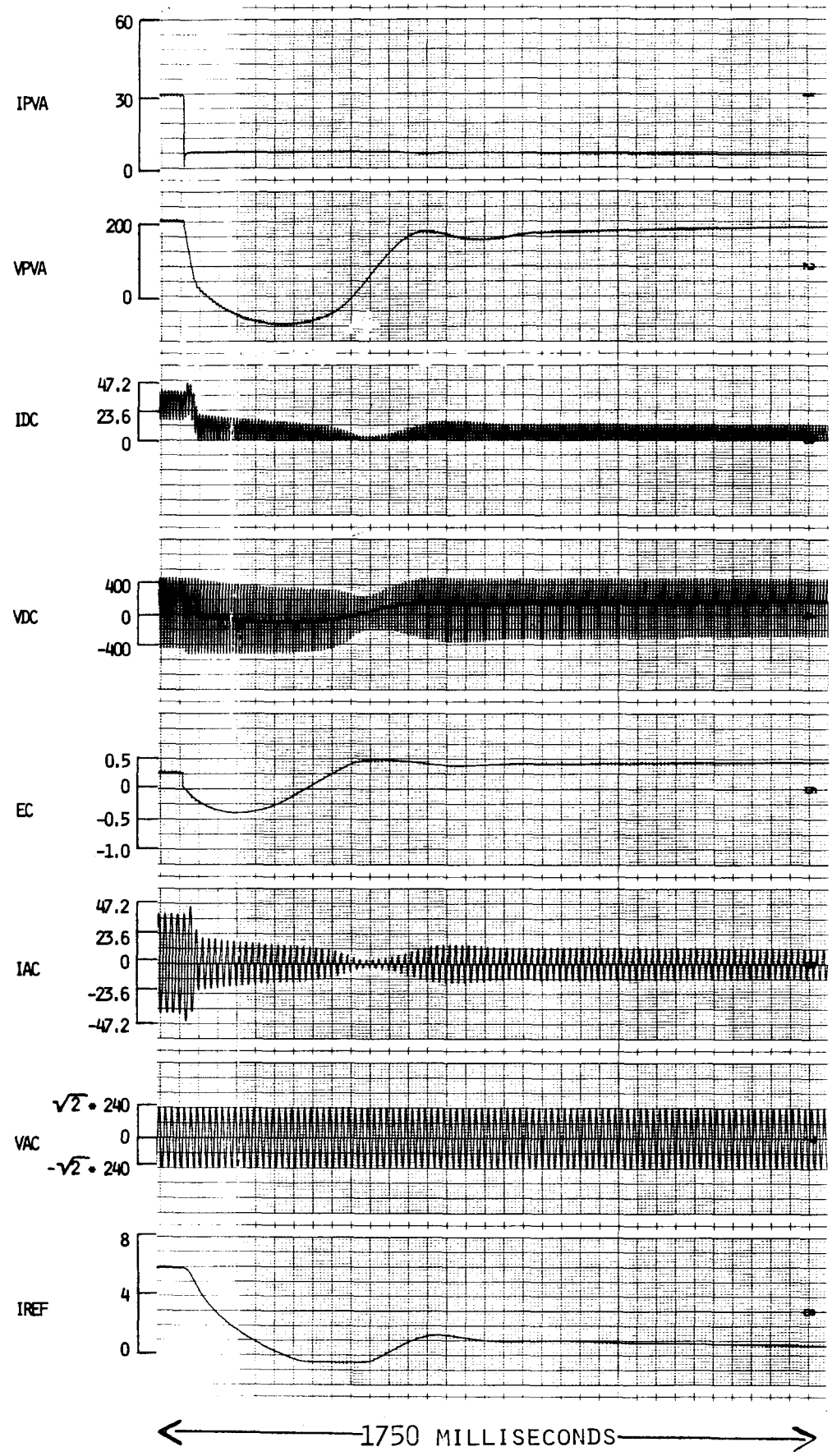

FIGURE C3-5 EMTP COMPUTES MODEL RESULTS OF GEMINI SPC STEADY STATE OPERATION WITH SOLAR INSOLATION = 20 MW/CM^2

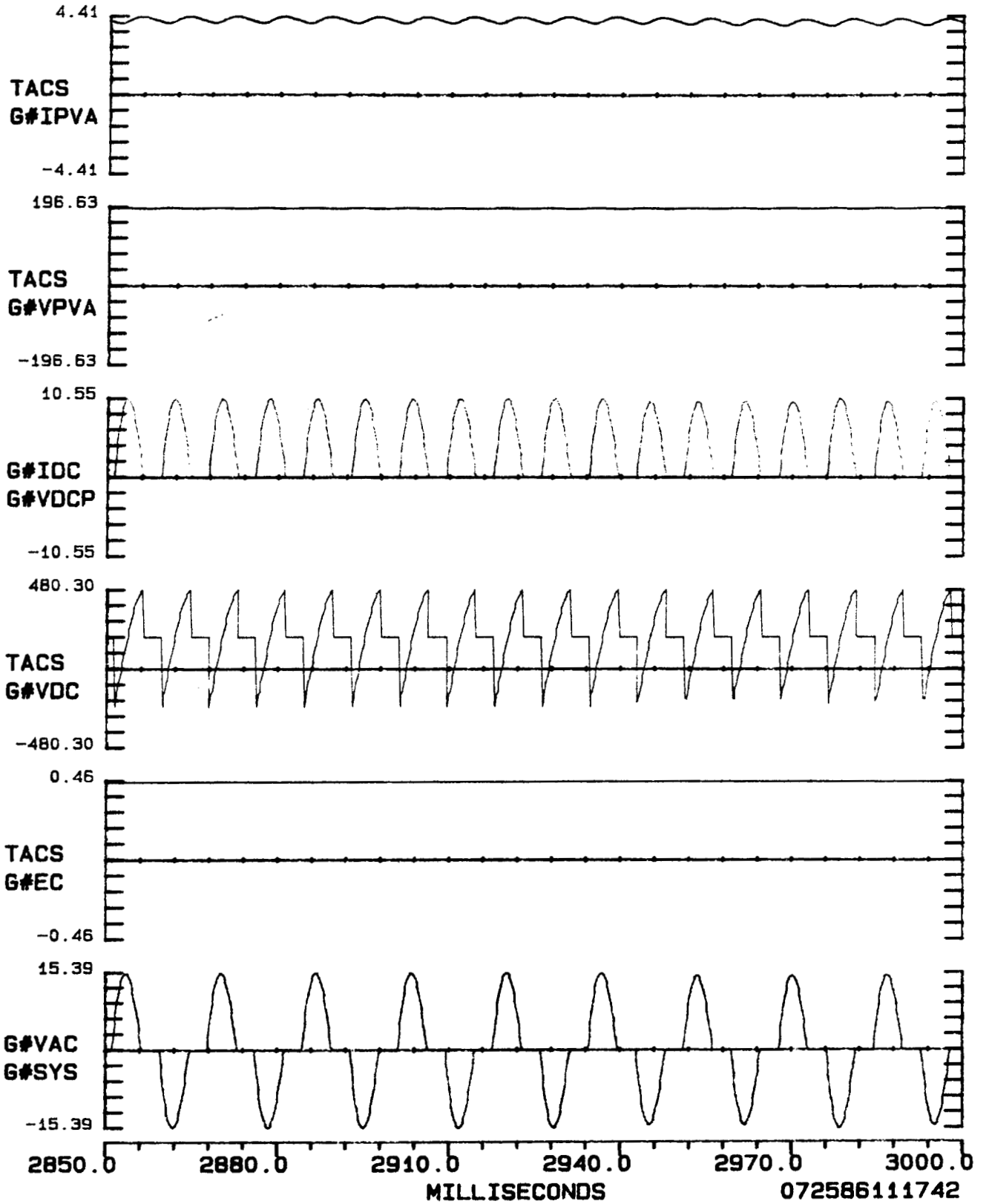

FIGURE C3-6 ANALOG COMPUTER MODEL RESULTS OF GEMINI SPC STEADY STATE OPERATION WITH SOLAR INSOLATION = 20 MW/CM^2

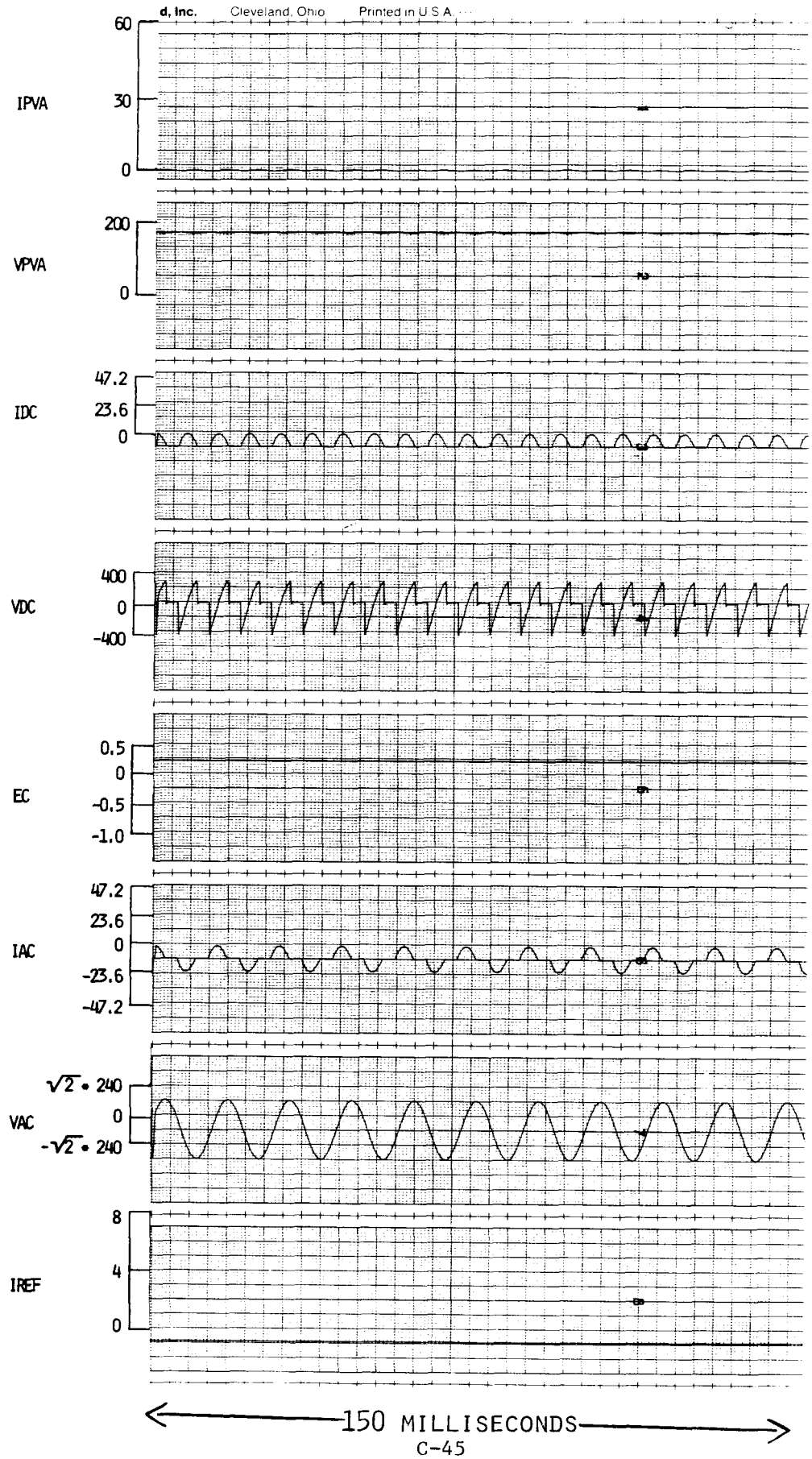

FIGURE C3-7 EMTP COMPUTER MODEL RESULTS OF GEMINI SPC WHEN SOLAR INSOLATION IS INCREASED FROM 20 MW/CM^2 TO 100 MW/CM^2

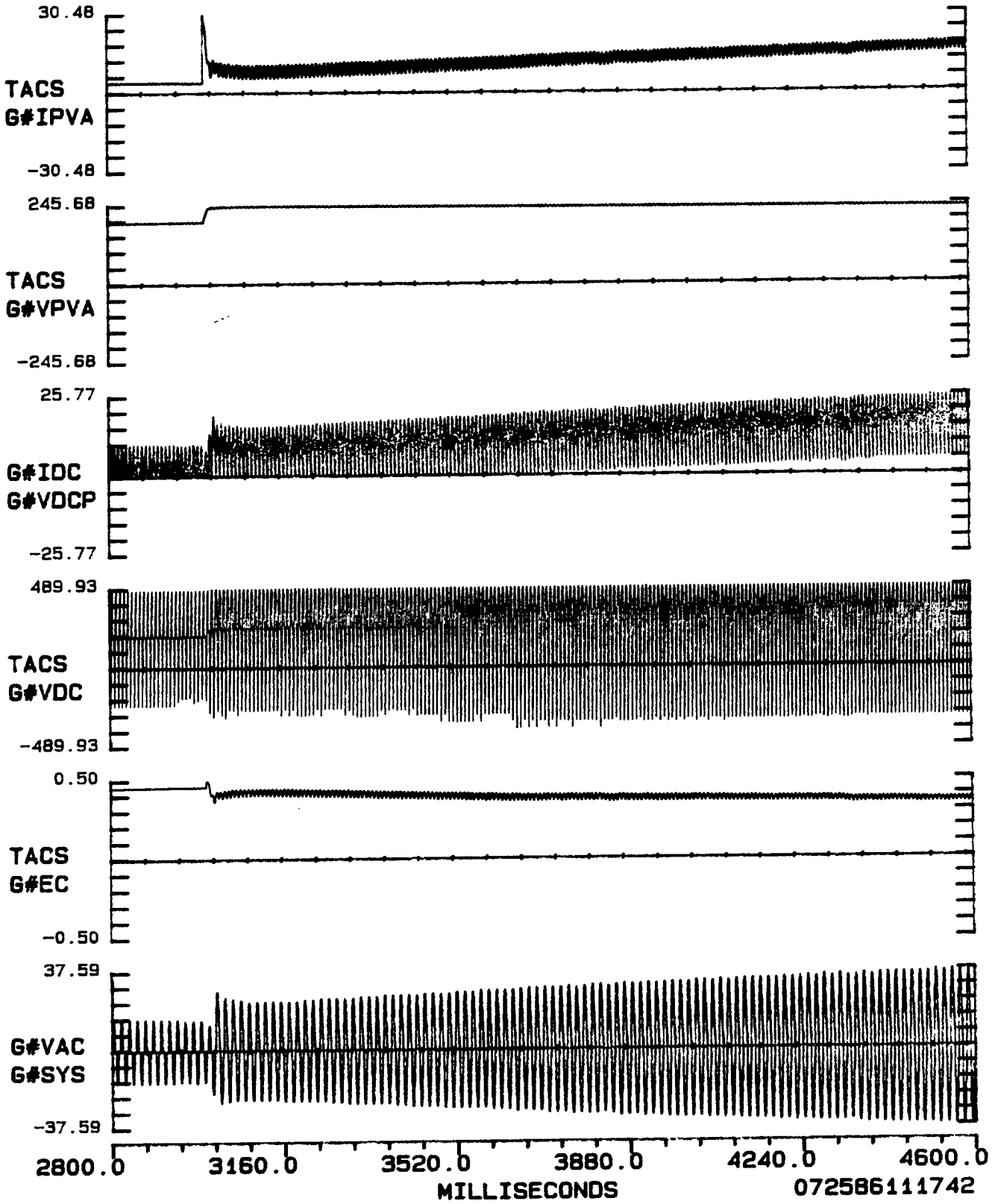

FIGURE C3-8 ANALOG COMPUTER MODEL RESULTS OF GEMINI SPC WHEN SOLAR INSOLATION IS INCREASED FROM 20 MW/CM^2 TO 100 MW/CM^2

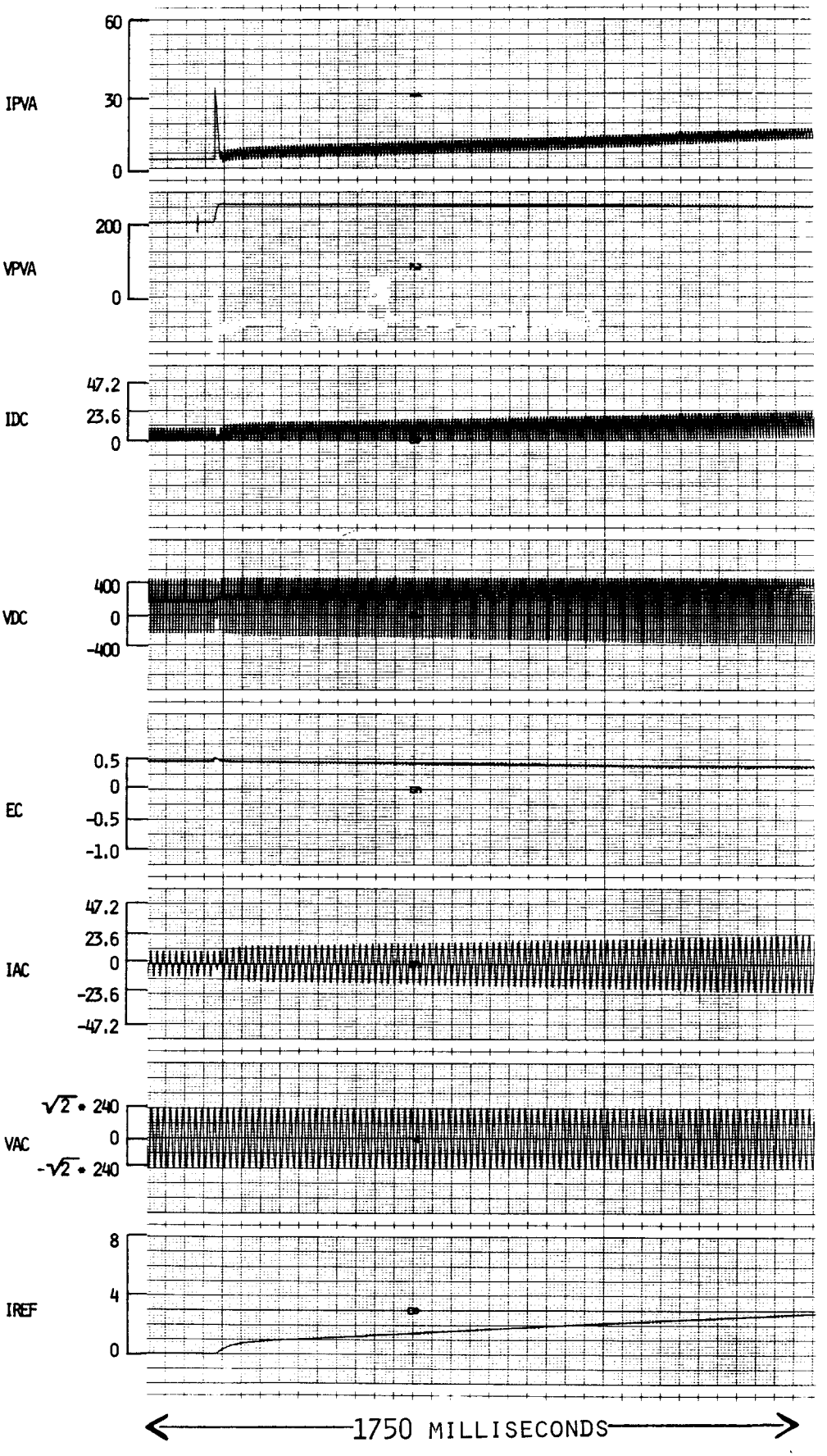

FIGURE C3-9 EMTP COMPUTER MODEL RESULTS OF GEMINI SPC WHEN REFERENCE VOLTAGE IS INCREASED FROM 200V TO 260V

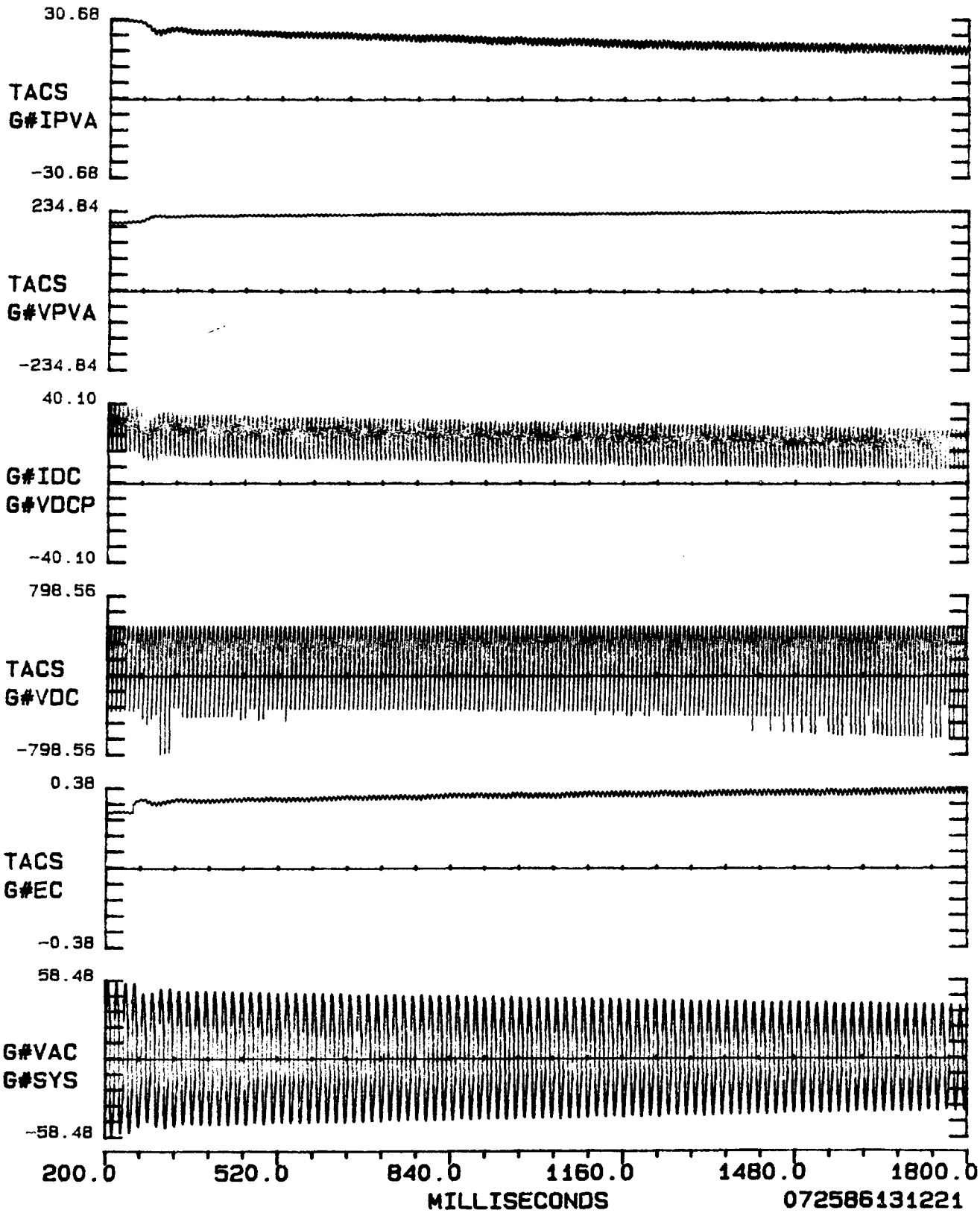

FIGURE C3-10 ANALOG COMPUTER MODEL RESULTS OF GEMINI SPC WHEN REFERENCE VOLTAGE IS INCREASED FROM 200V TO 260V

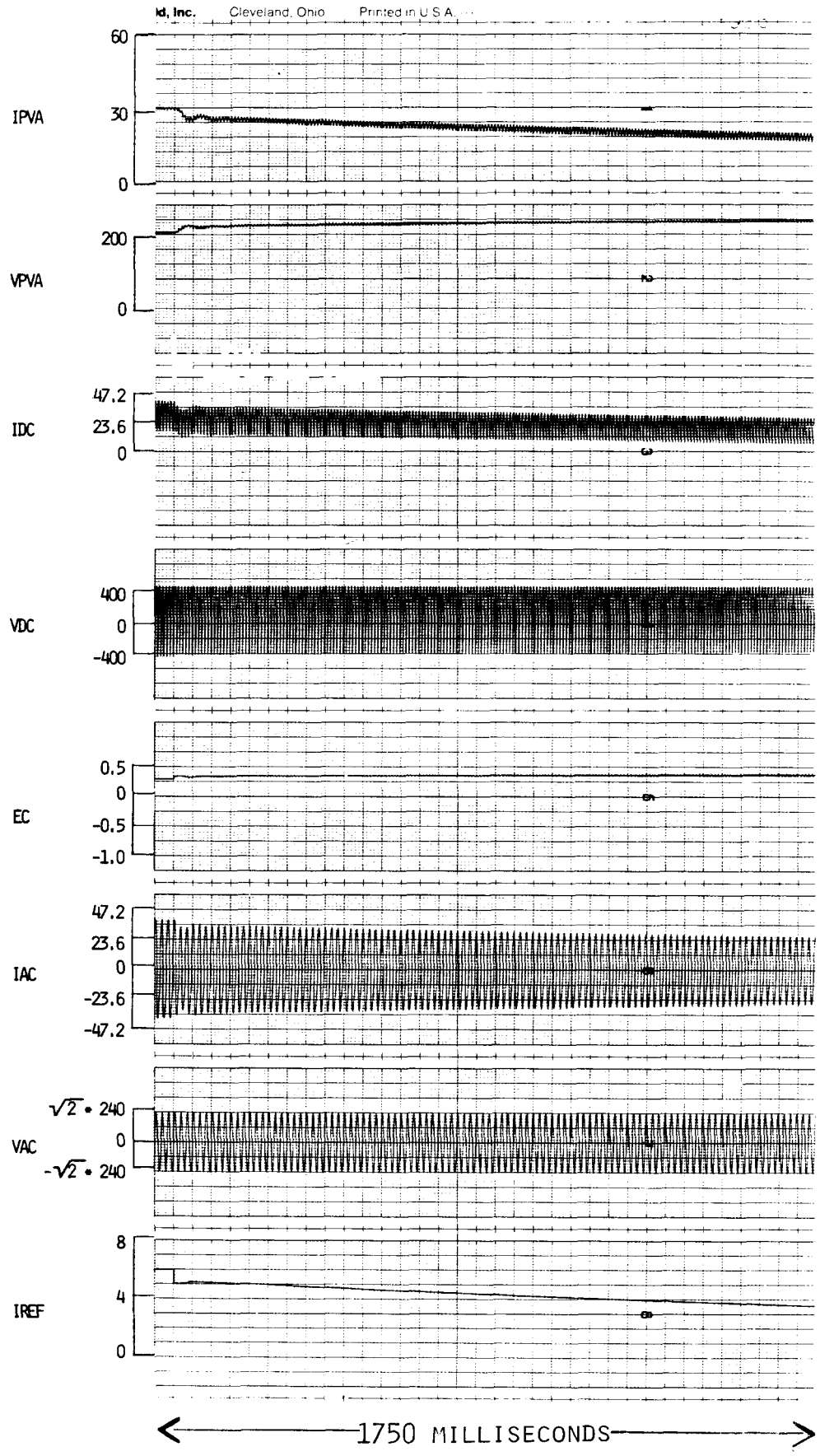

FIGURE C3-11 EMTP COMPUTER MODEL RESULTS OF GEMINI SPC
WHEN REFERENCE VOLTAGE IS DECREASED

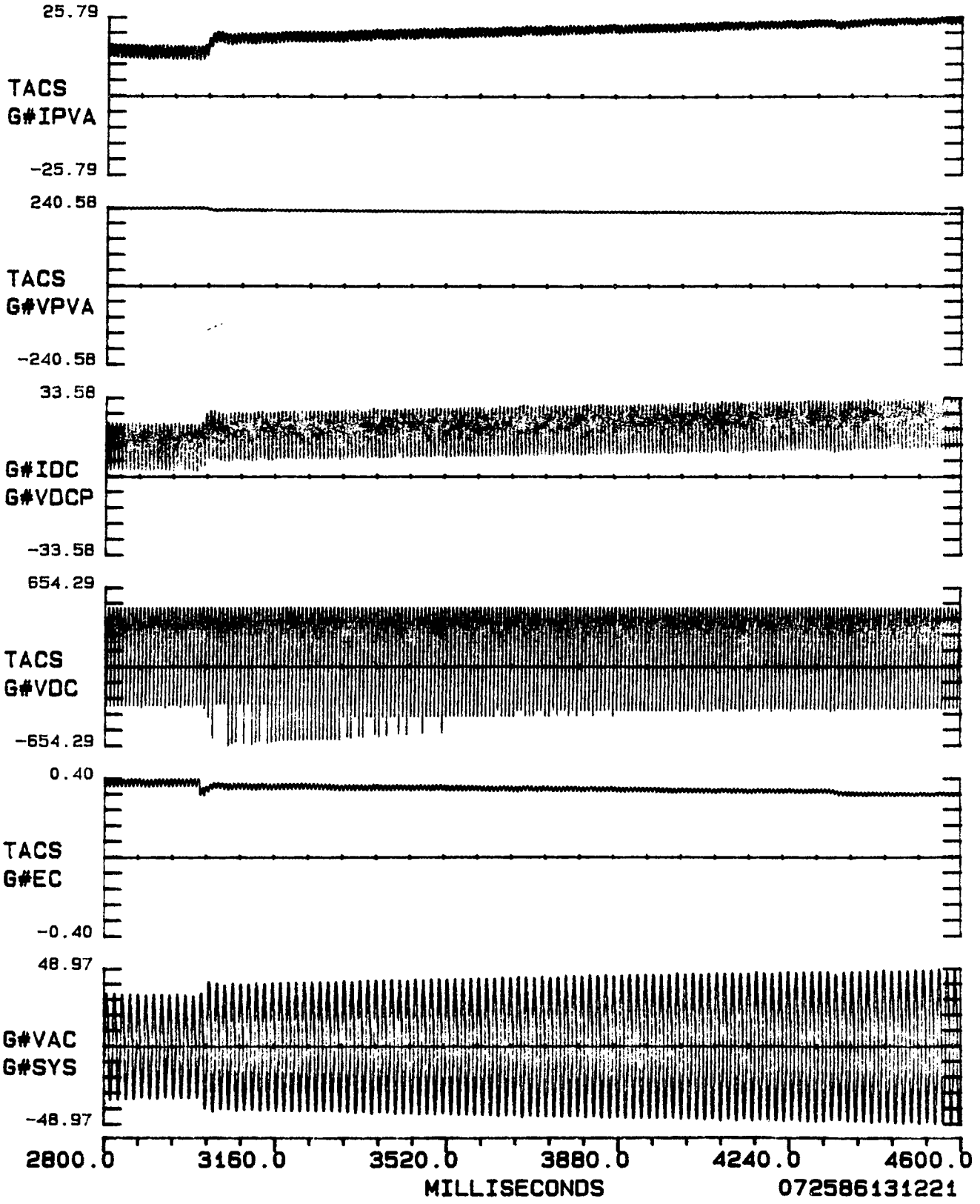

FIGURE C3-12 ANALOG COMPUTER MODEL RESULTS OF GEMINI SPC
WHEN REFERENCE VOLTAGE IS DECREASED

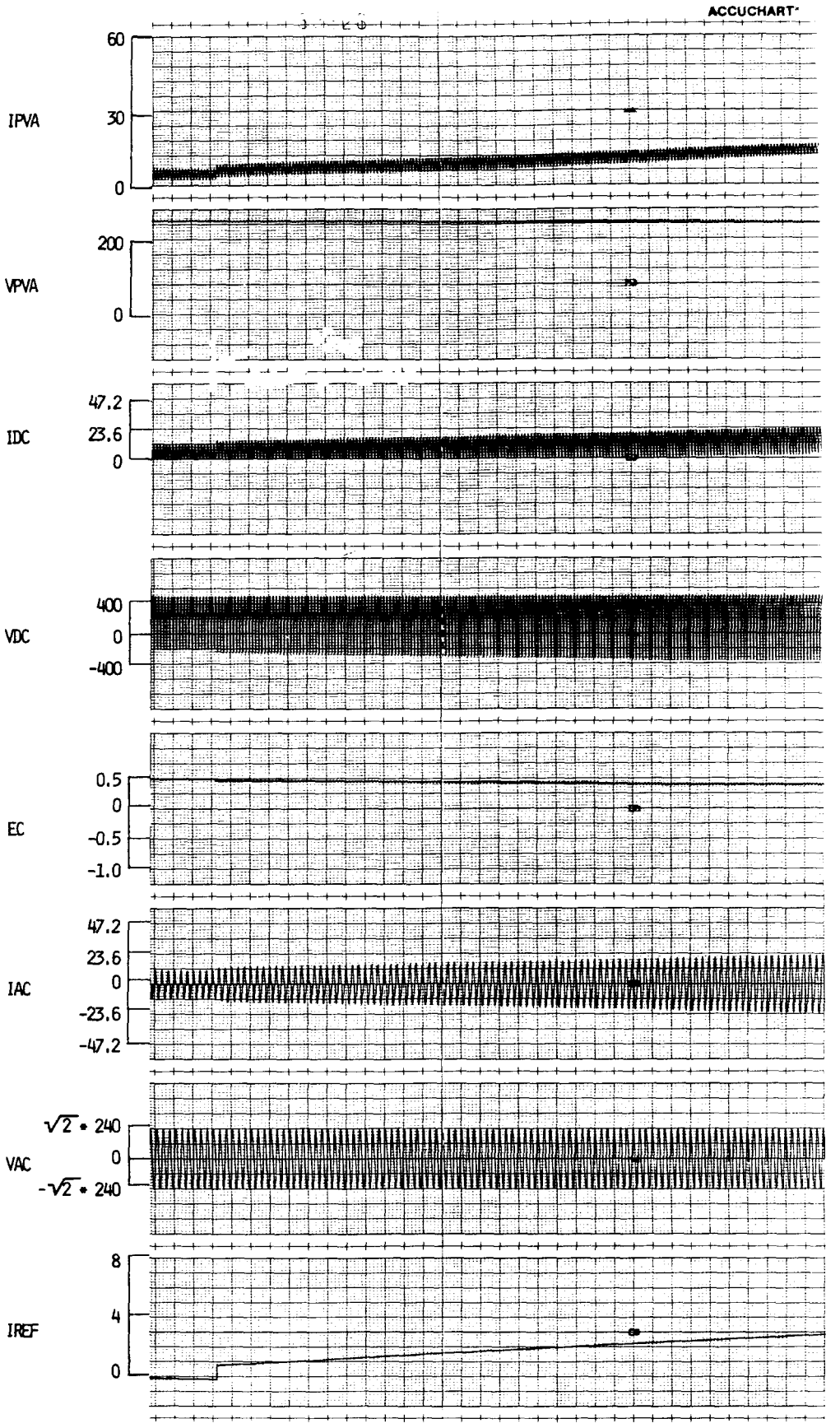

BLANK PAGE

APPENDIX D - SIMPLIFIED ANALYTICAL MODEL FOR THE APCC STATIC POWER CONVERTER

This appendix details the development of simplified computer models for the American Power Conversion Corporation's (APCC) Sunsine 2000 photovoltaic static power converter (SPC). Simulation studies are described using the simplified models, and results are compared to experimental data as well as to information available from detailed computer models.

The primary objective of this effort is to produce simple models that represent the dynamic behavior of the SPC under run-on conditions. The focal point of this endeavor is, therefore, to highlight those features of the inverter circuitry that are crucial in effecting inverter shut-down whenever the utility line is disconnected from the SPC-load combination.

This work is motivated by the need to provide utility personnel with a portable and easy-to-use tool to predict any possible islanding events and estimate their approximate duration, given the typical range of local load and power utility conditions. If such an approximate but readily available tool provides an indication of possible problem situations, then a more elaborate modeling and analysis effort may be undertaken to resolve these issues unquestionably.

In most situations, the modeling results reported herein are conservative, providing the user with significant trends as load conditions vary. Whereas more sophisticated computer models must exhibit a predictive capability

compatible with actual laboratory or field results if they are to be used as tools in assessing design and safety concerns, a simplified approach can only claim results with a reasonable resemblance to the actual case. Slow inverter dynamics or nonessential components to the run-on condition are neglected. The inverter designer, anticipating the need to shut the device down under emergency conditions, invariably incorporates electronic circuits that sense the resulting operating discrepancy and activate appropriate shut-off sequences. A simplified analytical model must, therefore, focus upon those features of the interconnected PV system- utility grid that affect significantly its isolated operation.

D.1 General Description

Detailed electrical diagrams of commercial power-conversion systems are usually considered proprietary and are not available in the open literature. Recently, Purdue University developed a hybrid computer model of the APCC Sunsine 2000 photovoltaic SPC through the assistance and cooperation of the APCC technical staff. The Purdue report [27] detailing this modeling effort formed the only available source of information regarding the Sunsine 2000 for the development of a simplified analytical tool. Mathematical descriptions of key inverter subsystems (the line filter, the loop filter, etc.) were taken directly from the Purdue development, since actual circuit diagrams are still considered proprietary. The results of this work are, therefore, dependent upon the credibility of the Purdue model. In general, for most practical situations, the computer results seem to match fairly well experimental data obtained from laboratory and field studies conducted by Georgia Power Company.

Figure D.1-1, reprinted from Wasynczuk [27], is a simplified electrical diagram of the APCC Sunsine PV system. The dc system, consisting of the PV array and a filter capacitor, is connected to a down converter, which produces an output current closely resembling a full wave rectified sine wave. The unwrapper circuit produces a sinusoidal output at the utility side of the isolation transformer by inverting every other half cycle of the down converter output.

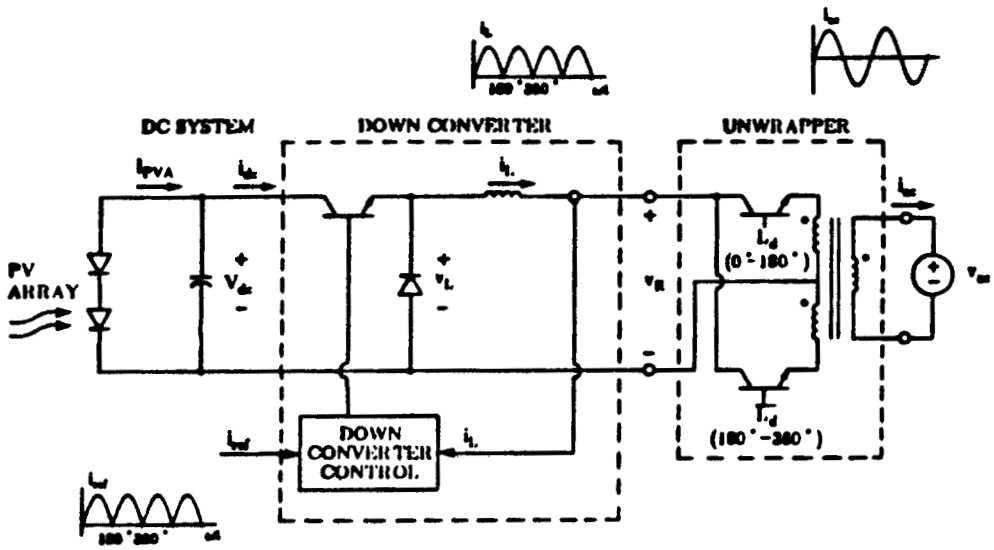

FIGURE D.1-1 SIMPLIFIED ELECTRICAL DIAGRAM OF APCC INVERTER.

The inverter ac output current is phase locked to the measured line voltage. A simplified block diagram of the inverter control system is shown in Figure D.1-2. A maximum power tracker (MPT) assures that maximum power is extracted from the array under varying environmental conditions. The voltage regulator adjusts a magnitude command signal, I_{mag}, which is tracked by the down converter during normal operation and is a measure of the peak ac current injected into the utility.

The function of the PLL is to provide a rectified sinusoidal reference signal and to control the switching of the unwrapper. A more detailed functional block diagram of the phase locked loop control system is shown as Figure D.1-3. For normal operation, the multiplying digital-to-analog converter (MDAC) produces a rectified sinusoidal reference signal, which must be synchronized with the line voltage. To accomplish this, the frequency of the voltage controlled clock (VCC) is varied in proportion to a control signal V_ω. When $V_\omega = 0$, the output frequency of the clock is approximately 30.72 kHz. At each clock pulse, the counter is incremented with a maximum count of 512. Thus, the frequency associated with a complete counter cycle is 60 Hz. As the control voltage V_ω varies from -10 to +10 volts, the frequency of a complete counter cycle will vary between 59.073 and 60.927 Hz. Synchronization is achieved using a feedback circuit, which increases or decreases the control voltage whenever the counter output leads or lags the line voltage. Details of the PLL VCC and nine-bit counter are depicted in Figure D.1-4.

Synchronization of the counter to the line frequency is achieved by monitoring the phase difference between the counter output and the line

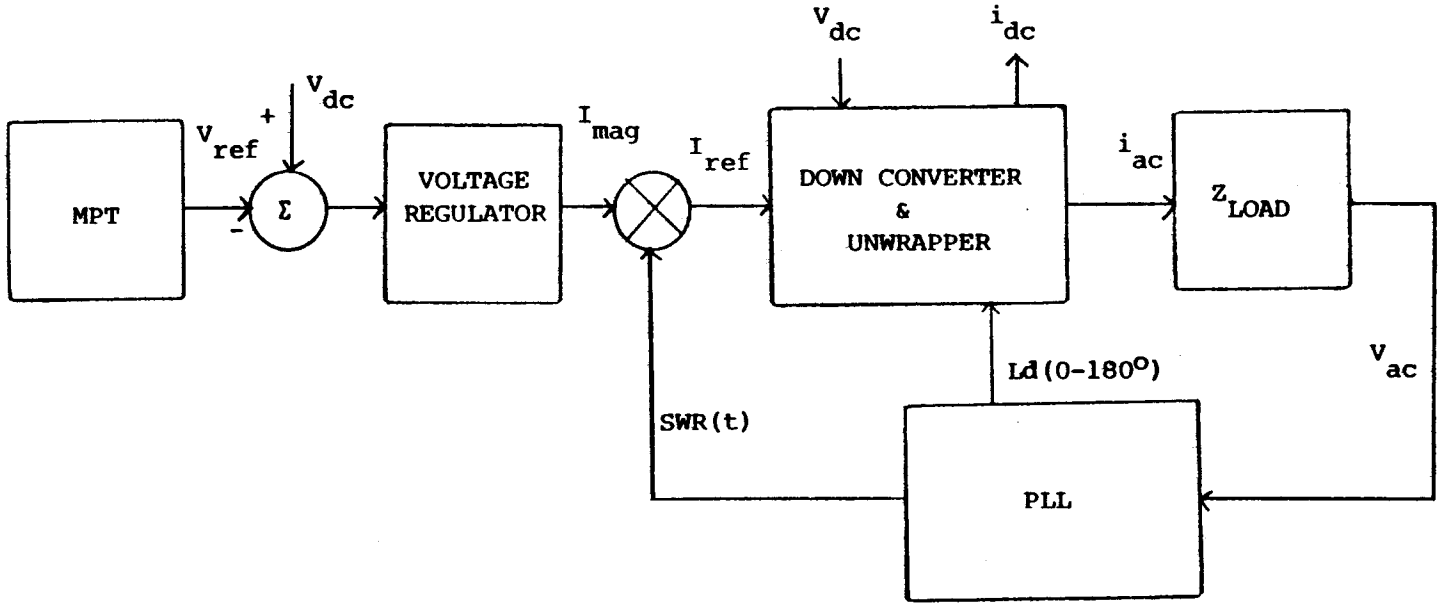

FIGURE D.1-2 SIMPLIFIED BLOCK DIAGRAM OF THE CONTROL SYSTEM.

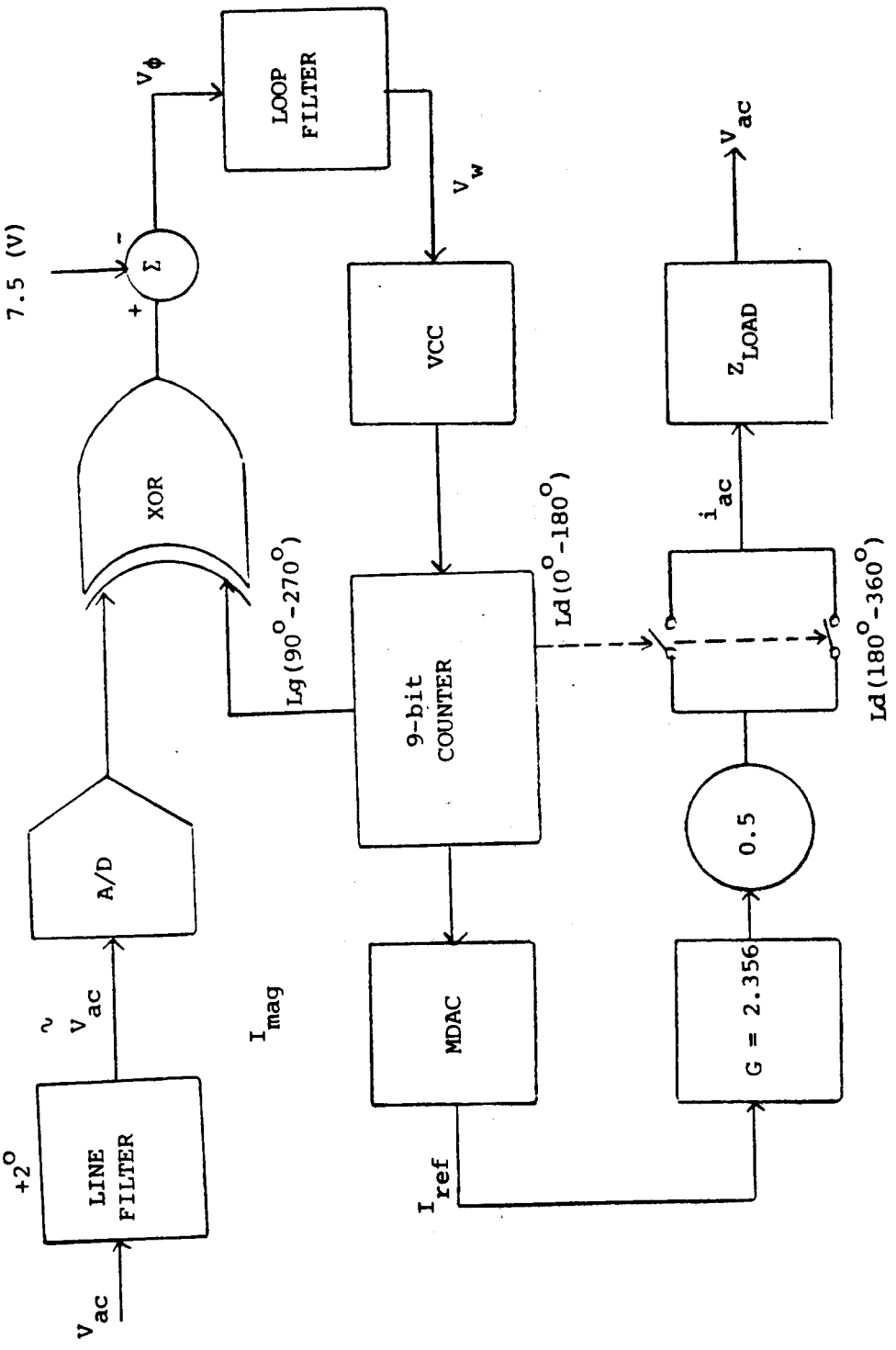

FIGURE D.1-3 BLOCK DIAGRAM OF THE APCC PLL CIRCUITRY.

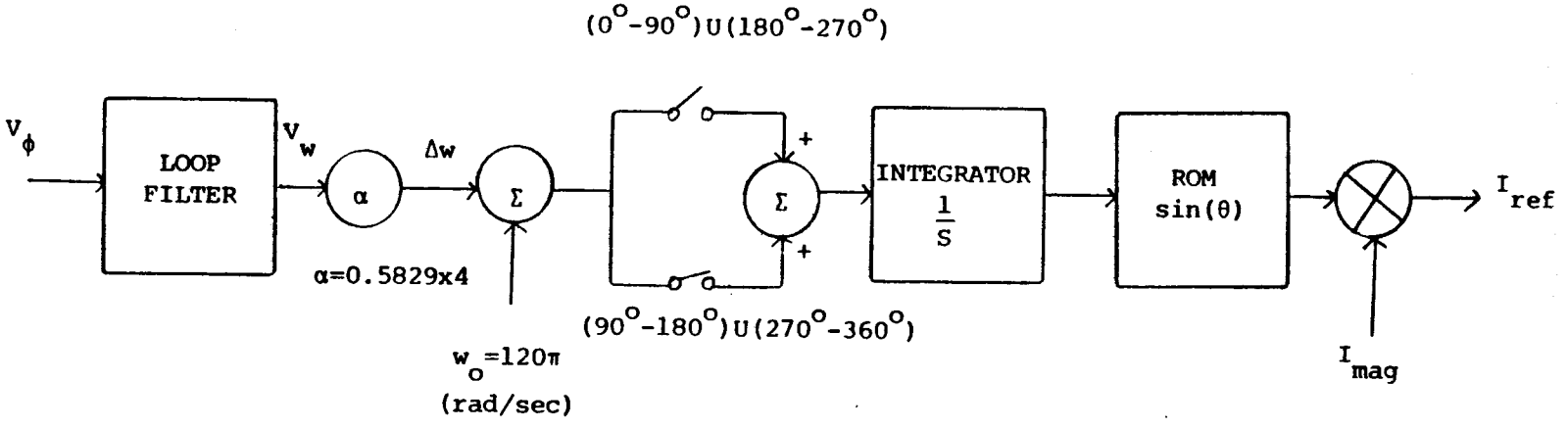

FIGURE D.1-4 BLOCK DIAGRAM OF THE PLL VCC AND 9-BIT COUNTER

voltage. The filtered line voltage is fed to an A/D comparator whose output represents one of two inputs to an exclusive OR (XOR) phase detector. Thus, the average value of the XOR output is a measure of the phase difference between the angular state of the counter and the line voltage.

D.2 Islanded Operation

Let us consider the interconnected operation of the PV system with the utility grid as shown in Figure D.2-1. It is of interest to observe the operation of the PV system in the event that the circuit breaker is suddenly opened. Particularly, it is important for operational and safety considerations to determine conditions under which the unit will run on for the maximum possible time. As a matter of fact, if the load current is carefully adjusted so that all of the current supplied by the inverter is consumed by the load, then the opening of the breaker will not be sensed by the inverter's protective control circuits. In this case, the inverter will, theoretically at least, run on indefinitely. Under all other load conditions, the PLL and its associated control circuitry undertake the task of sensing the appropriate phase angles before and after line disconnection and tripping a phase error detector whenever the phase error between the angular state of the phase locked oscillator and the filtered line voltage reference becomes greater than 2°. Thus, the dynamics of the PLL circuit are primarily responsible for the operation of the inverter under islanded conditions. For that reason, attention is focused below in the modeling effort on the behavior of the PLL circuitry.

Let us examine the action of the control circuit at the time of line disconnection. Let

ϕ_e = absolute phase error in degrees

ϕ_i = absolute phase difference between inverter voltage and current.

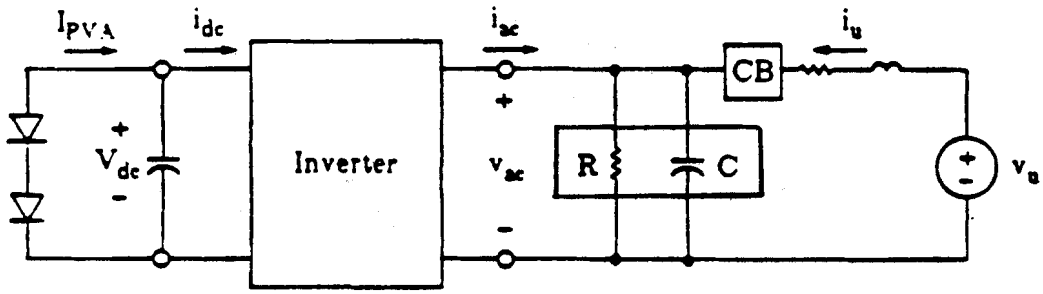

FIGURE D.2-1 PV-INVERTER-UTILITY INTERCONNECTION.

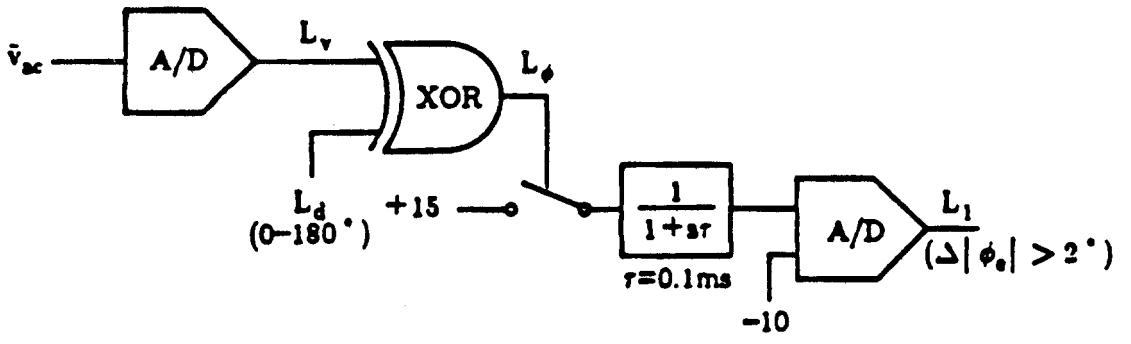

FIGURE D.2-2 THE PHASE ERROR DETECTOR CIRCUIT.

During steady-state conditions, before the circuit breaker is opened, ϕ_i is the phase lead angle introduced by the line filter, which is very close to 2°. The phase error ϕ_e is, of course, zero during steady-state conditions. When the circuit breaker is opened, the value of ϕ_i is determined by the load angle, ϕ_L of the passive load to which the inverter connects. Upon opening of the circuit breaker, ϕ_e will jump to the value so that $\phi_L + \phi_e = 2°$. Thereafter, the response of

ϕ_i , ϕ_e , and V_ω is primarily determined by the characteristics of the line filter, the load and loop filter associated with the phase locked loop.

The most significant design feature of the inverter involves a resonant peak of the line filter at 60 Hz. Thus, the phase load of the line filter increases as the frequency increases and at a significantly higher rate than that of the load (if it is capacitive) so that the resulting phase error increases as the frequency increases. A classic "positive feedback" instability results, since the ac system frequency will increase at a higher rate as the phase error increases.

Details of the phase-error-detector circuit responsible for disabling the inverter are shown in Figure D.2-2. If the load is resistive or inductive, then the initial jump in ϕ_e will always be greater than 2°, which is the trip point of the phase error detector resulting in almost instantaneous shutdown. The same condition will result if the load is capacitive but the magnitude of load angle is between 0° and 2°. The positive feedback instability is, therefore, essential for the shutdown mode only in the case of a capacitive load with a phase angle between 0° and 2°.

D.3 The Simplified Computer Model

Special attention is required in modeling the dynamics of the line filter and the loop filter of the PLL circuit. The significance of the first in the run-on mode was demonstrated in the previous section. Modeling of the remaining control circuit components is straightforward and follows classical approaches.

The Line-Filter Implementation

The line filter is implemented by a fifth-order state equation whose transfer function is as follows:

$$H(s) = \frac{9.803934E7*(s-2.8748E-14)(s^2+92.79882s+144998.1)}{(s+71005.7)(s+2511.29)(s+61.87084)(s^2+186.6827s+149752.5)} .$$

In Figures D.3-1 and D.3-2, the magnitude and phase responses are plotted using a CC program package. As was pointed out previously, the positive group delay at 60 Hz makes the PLL system unstable.

In state variable form, the equations are written as:

$$\frac{d}{dt}\begin{bmatrix} x_1 \\ x_2 \\ x_3 \\ x_4 \\ x_5 \end{bmatrix} = \begin{bmatrix} -70970.59 & -2303.92 & 1470.59 & 0 & 0 \\ -104.7237 & -104.7237 & 66.8449 & 0 & 0 \\ 1470.59 & 1470.59 & -2597.43 & 74.23905 & -4925.76 \\ 0 & 0 & 46.39941 & -46.39941 & 3078.60 \\ 0 & 0 & 46.39941 & -46.39941 & -46.39941 \end{bmatrix} \begin{bmatrix} x_1 \\ x_2 \\ x_3 \\ x_4 \\ x_5 \end{bmatrix}$$

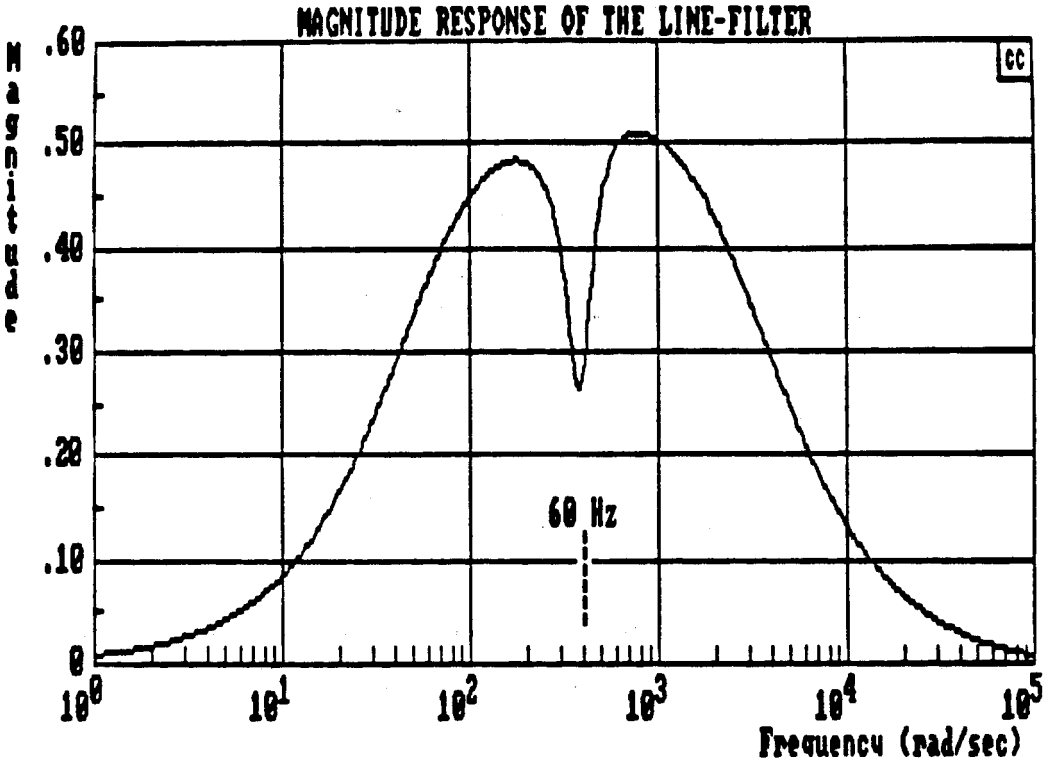

FIGURE D.3-1 THE MAGNITUDE RESPONSE OF THE LINE FILTER.

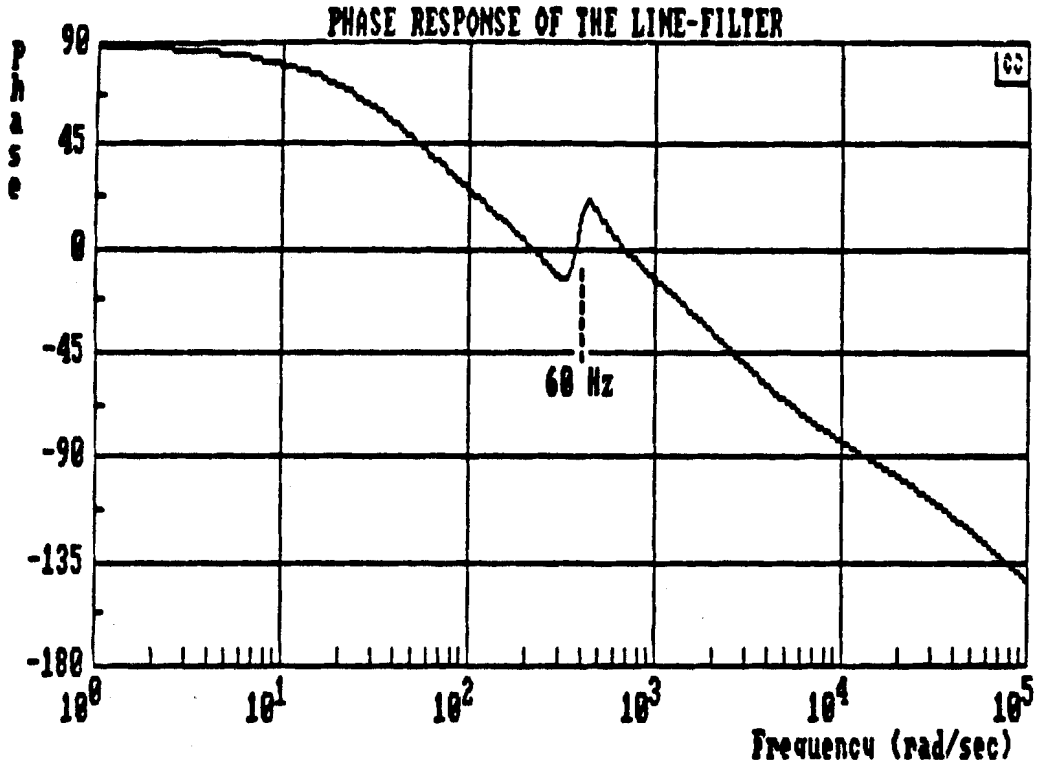

FIGURE D.3-2 THE PHASE RESPONSE OF THE LINE FILTER.

$$+\begin{bmatrix} 66666.67 \\ 0 \\ 0 \\ 0 \\ 0 \end{bmatrix} v_{ac}$$

$$\bar{v}_{ac} = [0\ 0\ 1\ 0\ 0]^{*}\underline{x},$$

where

$\underline{x} = [x_1\ x_2\ x_3\ x_4\ x5]^{T}$. The poles of the line-filter transfer function are

$$s_1 = -61.87084$$

$$s_2 = -93.34133 + j375.5528$$

$$s_3 = -93.34133 - j375.5528$$

$$s_4 = -2511.29$$

$$s^5 = -71005.7.$$

The Loop-Filter Implementation

The loop filter can be implemented by a third-order state equation whose transfer function is

$$H_{\ell}(s) = \frac{67188.53\ (s+3.002979)}{s(s+303.0303)(s+62.57823)}.$$

In Figures D.3-3 and D.3-4, the magnitude and phase responses are plotted using the CC program package. The

state representation is as follows:

$$\frac{d}{dt}\begin{bmatrix} x_1 \\ x_2 \\ x_3 \end{bmatrix} = \begin{bmatrix} 0 & 1 & 0 \\ 0 & 0 & 1 \\ 0 & -1.89631E4 & -3.656085E2 \end{bmatrix}\begin{bmatrix} x_1 \\ x_2 \\ x_3 \end{bmatrix} + \begin{bmatrix} 0 \\ 6.314712E3 \\ -2.289749E6 \end{bmatrix} V_{\phi},$$

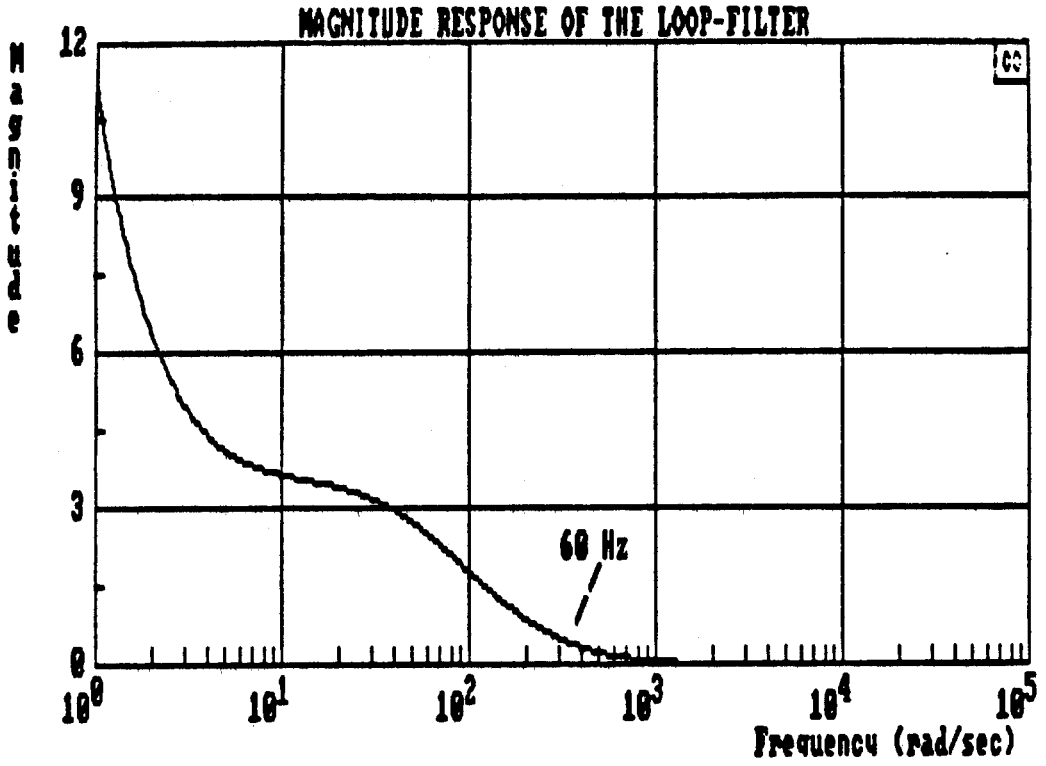

FIGURE D.3-3 THE MAGNITUDE RESPONSE OF THE LOOP FILTER.

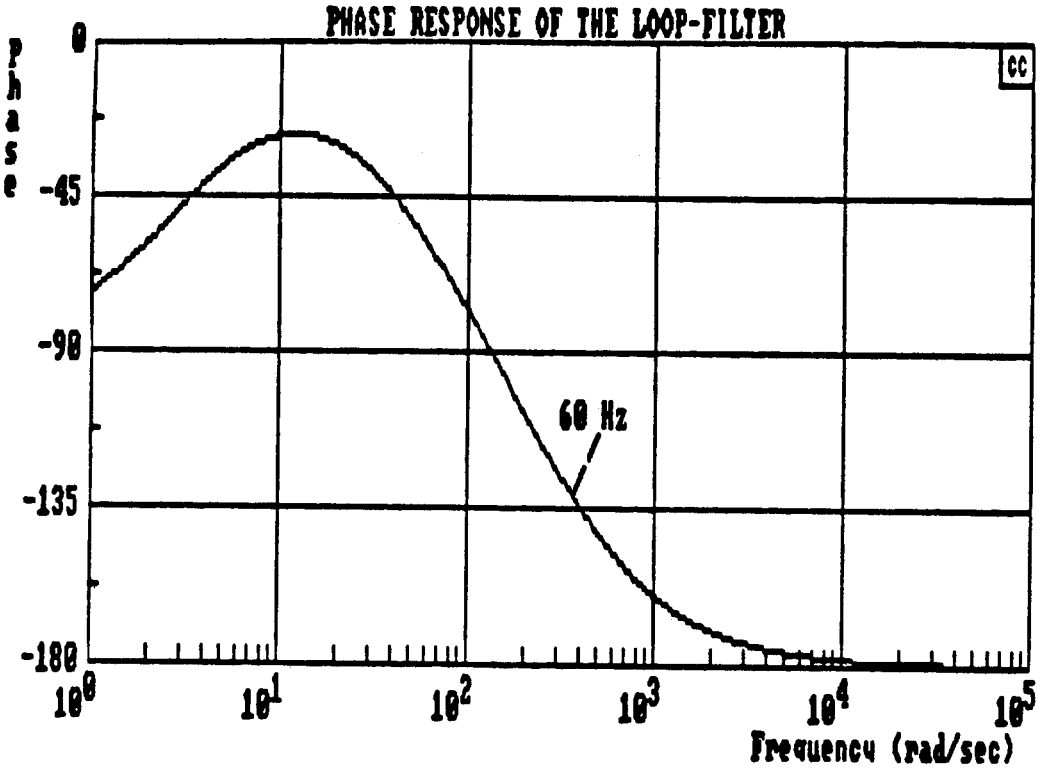

FIGURE D.3-4 THE PHASE RESPONSE OF THE LOOP FILTER.

$$V_\omega = [10.64 \quad 0 \quad 0]^* \underline{x},$$

where

$\underline{x} = [x_1 \; x_2 \; x_3]^T$. The poles of the loop filter are

$$s_1 = -62.57823$$

$$s_2 = -303.0303$$

$$s_3 = 0.$$

V_ϕ is the input to the loop filter.

The Line Impedance and the Load Impedance

The line impedance is modeled as the series combination of a resistor (with a nominal value of 0.072 ohm) and an inductor (0.072 ohm). The load impedance is specified by the user.

D.4 Simulation Studies

Figure D.4-1 depicts a flow chart of the simulation program. The following conditions are assumed:

(1) The inverter is operating in steady state before line disconnection so that the average value of the loop filter output V_ω is zero.

(2) The circuit breaker is opened when the utility current, $I_u(t)$, goes from a negative to a positive zero crossing.

(3) The initial value of $V_\omega(t)$ is adjusted to conform to condition (1).

In order to compare model results with test data available through GPC, simulated conditions were initially set to match those of the GPC tests. The system current, $I_{AC}(t)$, was chosen to be 23.56 amperes, and the

inverter voltage was made equal to 339.4 volts. The power dissipated by the load was 4200 (watts) - j280 (vars) under matched conditions - the same as in the GPC tests.

For a balanced condition with a capacitive load, R_L = 13.7 ohm and C_L = 12.895$_\mu$F. Table D.4-1 shows the sensitivity of the run-on time on load conditions as the load power is varied for fixed vars and fixed watts, respectively. The balanced load case produces the longest run-on time of only 7.943 ms.

Table D.4-2 depicts the comparison between the simulated and the experimental results. All run-on times are less than 8 ms. The inverter shuts down almost instantaneously. The computer results are considered acceptable, because they are well within the "window" of 200 ms. This time is considered important because it may affect the automatic reconnection of the PV system to the utility grid.

Table D.4-3 shows a breakdown of the simulation results according to the type of the load. It may be observed that the inverter shuts down almost immediately for practically all situations except when the load phase angle is between 0° and 2°.

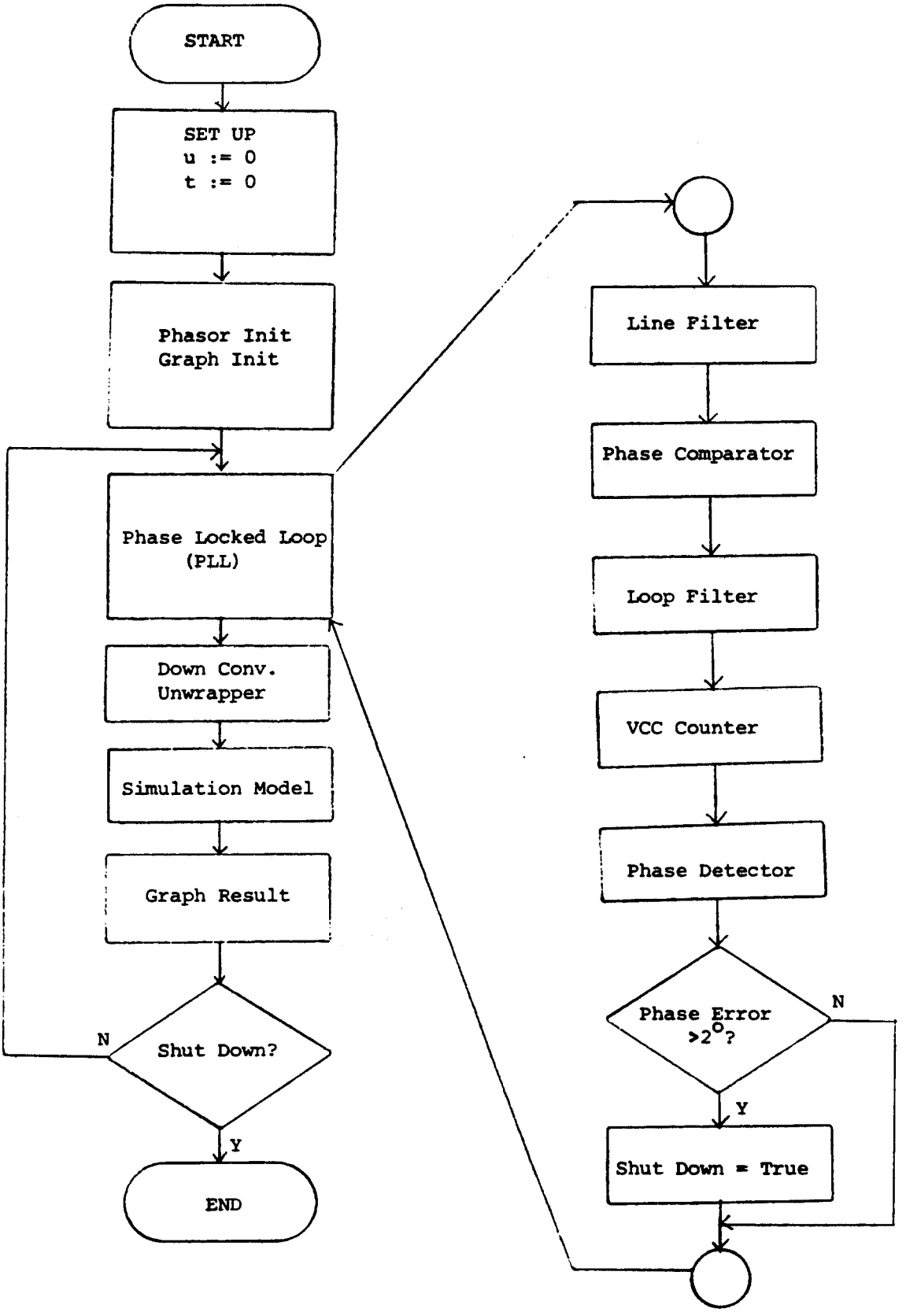

FIGURE D.4-1 FLOW CHART OF APCC SIMULATION PROGRAM.

TABLE D.4-1 SIMULATION RESULTS FOR CAPACITIVE LOAD
($\phi_L > 2°$)

Load Power	Load Impedance	V_{ao} Phase-Lag	Run-On Time
3720.93-j280.01	15.393-j1.158	4.302°	2.604 msec
4204.38-j280.01	13.64 -j0.908	3.8085°	7.943 msec
4600.64-j280.01	12.474-j0.759	3.482°	5.632 msec
4204.38-j325.72	13.618-j1.055	4.43°	0.326 msec
4204.38-j280.01	13.64 -j0.908	3.8085°	7.943 msec
4204.38-j147.66	13.683-j0.481	2.013°	5.664 msec

TABLE D.4-2 COMPARISON OF SIMULATED AND EXPERIMENTAL RESULTS

Case	GPC Test Results	Computer Simulation Results
#I.A.1 Matched Power	Load Power 4160 (Watts) -280 (Vars) System Amps 17.28 (A) SPC Volts 244.8 (V) Run-On Time 0.006 (sec)	Load Power 4204.38 (Watts) -280.01 (Vars) System Amps 237.66 (V) SPC Volts 237.66 (V) Run-On Time 0.007943 (sec)
#I.A.2 10% Less	Load Power 3720 (Watts) -288 (Vars) System Amps 17.36 (A) SPC Volts 244.8 (V) Run-On Time 0.004 (sec)	Load Power 3720.93 (Watts) -280.01 (Vars) System Amps 16.66 (A) SPC Volts 270.18 (V) Run-On Time 0.002604 (sec)
#I.A.3 10% More	Load Power 4600 (Watts) -276 (Vars) System Amps 17.28 (A) SPC Volts 243 (V) Run-On Time 0.001 (sec)	Load Power 4600.64 (Watts) -280.01 (Vars) System Amps 16.66 (A) SPC Volts 223.45 (V) Run-On Time 0.005632 (sec)

TABLE D.4-3 COMPUTER RESULTS AND COMPARISONS FOR THE APCC INVERTER

Case 1. ($\phi_L > 2°$)	ϕ_L	Load Watts	;	Vars	Run-On Time
R-L Load (Vac Leads Iac)	+3.953°	4199.73	;	290.22	2.018 msec
R-L Load (Vac Leads Iac)	-4.302°	3720.93	;	-280.01	2.604 msec
	-3.809°	4204.38	;	-280.01	7.943 msec
	-3.482°	4600.64	;	-280.01	5.632 msec
	-4.430°	4204.38	;	-325.72	0.326 msec
	-2.013°	4204.38	;	-147.66	5.664 msec
Case 2. ($\phi_L > 2°$)	ϕ_L	Load Watts	;	Vars	Run-On Time
R-L Load	-1.776°	4204.38	;	-130.40	8.984 msec
(Vac Leads Iac)	-0.592°	4204.38	;	-43.47	927.865 msec
Case 3. ($\phi_L > 0°$)	ϕ_L	Load Watts	;	Vars	Run-On Time
R-L Load	0.000°	4203.31	;	0.00	594.987 msec

DISTRIBUTION:

Abacus Controls, Inc.
Attn: G. A. O'Sullivan
P. O. Box 893
Somerville, NJ 08876

Alabama Power Co.
Attn: Greg Reardon
P. O. Box 2641
Birmingham, AL 35291

Alabama Solar Energy Center
Attn: Dr. D. B. Wallace
University of Alabama
in Huntsville
Huntsville, AL 35899

American Power Conversion Corp.
Attn: Dr. E. E. Landsman
89 Cambridge Street
Burlington, MA 01803

Arco Solar, Inc.
Attn: G. Shushnar
P. O. Box 6032
Camarillo, CA 93020

Arizona Public Service Co.
Attn: Thomas C. Lepley
P. O. Box 53999, Mail Sta. 3875
Phoenix, AZ 85072-3999

Arizona State University
Attn: Paul Russell
College of Engineering
Tempe, AZ 85287

Ascension Technology
Attn: Ed Kern
Box 314
Lincoln Center, MA 01773

Automotive Research
Attn: Bill Hyde, A/RE Manager
1685 Whitney
Idaho Falls, ID 83402

Best Power Technology, Inc.
Attn: Marguerite Paul
P. O. Box 280
Nedecah, WI 54646

Bechtel Group, Inc.
Attn: W. Stolte
P. O. Box 3965
San Francisco, CA 94119

Beckwith Electric Company
Attn: R. W. Beckwith
11811 62nd St. N.
Largo, FL 33543

Black & Veatch
Attn: S. Levy
P. O. Box 8405
Overland Park, KS 66211

Bonneville Power Admin.
Attn: Minje Ghim
P. O. Box 3621
Portland, OR 97208

Boston Edison Company
Attn: Michael Mulcahy
800 Boylston Street
Boston, MA 02199

Brookhaven National Labs
Attn: John Andrews
National Center for Analysis
of Energy Systems
Upton, NY 11973

Brown Boveri Corporation
1460 Livingston Avenue
North Brunswick, NJ 08902

Cal Tech
Attn: R. Middlebrook
116-81 Cal Tech
Pasadena, CA 91125

Carolina Power & Light Co.
Attn: Kent Hoffman
Center Plaza Bldg.
P. O. Box 1551
Raleigh, NC 27602

Chronar-TriSolar Corporation
Attn: R. W. Matlin
10 De Angelo Drive
Bedford, MA 01730

City of Austin Power & Light
Attn: John Hoffner
P. O. Box 1088
Austin, TX 78767

City of Austin Power & Light
Attn: David Panico
P. O. Box 1088
Austin, TX 78767

Clemson University
Attn: Jay W. Lathrop
Electrical Engr. Dept.
Clemson, SC 29631

Cleveland State University
Attn: Peter Groumpos
1983 E. 24th St.
Cleveland, OH 44115

Computer Power Inc.
Attn: J. R. Hoeffler
124 W. Main
High Bridge, NJ 08829

Cons. Edison Co. of NY
Attn: M. LeBow
Irving Place
New York, NY 10003

Cons. Edison Co. of NY
Attn: N. Tai
Irving Place
New York, NY 10003

Cummings Solar Corporation
Attn: D. F. Stapin
323 Andover Street
Wilmington, MA 01887

Cyberex
Attn: D. C. Griffith
7171 G Industrial Park Blvd.
Mentor, OH 44060

DROME-EA
USAMERADCOM
Robert Williams
Fort Belvoir, VA 22060

Dayton Power & Light Company
Attn: S. K. Aventsen
P. O. Box 1247
Courthouse Plaza
Dayton, OH 45401

Detroit Edison Co.
Attn: Bob Pratt
2000 2nd Ave.
Detroit, MI 48226

Duke University
Attn: T. C. Wilson
Dept. of Elec. Engr.
Durham, NC 27706

Duquesne Light Co.
Attn: J. L. Koepfinger
One Oxford Centre
301 Grant St.
Pittsburgh, PA 15279

Dynamote Corporation
Attn: Glynn Gooden
1200 W. Nickerson
Seattle, WA 98119

ENTECH, Inc.
Attn: M. J. O'Neill
P. O. Box 612246
DFW Airport, TX 75261

EPRI (4)
Attn: H. Mehta
R. Ferraro
J. Mitsche
J. Schaefer
3412 Hillview Avenue
Palo Alto, CA 94303

Eaton Corporation
Industrial Drives Oper.
3122 14th Avenue
Kenosha, WI 53140

Electric Research & Mgmt., Inc.
Attn: W. E. Feero
P. O. Box 165
State College, PA 16804

Energy Conversion Devices
Attn: Hank Bianchi
32400 Edward Street
Madison Heights, MI 45071

Energy System Consultants
Attn: Dana Sears
1532 79th Ave. NE
Brookland Park, MN 55444

Exide Electronics
Attn: J. Masser
3301 Spring Forest Road
Raleigh, NC 27604

Firing Circuits, Inc.
Attn: J. Miller
Mueller Avenue
P. O. Box 2007
Norwalk, CT 06852

Florida Power Corp. (3)
Attn: Tony Padilla
Christy Herig
Jim Crews
3201 34th Street South
St. Petersburg, FL 33711

Florida Power and Light
Attn: R. S. Allan
P. O. Box 14000
Juno Beach, FL 33408

Florida Power and Light
Attn: Gary L. Michel
P. O. Box 529100
Miami, FL 33152

Florida Solar Energy Center
Attn: Gobind Atmaran
300 State Road 401
Cape Canaveral, FL 32920

GE Energy Sys. Pro. Dept.
Attn: Paul C. Bogiages
1 River Road
Bldg. 5 - Rm. 425
Schenectady, NY 12345

Garrett Corporation
Airesearch Mfg. Co. Div.
Attn: A. W. Ferris
2525 West 19th St.
Torrance, CA 90509

Georgia Inst. Technology (2)
Attn: George Vachtsevanos
Roger Webb
School of Elec. Engr.
Atlanta, GA 30332

Georgia Power Company
Attn: Dennis Keebaugh
7 Solar Circle
Shenandoah, GA 30265

Georgia Power Company (28/270)
Attn: C. H. Griffin
P. O. Box 4545
Atlanta, GA 30302

Helionetics, Inc.
Attn: L. R. Suelzle
17312 Eastman Street
Irvine, CA 92714

Heliotrope (2)
Attn: Dave Parks
Malcolm Herbert
3733 Kenora Drive
Spring Valley, CA 92077

Houston Lighting and Power Co.
Attn: W. M. Menger
Chief Facility Engineer
P. O. Box 1700
Houston, TX 77001

Intersol Power Corporation
Attn: John Sanders
11901 W. Cedar Ave.
Lakewood, CO 80228

Jacksonville Electric Authority
Attn: Goerge Rizk
Box 53105
Jacksonville, FL 32201

James A. Ross
8480 Cliffridge Lane
La Jolla, CA 92037

Jet Propulsion Laboratory (2)
Attn: S. Krauthamer
J. Klein
4800 Oak Grove Drive
Pasadena, CA 91103

Fred Kalbach
920 Alta Pine Drive
Altadena, CA 91001

Kansas City Power & Light
Attn: David Martin
P. O. Box 679
Kansas City, MO 64141

La Marche Manufacturing Co.
Attn: T. Steinke
106 Bradrock Drive
Des Plaines, IL 60018

Long Island Lighting Co.
Attn: Joseph Miller
175 E. Old Country Road
Hicksville, NY 11801

Louis Allis Drives and Systems
16555 W. Ryerson Road
New Berlin, WI 53151

MARTA
c/o Andy Monger
2775 E. Ponce De Leon
Decatur, GA 30030

MIT (2)
Attn: J. G. Kassalkian
M. F. Schlecht
Elec. Power Systems Engr. Lab
Cambridge, MA 02139

Material Research Laboratory
Dr. Russell Messier
The Penn. State Univ.
University Park, PA 16802

McGraw Edison
Power Systems Division
Attn: R. Dugan
Cannonsburg, PA 15317

Meridian Corporation
Attn: Anil Cabraal
4300 King Street
Alexandria, VA 22302

Michigan State University
Attn: Jerry Park
Elec. Engr. Dept.
Engr. Bldg., Rm. 260
East Lansing, MI 48824

Minnesota Power Co.
Attn: John Kappenman
30 West Superior St.
Duluth, MN 55802

Mobil Solar Energy Corp. (2)
Attn: Paul Wormser
Tony Norbedo
4 Suburban Park Drive
Billerica, MA 02254

Montana State University
Attn: R. Johnson
Dept. of Elec. Engr.
Bozeman, MT 59717

Moylan Engineering Assoc., Inc.
Attn: W. J. Moylan
13530 Michigan Ave.
Suite 237
Dearborn, MI 48126

NASA/Lewis Research Center
Attn: Richard DeLombard
21000 Brookpark Road
Cleveland, OH 44135

Natl. Research Council
of Canada (2)
Attn: G. Rumbold
John Ayer
Photovoltaic Division
Montreal Road
Ottawa, Canada K1A OR6

Natural Power, Inc.
Attn: Brian Gordon
Francestown Turnpike
New Boston, NH 03070

Naval Civil Engineering Lab
Attn: Kwang Ta Huang
CODE L 72
Port Hueneme, CA 93043

New England Power Service
Attn: Ed Gulachenski
25 Research Drive
Westborough, MA 01581

New Mexico Solar Energy Inst.
Attn: Vern Risser
Box 3 SOL
Las Cruces, NM 88003

New Mexico State University
Attn: Satish Ranade
Dept. of Elec. Engr.
Las Cruces, NM 88003

New York State Energy Research
and Dev. Authority
Attn: Fred Strnisa
2 Rockefeller Plaza
Albany, NY 12223

New York State Pub. Serv. Comm.
Attn: Edward Schrom
Empire State Plaza
Albany, NY 12223

No. Carolina Central University
Attn: Arthur R. Eckels
Durham, NC 27707

Nova Electric Mfg. Corp.
Attn: K. Niovitch
263 Hillside Avenue
Nutley, NJ 07110

Oak Ridge National Lab
Attn: Paul Gnadt, Energy Div.
Building 5500A
P. O. Box X
Oak Ridge, TN 37830

Oklahoma Gas and Electric
Attn: J. D. Hampton
P. O. Box 321
Oklahoma City, OK 73101

Omnion Power Engineering
W297 S11085 Hwy. ES
Mukwonago, WI 53149

Pacific Gas and Electric Co.
Attn: Steve Hester
3400 Crow Canyon Rd.
San Ramon, CA 94583

Pacific Power and Light
Attn: Steve Carr
920 SW 6th Avenue
Portland, OR 97204

Pennsylvania Power & Light Co.
Attn: R. J. Fernandez
North Ninth St.
Allentown, PA 18101

Philadelphia Electric Co.
Attn: Don Fagnan
2301 Market Street 510-1
Philadelphia, PA 19101

Photovoltaic Energy Systems
Attn: Paul Maycock
P. O. Box 290
Casanova, VA 22017

Platte River Power Authority
Attn: Carol Dollard
Timberline and Horsetooth Roads
Fort Collins, CO 80525

Power Math Assoc., Inc.
Attn: Dr. P. Anderson
Southfair, Suite 314
2002 Jimmy Durante Blvd.
Del Mar, CA 92014

Public Service Co. of Colorado
Attn: Jim Wilson
P. O. Box 840, Room 420
Denver, CO 80201

Public Service Co. of NM (3)
Attn: A. Akhil
M. Lechner
J. F. Burcham
Alvarado Square
Albuquerque, NM 87158

Public Service Electric & Gas (2)
Attn: Harry Roman
B. Radimer
P. O. Box 570
Newark, NJ 07101

Purdue University (25)
Attn: Oleg Wasynczuk
School of Elec. Engr.
West Lafayette, IN 47907

Queens University
Attn: P. C. San
Dept. of Elec. Engr.
Kingston, Ontario
Canada K7L 3N6

Ratelco, Inc.
Attn: R. Detering
1260 Mercer Street
Seattle, WA 98109

Rational Alternatives, Inc.
Attn: Mark Conkling
16 Espira Court
El Dorado
Santa Fe, NM 87501

Real Gas and Electric Co.
P. O. Box F
Santa Rosa, CA 95402

Rensselaer Polytechnic Inst.
Attn: Jose M. Borrego
EESE Dept. JEC 7020
Troy, NY 12181

Research Triangle Institute
Attn: Carl Parker
P. O. Box 12194
Research Triangle Park, NC 27709

SERI (3)
Attn: P. Longrigg
Lynn Coles
R. DeBlasio
1536 Cole Blvd.
Golden, CO 80401

SMUD
Attn: D. Collier
Box 15830
Sacramento, CA 95852-1830

Salt River Project (3)
Attn: Jim Morris
S. Chalmers
A. B. Cummings
P. O. Box 1980
Phoenix, AZ 85001

San Diego Gas & Electric Co. (3)
Attn: Marlene Mishler
Robert Potthoff
Skip Fralick
P. O. Box 1831
San Diego, CA 92112

San Jose State University
Attn: Helmer Nielsen
Dept. of Mech. Engr.
Washington Square
San Jose, CA 95192

Saudi Arabian National Center
for Science and Technology
Attn: Abbas A. Salim
P. O. Box 15164, Riyadh 11444
Saudi Arabia

Sierra Pacific Power Co.
Attn: R. G. Richards
P. O. Box 10100
Reno, NV 89520

So. California Edison Co.
Attn: N. Patapoff
Research & Development
P. O. Box 800
Rosemead, CA 91770

So. California Edison Co.
Attn: W. Rothenbuhler
P. O. Box 800
Rosemead, CA 91770

So. California Edison Co.
Attn: Darshan Kaushal
System Oper., Rm. 290
P. O. Box 800
Rosemead, CA 91770

So. Company Services, Inc. (27)
Attn: Tim Petty
K. Chakravarthi
Bob Jones (25)
R&D Department
P. O. Box 2625
Birmingham, AL 35202

Solarex Corporation
Attn: Paul Garvison
1335 Piccard Drive
Rockville, MD 20850

Sovonics Solar Systems
Attn: Larry Slominski
1100 West Maple Road
Troy, MI 48084

Stone & Webster Engr.
Attn: Dave Agneta
245 Summer St.
Boston, MA 01921

Strategies Unlimited
Attn: R. Winegarner
201 San Antonio Circle
Suite 205
Mountain View, CA 94040

TESCO
Attn: Linda Terrel
P. O. Box 970
Fort Worth, TX 76101-0970

TESLACo
Attn: R. D. Middlebrook
490 S. Rosemead, Suite 6
Pasadena, CA 91107

Tennessee Valley Authority
Attn: Sharon Ogle
Solar Applications Branch
B 513 Signal Place
Chattanooga, TN 37401

The Citadel
Atn: J. F. Schaefer
Dept. of Elec. Engr.
Charleston, SC 29409

U. S. Dept. of Energy
Attn: D. C. Krenz
Energy Tech. Division
Albuquerque Oper. Office
Albuquerque, NM 87115

U. S. Dept. of Energy
Attn: J. Rumbaugh
DOE/Wind Systems
1000 Independence Ave. SW
Washington, DC 20585

U. S. Dept. of Energy
Div. of PV Energy Systems
Attn: R. Annan
1000 Independence Ave. SW
Washington, DC 20585

U. S. Dept. of Energy
Div. of PV Energy Systems
Attn: A. Krantz
1000 Independence Ave. SW
Washington, DC 20585

U. S. Dept. of Energy
Div. of PV Energy Systems
Attn: A. Bulawka
1000 Independence Ave. SW
Washington, DC 20585

U. S. Dept. of Energy
Div. of PV Energy Systems
Attn: M. Pulscak
1000 Independence Ave. SW
Washington, DC 20585

U. S. Dept. of Energy
Div. of Elec. Energy Sys.
Attn: D. Roesler
1000 Independence Ave. SW
Washington, DC 20585

U. S. Dept. of Energy
Div. of Elec. Energy Sys.
Attn: K. Klein
1000 Independence Ave. SW
Washington, DC 20585

Univ. of California, Berkeley
Attn: C. Hu
Dept. of Elec. Engr.
Berkeley, CA 94720

University du Quebec,
Trois-Rivieres
Attn: V. Rajegopalan
Dept. d'Ingehierie - C.P. 500
Trois-Rivieres, Quebec
CANADA G9A 5H7

University of British Columbia
Attn: W. G. Dunford
Dept. of Elec. Engr.
Vancouver, BC
Canada V6T 1WS

University of Colorado
Attn: R. W. Erickson
Dept. of Elec. Engr.
Boulder, CO 80309

University of Delaware
Attn: Allen Barnett
Dept. of EE
Newark, DE 19711

University of Hawaii
Attn: Patrick Takahashi
Hawaii Natural Energy Inst.
2540 Dole Street
Honolulu, HI 96822

University of Lowell
Attn: Thomas Costello
1 University Avenue
Lowell, MA 01854

University of Lowell
Attn: Fahd Wakim
1 University Avenue
Lowell, MA 01854

University of New Mexico
Attn: A. O. Lebeck
Farris Engineering Center
Room 124
Albuquerque, NM 87131

Univ. of Texas at Arlington
Attn: Jack Fitzer
West 6th at Speer Street
Arlington, Tx 76019

University of Toronto
Attn: S. B. Dewan
Dept of Elec. Engr.
Toronto, Ontario
Canada M5S 1A4

University of Wisconsin
Attn: T. A. Lipo
Dept. of Elec. Engr.
and Computer Science
Madison, WI 52706

Utility Power Group
Attn: M. Stern
9410 DeSoto Ave., Unit G
Chatsworth, CA 91311

Virginia Power Co.
Attn: Tim Bernadowski
Corp. Tech. Assess.
5000 Dominion Boulevard
Glen Allen, VA 23060

Virginia Polytechnic Inst.
and State University (3)
Attn: Dan Chen
F. C. Lee
Saifur Rahman
Dept. of Elec. Engr.
Blacksburg, VA 24061

Westinghouse R&D Center
Attn: Peter Wood
1310 Beulah Road
Pittsburgh, PA 15235

Wichita State University
Center for Energy Studies
Attn: Dr. Ward Jewell
Box 44
Wichita, KS 67208

2363 H. M. Barnett
2525 R. Clark
3141 S. A. Landenberger (5)
3154 C. L. Ward (8) DOE/OSTI
3151 W. I. Klein (3)
6220 D. G. Schueler
6221 E. C. Boes
6223 G. J. Jones
6223 J. W. Stevens (10)
6223 R. N. Chapman
6223 T. S. Key
6223 W. I. Bower
6223 H. N. Post
6223 M. G. Thomas
6223 J. W. Strachan
6224 D. E. Arvizu
8524 J. A. Wackerly
6220 A. V. Poore